University of Alberta

Identification of novel genes involved in the genesis of Wilms tumor of the kidney

by

©

Tanya L. Gillan

A thesis submitted to the Faculty of Graduate Studies and Research in partial fulfillment of the requirements for the degree of

Doctor of Philosophy

In

Medical Sciences – Oncology

Edmonton, Alberta

Fall, 2004

Library and
Archives Canada

Published Heritage
Branch

395 Wellington Street
Ottawa ON K1A 0N4
Canada

Bibliothèque et
Archives Canada

Direction du
Patrimoine de l'édition

395, rue Wellington
Ottawa ON K1A 0N4
Canada

Your file Votre référence
ISBN: 0-612-95936-8
Our file Notre référence
ISBN: 0-612-95936-8

The author has granted a non-exclusive license allowing the Library and Archives Canada to reproduce, loan, distribute or sell copies of this thesis in microform, paper or electronic formats.

L'auteur a accordé une licence non exclusive permettant à la Bibliothèque et Archives Canada de reproduire, prêter, distribuer ou vendre des copies de cette thèse sous la forme de microfiche/film, de reproduction sur papier ou sur format électronique.

The author retains ownership of the copyright in this thesis. Neither the thesis nor substantial extracts from it may be printed or otherwise reproduced without the author's permission.

L'auteur conserve la propriété du droit d'auteur qui protège cette thèse. Ni la thèse ni des extraits substantiels de celle-ci ne doivent être imprimés ou aturement reproduits sans son autorisation.

In compliance with the Canadian Privacy Act some supporting forms may have been removed from this thesis.

Conformément à la loi canadienne sur la protection de la vie privée, quelques formulaires secondaires ont été enlevés de cette thèse.

While these forms may be included in the document page count, their removal does not represent any loss of content from the thesis.

Bien que ces formulaires aient inclus dans la pagination, il n'y aura aucun contenu manquant.

Canada

In Memoriam

In memory of my mum, Helen Joan Gillan.

Dedication

This thesis is dedicated to my father and friend, Norman R. Gillan. Thank you for your love and support and for being a great dad!

Acknowledgements

My time at the CCI has been a rewarding and memorable experience to which I am very thankful to the numerous people who have opened up their hearts, experience, knowledge and labs to me and who have all contributed to the success and enjoyment of my many years in the Department. First I would like to thank my supervisor, Dr. Paul Grundy, for his help and support and for giving me the opportunity to follow my instinct and go off on a potential "wild goose chase". A big thank-you to my co-supervisor Dr. Roseline Godbout for her friendship and support and for answering all of my countless questions (and also for pumping me with chocolate especially when I was down!). Another thank-you goes to Dr. Joan Turner for allowing me to setup camp in her lab and making me feel welcomed and part of the Turner Lab. For everyone, both past and present in the Grundy Lab (especially Kevin Dietrich and Kay Ziebart who have been there from day one and Holly Mewhort who was the best summer student anyone could have asked for), the Turner Lab and Godbout Lab, Thank-you, Thank-you, Thank-you!!! Without everyone's help and support I would probably still be trying to figure out how to work the PCR machines!! I also must say a big thank-you to Gina Kennedy who was always one step ahead of me and had the amazing ability to fix and finds things that I never could. Also thanks to Linda Harris for obtaining so many journal articles for me and for the many cookies, stories and laughs that were shared. Finally, thank you to my supervisory/examining committee: Drs. Heather McDermid, Rachel Wevrick, Susan Cohn and Andrew Shaw.

To my friend and mentor Dr. Anne Galloway, I can't tell you how much I appreciate all of the advice, support, suggestions, wisdom, laughs, friendship and cat that you have provided me with over the years – thank-you so much. To the rest of my friends, both my old and dear friends and the new ones made since I've been in Edmonton. I just want you all to know that your unconditional friendship has been the best gift I could have asked for - thank-you. "Life is partly what we make it and partly what is made by the friends we choose – Tehyi Hsieh".

To my family, my father Norman Gillan, my brother Paul Gillan, my sister Norma Hustins and my grandmother Helen Rafuse, thank you for all of your love and support and for understanding when I decided to move to the other side of the country. Although we were separated by many miles, you have all been alongside of me every step of the way. Finally, thank you to Nicholas Budge for being the best friend anyone could ask for. Words cannot express how much your unconditional friendship, love and support has meant to me both now and always – thank-you.

Table of Contents

Page

CHAPTER 1 1

Introduction

1.1 Wilms tumor 1

- **1.1.1** History of Wilms tumor 1
- **1.1.2** Epidemiology 1
- **1.1.3** Normal kidney development 2
- **1.1.4** Development of Wilms tumor 5
- **1.1.5** Nephrogenic rests 8

1.2 Clinical Features of Wilms tumor 9

- **1.2.1** Diagnosis of Wilms tumor 9
- **1.2.2** Treatment of Wilms tumor 10
- **1.2.3** Late side effects of treatment and follow-up 13
- **1.2.4** Secondary neoplasms and metastases 14

1.3 Molecular Genetics of Wilms tumor 14

- **1.3.1** Wilms tumor suppressor gene 1 (*WT1*) 14
  - **1.3.1.1** Expression of *WT1* 15
  - **1.3.1.2** *WT1* mutations 16
  - **1.3.1.3** WAGR syndrome 18
  - **1.3.1.4** Denys Drash Syndrome (DDS) 18
  - **1.3.1.5** Other Wilms tumor predisposing syndromes 19
  - **1.3.1.6** WT1 function 20

- 1.3.1.7 WT1 and other cancers 21
- 1.3.1.8 *WT1* and β-catenin mutations 21
- 1.3.2 Beckwith-Wiedemann syndrome (BWS) 22
  - 1.3.2.1 *WT2* 22
  - 1.3.2.2 The *WT2* region is imprinted 23
  - 1.3.2.3 Insulin-like Growth Factor 2 (*IGF2*) 24
  - 1.3.2.4 *H19* 25
  - 1.3.2.5 $p57^{KIP2}$ 25
- 1.3.3 Familial Wilms tumor 28
- 1.3.4 Loss of heterozygosity in Wilms tumors 30
  - 1.3.4.1 Chromosome16q LOH 30
  - 1.3.4.2 Chromosome 1p LOH 34
  - 1.3.4.3 Other regions of chromosomal LOH 34
- 1.3.5 The *p53* gene, anaplasia and Wilms tumor 35

1.4 Simpson Golabi Behmel Syndrome (SGBS) 36
- 1.4.1 Glypican 3 (*GPC3*) 37
- 1.4.2 *GPC3* expression 38
- 1.4.3 *GPC3* mutations 39
- 1.4.4 Proteoglycans: Syndecans and Glypicans 40
- 1.4.5 Glypican structure 40
- 1.4.6 Glypican function 41
- 1.4.7 GPC3 and IGF2 42
- 1.4.8 GPC4 – A contiguous gene syndrome? 43

1.4.9 GPC3 and other cancers 45

1.5 The Cadherin gene family 48

1.5.1 Cadherin structure 48

1.5.2 Classical cadherins 49

1.5.3 Other cadherin sub-families 52

1.5.4 Cadherin inactivation in cancer 54

1.5.5 Cadherin switching 59

1.5.6 Catenin alterations in cancer 60

1.5.7 Wnt signaling pathway 62

1.5.8 Ksp-cadherin 65

1.5.8.1 Ksp-cadherin expression 66

1.5.8.2 Ksp-cadherin function 67

1.5.8.3 Ksp-cadherin promoter 68

1.6 Gene Expression profiling 68

1.6.1 Differential display PCR 69

1.6.2 *In silico* methods of candidate gene searching 75

1.7 Global Objectives 76

CHAPTER 2 79

Material and Methods

2.1 Patient samples 79

2.2 Nucleic acid and protein extractions 79

2.2.1 Tissue preparation 79

2.2.2 Nucleic acid extraction 80

2.2.3 Preparation of whole cell lysates 81

2.2.4 Quantitation of nucleic acids and protein 81

2.3 Southern and Northern blot hybridization 81

2.3.1 Southern blot analysis 81

2.3.2 Northern blot analysis 82

2.3.3 Preparation of probes 84

2.3.4 Random primed synthesis 84

2.4 Western blot analysis 85

2.4.1 SDS-polyacrylamide gel electrophoresis 85

2.4.2 Preparation of protein samples 85

2.4.3 Western blot transfer 86

2.4.4 Western blotting 86

2.4.5 Protein detection 87

2.5 Reverse transcription 87

2.6 Polymerase chain reaction 88

2.6.1 PCR primers 89

2.7 Heteroduplex analysis 89

2.8 Automated DNA sequencing 90

2.8.1 ABI prism 310 genetic analyzer sequencing preparation 90

2.8.2 CEQ8000 genetic analysis sequencing preparation 91

2.9 Differential Display PCR 92

2.9.1 Wilms tumor samples 92

2.9.2 Differential display reverse transcription 92

2.9.3 Differential display PCR 93

2.9.4 Denaturing polyacrylamide gel electrophoresis 93

2.9.5 Excision of cDNA fragments 94

2.9.6 Reamplification of cDNA fragments 95

2.9.7 Cloning of cDNA fragments 96

2.9.8 Plasmid isolation and restriction digest 97

2.9.9 Characterization of sequenced cDNAs 97

2.9.10 Semi-quantitative RT-PCR 97

2.10 DNA methylation analysis 98

2.10.1 Sodium bisulfite modification 98

2.10.2 Bisulfite-specific and methylation specific PCR 99

CHAPTER 3: Analysis of the Simpson-Golabi-Behmel syndrome (SGBS) gene locus, *GPC3* in sporadic Wilms tumors 106

3.1 Wilms tumor sample population 108

3.2 Identification of *GPC3* mutations by southern blot analysis 108

3.3 Identification of small *GPC3* mutations by heteroduplex analysis 115

3.4 RNA expression analysis of *GPC3* 134

3.5 Discussion 138

CHAPTER 4: Identification of Wilms tumor genes by DD-PCR and database searching 141

4.1 Loss of heterozygosity of chromosome 16q in Wilms tumors 142

4.2 Techniques used to identify candidate genes 142

4.3 Differential Display PCR 144

4.3.1 Tumor selection for DD-PCR 144

4.3.2 Identification of differentially expressed cDNAs 145

4.3.3 Review of the differentially expressed cDNAs 149

4.3.4 Analysis of the candidate Wilms tumor genes by semi-quantitative PCR 153

4.3.5 Results of semi-quantitative RT-PCR 154

4.3.6 Analysis of *MLLT10* RNA in additional Wilms tumors 165

4.3.7 Analysis of *EIF4b* RNA in additional Wilms tumors 168

4.4 Database searching 170

4.4.1 Genes localized within the minimal region of 16q LOH 170

4.4.2 Exclusion of candidate Wilms tumor genes 172

4.4.3 Candidate Wilms tumor genes 178

4.4.4 Highest priority Wilms tumor candidate genes 181

4.5 Discussion 185

CHAPTER 5: Evaluation of Ksp-cadherin in Wilms tumor 199

5.1 Ksp-cadherin 200

5.2 Tumor sample population 203

5.3 RNA analysis of Ksp-cadherin 203

5.4 Western blot analysis of Ksp-cadherin 210

5.5 Ksp-cadherin Immunohistochemistry 212

5.6 Methylation analysis of the Ksp-cadherin promoter region 215

5.6.1 Review of the methylation detection techniques used 215

5.6.2 Methylation primers 220

5.6.3 Ksp-cadherin promoter methylation is not found in Wilms tumors 222

5.7 Mutation analysis of the Ksp-cadherin gene 229

5.8 Sequencing of the *HNF-1* binding region 230

5.9 Discussion 234

CHAPTER 6 244

6.1 Final Discussion 244

6.1.1 Ksp-cadherin and Wilms tumor: Models for tumorigenesis 252

6.2 Future Directions 254

6.2.1 Further evaluation of Wilms tumor candidate genes 255

6.2.2 Mutation analysis of the Ksp-cadherin gene 255

6.2.3 Ksp-cadherin gene knock-out studies 256

6.2.4 Evaluation of epigenetic events controlling gene regulation 257

6.2.5 Evaluation of additional cadherins and the role of cadherin switching in Wilms tumor 260

6.3 Concluding Remarks 262

CHAPTER 7: References 264

Appendix I 290

List of Tables

Table	Title	Page
1.1	The National Wilms Tumor Study Group staging classification for Wilms tumors	11
2.1	*GPC3* PCR primer sequences, PCR product size and PCR and WAVE annealing temperature	101
2.2	Primer sequences for the anchored and internal primers used in the differential display analysis	102
2.3	Primer sequence, PCR product size and annealing temperature of candidate genes analysed by semi-quantitative RT-PCR	103
2.4	Ksp-cadherin gene and promoter primer sequences PCR product size and annealing temperature	104
2.5	Primer sequences, PCR product size and annealing temperatures for *β-actin* and *GAPDH* as well as M13 and Universal sequencing primers	105
3.1	Summary of Wilms tumor cases with *GPC3* polymorphisms/mutations	137
4.1	Categorization of the sequenced candidate transcripts according to anchored primer utilized and sequencing results	146
4.2	List of known genes identified by dd-PCR, their chromosomal location, number of times isolated and whether they were analysed by RT-PCR	150
4.3	Tissue expression pattern of the dd-PCR candidate genes	152
4.4	Summary of dd-PCR and semiquantitative RT-PCR expression results normalized to *GAPDH*	159
4.5	Semi-quantitative RT-PCR results for *MLLT10* expression normalized to *GAPDH* RNA expression	163
4.6	Semi-quantitative RT-PCR results for *EIF4b* expression normalized to *GAPDH* RNA expression	169

4.7	List of known genes within the minimal region of LOH according to 16q location	174
4.8	List of known genes on chromosome 16q excluded as Wilms tumor candidates	179
4.9	List of genes from chromosome 16q that are known or believed to be implicated in tumorigenesis	180
4.10	List of cadherin genes located within the minimal region of LOH on chromosome 16q	182
4.11	List of genes located on chromosome 16q with limited tissue expression including the kidney	183
4.12	List of genes on chromosome 16q implicated in a potential Wilms tumor associated syndrome	183
5.1	Comparison of Northern blot and RT-PCR results, chromosome 16q LOH status and histology in 8 representative Wilms tumors	209
5.2	Methylation sequencing results from the MSP primer set MSP03-1	223
5.3	Methylation sequencing results from the MSP primer set MSP03-2	224
5.4	Methylation sequencing results from the BSP primer set MSP3-1n	225
5.5	Methylation sequencing results from the BSP primer set MSP3-2n	226

List of Figures

Figure	Title	Page
1.1	Normal kidney development	3
1.2	Kidney development and Wilms tumor	6
1.3	Imprinting and the *WT2* locus	26
1.4	Location of genes associated with *WT1* and putative *WT2* loci	29
1.5	Incidence of LOH for each chromosomal arm in Wilms tumor	31
1.6	Location of genes putative Wilms tumor genes	32
1.7	Cadherin mediated cell-cell adhesion	50
1.8	Cadherins and tumorigenesis	53
1.9	Schematic diagram of 9 of the cadherin subfamilies	55
1.10	Cadherin genes localize to the minimal region of chromosome 16q LOH	58
1.11	Wnt signaling pathway	63
1.12	Differential display PCR	72
3.1	Southern blot of Wilms tumor WT-42T hybridized with *GPC3*	110
3.2	Ideogram of the X chromosome	111
3.3	X chromosome microsatellite analysis of sample WT-42	113
3.4	Southern blot analysis of *Taq 1* digested Wilms tumor and corresponding constitutional DNA hybridized with *GPC3*	114
3.5	Southern blot analysis of *Taq 1* digested DNA with segments of the *GPC3* gene	116
3.6	*GPC3* exon 2 WAVE and sequencing results for sample WT-46	119

3.7 *GPC3* exon 2 WAVE and sequencing results for sample WT-47T 121

3.8 *GPC3* exon 7 WAVE and sequencing results for sample WT-44 124

3.9 *GPC3* exon 7 WAVE and sequencing results for sample WT-49T 126

3.10 *GPC3* exon 8 WAVE and sequencing results for sample WT-51T 129

3.11 *GPC3* exon 8 WAVE and sequencing results for sample WT-48T 131

3.12 RNA expression of *GPC3* in Wilms tumor and normal mature kidney 135

4.1 Differential display PCR autoradiogram (1) 147

4.2 Differential display PCR autoradiogram (2) 148

4.3 Average *GAPDH* RNA expression for each tumor sample evaluated 156

4.4 Northern blot of tumors used in the DD-PCR analysis Hybridized with β-actin 157

4.5 RT-PCR results, uncorrected for *GAPDH*, for 5 of the tumor samples for 6 of the genes evaluated (1) 161

4.6 RT-PCR results, uncorrected for *GAPDH,* for 5 of the tumor samples for 6 of the genes evaluated (2) 163

4.7 RT-PCR analysis of *MLLT10* in additional Wilms tumors uncorrected for *GAPDH* 167

4.8 RT-PCR analysis of *E1F4b* in additional Wilms tumors and normal kidney uncorrected for *GAPDH* 171

4.9 Categorization of the genes localized to the minimal region of LOH on chromosome 16q 173

5.1 RT-PCR analysis of Ksp-cadherin in Wilms tumor 205

5.2	Northern blot analysis of Ksp-cadherin in Wilms tumor	207
5.3	Summary of Ksp-cadherin RNA expression in Wilms tumors	211
5.4	Western Blot Analysis of Ksp-cadherin	213
5.5	Representative immunohistochemistry results	214
5.6	Sodium bisulfite modification and BSP and MSP analysis	217
5.7	Design of MSP primers	219
5.8	Regions of the Ksp-cadherin gene and promoter analysed for methylation	221
5.9	Representative BSP methylation sequencing results	227
5.10	Southern blot analysis of digested Wilms tumor DNA hybridized with Ksp-cadherin cDNA	231
5.11	Sequencing results of *HNF-1ß* binding region	232

List of Abbreviations

dATP	deoxyadenosine triphosphate
dCTP	deoxycytidine triphosphate
APS	ammonium persulfate
β-ME	β-mercaptoethanol
bp	base pair(s)
BSA	bovine serum albumin
BWS	Beckwith Weidemann Syndrome
C	constitutional
°C	degrees celsius
cDNA	complementary deoxyribonucleic acid
Ci	curie(s)
cpm	counts per minute
CTPS	2,4,4-Trimethylpyridinium p-toluenesulfonate
dd-PCR	differential display PCR
DDS	Denys-Drash Syndrome
dH$_2$0	distilled water
DNA	deoxyribonucleic acid
DNTPs	deoxynucleoside triphosphates
DTT	dithiothreitol
E	embryonic day
EDTA	ethylenediaminetetraacetic acid
EST	expressed sequence tag(s)
EtBr	ethidium bromide
EtOH	ethanol
FH	favorable histology
GPC3	Glypican 3
h	hour
HCC	hepatocellular carcinoma

HCl	hydrochloric acid
HPLC	high performance liquid chromotography
HRP	horseradish peroxidase
IGF2	Insulin-like growth factor 2
IHC	immunohistochemistry
ILNR	intralobar nephrogenic rests
IPTG	Isopropyl-beta-D-thiogalactopyranoside
KDa	kilodalton(s)
LB	luria broth
LOH	loss of heterozygosity
M	molar
mA	milliamp
MeOH	methanol
mg	milligram(s)
$MgCl_2$	magnesium chloride
min	minute
ml	milliliter(s)
mm	millimeter
mM	millimolar
mmol	millimole
MOPS	3-[N-Morpholino]propane-sulfonic acid
mRNA	messenger ribonucleic acid
MSP	methylation specific PCR
N	normal
NaOAc	sodium acetate
NH_4OAc	ammonium acetate
$NaHCO_3$	sodium bicarbonate
NaOH	sodium hydroxide
ng	nanogram(s)
OD	optical density
O/N	overnight

OPG	random DD-PCR primers
PAGE	polyacrylamide gel electrophoresis
PCR	polymerase chain reaction
PEG	polyethylene glycol
PLNR	perilobar nephrogenic rests
pmol	picomole
PVP	polyvinylpyrrolidone
RNA	ribonucleic acid
RNase	ribonuclease(s)
rpm	revolutions per minute
RT	room temperature
RT	reverse transcription
RT-PCR	reverse transcription polymerase chain reaction
s	second
SDS	sodium dodecyl sulfate
SGBS	Simpson Golabi Behmel Syndrome
SLS	sample loading solution
T	tumor
TBE	tris-borate-EDTA
TBS	tris buffered saline
TE	tris-EDTA
TEMED	N,N,N’.N’-tetramethylethylenediamine
TSR	template suppression reagent
T-TBS	tween-tris buffered saline
U	units
µg	microgram
µl	microliter
µM	micromolar
UV	ultraviolet
V	volts

vol	volume
WAGR	Wilms tumor, aniridia, genitourinary malformations, mental retardation
WT	Wilms tumor sample
WT1	Wilms tumor 1 gene
WT2	Wilms tumor 2 gene
X-Gal	5-brom-4-chloro-3-indolyl-beta-D-galactopyranoside

CHAPTER 1 - Introduction

1.1 Wilms tumor

1.1.1 History of Wilms tumor

Wilms tumor or nephroblastoma is a childhood renal tumor first described by Rance (1814). The oldest specimen dates back to 1793 and is from an infant who was described as having a bilateral renal tumor now believed to be a Wilms tumor (Beckwith, 1986). The first well-characterized histological description was published by Eberth (1872) with several other publications following. It was, however, the new observations and the thorough review of the literature published by Dr. Max Wilms in 1899 that forever linked his name to the tumor that is now commonly referred to as Wilms tumor. Dr. Wilms, in his famous monograph "Die Mischgeschwülste der Niere" was the first to describe Wilms tumor as a cancer arising from cells within the germline and leading to its classification as an embryonal tumor (Wilms, 1899).

1.1.2 Epidemiology

Wilms tumor is the most common form of childhood renal tumor with an estimated incidence of 1 in 10 000 live births, making it the fourth most common childhood malignancy in North America (Miller et al., 1995). Children can present with either unilateral (one kidney) or bilateral (both kidneys) Wilms tumor. Wilms tumors are usually diagnosed by 15 years of age with the average age of diagnosis between 3-4 years of age for unilateral Wilms tumor and 2.5 years of age for the bilateral form (Breslow et al., 1988; Breslow et al., 1993). However, in rare cases, adults have also been diagnosed with the disease (Huser et al., 1990). Wilms tumor is equally distributed amongst sexes, races and geographically, although a slightly higher incidence has been reported in African Americans (Fukuzawa et al., 2004). Several syndromes have also been reported to be associated with the development of Wilms tumor as described later in this chapter (Hastie et al., 1994).

1.1.3 Normal Kidney Development

The kidney develops from 3 separate components: the pronephros, mesonephros and metanephros. The pronephros is a rudimentary and transient structure that represents the beginning of kidney formation. The pronephros gradually disappears as the mesonephros develops and gives rise to gonadal structures including the Wolffian (mesonephric) duct and Bowman's capsule. The mesonephric duct then develops into the metanephros which gives rise to the permanent kidney. At this point, the metanephric mesenchyme, which is comprised of undifferentiated renal blastemal cells, signals the Wolffian duct to initiate the formation of the ureteric bud. The ureteric bud then grows into the metanephric mesenchyme initiating a reciprocal induction. The metanephric mesenchyme induces the ureteric bud to branch and grow beginning the formation of the collecting duct system. In turn the ureteric bud induces the blastemal cells of the metanephric mesenchyme to begin to differentiate ultimately forming the mature nephron (Figure 1.1) (Davies, 1993; Bard et al.,

Figure 1.1: Normal kidney development. The ureteric bud, an outgrowth of the wolffian duct, grows and comes in contact with a group of undifferentiated cells comprising the metanephric mesenchyme. This contact leads to a reciprocal inductive event whereby the metanephric mesenchyme induces the ureteric bud to proliferate and branch thus forming the beginning of the renal collecting duct system. The branching of the ureteric bud in turn induces the metanephric mesenchyme to differentiate into epithelial cells and begin the formation of nephrons and connective tissue. This figure was adapted from: Brown and Malik (2001).

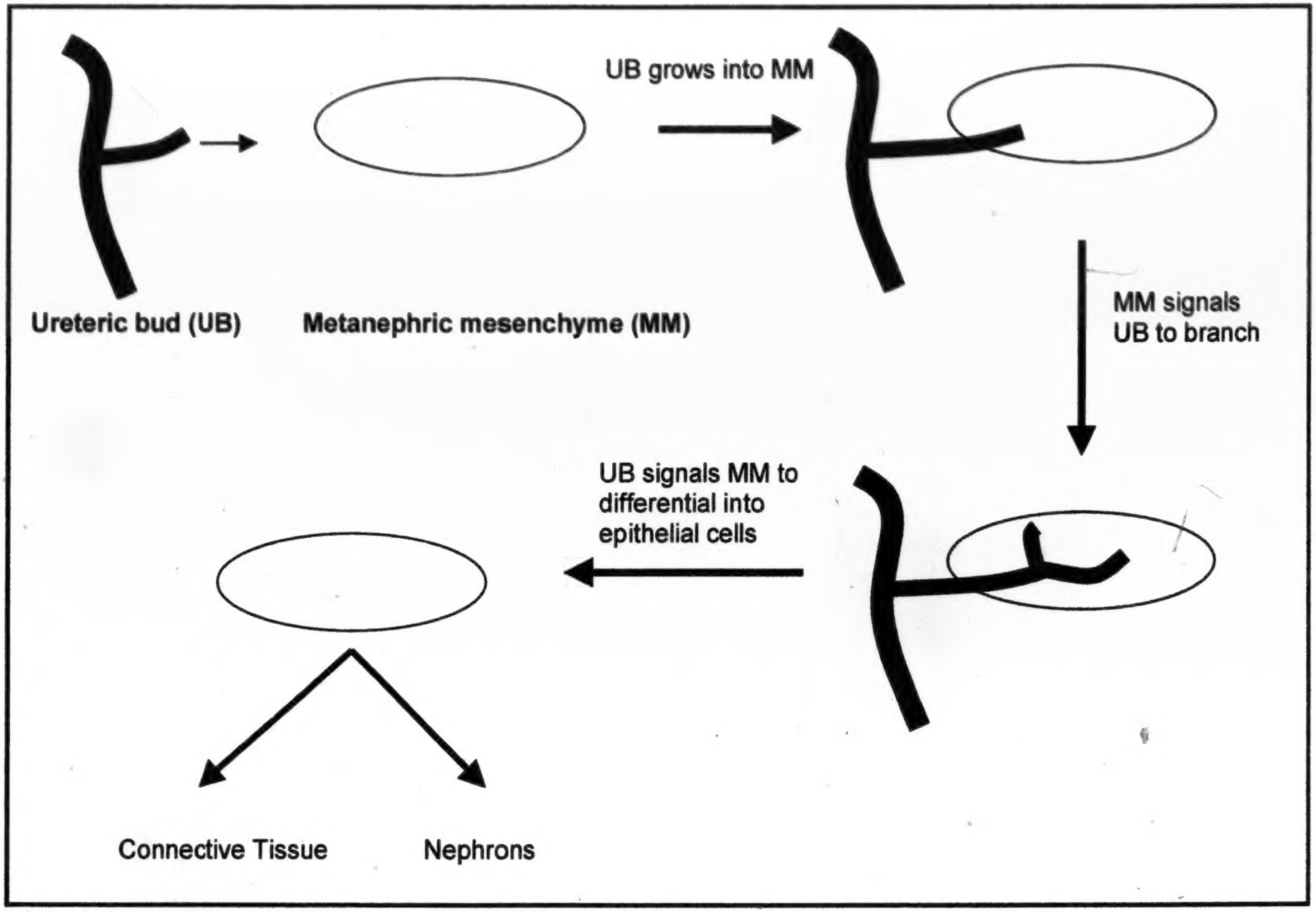
Ureteric bud (UB)
Metanephric mesenchyme (MM)
UB grows into MM
MM signals UB to branch
UB signals MM to differential into epithelial cells
Connective Tissue
Nephrons

1994). These cells undergo a mesenchyme to epithelial transition and are organized to form the epithelial renal vesicle. The renal vesicle elongates and twists to form first a comma-shaped and then the S-shaped body in which the lower segment develops into the glomerulus, comprised of epithelial cells that revert to resemble mesenchymal cells. The middle develops into the proximal tubule and the upper segment forms the distal tubule. The mature kidney is comprised primarily of epithelial nephrons and collecting ducts with a minor proportion comprised of mesenchyme or mesenchymal-like and stromal cells (Sariola and Sainio, 1998; Pritchard-Jones and Fleming, 1991).

1.1.4 Development of Wilms tumor

Wilms tumor is thought to arise from undifferentiated or partly differentiated metanephric blastema that undergoes malignant transformation (Figure 1.2). Wilms tumors are a classic example of embryonal tumors as they recapitulate almost every stage of normal kidney development. They are histologically diverse and are often comprised of varying proportions of epithelial, stromal and blastemal cells. Some tumors are comprised of a mixture of the three cell types while others are predominantly or exclusively made up of only one cell type (Murphy et al., 2004). This histological variation illustrates the fact that Wilms tumors can arise throughout various stages of renal development as some Wilms tumors resemble undifferentiated metanephric mesenchyme indicating they arose early in kidney development. Other tumors exhibit various degrees of differentiation (epithelial and stromal elements present) and resemble

Figure 1.2: Kidney development and Wilms tumor. Wilms tumors are thought to arise from the metanephric mesenchyme which is unable to undergo differentiation into renal epithelial cells. This leads to the persistence of undifferentiated or partly differentiated cells that give rise to a Wilms tumor. This figure adapted from: www-ermm.cbcu.cam.ac.uk.

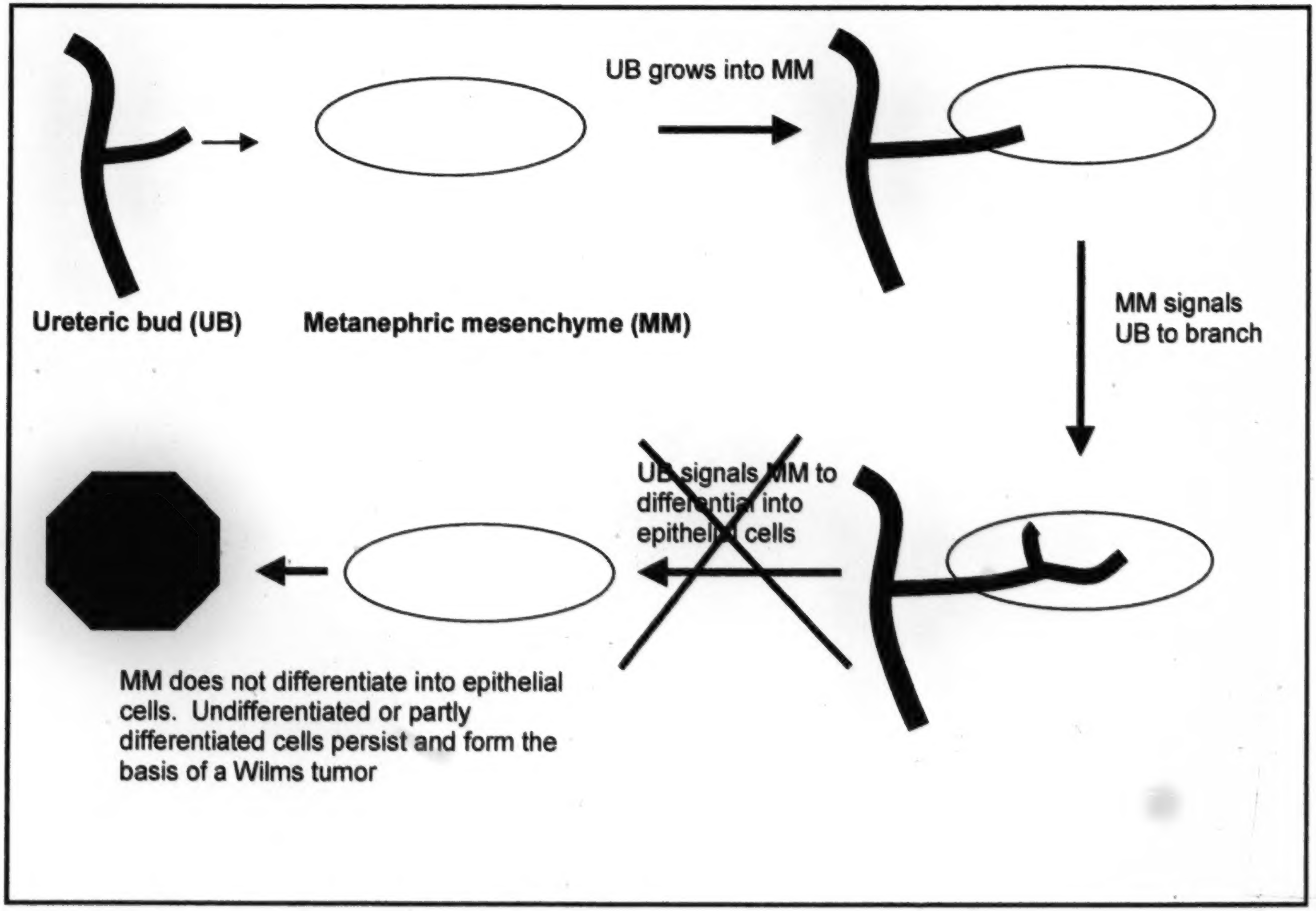
Ureteric bud (UB)
Metanephric mesenchyme (MM)
UB grows into MM
MM signals UB to branch
~~UB signals MM to differentiate into epithelial cells~~

MM does not differentiate into epithelial cells. Undifferentiated or partly differentiated cells persist and form the basis of a Wilms tumor the pathways undertaken during normal kidney development and these tumors likely arose during later stages of kidney development (Pritchard-Jones and Fleming, 1991).

1.1.5 Nephrogenic rests

Interestingly, approximately 40% of kidneys with Wilms tumors contain putative precursor lesions called nephrogenic rests. These lesions represent an abnormal persistence of embryonal cells and/or their derivatives into postnatal life, some of which are believed to be able to develop into Wilms tumors (Beckwith et al., 1990). The presence of nephrogenic rests seems to conform to Cohneim's "cell rest" theory of tumor formation which states that tumorigenesis may arise from the excessive production or abnormal retention of undifferentiated embyronal cells or cells that retain embryonal potentialities (Beckwith, 1998). Nephrogenic rests can undergo a variety of different fates and not all lead to the development of Wilms tumor. Nephrogenic rests can: (1) persist in a dormant state for years; (2) regress and eventually disappear; (3) become cystic and mature into structures resembling renal dysplasia; (4) lead to hyperplastic proliferation or (5) lead to malignant (Wilms tumor) growths (Beckwith, 1998). Furthermore, nephrogenic rests can also undergo more than one of these transformations. For example, dormant rests have been found to undergo hyperplastic proliferation leading to tumorigenesis.

There are two types of nephrogenic rests, perilobar nephrogenic rests (PLNR) and intralobar nephrogenic rests (ILNR), both of which have been found associated with Wilms tumors (Beckwith et al., 1990; Beckwith, 1993). PLNRs are located on the periphery of the renal lobe, are well demarcated, are composed of blastemal and/or embryonal epithelial cells and arise late in kidney development. ILNRs are found within the renal lobe, are comprised of multiple cell types including stromal, blastemal and epithelial and arise early during kidney development (Beckwith, 1998). Nephrogenic rests are found in routine autopsies of infants and children unaffected with Wilms tumor with a frequency of 1% for PLNRs and 0.01% for ILNRs. These numbers increase substantially in kidneys with Wilms tumors. The frequency of PLNRs and ILNRs in individuals with unilateral Wilms tumor is 25% and 15%, respectively. The frequency increases further in individuals with bilateral Wilms tumor with PLNRs and ILNRs occurring at a frequency of 42-79% and 34-75%, respectively, depending on whether the bilateral tumors are metachronous or synchronous (Beckwith, 1993). It has been found that ILNRs more frequently progress to Wilms tumors than the PLNRs.

1.2 Clinical Features of Wilms tumor

1.2.1 Diagnosis of Wilms tumor

Wilms tumors are generally asymptomatic in the early stages of the disease and the majority of cases are detected due to the presence of a large abdominal mass (Aron, 1974). Many children also complain of abdominal pain and in some cases hematuria and hypertension are present in addition to the ambiguous symptoms of anorexia, vomiting, fever and general malaise

(Greenwood and Holland, 1984). Diagnosis of Wilms tumor is usually accomplished by abdominal ultrasonography, CT-scan, and/or MRI followed by biopsy and pathological analysis. Morphologically, Wilms tumors are usually well demarcated and a uniform grey/tan color. Some tumors, however, may be variegated due to hemorrhage and necrosis and often contain cysts. Clinical, surgical and pathological analysis of Wilms tumors classifies them into stages and the course of treatment is dependent on the tumor stage (reviewed in Murphy et al., 2004). Table 1.1 provides a brief summary of the current staging system.

1.2.2 Treatment of Wilms tumor

The current multi-modal treatment regimens are successful with an overall survival rate exceeding 85% (D'Angio et al., 1988). Interestingly, the course of treatment differs between countries/continents. In North America, the standard treatment protocol is surgical resection of the tumor by complete nephrectomy, followed by tailored chemotherapy and radiation regimens according to histopathologic and staging criteria. In some instances, pre-operative chemotherapy or radiation therapy is prescribed to patients with infiltrative tumors or bilateral renal tumors (Ritchey et al., 1993). Pre-operative treatment is prescribed for all children with Wilms tumor in Europe/Asia/Africa. Treatment with therapeutic agents, prior to surgical resection, aids in reducing tumor mass, thus allowing for easier surgical resection of the tumor and thereby reducing

Table 1.1: The National Wilms Tumor Study Group staging classification for Wilms tumors (Tumors of the Kidney, Bladder, and Related Urinary Structures, 2004).

Stage I	Tumor limited to the kidney and completely resected. No penetration of the renal capsule or involvement of renal sinus vessels.
Stage II	Tumor extends beyond the kidney but is completely resected (negative margins and lymph nodes). At least one of the following has occurred: (1) penetration of the renal capsule; (2) invasion of the renal sinus vessels; (3) biopsy of tumor prior to removal; (4) spillage of tumor locally during removal
Stage III	Gross or microscopic residual tumor remains postoperatively including: inoperable tumor, positive surgical margins, tumor spillage involving peritoneal surfaces, regional lymph node metastases, or transected tumor thrombus.
Stage IV	Hematogenous metastases or lymph node metastases outside the abdomen (lung, brain, bone, liver)
Stage V	Bilateral renal Wilms tumor at onset

surgical complications.

The treatment of Wilms tumor is not only aided by accurate histological staging, but its success is also attributed to the high rate of responsiveness of tumors to chemotherapeutic agents and radiation therapy. The efforts of the National Wilms Tumor Study Group have provided valuable information on effective treatments for this tumor. Wilms tumors were first found to be responsive to the chemotherapeutic agent dactinomycin. This led to the discovery that additional agents including vincristine, doxorubicin and cyclophosphamide were all active against Wilms tumors (Farber, 1966; D'Angio 1981). Wilms tumors are also extremely responsive to radiation therapy which was initially administered to all patients post-operatively. However, with the advent of effective chemotherapeutic drugs and the desire to minimize side effects and loss of normal tissue, radiation therapy is usually only prescribed for patients with advanced stages of Wilms tumor (Stages III, IV) (Thomas et al., 1991).

The most significant outcome predictor is the classification of tumors as either favorable histology (FH) or unfavorable or anaplastic histology, which is characterized by atypical mitotic figures and enlarged nuclei (Vujanic et al., 1999). FH tumors do not show evidence of anaplasia and generally have a good outcome, responding well to surgical resection and treatment with chemotherapeutic agents. Anaplastic tumors are generally more resistant to current therapies and have a worse outcome, even when radiation and more toxic chemotherapeutic drugs are included in the treatment regimen (Beckwith and Palmer, 1978).

Approximately 15% of children with Wilms tumor relapse after treatment for the disease. Recommended therapies for relapsed patients depend on their initial diagnosis and treatment, the site of relapse and the duration between initial diagnosis and relapse. Generally, children who relapse after initial diagnosis with low stage FH tumors are treated aggressively and respond well to the therapies (Grundy et al., 1989). However, children who relapse following treatment for late stage and anaplastic Wilms tumors generally respond poorly to subsequent treatment and have a poor prognosis (Grundy et al., 1989).

1.2.3 Late side effects of treatment and follow-up

The occurrence of late side effects of treatment is significant among Wilms tumor survivors and therefore subsequent long-term follow-up is recommended. The side-effects that can arise following therapy include: cardiac dysfunction, pulmonary fibrosis in patients with metastatic disease, hematological toxicity, impairment of gonadal function (particularly in males), high risk pregnancies in females, scoliosis and secondary neoplasms (Green et al., 1995). Surprisingly, serious renal dysfunction is not prevalent among survivors. The best defense against the occurrence of these side effects is the development of more effective and less toxic cancer therapies, diligent long-term follow-up and early detection of symptoms. Therefore, research into the genetics and biochemistry will not only lead to a better understanding of Wilms tumor, but may aid in the development of more sensitive diagnostic and prognostic indicators and refinement of therapies which could lead to more specific therapies and possibly reducing the occurrence of late side effects.

1.2.4 Secondary neoplasms and metastases

A small proportion of Wilms tumors are metastatic with the most common target site being the lung, followed by the liver, brain and regional nodes (Breslow et al., 1986). Wilms tumor survivors also have an approximate 1.6% increased risk for the development of secondary neoplasms. These neoplasms can arise from an inherited genetic predisposition or from chemotherapy or radiation damage.

1.3 Molecular Genetics of Wilms tumor

1.3.1 Wilms tumor suppressor gene 1 (WT1)

Identification of the first Wilms tumor gene was aided by the discovery that approximately 1% of individuals with Wilms tumor also had aniridia, genitourinary defects and mental retardation. This grouping of anomalies was termed the WAGR syndrome which stands for **W**ilms tumor, **a**niridia, **g**enitourinary defects and mental **r**etardation. Constitutional deletions at chromosome 11p13 were identified in individuals with the WAGR syndrome (Riccardi et al., 1978). These findings together with those of Koufos et al. (1984) and Orkin et al. (1984), who found that 40% of Wilms tumors lose heterozygosity of chromosome 11p, suggested that this chromosomal region contained a Wilms tumor gene. In 1988, a Wilms tumor containing a homozygous deletion was identified that localized the putative Wilms tumor gene to a 350 kb region, at 11p13. This discovery aided in the cloning of the Wilms tumor suppressor gene 1 (*WT1*) by two independent groups in 1990 (Call et al., 1990; Gessler et al., 1990).

WT1 is comprised of 10 exons, spans approximately 50 kb, produces a 3.5 kb mRNA transcript and a 499 amino acid protein (Call et al., 1990). The carboxyl terminus of WT1 contains four zinc finger domains and two alternative splice sites, one of which regulates the presence or absence of exon 5 (splice site 1). The second alternative splice site encodes a variable splice donor site in exon 9 resulting in the addition of three extra amino acids that interrupt the third and fourth zinc finger binding sites (splice site 2). These three amino acids (lysine, threonine and serine) have subsequently been termed KTS. The presence of these two alternative splice sites result in four different WT1 isoforms: (1) + exon 5, +KTS; (2) + exon 5, -KTS; (3) – exon 5, +KTS; (4) – exon 5, -KTS (Call et al., 1990; Rauscher, 1993; Haber et al., 1991).

1.3.1.1 Expression of WT1

WT1 is expressed in both fetal and adult kidney. Low levels of *WT1* are first seen in the undifferentiated metanephric mesenchyme. *WT1* expression increases significantly upon induction of the metanephric mesenchyme to differentiate and remains expressed in the mature nephron (Hastie, 1994). In addition to the kidney, *WT1* is also expressed in the stromal cells of the spleen and gonad and the mesothelial cells lining the heart, diaphragm and peritoneum

(Armstrong et al., 1992). Analysis of *WT1* mRNA shows variable expression between Wilms tumors. Immunohistochemical analysis has shown that *WT1* is highly expressed in the blastemal and immature epithelial cells. This explains the variable mRNA expression seen, as Wilms tumors are comprised of varying proportions of cell types, some of which do not express *WT1*.

1.3.1.2 WT1 Mutations

The *WT1* gene functions as a tumor suppressor gene. Thus inactivation of both copies of the *WT1* gene is needed for the development of Wilms tumor, as defined by Knudson's "two-hit" hypothesis (Knudson, 1975). Inactivation of each *WT1* allele can arise via somatic or germline mutations, deletions or recombination. Loss of heterozygosity (LOH) of chromosome 11p has been found to occur in approximately 30-40% of Wilms tumors. This loss of chromosomal material where the *WT1* gene resides often represents the "second-hit" needed for *WT1* gene inactivation according to the "two-hit" hypothesis model. A variety of *WT1* mutations have been identified in Wilms tumor including insertions/deletions, frameshift, missense and nonsense mutations. Although *WT1* mutations are found throughout the gene, a high proportion of insertion/deletion mutations have been found within the first exon, suggesting the presence of a mutational hotspot (Huff, 1996).

Both germline and somatic *WT1* mutations have been identified in Wilms tumor patients. Surprisingly, *WT1* mutations are found in only 10-20% of Wilms tumors. Furthermore, its involvement appears to be primarily associated with bilateral Wilms tumor or syndrome-associated Wilms tumors. A study by Huff (1998) found that 100% of the bilateral tumors they evaluated carried a *WT1* germline mutation while only 7% of unilateral tumors carried a *WT1* germline mutation. However, it has been found that not all bilateral Wilms tumors carry *WT1* germline mutations. This is in accordance with the genetic model that germline mutations predispose to the development of multiple tumors while somatic mutations give rise to unilateral tumors (Huff, 1998). Furthermore, germline *WT1* mutations have also been found in the 3-4% of Wilms tumors associated with the Denys-Drash syndrome (DDS) and the WAGR syndrome. Surprisingly, somatic mutations of *WT1* occur in only 5-10% of sporadic Wilms tumor (reviewed in Hastie, 1994). It is possible that other mechanisms of gene inactivation, such as epigenetic events, may be present in Wilms tumors with no apparent *WT1* mutations. However, due to the fact that the majority of Wilms tumors express *WT1*, this possibility is unlikely (Huff, 1998). Therefore, the role of *WT1* in sporadic Wilms tumorigenesis is limited, suggesting that additional genes are likely to be involved in the pathogenesis of Wilms tumor. Review of individuals heterozygous for germline *WT1* mutations associated with either the WAGR syndrome or DDS showed a cumulative risk of 62% and 32%, respectively, for the development of renal failure 20 years after initial diagnosis. In contrast, the risk for non-syndrome associated Wilms tumor patients developing renal failure later in life was only 1% (Breslow et al., 2000).

1.3.1.3 WAGR Syndrome

The WAGR syndrome is a contiguous gene syndrome that involves at least 2 genes, the *PAX6* gene and *WT1 gene,* on chromosome 11p13. Thirty percent of individuals with aniridia and the WAGR syndrome develop Wilms tumor, often of the bilateral form. These individuals usually have various genitourinary defects and mental retardation. In WAGR patients, loss of one *PAX6* allele gives rise to aniridia while loss of one *WT1* allele contributes to genitourinary defects and represents the "first-hit" predisposing to Wilms tumor. A "second-hit" which inactivates the remaining *WT1* allele, is then needed for the development of Wilms tumor (Pelletier et al., 1991). The genetic defects underlying mental retardation are not known.

1.3.1.4 Denys Drash Syndrome (DDS)

DDS is a rare syndrome characterized by severe nephropathy and pseudo-hermaphrodism. Approximately 70-80% of individuals with DDS also develop Wilms tumors (Jadresic et al., 1990). Analysis of the *WT1* gene in those DDS patients with Wilms tumor revealed the presence of point mutations within exon 9 corresponding to the zinc finger DNA-binding domain (Coppes et al., 1993). Interestingly, these mutations were found to be heterozygous, implying that a mutant protein may act in a dominant-negative fashion interfering with and inhibiting the wild-type *WT1* protein. It is this dominant-negative effect that is believed to cause the more severe renal and genitourinary abnormalities seen in DDS patients as compared to WAGR patients with heterozygous *WT1* deletions.

Rare dominant-negative mutations have also been identified in sporadic Wilms tumors (Little et al., 1992; Haber et al., 1993).

1.3.1.5 Other Wilms tumor predisposing syndromes

Both Frasier and Perlman syndromes have been reported to have an increased incidence of Wilms tumor. However the occurrence of tumors is much lower than that reported for the DDS and WAGR syndromes. Frasier syndrome is a rare disorder characterized by male pseudo-hermaphrodism, renal abnormalities and genitourinary tumors such as gonadoblastoma and occasionally Wilms tumor. An individual with Frasier syndrome was found to have a point mutation within the intron 9 donor splice site which resulted in decreased expression of the WT1+KTS isoform (Barbaux et al., 1997 and reviewed in Dome and Coppes, 2002) suggesting that *WT1* may be involved in this syndrome.

Perlman syndrome is a rare condition with a high neonatal mortality that clinically resembles both the Beckwith-Weidemann (BWS) and Simpson-Golabi-Behmel (SGBS) overgrowth syndromes (which will be described later). A review of 16 patients with Perlman syndrome found that 5 (31%) individuals also developed Wilms tumor (Henneveld et al., 1999). There are conflicting reports of *WT1* involvement as loss of chromosome 11 was found in the tumor tissue of one patient but no chromosome 11 involvement was found in the others (Chernos et al., 1990). Due to the small sample size it cannot be determined if *WT1* and/or loss of chromosome 11p contributes to Perlman syndrome.

1.3.1.6 WT1 Function

Mouse gene knock-out studies have provided convincing evidence that *WT1* is crucial during embryonic development. Homozygous *WT1*$^{-/-}$ mice die *in utero* around embryonic day 13 (E13). These embryonic mice display heart, thoracic and diaphragmatic abnormalities. Furthermore, in the *WT1* null mice, the ureteric bud does not form and metanephric mesenchyme undergoes apoptosis preventing the urogenital system from developing. *WT1*$^{+/-}$ heterozygous mice, which should theoretically be similar to an individual with the WAGR syndrome, surprisingly exhibit no renal or gonadal abnormalities or predisposition to Wilms tumors (Kreidberg et al., 1993).

WT1 functions as a tumor suppressor gene and has an anti-proliferative role that presumably leads to the stimulation of specific differentiation processes (Little et al., 1999). In addition to WT1's tumor suppressor activity, the presence of four zinc finger motifs suggests that WT1 also functions as a transcription factor and has been shown to induce both transcriptional activation and repression of various genes (Wang et al., 1993). WT1 regulates its own expression as well as the expression of other proteins including transcription factors, growth factors and their receptors and proteins involved in the extracellular matrix (Rupprecht et al., 1994). It is thought that the various protein partners of WT1 contribute to its role in different developmental stages and tissues. Surprisingly, studies of WT1 found that in addition to binding DNA, WT1 can also bind RNA via zinc finger motifs similar, but not identical to the zinc finger motifs used for DNA binding. Furthermore, the WT+KTS isoform has a higher affinity to RNA whereas the WT-KTS isoform preferentially binds DNA, suggesting that the DNA/RNA binding is regulated at the isoform level.

1.3.1.7 WT1 and other cancers

There is growing evidence that *WT1* may be involved in non-Wilms tumor malignancies. Furthermore, it has been proposed that *WT1* may have an oncogenic function as it has been found to be overexpressed in a variety of cancers including acute leukemias, ovarian cancers, malignant mesotheliomas and granulosa cell tumors. Aberrant expression of *WT1* has been found in leukemias, breast cancer and HNSCC and has been correlated with worse prognosis in these instances. A point mutation within exon 6 of *WT1,* that changed the function of *WT1* from a transcriptional repressor to a transcriptional activator, was identified in one case of malignant mesothelioma (reviewed in Bruening et al., 1995). Recently, *WT1* mutations have also been found in 20% of AML/ALL patients, suggesting that *WT1* may have a role in hematopoiesis (Little et al., 1999).

1.3.1.8 WT1 and β-catenin *mutations*

β-catenin is a cell adhesion molecule involved in the maintenance of cell adhesion as well as a signaling molecule of the Wnt/wingless signal transduction pathway. Heterozygous mutations of β-catenin have been found to occur in approximately 15% of Wilms tumors, the majority of which also contain inactivating *WT1* mutations. A study by Koesters et al. (1999) showed that of the

21 tumors that had β-catenin mutations, 19/21 (90%) also had a mutation of *WT1*. No correlation between the presence of β-catenin and a particular Wilms tumor phenotype has been observed as β-catenin mutations have been identified in unilateral and bilateral tumors as well as tumors associated with both DDS and WAGR syndromes (Maiti et al., 2000). These data suggest that β-catenin mutation and subsequent deregulation of the Wnt/wingless signaling pathway plays a role in at least a subset of Wilms tumors. Further discussion of β-catenin and the Wnt pathway will be presented in the cadherin sections to follow.

1.3.2 Beckwith-Wiedemann Syndrome

The Beckwith-Wiedemann syndrome (BWS) is an overgrowth syndrome characterized by macroglossia, umbilical hernia, hemihypertrophy, nevus flammeus, visceromegaly, diaphragmatic defects, postnatal gigantism, and omphalocele (Beckwith, 1969). Individuals with BWS are also at risk for developing childhood tumors, the most common being Wilms tumor with adrenocortical carcinoma, hepatoblastoma and rhabdomyosarcoma occurring less frequently (Wiedemann, 1983). The BWS gene has been localized to chromosome 11p15 by linkage analysis (Koufos et al., 1989; Mannens et al., 1994).

1.3.2.1 WT2

LOH of chromosome 11p in Wilms tumors often encompasses a large portion of the chromosome. Interestingly, LOH at 11p13 in many Wilms tumors includes a second distinct region telomeric to *WT1* at 11p15 (Reeve et al., 1989). Furthermore, linkage analysis of a small subset of patients with familial BWS mapped the BWS gene to chromosome 11p15 (Koufos et al., 1989). Since individuals with BWS are predisposed to developing Wilms tumor with an incidence of 5-10%, it is therefore proposed that the same gene(s) may be responsible for BWS and the development of BWS-associated Wilms tumors. A similar situation is seen with respect to *WT1* mutations and DDS and WAGR syndromes. It is also possible that the *BWS/WT2* locus may represent another contiguous gene syndrome similar to the WAGR syndrome locus. Although the gene(s) responsible for Wilms tumor and BWS at this locus have not yet been identified, the locus has been named *WT2*.

1.3.2.2 The WT2 region is imprinted

Interestingly, LOH of 11p15 is found to exclusively involve the maternal chromosome suggesting that this region may be imprinted (Schroeder et al., 1987). In fact, loss of the maternal chromosome 11p15 region and/or chromosome accompanied by constitutional duplication of the paternal 11p15 region or chromosome, resulting in the presence of 2 identical copies of the paternal chromosome region is seen in a proportion of BWS patients and Wilms tumors (Grundy et al., 1991; Henry et al., 1991). This provides strong evidence that this region is subject to genomic imprinting. The preferential loss of the maternal chromosome with duplication of the paternal chromosome is referred to as uniparental paternal disomy. There are at least 10 imprinted genes in this region that are preferentially expressed from either the paternal or maternal allele. Three of these imprinted genes, *IGF2*, *H19* and *p57*^{kip2}, have been extensively studied in Wilms tumors.

1.3.2.3 Insulin-like Growth Factor 2

Insulin-like Growth Factor 2 (*IGF2*) is an embryonal growth factor that acts as a mitogen in cultured cells and is involved in muscle growth and differentiation. In normal tissues *IGF2* is preferentially expressed from the paternal allele and is silenced on the maternal allele (Pedone et al., 1994). In Wilms tumors that exhibit chromosome 11p15 LOH, the loss of the maternal allele/chromosome is always accompanied by duplication of the paternal region/chromosome resulting in two paternal copies of *IGF2* being actively transcribed (Scott et al., 1985). Furthermore, in many tumors that do not exhibit LOH of 11p15, a phenomenon called loss of imprinting (LOI) is seen. In these instances, both the maternal and paternal *IGF2* alleles are expressed (Ogawa et al., 1993). Both of these events theoretically result in a two-fold increase in *IGF2* mRNA levels relative to tumors with no such alterations. Since *IGF2* represents a growth factor, an increase in its expression could lead to overgrowth and subsequently contribute to the development of BWS and Wilms tumor due to an increase in cell growth and proliferation.

1.3.2.4 H19

Another imprinted gene located on chromosome 11p15 believed to be involved in BWS and Wilms tumor is the *H19* gene, which encodes an untranslated mRNA, suggesting that it may act as a regulatory RNA molecule (Bartolomei et al., 1991). *H19* is imprinted in the reciprocal manner to *IGF2* and is preferentially expressed from the maternal allele (Zhang and Tycko, 1992). Therefore, unlike the doubling of expression seen with *IGF2*, loss of 11p15 due to either LOH or LOI, results in reduction of *H19* expression. This suggests that *H19* may act as a tumor suppressor in Wilms tumors unlike *IGF2* which is proposed to be a growth promoting gene. This is supported by *in vitro* studies whereby overexpression of *H19* in Wilms tumor-like and rhabdomyosarcoma cell lines suppressed cell growth and tumorigenicity (Hao et al., 1993). It has been shown that *IGF2* and *H19* are co-ordinately regulated and LOI of *IGF2* is associated with silencing of H19 and vice versa. Therefore, in many Wilms tumors loss of the tumor suppressor gene, *H19*, and gain of growth promoting gene, *IGF2*, occurs (Figure 1.3).

1.3.2.5 $p57^{KIP2}$

A third candidate imprinted Wilms tumor/ BWS gene is $p57^{KIP2}$, a cyclin-dependent kinase inhibitor preferentially expressed from the maternal allele (Matsuoka et al., 1996). Reduced or absent expression of $p57^{KIP2}$ is seen in some Wilms tumors (Hatada et al., 1996; Thompson et al., 1996). Transfection

Figure 1.3: Imprinting and the *WT2* locus. A. Normal imprint: Normally, *H19* is exclusively expressed from the maternal allele and *IGF2* is exclusively expressed from the paternal allele. **B. LOH:** When LOH of 11p15 occurs, this results in the duplication of the paternal allele which leads to an increase (doubling) of *IGF2* expression (due to the presence of two paternal alleles) and a loss of *H19* expression (due to the loss of the maternal allele). **C. LOI:** When LOI of 11p15 occurs, the maternal imprint is lost resulting in the abnormal expression of *IGF2* from the maternal allele and loss of maternal *H19* expression. This produces the same effect as LOH; a doubling in *IGF2* expression and loss of *H19* expression.

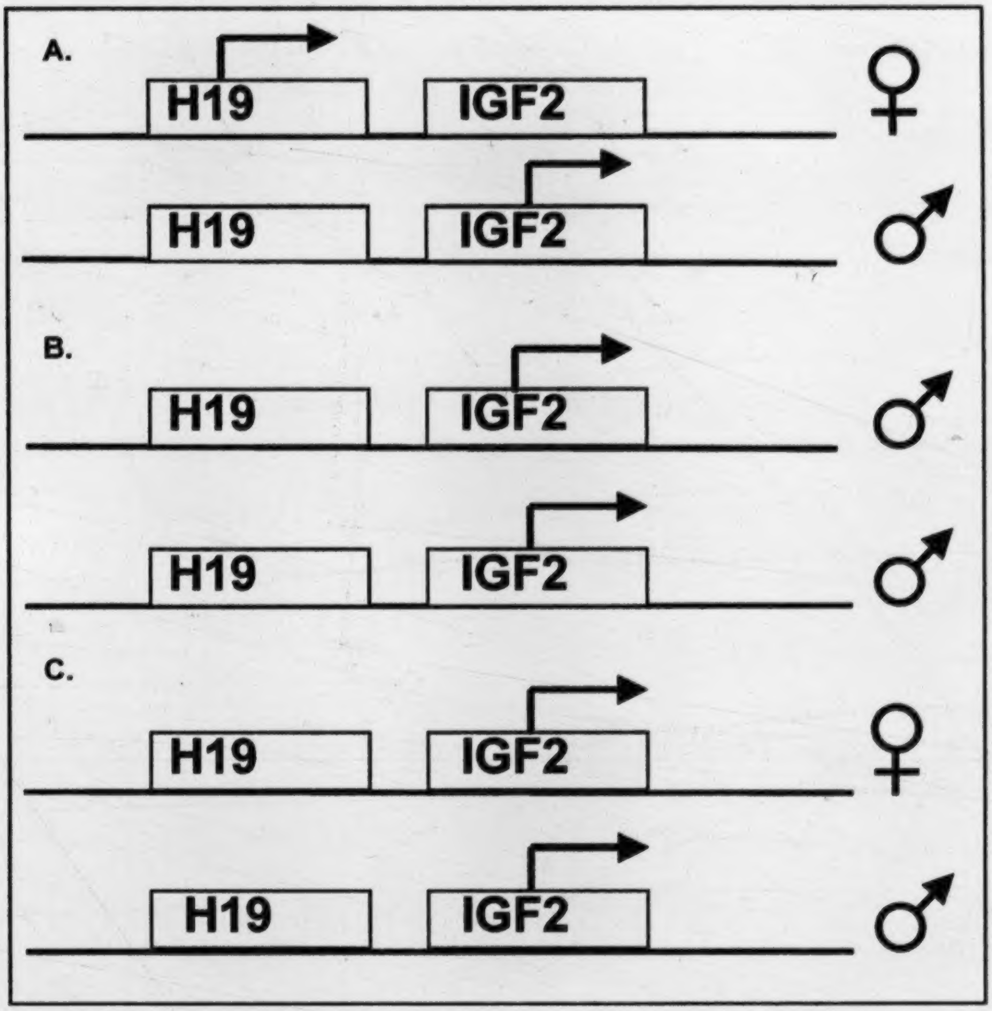
A.
H19
IGF2
♀
H19
IGF2
♂
B.
H19
IGF2
♂
H19
IGF2
♂
C.
H19
IGF2
♀
H19
IGF2
♂

of a subchromosomal fragment of 11p15 containing *p57*^{KIP2} but neither *IGF2* nor *H19* resulted in suppression of both growth and tumorigenicity suggesting that *p57*^{KIP2} also functions as a tumor suppressor gene (Koi et al., 1993). However, other Wilms tumors have been reported to express *p57*^{KIP2} equally from both the maternal and paternal alleles. Clearly, further elucidation of *p57*^{KIP2} and its involvement in Wilms tumor is needed.

Although evidence suggests an imprinted gene(s) is involved in the etiology of Wilms tumor and BWS, the exact genes and the extent of their effects is still unclear. In addition to the three imprinted genes mentioned above, there are several other imprinted genes in this region that need to be, or are in the process of being evaluated, in Wilms tumor and BWS. Figure 1.4 illustrates the chromosomal locations of the 3 imprinted candidate Wilms tumor genes with respect to *WT1*.

1.3.3 Familial Wilms tumor

The incidence of familial Wilms tumor is low comprising only 1-2% of all Wilms tumors. The familial form of the tumor is inherited in an autosomal dominant manner, with incomplete penetrance (Matsuoka, 1981). Linkage analysis has identified two distinct chromosomal regions, the first is on chromosome 17q and has been named *FWT1*, while the second loci, *FWT2*, is located on chromosome 19q (Rahman et al., 1997; McDonald et al., 1998). Surprisingly, additional families exist that do not show linkage to either of these

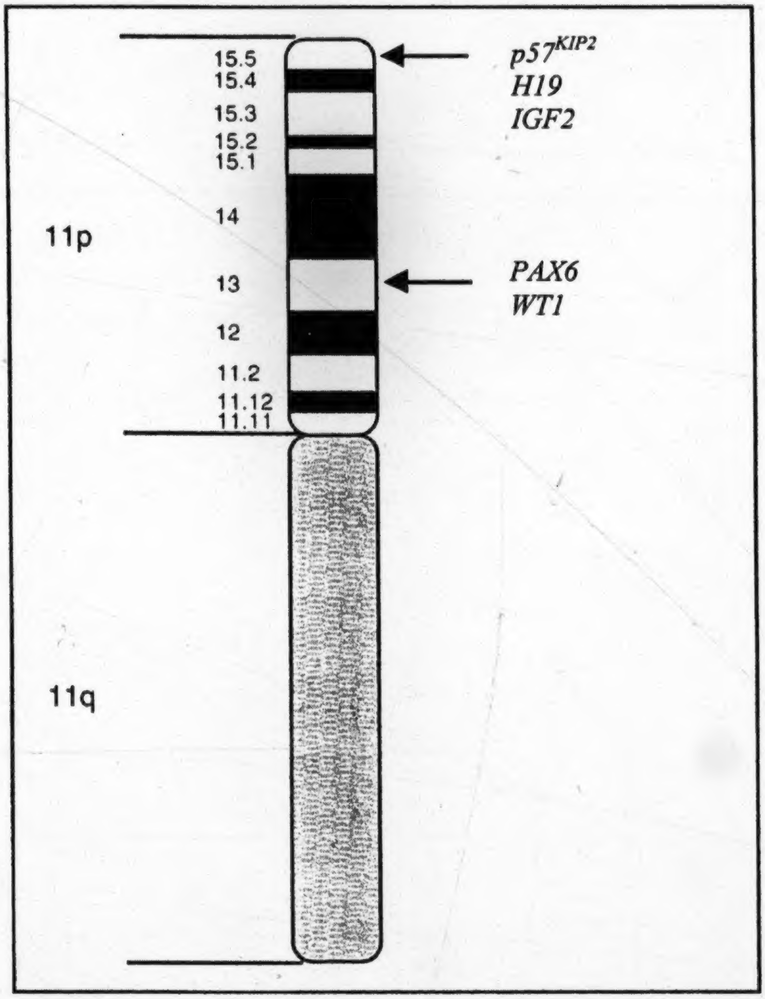
15.5
15.4
15.3
15.2
15.1
14
11p
13
12
11.2
11.12
11.11
11q
p57KIP2
H19
IGF2
PAX6
WT1

Figure 1.4: Location of genes associated with *WT1* and putative *WT2* loci. Figure taken from Coppes et al. (1994).

loci, nor do they demonstrate linkage to chromosome 11p13 or any other of the known or reported putative Wilms tumor loci, suggesting that at least a third familial Wilms tumor loci exists. Such results further emphasize the complexity and genetic heterogeneity of Wilms tumors.

1.3.4 Loss of heterozygosity in Wilms tumors

The presence of loss of heterozygosity (LOH) in tumors is associated with inactivation of a tumor suppressor gene. Therefore, LOH studies are often performed to determine: (1) if inactivation of a tumor suppressor gene is involved in the etiology of the tumor and (2) the chromosomal region where the putative tumor suppressor gene resides. Many cancers are genetically unstable and display high levels of global chromosomal loss. Wilms tumors, however, generally have a low background level of chromosomal loss with only a few, well defined chromosomal regions of LOH (Figure 1.5). In addition to the frequent LOH at chromosome 11p that occurs in approximately 40% of Wilms tumors, LOH of chromosomes 16q, 1p, 7p and 22q also occurs (reviewed in Dome and Coppes, 2002). Figure 1.6 shows the chromosomal regions believed to harbour Wilms tumor genes.

1.3.4.1 Chromosome 16q LOH

Next to chromosome 11p, chromosome 16q exhibits the highest frequency of LOH, occurring in approximately 20% of sporadic Wilms tumors. Interestingly, in some tumors a significant reduction, but not complete loss, of one allele has

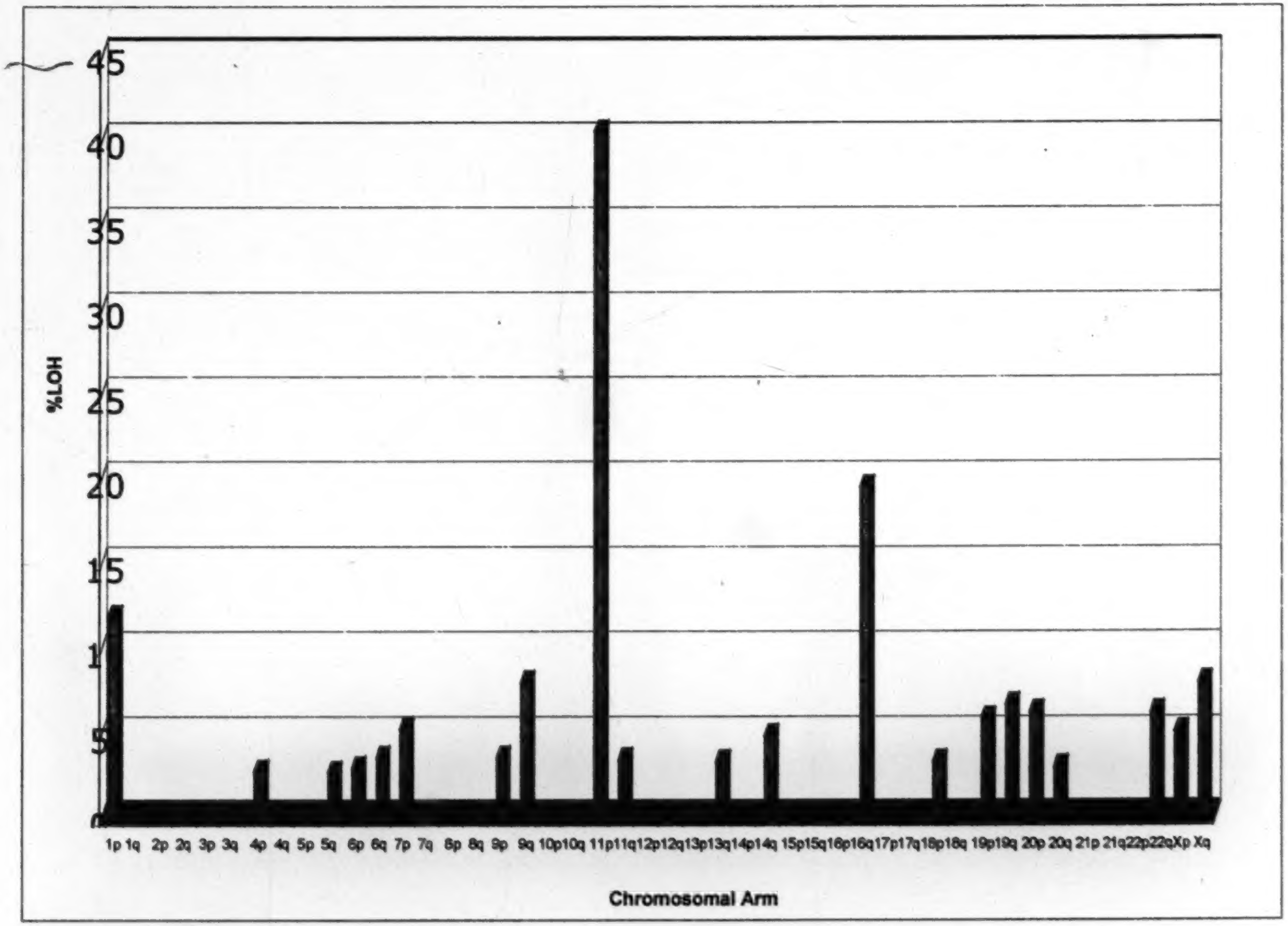

Figure 1.5: Incidence of LOH for each chromosomal arm in Wilms tumor. (Grundy, unpublished results).

Figure 1.6: Location of putative Wilms tumor genes. Pink bars to the right-hand side of each chromosome represent the regions in which Wilms tumor genes or putative Wilms tumor genes are thought to reside based on linkage and LOH studies. Ideogram adapted from the University of Washington, Department of Pathology website:

http://www.pathology.washington.edu/research/cytopages/idiograms/human/

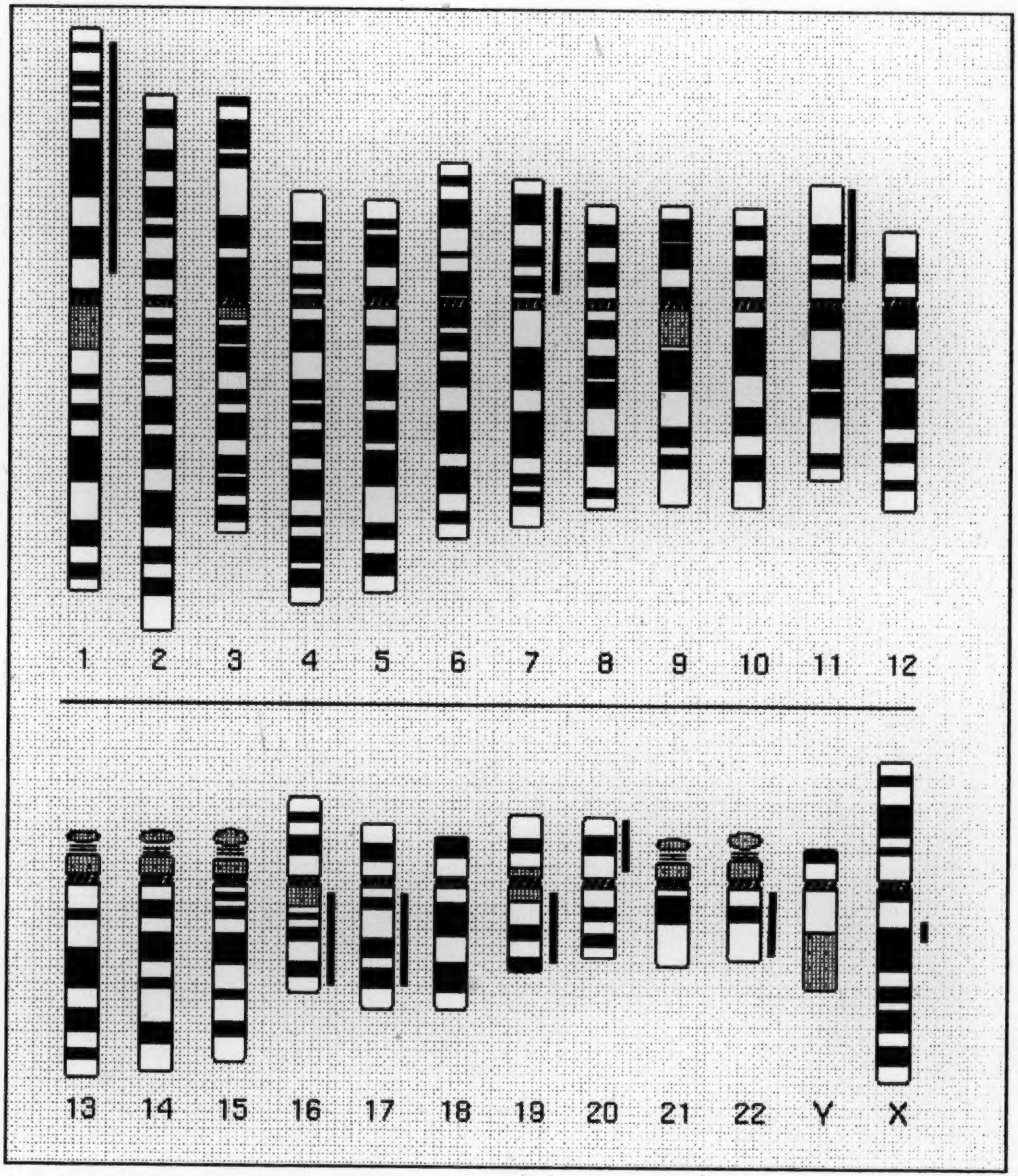
Y
X

been observed (P. Grundy, unpublished data). The presence of 16q LOH in only a subset of the tumor cells (partial loss) suggests that chromosome 16q LOH occurs after the tumor is established and may be involved in tumor progression rather than initiation. This is supported by the fact that correlation of chromosome 16q LOH with clinicopathological characteristics indicated that loss of chromosome 16q appears to be associated with a statistically significantly poorer prognosis and overall survival (Grundy et al., 1994). The minimal region of LOH has been defined to a 6.7 Mb region localized to chromosome 16q21-q24 (Stafford et al., 2003; P. Grundy, unpublished data).

1.3.4.2 Chromosome 1p LOH

Loss of heterozygosity of chromosome 1p occurs in approximately 11% of Wilms tumors (Grundy et al., 1994). The region of loss is quite large, encompassing the telomeric end and spanning half of the p arm. Analysis of clinicopathological correlations with loss of 1p reveals a slight association with adverse outcome, but not one of statistical significance (Grundy et al., 1994). Recently, data from our laboratory have shown a correlation between adverse outcome and concurrent loss of both chromosomes 1p and 16q (manuscript in preparation).

1.3.4.3 Other regions of Chromosomal LOH

Loss of heterozygosity of chromosome 7p has been found to occur in approximately 5% of Wilms tumors and is localized to chromosome 7p15-p21.

One Wilms tumor was identified that had a constitutional balanced translocation between chromosomes 1 and 7 t(1;7) (q42;p15) (Wilmore et al., 1994). However, no clinicopathological correlation studies have been performed so it is not known if loss of 7p may be involved in a certain subset of Wilms tumors. Frequent loss of chromosome 22q is also seen in Wilms tumors and often occurs together with loss of chromosomes 1p and 11q. Correlations of chromosome 22q LOH with clinicopathological characteristics revealed an association with anaplasia and relapse, similar to that found with chromosome 16q LOH (Klamt et al., 1998).

1.3.5 The p53 gene, anaplasia and Wilms tumor

The *p53* gene is the most commonly mutated gene in human cancers. Defects in this gene are found in over 50% of adult cancers but occur to a lesser extent in childhood cancers (Hollstein et al., 1991). Mutation analysis of *p53* in Wilms tumors found that 4% of tumors had a mutated *p53* allele. Interestingly, the presence of a *p53* alteration correlated with tumors with both focal and diffuse anaplastic histology. Further evaluation of *p53* in Wilms tumors revealed that *p53* mutations were present in 75% of anaplastic Wilms tumors but occurred rarely in favorable histology tumors (Malkin et al., 1994; Bardeesy et al., 1995.). These results suggest that acquisition of a *p53* mutation may be a prerequisite for the development of anaplastic tumors which are associated with poor prognosis and outcome.

1.4 Simpson-Golabi-Behmel Syndrome (SGBS)

SGBS is a congenital overgrowth syndrome that shares considerable phenotypic overlap with BWS and was first described by Simpson et al. (1975). SGBS is a recessive X-linked disease, predominantly found in males. It has been estimated that approximately 50% of affected males die at birth or shortly thereafter (Neri et al., 1988). A subset of females are affected with a less severe form of the disease and often act as carriers of the disease due to the presence of one normal copy of the X chromosome. The incidence of SGBS is not known due to its low frequency and the difficulties in accurately diagnosing and distinguishing the disease from other overgrowth syndromes including BWS and Perlman syndrome (Verloes et al., 1995).

Diagnosis of SGBS is based on clinical manifestations; however, due to the phenotypic overlap between SGBS and BWS, misdiagnosis can occur. Individuals with BWS or SGBS are both characterized by coarse facial features, macroglossia, umbilical hernias, visceromegaly, and congenital hypotonia. In addition to these characteristics, supernumerary nipples, skeletal defects, diaphragmatic defects, congenital heart defects and polydactyly are unique to SGBS, while hemihyperplasia, facial nevus flammeus, ear pits/creases and the increased risk of other childhood tumors are characteristics specific to BWS patients (Verloes et al., 1995). Interestingly, individuals with either syndrome are predisposed to developing Wilms tumor (reviewed in DeBaun et al., 2001). It is unclear whether this syndrome causes mental retardation as individuals with severe SGBS usually display a mild form of mental retardation while IQ scores from individuals with a milder form of SGBS range from low-normal to normal. At present no molecular diagnostic tests are available for diagnosing SGBS versus BWS, although the development of such tests would be beneficial for accurate diagnosis.

1.4.1 Glypican 3 (GPC3)

Linkage analysis of a Dutch-Canadian family initially localized the SGBS gene to chromosome Xqcen-q21 (Hughes-Benzie et al. 1992). The location was redefined by the same group to chromosome Xq25-q27 aided by the presence of a recombination event in one of the SGBS families (Xuan et al., 1994). The gene responsible for SGBS was identified using a positional cloning approach by Pilia et al. (1996) using a cell line derived from an individual misdiagnosed with BWS carrying a *de novo* X;1 translocation. They found that the translocation breakpoint in this individual disrupted a gene called Glypican 3 (*GPC3*). A second individual presenting with an overgrowth syndrome and a X;16 translocation was also found to have a disruption of the *GPC3* gene. These individuals were rediagnosed with SGBS and it was proposed that *GPC3* represented the SGBS gene. Three additional SGBS families were evaluated for defects in the *GPC3* gene and it was found that these SGBS individuals contained deletions within the *GPC3* gene. An extensive analysis and characterization of the *GPC3* gene in SGBS families was performed by Huber et al. (1997).

Surprisingly, the infantile, lethal form of SGBS was found, by linkage analysis, not to map to chromosome Xq26 but rather to Xp22 (Brzustowicz et al., 1999). The gene responsible for this variant form of SGBS is not yet identified due to the limited number of families available for analysis but the critical gene region has been localized to a 6 cM region between markers DXS8022 and DXS1195. The identification of this second SGBS locus may also explain the phenotypic variation seen in SGBS patients as defects in the gene at Xp22 either by itself or in combination with *GPC3* may be necessary for the severe form of the disease.

1.4.2 GPC3 Expression

GPC3 is widely expressed during development and is particularly highly expressed in mesodermal tissue. However, its expression in adult tissue is limited to placenta, lung, ovary, small intestine and colon (Pilia et al., 1996). No *GPC3* expression has been found in either fetal or adult brain or blood (Filmus et al., 1995; Pilia et al., 1996). *In situ* hybridization led to the discovery that expression of *GPC3* peaks around 11.5-14.5 days post coitum (dpc) in mice and is predominantly expressed in mesoderm and mesoderm-derived tissues including somitic, intermediate and lateral mesoderm and their derivatives (Pellegrini et al., 1998). With respect to the developing kidney, *GPC3* is only expressed in the mesenchyme components. Based on expression studies it can be proposed that *GPC3* may be an important modulator of the growth of many tissues and organs and may be important during development. Since *GPC3* is expressed in many tissues, this may also explain why a large spectrum of phenotypic variability is seen amongst SGBS patients as the type of mutation and the extent to which GPC3 function is altered may depend on the tissue and/or stage of development.

1.4.3 GPC3 Mutations

GPC3 localizes to chromosome Xq26 and is a large gene comprised of 8 exons spanning approximately 500 kb producing a 2.2 kb transcript and 80 kDa protein. Both deletions and point mutations of the *GPC3* gene have been identified in SGBS patients with approximately 50% of mutations identified as deletions within exon 8 of *GPC3* (Veugelers et al., 1998, Veugelers et al., 2000). The *GPC3* exonic deletions either interfere with the start codon or introduce a premature stop codon resulting in an unstable, truncated or absent GPC3 protein. The point mutations vary from nonsense and frameshift mutations to splice-site mutations, all of which create premature stop codons within the transcript, resulting in protein truncation (Veugelers et al., 2000). All of the mutations that give rise to the SGBS phenotype are true loss of function mutations that give rise to the SGBS phenotype.

Hemizygous *GPC3* knock-out mice display several SGBS clinical characteristics including perinatal death, developmental overgrowth, cystic and dysplastic kidneys, abnormal lung development as well as imperforate vagina and mandibular hypoplasia, two features not found in SGBS (Cano-Gauci et al., 1999). The *GPC3* hemizygous male mice are viable *in utero* but die prior to weaning. The *GPC3* deficient mice also show an increased rate of epithelial cell proliferation in the ureteric bud and collecting systems suggesting that *GPC3* may act as a negative regulator of cell proliferation (Cano-Gauci et al., 1999).

1.4.4 Proteoglycans: Syndecans and Glypicans

Proteoglycans are proteins composed of long, unbranched chains of polysaccharides (sugar polymers and glycosaminoglycans) that are covalently bound to serine residues of the protein core. Proteoglycans are major components of the extracellular matrix and are involved in the formation of cartilage, connective tissue and basement membranes. Proteoglycans are also commonly found on the surface of cells (Bernfield et al., 1999). The two most predominant groups of cell surface proteoglycans are the syndecans and the glypicans (Bernfield et al., 1999). Syndecans are a family of transmembrane molecules containing a short carboxy-terminal cytoplasmic domain that links to serine residues distal from the plasma membrane. Conversely, glypicans, which are part of the heparan sulfate proteoglycan sub-family, attach to the exocytoplasmic surface of the plasma membrane via a glycosyl-phosphatidylinositol (GPI) anchor (reviewed in Grisaru and Rosenblum, 2001; Song and Filmus, 2002).

1.4.5 Glypican Structure

To date, 6 mammalian glypican genes, *GPC1-6,* have been identified. Two *Drosophila* glypican genes, *Dally1* and *Dally-like* have also been identified and have been key in elucidating glypican function (Baeg et al., 2001; Nakao et al., 1995). Glypicans have been found to cluster on different chromosomal regions. *GPC3* and *GPC4* are located on chromosome Xq26 while *GPC5* and *GPC6* are found on chromosome 13q31-q32 (Saunders et al., 1997; Veugelers et al., 1998; Veugelers et al., 2000). This clustering of genes suggests that the glypican family arose from gene duplication.

Glypicans belong to the heparan sulfate proteoglycan (HSPG) family which have been implicated in cell adhesion, proliferation, motility, differentiation and morphogenesis (Perrimon and Bernfield, 2000). Glypicans consist of a protein core of approximately 50-60 kDa in size, to which two heparan sulfate chains are attached. The protein cores of glypicans and other HSPGs display a considerable degree of variation allowing them to be involved in many different biological processes. The protein cores of glypicans share between 20-50% homology with GPC3 and GPC5 showing the highest degree of similarity. (Grisaru and Rosenblum, 2001).

1.4.6 Glypican Function

Glypicans act as regulators of growth factor signaling during development as illustrated by the fact that cell surface heparan sulfate is necessary for fibroblast growth factor (FGF) signaling *in vitro*. Functional studies using the *Drosophila* glypican homolog gene, *division abnormally delayed* (*dally*) found that *Dally* mutants had cell division abnormalities in the larval brain, eye, wing, antenna and genitalia suggesting a role for *dally* in cell division patterning and morphogenesis (Nakato et al., 1995).

Although the exact function of GPC3 is not known, it is believed to have similar functions as the other glypican family members and be involved in: (1) regulation of growth factor signaling; (2) cell-cell recognition and (3) cell-matrix adhesion. In addition to these, a role for GPC3 in cell proliferation and apoptosis has been identified (Gonzalez et al., 1998). It has been shown that GPC3 can induce apoptosis in a cell line-specific manner. This suggests that inactivating mutations of *GPC3* could prevent apoptosis in certain cell types. This could provide an explanation for some of the phenotypic characteristics such as syndactyly seen in SGBS patients (Gonzalez et al., 1998). Therefore, GPC3 has also been proposed to be a negative regulator of cell proliferation.

1.4.7 GPC3 and IGF2 Interactions

Several studies have come forth discussing, with much debate, the possible relationship between GPC3 and IGF2. In individuals with BWS and BWS-associated Wilms tumor, overexpression of IGF2 is thought to contribute to the overgrowth phenotype of BWS and development of Wilms tumor. It has been suggested that GPC3 is a negative regulator of IGF2, which competes with the IGF2 receptor for IGF2 binding. Therefore, defects in GPC3 could prevent it from binding IGF2, which would lead to an excess of unbound IGF2, resulting in overexpression of IGF2 (Weksberg et al., 1996). This is supported by studies in mice over-expressing IGF2 which display characteristics similar to BWS and

SGBS including skeletal defects which are unique to individuals with SGBS (Eggenschwiler et al., 1997). However, Song et al. (1997) were unable to show that GPC3 directly binds to IGF2 *in vitro*. Furthermore, it has been shown that IGF2 levels in the serum, liver, kidney and lung of *GPC3* deficient mice are similar to IGF2 levels in wild type mice. If GPC3 were a negative regulator of IGF2, higher levels of free IGF2 would be expected in the *GPC3* deficient mice. An increase in IGF2 serum levels are seen in *IFG2 receptor* deficient mice. It is possible that GPC3 interacts with the IGF2 pathway indirectly and regulates cell proliferation using a pathway independent of IGF2. The relationship of GPC3 and IGF2 and whether or not they interact directly, indirectly or not at all is still a question that remains unanswered.

1.4.8 GPC4 – A contiguous gene syndrome?

One hundred and twenty kilobase pairs centromeric to the 3' end of *GPC3* is another glypican gene called *GPC4* (Veugelers et al., 1998; Huber et al., 1998). Unlike *GPC3*, *GPC4* displays high expression in fetal lung and kidney and is widely expressed in adult tissues (Huber et al., 1998; Veugelers et al., 1998). In addition to analysis of the *GPC3* gene, mutation analysis of *GPC4* in some SGBS patients has been performed. Several SGBS individuals were identified with large deletions within the *GPC3* gene that also included part or all of the *GPC4* gene. However, no mutations confined to the *GPC4* gene were identified indicating that disruption of this gene does not cause SGBS, although it is possible that its disruption together with loss of *GPC3* function may contribute to the phenotypic variability seen in the SGBS syndrome. It has been proposed that disruption of *GPC4* may contribute to the mental retardation and abnormalities of the central nervous system as *GPC4*, but not *GPC3*, is expressed in the brain (Veugelers et al., 1998; Veugelers et al., 2000). However, further research into this association needs to be explored.

Studies in mice support an association between *GPC4* and certain characteristics of the SGBS phenotype as loss of expression of *GPC4* in the adrenal gland, kidney and facial mesenchyme may give rise to some of the phenotypic features of SGBS including neuroblastoma, Wilms tumor, renal tract abnormalities and coarse facies respectively (Watanabe et al., 1995; Veugelers et al., 1998). However, it can be argued that some SGBS patients with mutations exclusively within *GPC3* also exhibit some of the above phenotypic traits, including Wilms tumor and renal tract abnormalities. Therefore, further evaluation of both the *GPC3* and *GPC4* genes in SGBS patients together with correlation to the clinicopathological phenotype is warranted to better understand the role of these genes in SGBS.

With the phenotypic variation of SGBS ranging from asymptomatic carriers to a lethal infantile form in some hemizygous males, the identification of at least two SGBS loci and the absence of *GPC3* or *GPC4* mutations in some SGBS patients, there is still much to be learned about the genetics and biochemistry of SGBS. Identification and mutational analysis of the putative gene on chromosome Xp22 would provide further insight into whether defects in this gene are responsible for the severe and often lethal form of this syndrome or if it works as part of a pathway together with *GPC3* and possibly *GPC4*.

1.4.9 GPC3 and cancer

Individuals with SGBS are predisposed to developing Wilms tumor and neuroblastoma; however, the frequency of tumors is low (DeBaun et al., 2001). It has been proposed that a cancer screening program for SGBS individuals, similar to that recommended for BWS patients, would be beneficial for early cancer detection and treatment of SGBS patients. The association between SGBS and Wilms tumor was first reported by Hughes-Benzie et al. (1992) who described two SGBS individuals from a Dutch-Canadian family with renal dysplasia and Wilms tumor. A study by Li et al. (2001) identified deletions within *GPC3* exons 1-3 in SGBS patients with Wilms tumors suggesting a possible association between *GPC3* and Wilms tumor.

Recently, a study by White et al. (2002) reported *GPC3* mutations in 2/41 (4.9%) Wilms tumors. One mutation was a tumor specific C → T transition mutation in exon 3 at position 558, while the second was a tumor specific G → A transition mutation at position 1902 in exon 8. Investigators proposed that disruption of *GPC3* may be involved in the initiation and/or progression of some Wilms tumors. Furthermore, Saikali and Sinnett (2000) used differential display PCR to identify differentially expressed genes in Wilms tumor and neuroblastoma, identified *GPC3* which was found to be up-regulated in several neuroblastomas, and all Wilms tumors tested. Studies by Toretsky et al. (2001)

also identified high levels of *GPC3* expression in Wilms tumors and hepatoblastomas as compared to normal kidney. Further research is needed to define the role of *GPC3* in Wilms tumor and other cancers.

GPC3 is silenced in numerous adult cancers including ovarian, breast and malignant mesothelioma (Lin et al., 1999; Murthy et al., 2000; Xiang et al., 2001). Lin et al. (1999) reported that aberrant promoter hypermethylation silenced *GPC3* in 4/13 (31%) ovarian cancer cell lines as compared to the normal controls which were unmethylated. Furthermore, chromosome Xq26 LOH is found in approximately 30% of ovarian tumors suggesting that *GPC3* may represent an ovarian cancer tumor suppressor gene. Similarly, reduced and/or absent *GPC3* RNA has been found in malignant mesothelioma cell lines and primary tumors (Murthy et al., 2000). Aberrant promoter hypermethylation was found in the majority, but not all of tumor samples evaluated, suggesting that *GPC3* may play a role in the development of malignant mesothelioma. However, promoter hypermethylation is likely not the only mechanism of *GPC3* gene inactivation occurring in this cancer. In studies involving hypermethylated GPC3, expression could be restored by treatment with the demethylating agent 5-aza-2'-deoxycytidine in most cases.

In situ hybridization was performed on 12 primary breast cancer samples and it was found that *GPC3* was reduced or absent in the tumor cells as compared to normal breast epithelium (Xiang et al., 2001). Furthermore, although the sample size was small, a correlation between degree of *GPC3* expression and tumor stage was found. As in the previous studies, the *GPC3* promoter was hypermethylated and treatment of breast cancer cell lines with the demethylating agent, 5-aza-2'-deoxycytidine, restored *GPC3* expression in all cell lines evaluated. The lack of *GPC3* RNA and the presence of aberrant promoter methylation in ovarian, breast and malignant mesothelioma suggest that *GPC3* may act as a negative regulator in these cancers and may represent a putative tumor suppressor gene.

GPC3 has also been found to be overexpressed in hepatocellular carcinoma (HCC) and may represent an early detection marker for HCC (Hsu et al., 1997; Hippo et al., 2004). Elevated levels of a soluble NH_2-terminal GPC3 protein fragment were detected in individuals with early stage HCC as well as in individuals with liver cirrhosis who were at risk of developing HCC. Interestingly, those individuals with liver cirrhosis later went on to develop HCC within 6 months of testing positive for *GPC3.* These results indicate that *GPC3* could be a useful early detection HCC marker, increasing detection sensitivity from 50% to 72% when used in combination with the current detection marker, α-fetoprotein, (Hippo et al., 2004).

In summary, *GPC3* may play a variety of roles in tumorigenesis. It is silenced in malignant mesotheliomas, breast and ovarian cancers as compared to their normal counterparts and may contribute to the tumorigenic phenotype in some cases. Conversely, expression of *GPC3* is seen in some Wilms tumors, neuroblastomas and HCC as compared to normal, mature kidney. While *GPC3* expression in Wilms tumor and neuroblastoma is likely attributed to the fact that these are embryonal tumors and are more representative of a fetal-like tissue, *GPC3* expression in HCC may represent an oncofetal protein.

1.5 The cadherin gene family

Cadherins belong to a large family of evolutionarily conserved cell adhesion molecules involved in calcium-dependent, homotypic cell-cell adhesion. Not only are cadherins important in the establishment and maintenance of cell-cell adhesion, but they have also been implicated in development, cell polarity, cytoskeletal organization and tumorigenesis (reviewed in Angst et al., 2001). Cadherins are prevalent in vertebrates but have also been identified in *Droshophila* and *C. elegans*. The cadherin superfamily can be divided into at least 8 different cadherin sub-families which include: (1) Classical cadherins (type I and II); (2) Fat-like cadherins; (3) Seven-pass transmembrane; (4) Desmosomal cadherins; (5) Protocadherins; (6) Protein kinase cadherins; (7) Dcad 102F-like cadherins; (8) 7D-cadherins (Tepass et al., 2000). The majority of the cadherin superfamily members are transmembrane proteins; however, there are some exceptions like T-cadherin, which binds to the cell membrane via a GPI-linkage (Wheelock and Johnson, 2003).

1.5.1 Cadherin structure

All of the cadherin superfamily members share similar regions of homology, the most common being the presence of a calcium-binding region in the extracellular domain. This extracellular domain is evolutionarily conserved and comprised of varying numbers (5-34) of negatively charged calcium binding domains (DXDN, DXD, LDRE) (Shapiro et al., 1995). However, the cytoplasmic regions of cadherin family members are quite diverse, allowing for their ability to interact specifically with their intracellular partners thus enabling their tissue and cell type specificity.

1.5.2 Classical cadherins

The best characterized cadherins are those that belong to the classical cadherin family and include E-cadherin, N-cadherin, VE-cadherin and P-cadherin. Classical cadherins, although the best characterized, represent a small proportion of the total number of cadherin family members. The first cadherin described was E-cadherin, identified in 1983 (Peyreias et al., 1983) followed by the cloning of N-cadherin in 1987 (Hatta et al., 1987). Classical cadherins mediate homophilic cell-cell adhesion via interaction with the actin cytoskeleton within the adherens junctions in normal epithelium (Ozawa et al., 1989). The His-Ala-Val (HAV) amino acids and flanking residues, present in the extracellular domain are thought to contribute to homophilic cell-cell adhesion seen in classical cadherins (Shapiro et al., 1995). Cell-cell adhesion, in the presence of calcium, occurs through the interactions of the five extracellular calcium-binding repeats present in classical cadherins with extracellular domains of adjacent cadherin molecules forming a molecular zipper (Nagar et al., 1996) (Figure1.7). Classical cadherins are linked to the actin cytoskeleton via interaction with catenin molecules, which belong to the armadillo family of

Figure 1.7: Cadherin mediated cell-cell adhesion. The N-terminal calcium binding repeats of E-cadherin form a homotypic, intracellular molecular zipper in the presence of calcium. The E-cadherin cytoplasmic tails form stable complexes with the actin cytoskeleton via the interactions with various proteins from the armadillo family of proteins (catenins). The cytoplasmic tail of E-cadherin can bind to β-catenin and γ-catenin which in turn binds to α-catenin. α-catenin can either indirectly, via α-actin, or directly bind to the actin cytoskeleton, stabilizing the interactions. Figure adapted from Haijra and Fearon (2002).

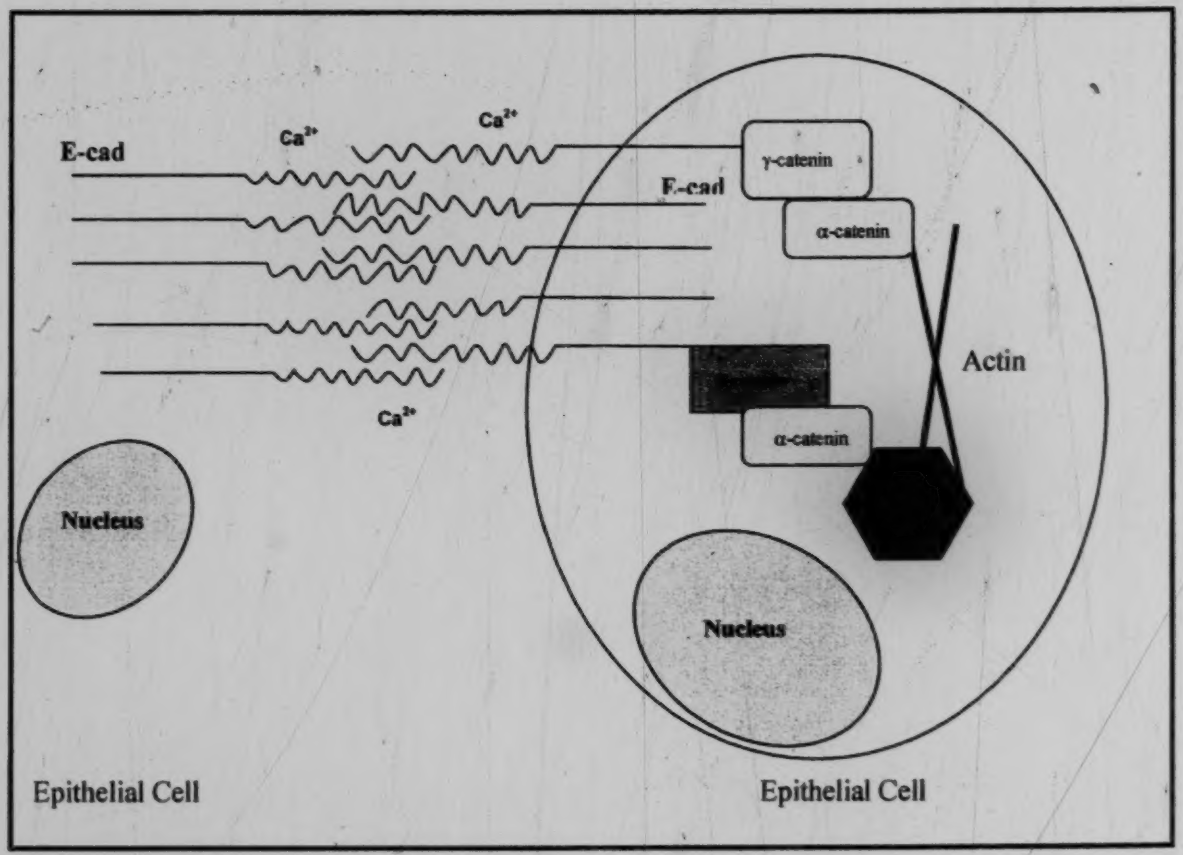
E-cad
Ca^{2+}
Ca^{2+}
E-cad
γ-catenin
α-catenin
Actin
Ca^{2+}
α-catenin
Nucleus
Nucleus
Epithelial Cell
Epithelial Cell

proteins. The cytoplasmic domain of cadherins bind to β- or γ-catenin which subsequently bind to α-catenin which in turn is bound to the actin cytoskeleton (Yap et al., 1997). It is thought that disruption of cadherin-catenin interactions leads to reduced cell adhesiveness and a cancer-promoting environment (Figure 1.8). It has been shown that mutations within the N-terminus extracellular binding domain or disruption of the cytoplasmic, catenin binding domain compromise cell-cell adhesiveness (reviewed in Hirohashi, 1998). It has been proposed that loss of cadherin function may also allow for the separation of cancer cells from the primary cancer site and is thus associated with metastasis.

1.5.3 Other cadherin sub-families

Desmosomal cadherins have an extracellular domain similar to that found in the classical cadherins. However, their cytoplasmic domain differs allowing for attachment to the intermediate filament network (Troyanovsky et al., 1994). Protocadherins contain structurally diverse calcium-dependent cell adhesion molecules that are preferentially expressed in the central nervous system and regulate neural cell-cell adhesion (Sano et al., 1993). T-cadherins are similar to classical cadherins with 5 extracellular domains; however, they bind to the cell membrane via a GPI-anchor (Wheelock and Johnson, 2003). Fat-like cadherins are named for the presence of a large number (19-34) of calcium-binding domains (Yagi and Takeichi, 2000). Seven-pass transmembrane cadherins pass through the membrane seven times and have an extracellular domain comprised of 8-9 cadherin repeats. In addition, these cadherins also have an LG (laminin)

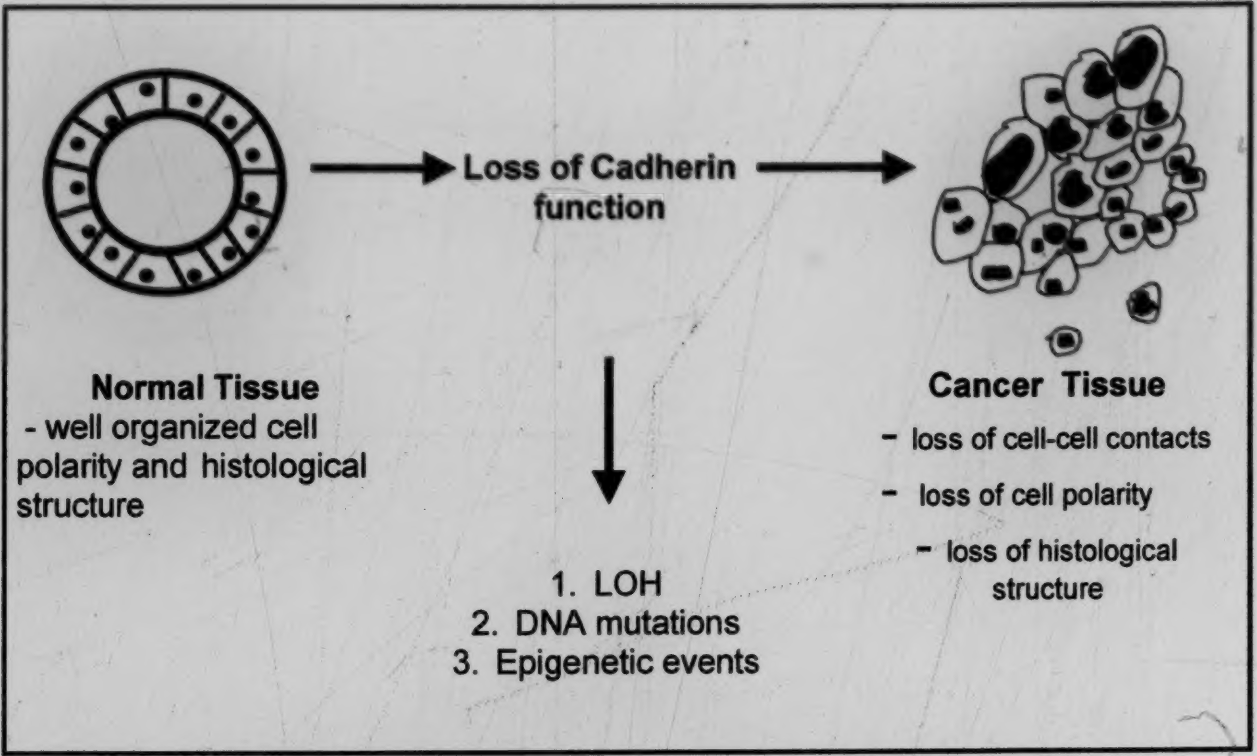
Loss of Cadherin function
Normal Tissue
- well organized cell polarity and histological structure
1. LOH
2. DNA mutations
3. Epigenetic events
Cancer Tissue
- loss of cell-cell contacts
- loss of cell polarity
- loss of histological structure

Figure 1.8: Cadherins and tumorigenesis. Loss of cadherin function via LOH, mutation or epigenetic events results in loss of cell contacts, polarity and histological structure, which can contribute to tumorigenesis. Figure adapted from Hirohashi (1998).

domain, an EGF (epidermal growth factor) domain and a flamingo box (Tepass et al., 2000). Protein kinase cadherins are comprised of 2 cadherin-binding domains and a cytoplasmic tyrosine kinase domain while Dcad 102F-like cadherins are a novel, evolutionarily conserved group comprised of 2 cadherin-binding domains and an LG domain (reviewed in Tepass et al., 2000; Yagi and Takeichi, 2000). The 7D-cadherins contain 7 cadherin-binding domain repeats and have a short cytoplasmic tail that does not interact with catenins or the actin cytoskeleton (Wong et al., 2003). Figure 1.9 illustrates the structure of the various cadherin families outlined above. The remainder of this discussion will focus mainly on the classical and 7D-cadherins.

1.5.4 Cadherin inactivation in cancer

The best characterized cadherin is E-cadherin, silencing of which occurs in a variety of human cancers. Both somatic and germline mutations of *E-cadherin* are common with germline mutations being found in patients with diffuse-type gastric (Gayther et al., 1998; Guilford et al., 1998), colorectal, prostate and breast cancers, and somatic mutations being identified in those cancers as well as endometrial and signet-ring cell type gastric cancers (Gayther et al., 1998; Guilford et al., 1998; Keller et al., 1999, Richards, 1999; Becker et al., 1994; Berx et al; 1996). E-cadherin is expressed in favorable histology, well differentiated cancers, but not in unfavorable, undifferentiated, invasive cancers, suggesting that inactivation of E-cadherin and the associated loss of cell-cell contacts may predispose the cell to a more invasive phenotype. The majority of

Figure 1.9: Schematic diagram of 9 of the cadherin subfamilies. (1) Classical cadherins; **(2)** 7D-cadherins; **(3)** Desmosomal cadherins; **(4)** Fat-like cadherins; **(5)** Protein kinase cadherins; **(6)** Protocadherins; **(7)** Seven-pass transmembrane cadherins; **(8)** Dcad102-like cadherins; **(9)** T-cadherin. Yellow blocks represent calcium binding repeats; PM = plasma membrane. Adapted from Yagi and Takeichi, 2000).

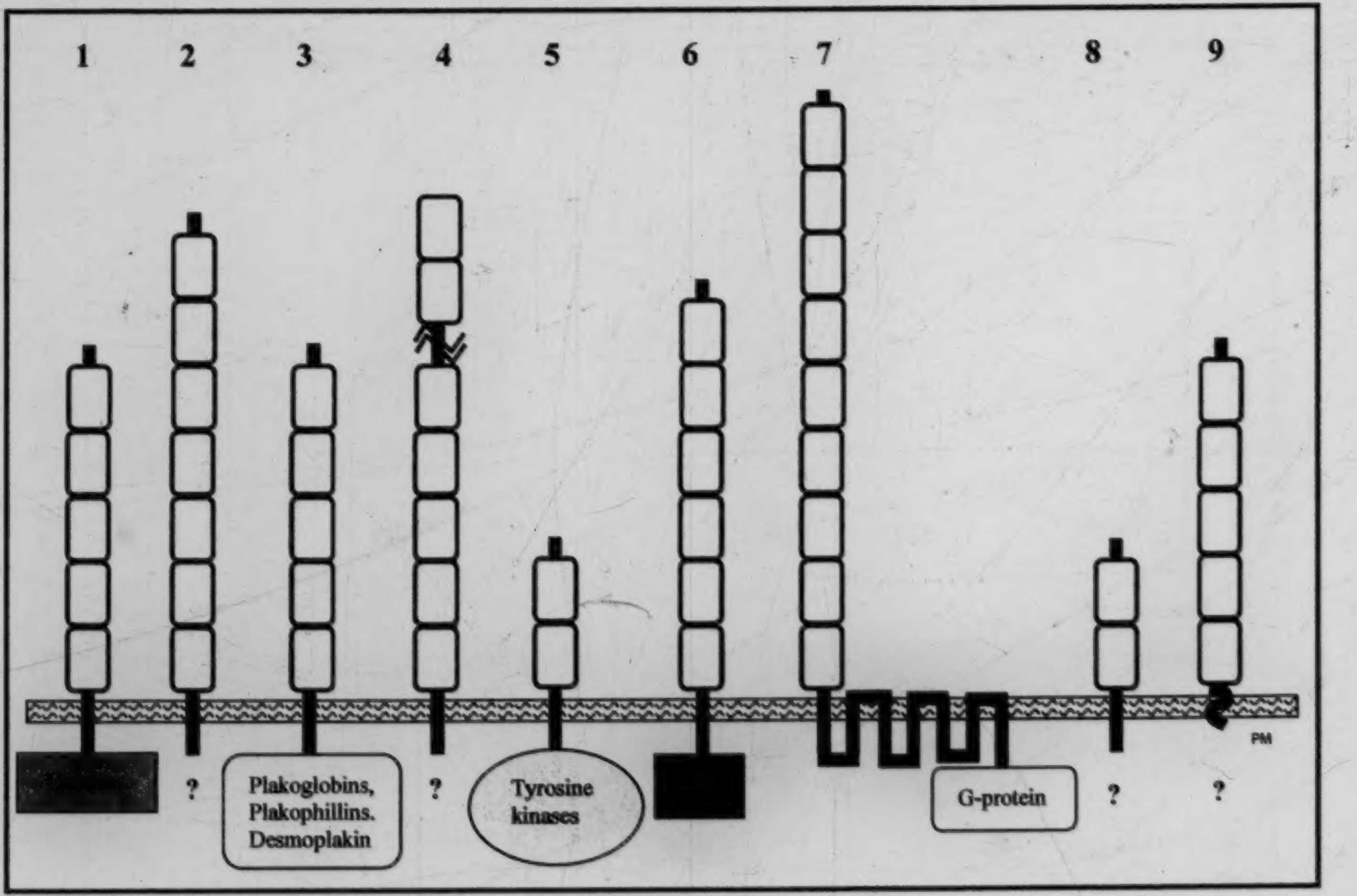
1
2
3
4
5
6
7
8
9
?
Plakoglobins, Plakophillins. Desmoplakin
?
Tyrosine kinases
G-protein
?
?
PM

mutations identified in the E-cadherin gene include exon skipping, in-frame and frame-shift deletions/insertions and point mutations, many of which arise between exons 6 to 10. E-cadherin seems to function as a recessive gene as cell lines with one inactivated E-cadherin allele are normal, while cell lines in which both E-cadherin alleles are inactivated have a tumorigenic-like phenotype (Berx et al., 1998). Furthermore, many cancers exhibit chromosomal LOH in regions where several cadherin genes reside. For example, chromosome 16q LOH is associated with many cancers including Wilms tumor, breast cancer, hepatocellular carcinoma and prostate cancer (Maw et al., 1992; Doggett et al., 1995; Nishida et al., 1992; Cher et al., 1995). Interestingly, this chromosomal region harbours 8 cadherin genes (Figure 1.10). Chromosome 18q LOH, which is seen in gastric and colorectal cancers, adenocarcinoma and head and neck squamous cell carcinoma, contains 4 cadherin genes and chromosome 5p LOH, which is found in sporadic colorectal cancer contains 4 cadherin genes (Jones et al., 1997; Xu et al., 2003).

In addition to gene mutation, epigenetic events such as promoter hypermethylation have been documented in several cadherin genes in cancer. Evidence of E-cadherin promoter hypermethylation has been found in cancer cell lines and primary breast, prostate, gastric and thyroid tumors (Graff et al., 1995; Yoshiura et al., 1995; Tamura et al., 2000). Furthermore, treatment of hypermethylated cancer cell lines with 5-aza-cytidine, a demethylating agent, has been shown to restore E-cadherin expression and reverse the tumorigenic phenotype in some cell lines. E-cadherin promoter hypermethylation has been

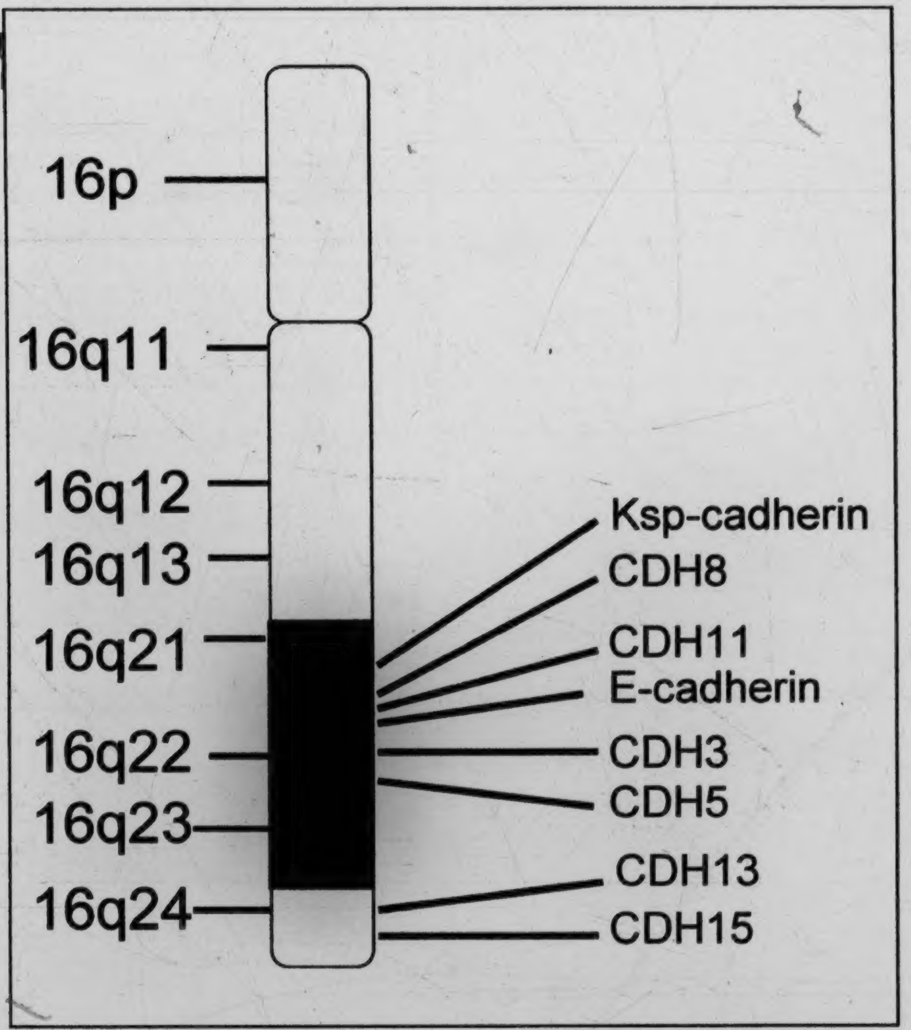
16p
16q11
16q12
16q13
16q21
16q22
16q23
16q24
Ksp-cadherin
CDH8
CDH11
E-cadherin
CDH3
CDH5
CDH13
CDH15

Figure 1.10: Cadherin genes localize to the minimal region of chromosome 16q LOH. The shaded blue region represents the 6.7 Mb minimal region of LOH identified in Wilms tumors shown in blue and the list of cadherin genes in order shown on the right. Note that 6 of the cadherin genes, including *Ksp-cadherin*, localize within the minimal region of LOH.

shown to be the mechanism of allele inactivation in cancers in which one allele is already inactivated. This suggests that aberrant gene promoter hypermethylation is another mechanism of gene inactivation. Other epigenetic events such as dysregulation of cadherin transcriptional regulators and chromatin condensation have also been reported to contribute to gene silencing but their incidence and extent are unknown (Hajra and Fearon, 2002; Hirohashi, 1998). It is likely that these three events are not mutually exclusive but rather occur together with or as a result of one or more of these mechanisms.

1.5.5 Cadherin Switching

It has been shown that loss or disruption of cadherin function causes a reduction in cell-cell adhesiveness, which may lead to tumor growth, invasiveness or metastasis. Evidence suggests that cadherin switching, defined as the inappropriate expression of cadherins in tissues where they are normally silenced, may also contribute to carcinogenesis. It has recently been demonstrated that loss of E-cadherin expression coincides with the upregulation of N-cadherin in some invasive tumors and cell lines from gastric signet ring carcinoma, breast and prostate cancers (Shibata et al., 1996; Tomita et al., 2000; Nieman et al., 1999). Overexpression of N-cadherin in a squamous tumor cell line resulted in cells that were more motile and invasive and metastatic when transfected into mice (Nieman et al., 1999 and reviewed in Hazan et al., 2004). It has been proposed that inappropriate cadherin expression could be responsible for a switch from epithelial tumors to more invasive mesenchymal tumors.

Furthermore, it has been suggested that inactivation of cadherins may not represent the primary event for tumor progression or invasiveness in some cancers but rather may represent the first step of initiation which is then followed by a switch in cadherin expression that may lead to tumor progression and invasiveness. Additional transfection studies have found that overexpression of N-cadherin in E-cadherin expressing cell lines did not cause a reduction in E-cadherin but did cause cells to change to a more invasive phenotype (Hazan et al., 2000). Similarly, overexpression of E-cadherin in a N-cadherin-expressing tumor cell line did not reduce N-cadherin expression nor did it reduce the invasive potential of the cells. This suggests that aberrant expression of N-cadherin is effective in conferring invasive properties to cells whether or not E-cadherin is expressed; however, the mechanism in which it confers these properties remains unknown (Hazan et al., 2004). In addition to N-cadherin, aberrant expression of cadherin-11 has been reported in aggressive breast and prostate cancer cell lines and tissues and is associated with invasiveness and poor prognosis (Pishvaian et al., 1999).

1.5.6 Catenin alterations in cancer

Inactivation of cadherins is not the only alteration that can reduce cell-cell adhesiveness and promote tumorigenesis; inactivation of catenins can also induce similar effects. In fact, catenin mutations have been identified in a variety of cancers. Inactivating mutations of α-catenin have been identified in lung, breast, prostate and colon cancer cell lines and primary tumors (Breen et al., 1993; Morton et al., 1993; Vermeulen, 1999). Furthermore, transfection of wildtype α-catenin into cells with inactive α-catenin reverses the tumorigenic phenotype (Bullions et al., 1997). These results suggest that even in the presence of functional cadherins, loss of α-catenin is able to contribute to the loss of calcium-dependent cell-cell adhesion and induce carcinogenesis.

Loss of expression of γ-catenin and β-catenin has been identified in cancers that show no evidence of catenin mutations. It has been proposed that disruption of post-translational events may explain the loss of catenin function in some cases. Tyrosine phosphorylation of catenins by either the Src family kinases or receptor tyrosine kinases has been shown to alter cell-cell adhesiveness. Phosphorylation of α-, β- and γ-catenins by Src kinases and receptor tyrosine kinases (RTKs) leads to decreased cell-cell adhesion, while dephosphorylation of catenins increases cell-cell adhesion (Hirohashi, 1998). Furthermore, GTPases have also been implicated in cadherin-catenin mediated cell-cell adhesion. GTPases cycle between inactive GDP-bound form and an active GTP-bound form. Studies with the Rho family of GTPases have shown that when Rho GTPases (RhoA, Cdc42, Rac1) are in their inactive state they can inhibit downstream signaling or cause their effector protein, IQGAP1, to bind to the cytoplasmic domain of E-cadherin and β-catenin. This causes α-catenin to dissociate from the cadherin-catenin complex causing a decrease in cell adhesion (Fukata et al., 1999; Kuroda et al., 1998; Hajra and Fearon, 2002). Conversely, when Rac1 and Cdc42 are in their active conformation they can bind IQGAP1, thereby preventing its interaction with β-catenin leading to stabilization of the cadherin-catenin complex. Therefore, disruption of downstream signaling events such as an increase in catenin phosphorylation or inactivation of GTPases can disrupt cell-cell adhesion and contribute to tumorigenesis.

1.5.7 Wnt Signaling Pathway

Both WT1 and β-catenin are part of the Wnt signal transduction pathway. There are two distinct pools of β-catenin in cells: the cadherin, cell membrane associated pool, as described previously, and the nuclear, Wnt signaling/gene transcription pool. Wnt-associated β-catenin is regulated by the adenomatous polyposis coli (APC) protein, AXIN proteins and glycogen synthase kinase 3β (GSK3β). In this pathway, β-catenin acts as a transcriptional regulator of Tcf/Lef signaling and is able to regulate gene transcription via the presence or absence of a Wnt signal. In the absence of a Wnt signal, β-catenin forms a complex with APC and AXIN proteins. The β-catenin N-terminal domain is then subjected to serine/threonine phosphorylation via GSK3β. β-catenin is then targeted for ubiquination and proteosomic degradation, leaving no β-catenin available for transcriptional activation (Polakis, 2001). However, in the presence of a Wnt signal, proteins that inhibit GSK3β activity and subsequent β-catenin phosphorylation are activated. β-catenin is stabilized, shuttled to the nucleus, and interacts with Tcf/Lef proteins, altering their transcriptional activity leading to activation of *Tcf/Lef* target genes (Behrens et al., 1996). This is illustrated in Figure 1.11.

Figure 1.11: Wnt signaling pathway. A. In the absence of a Wnt signal, β-catenin forms a multiprotein complex with AXIN and APC and GSK3β. GSK3β phosphorylates the N-terminal domain of β-catenin, targeting it for degradation by the ubiquination/proteosome pathway. As a result, β-catenin is unable to regulate gene transcription. **B.** The presence of a Wnt signal results in the formation of a multiprotein complex with AXIN, LRP5/6 and frizzled. This complex inhibits the function of GSK3β resulting in stabilization of β-catenin due to decreased β-catenin phosphorylation. As a result, β-catenin is recruited to the nucleus where it forms a complex with members of the Tcf/Lef transcription factor family and regulates transcription of β-catenin-Tcf/Lef target genes. Figure adapted from Hajra and Fearon (2002).

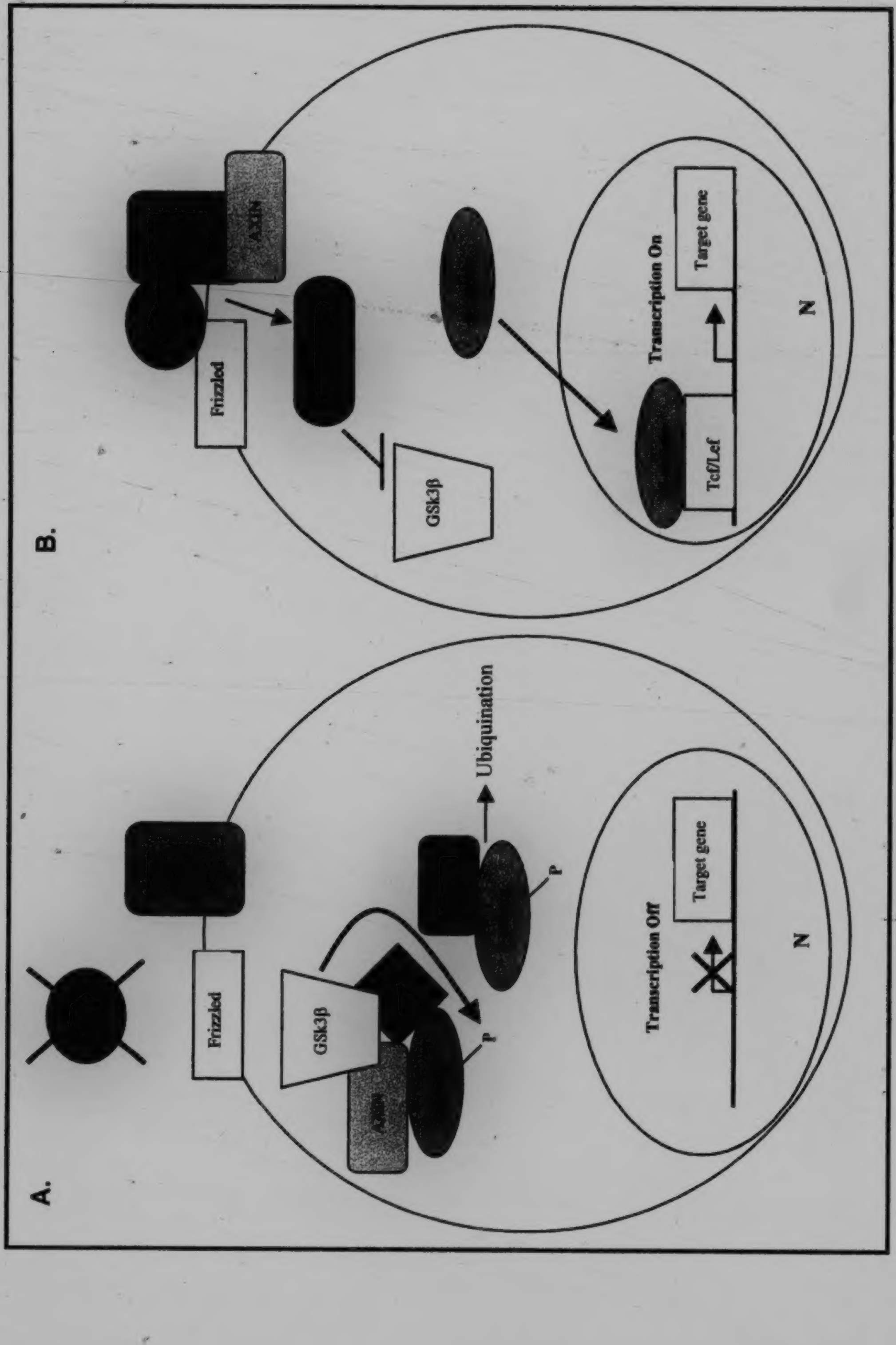
A.
Frizzled
GSk3β
AXIN
P
P
Ubiquination
Transcription Off
Target gene
N
B.
Frizzled
AXIN
GSk3β
Tcf/Lef
Transcription On
Target gene
N

Mutations or deregulation of genes involved in the Wnt pathway have been described in many cancers including melanoma, HCC, hepatoblastoma, ovarian and thyroid, indicating that disruption of this pathway contributes to tumorigenesis (Morin, 1999; Polakis, 2000). Activating or oncogenic *β-catenin* mutations occur in the N-terminus, which inhibits the mutant β-catenin protein from being phosphorylated by GSK3β. This leads to the inappropriate upregulation of Tcf/Lef target genes. Furthermore, inactivation of APC and AXIN proteins can also lead to elevated levels of β-catenin in the nucleus resulting in the continuous formation of β-catenin-Tcf/Lef complexes and the upregulation of Tcf/Lef target genes including *Tcf-1*, *Lef-1*, *MYC*, cyclin D1, matrix metalloproteinase 7, peroxisome proliferator-activator receptor delta and gastrin. The abnormal expression of the *Tcf/Lef* target genes may contribute to the cancer phenotype (reviewed in Hajra and Fearon, 2002). Surprisingly, the oncogenic mutations of β-catenin do not appear to affect cadherin-catenin mediated cell adhesion suggesting that β-catenin functions in two distinct and independent pathways.

1.5.8 Ksp-cadherin

Ksp-cadherin was identified in 1995 and along with LI-cadherin, belongs to the 7D-cadherin sub-family previously described (Thomsom et al., 1995). Ksp-cadherin contains the evolutionarily conserved extracellular domain comprised of the LDRE, DXND and DXD sequence motifs that are present in the extracelluar domains of most cadherin molecules. However, unlike the classical cadherins, the 7D-cadherins lack the prosequence and HAV adhesion recognition sequence and have a truncated cytoplasmic tail comprised of only 18-22 amino acids. Genomic studies found that Ksp-cadherin is comprised of 18 exons and produces a 2.2 kb transcript and a 130 kDa protein. Expression analysis of Ksp-cadherin revealed that it is expressed exclusively in the developing and adult kidney (Thomson et al., 1999).

1.5.8.1 Ksp-cadherin Expression

Expression of Ksp-cadherin in mice is first detected at embryonic day 10.5 (E10.5) in epithelial tissues of the Wolfian duct, followed by expression in the ureteric bud at E11. Expression of Ksp-cadherin seems to be limited to the basolateral membrane of renal epithelial tubular cells of maturing nephrons including the distal and proximal tubules, loops of Henle, ureters and renal collecting ducts of the embryonic and adult metanephros. It is not expressed in the metanephric mesenchyme, renal vesicles and comma- and S-shaped bodies. Ksp-cadherin expression continues to rise during late gestation and remains high in the adult kidney (Wertz and Herrmann, 1999; Igarashi, 2003). The expression pattern of Ksp-cadherin indicates that it may one of the most abundant cadherins in the mammalian kidney and is likely to play a role in kidney development and maintenance of epithelial tubular differentiation (Thompson and Aronson, 1999). Ksp-cadherin has also been shown to display transient expression in the lung and genitourinary tract as it is expressed in these tissues during development but expression is lost in mature and adult tissues (Thomson, 1999, Wertz and Herrmann, 1999).

1.5.8.2 Ksp-cadherin Function

The exact function of Ksp-cadherin is not known; however, it is thought to be similar to that of other cadherin family members. Studies with CHO cells transfected with Ksp-cadherin, LI-cadherin or the classical E-cadherin revealed that the three transfectants demonstrated similar levels of cell-cell adhesion (Wendeler et al., 2003). However, the cell aggregates differed with E-cadherin transfected cells forming large, highly compacted spherical cell clusters with sharp edges, while the LI- and Ksp-cadherin transfected cells formed large, irregular cell clusters with soft edges. This suggests that the two cadherin groups differ in their molecular mode of action. Elimination of Ca^{2+} ions reduced the level of cell aggregation for all 3 cadherins to basal levels seen in the untransfected CHO cells suggesting that, like the classical cadherins, 7D-cadherins mediate calcium-dependant cell-cell adhesion (Wendeler et al., 2003). However, unlike the classical cadherins, both LI- and Ksp-cadherins lack the cytoplasmic β-catenin binding region and thus do not form interactions with β-catenin. This suggests that calcium-dependent cell-cell adhesion occurs in a manner different from that of the classical cadherins (Wendeler et al., 2004).

1.5.8.3 Ksp-cadherin promoter

Deletion analysis of the Ksp-cadherin promoter region has defined the minimal region needed for transcriptional activity (Whyte et al., 1999; Bai et al., 2002). It was found that significant truncation of the Ksp-cadherin promoter from –2608 to –250, with respect to the transcription start site, did not compromise promoter activity. However, further truncation to –113 bp reduced promoter activity by 40%, while truncation to –31 eliminated promoter activity completely (Whyte et al., 1999). A binding site for hepatocyte nuclear factor-1α and 1β (*HNF-1*) has been found within the minimal promoter region, and it has been proposed that one or both regulate Ksp-cadherin transcription. Co-transfection of *HNF-1α* and *HNF-1β* transactivates the Ksp-cadherin promoter. Furthermore, mutations within the *HNF-1* binding region of the Ksp-cadherin promoter prevent *HNF-1* binding and abolish promoter transactivation. In addition, *HNF-1β* dominant gain-of-function mutations induced Ksp-cadherin promoter activity, while dominant negative mutations inhibit promoter activity. This suggests that the *HNF-1* genes are direct regulators of Ksp-cadherin (Bai et al., 2002).

1.6 Gene Expression Profiling

The identification of genes responsible for human disease and cancer is vital to increasing our knowledge of how and why diseases/cancers arise and is important for the development of novel or improved therapies. With the sequencing of the human genome, the number of genes identified and their subsequent association to human disease and cancer has increased considerably.

A variety of techniques have been developed to identify candidate genes, many of which are based on differential RNA or protein expression. These studies often compare the expression profiles between two or more cell populations (i.e.: tumor versus normal, disease versus non-diseased, induced versus non-induced) and identify candidate genes that are either up- or down-regulated in one population versus the other. Subtraction hybridization and differential display PCR (DD-PCR) are two of the classic gene profiling techniques that have been successful in identifying numerous differentially expressed genes. These techniques have led to the development of more refined technologies, many of which are still based on these initial two methods and will be described later.

1.6.1 Differential Display PCR

Differential display PCR (DD-PCR), often referred to as RT-DD-PCR or mRNA DD-PCR, was first described in 1992 by Liang and Pardee. DD-PCR has been successfully used to identify genes important in a variety of biological processes. The human genome is comprised of approximately 30-35 000 genes with each cell expressing only 10-15% of these, the number and type of gene, varying depending on cell type and developmental stage. DD-PCR compares levels of expression of thousands of transcripts between two cell populations, tissue type etc., and identifies cDNAs that are differentially expressed between these two populations. DD-PCR has been successfully used to identify differentially expressed genes implicated in cancer (Manda et al., 1999; Miller et al., 1999; Maeda et al., 1999), V(D)J recombination (Verkoczy and Berinstein, 1998), young versus senescent cells (Linskens et al., 1995), drug resistance (Bertram et al., 1998), infection (Domachowske et al., 2000) and hematopoiesis (Bond et al., 1998), to name a few.

DD-PCR utilizes reverse transcription and PCR to amplify various sized transcripts from the populations of interest. An important factor for successful DD-PCR is the use of properly designed arbitrary and anchored primers. Initially, poly A+ RNA from each population is reverse transcribed. This reverse transcription process requires the use of an anchored oligo-dT primer consisting of a stretch of 12 T's, which bind to the polyA+ tail, followed by 2 extra 3' bases. The penultimate 3' base in the anchored primer is a random mixture of all 4 nucleotides while the final 3' base is a designated nucleotide, thus allowing for the amplification of subsets of mRNA transcripts. Thus, the 4 different anchored primers, T_{11}MA, T_{11}MC, T_{11}MG, T_{11}MT, where M represents any base, are used separately in 4 different reverse transcription reactions. Under optimal conditions, this combination of four primers should bind to and transcribe parts of all of the different mRNA species expressed by the cell. For the PCR amplification step, each of the 4 anchored primers is paired with a 10mer random primer. Liang et al. (1993) found that the 4 anchored primers in combination with 20 arbitrary primers (total reactions = 80) was sufficient to amplify approximately 10 000 mRNAs present in mammalian cells. Each PCR reaction typically amplifies 100-200 cDNAs or parts thereof (cDNA fragments) which are subsequently resolved on a denaturing polyacrylamide gel. cDNA fragments, which are represented as bands on a gel, that are more abundant in one population versus the other, are excised, re-amplified, cloned and further analysed (Figure 1.12).

A variety of techniques can be employed to confirm differential expression of transcripts identified in the DD-PCR assay. The two most common methods are Northern blot analysis and quantitative RT-PCR. However, reverse Northerns, slot blots and RNase protection assays have also been used. If differential expression is confirmed, the cDNA fragments can be sequenced and the corresponding gene identified.

There are several advantages and disadvantages of DD-PCR over other differential gene expression techniques. Advantages of DD-PCR include: (1) the ability to identify both known and unknown genes; (2) the comparison of a large number of mRNAs in a single experiment; (3) simultaneous detection of genes that are up-regulated or down-regulated; (4) less labor intensive than some of the other approaches; (5) cost effectiveness and (6) the requirement of only a small amount of mRNA (Zhang et al., 1998).

The major disadvantage of DD-PCR is its high probability of isolating false positives, which are transcripts that appear to be differentially expressed in the original DD-PCR assay, but which cannot be confirmed by other expression studies. It has been reported that up to 90% of the differentially expressed

Figure 1.12: Differential display PCR. Poly(A)+ RNA from two different populations (i.e. normal vs tumor) is reversed transcribed using anchored primers corresponding to the Poly(A)+ tail in which the penultimate base represents a random nucleotide and the 3' base is one of the 4 nucleotides. The cDNA is amplified by PCR using one of the anchored primers and a random 10mer arbitrary primer. PCR products are resolved by electrophoresis on a denaturing PAGE (sequencing) gel. Differential expression of transcripts between the two populations are identified and bands are excised and further characterized.

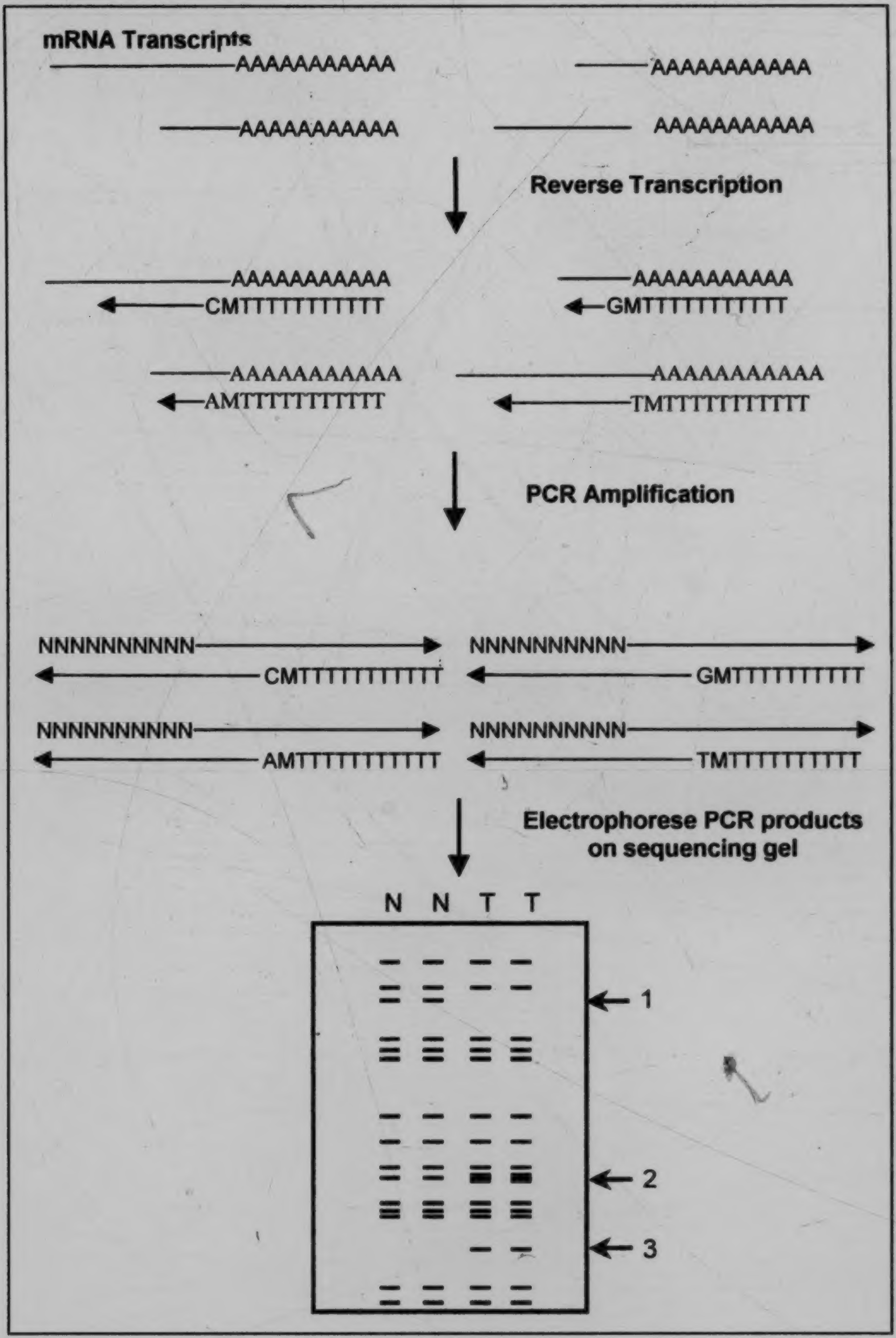
mRNA Transcripts
AAAAAAAAAAA
AAAAAAAAAAA
AAAAAAAAAAA
AAAAAAAAAAA
Reverse Transcription
AAAAAAAAAAA
CMTTTTTTTTTTT
AAAAAAAAAAA
GMTTTTTTTTTTT
AAAAAAAAAAA
AMTTTTTTTTTTT
AAAAAAAAAAA
TMTTTTTTTTTTT
PCR Amplification
NNNNNNNNNN
CMTTTTTTTTTTT
NNNNNNNNNN
GMTTTTTTTTTT
NNNNNNNNNN
AMTTTTTTTTTTT
NNNNNNNNNN
TMTTTTTTTTTT
Electrophorese PCR products on sequencing gel
N N T T
1
2
3

fragments may represent false positives (Sompayrac et al., 1995). Factors contributing to the generation of these false positive transcripts include partial RNA degradation, primer design and contamination of mRNA with DNA. Furthermore, a single DD-PCR band can be comprised of two or more RNA species due to the low resolution capacity of the denaturing polyacrylamide gels used for electrophoresis. This can lead to masking of differentially expressed fragments and isolation of fragments that are not truly differentially expressed (Linskens et al., 1995). As a result, it is critical that all selected bands be confirmed. However, confirmation of the differentially expressed fragments (which can number in the hundreds) can turn this technique into a labor intensive exercise.

Other disadvantages of DD-PCR include its preference for the 3' ends of mRNAs, which may not include coding regions and for the more abundant mRNAs. A study by Bertioli et al. (1995) showed that in a model biological system, DD-PCR failed to detect transcripts representing <1.2% of the total mRNAs. Sensitivity can be improved by more stringent PCR conditions and utilization of longer and more specific primers; however, this can also reduce the overall number of transcripts identified (Zhang et al., 1998). Another concern of DD-PCR is limited reproducibility as different DD-PCR patterns can be seen when DD-PCR is performed in duplicate; however, more stringent PCR conditions can help minimize this problem.

To aid with some of the pitfalls of DD-PCR, several related techniques, based on DD-PCR, have emerged and include targeted differential display

(Donohue et al., 1995), ordered differential display (Matz et al., 1997) and RFLP-coupled domain-directed differential display (Joshi and Nguyen, 1997). These techniques have been used with varying degrees of success. However, DD-PCR still remains the preferred choice among these methods, as it has been the most successful in identifying genes and/or mRNAs associated with a particular disease/state. Other non-DD-PCR based methods have been designed to identify differentially expressed genes, including subtraction hybridization, microarray analysis and protein arrays, all of which have been successful in identifying differentially expressed transcripts and each have their own set of advantages and disadvantages as discussed in Chapter 4.

1.6.2 In silico methods of candidate gene searching

A method that has become more prominent and relevant with the sequencing of the human genome is the *in silico* approach of database searching for candidate genes. This is a very simple, efficient, cost-effective approach to identify putative candidate genes. This method is useful only when a candidate gene region has been defined by LOH, linkage analysis, translocations etc. If a chromosomal region of interest is known, the researcher can review the known genes in the region using a database such as NCBI's Online Mendelian Inheritance in Man (OMIM) (http://www.ncbi.nlm.nih.gov:80/entrez/Omim/getmap.cgi) genemap database. A list of known genes in the critical region can be compiled and literature reviews on each gene can be performed to see if its expression pattern and/or proposed function are consistent with the disease/cancer being studied. The drawback of this approach is that it can only identify known genes and therefore candidate gene selection is made based only on the information known about the gene and disease/cancer being studied. However, it provides a relatively simple way of identifying candidate genes to be further screened by RT-PCR or Northern blot analysis to evaluate RNA expression in the tissue of choice.

1.7 Global Objectives

Wilms tumors are heterogeneous and genetically complex. Only one Wilms tumor gene, *WT1*, has been identified and shown to have a proven role in the etiology of Wilms tumors. Surprisingly, *WT1* has only been implicated in 10-20% of Wilms tumors. Loss of heterozygosity studies by our lab and others have identified several chromosomal regions thought to harbour putative candidate Wilms tumor genes. The identification of genes involved in the initiation and/or progression of Wilms tumor would be beneficial in furthering our understanding of this cancer, aiding in the development of diagnostic and/or prognostic markers and tailoring current therapies. Therefore, the global objective of this thesis was to identify and characterize novel Wilms tumor genes using a combination of methodologies.

Objective 1: To determine the role of the Simpson-Golabi-Behmel gene, *GPC3* in sporadic Wilms tumors

The Simpson-Golabi-Behmel syndrome (SGBS) is an X-linked, overgrowth syndrome often misdiagnosed as BWS. Individuals with SGBS are predisposed to developing various embryonal tumors such as Wilms tumor during childhood. The gene responsible for SGBS, glypican 3 (*GPC3*) is located at Xq26 and encodes a heparan sulfate proteoglycan involved in cell growth and differentiation. Interestingly, alterations of *WT1* and the putative *WT2* genes are involved in both syndrome and non-syndrome-associated Wilms tumors. Therefore, since individuals with SGBS have a predisposition to developing Wilms tumor, we hypothesized that some tumors from non-SGBS individuals, which do not involve loci on 11p, may harbor somatic *GPC3* mutations. We therefore proposed to conduct an extensive analysis of the *GPC3* gene by Southern blot analysis, denaturing HPLC, sequencing and Northern blot analysis in 64 sporadic Wilms tumors.

Objective 2: To identify the putative Wilms' tumor gene(s) on chromosome 16q and/or its downstream targets utilizing differential display PCR *and in silico* approaches.

Loss of heterozygosity of chromosome 16q occurs in 20% of Wilms tumors suggesting the presence of a Wilms tumor gene in this region. Identification of the gene(s) on chromosome 16q is necessary for a better understanding of Wilms tumorigenesis and for the development of diagnostic and prognostic indicators. We proposed to identify and characterize candidate Wilms tumor suppressor or progression genes on 16q and/or its downstream targets utilizing differential display PCR (DD-PCR) and the *in silico* approach of database searching.

Objective 3: Analysis of the candidate gene, *Kidney-specific-cadherin*, in Wilms tumor

Approximately 20% of Wilms tumors lose heterozygosity of chromosome 16q and this loss is associated with adverse outcome. This suggests that the 16q gene may be involved in the progression of this aggressive form of Wilms tumor. We investigated the possibility that one of the cadherin genes, Ksp-cadherin, may be involved in Wilms tumorigenesis. Ksp-cadherin is located on chromosome 16q, is exclusively expressed in fetal and adult kidney, and is part of a gene family that has been implicated in tumorigenesis. We hypothesized that Ksp-cadherin may be the chromosome 16q Wilms tumor gene associated with poor outcome. We therefore proposed to perform RNA and protein expression studies, methylation studies and mutation analysis to characterize the *Ksp-cadherin* gene in 34 sporadic Wilms tumors.

CHAPTER 2: Materials and Methods

2.1 Patient Samples

Wilms tumors and adjacent normal kidney and/or DNA from patient or parent blood samples, were obtained from the National Wilms Tumor Study Group Bank. Ethical approval for use of these samples was granted by the Alberta Cancer Board Research Ethics Committee. Fetal kidney was obtained from the University of Washington, Seattle. DNA from 89 non-Wilms tumor patients was kindly donated by Dr. Heather McDermid, Department of Biological Sciences, University of Alberta for the heteroduplex analysis. Anonymous blood was obtained from the Canadian Blood Services for a normal DNA control for heteroduplex analysis.

2.2 Nucleic Acid and Protein Extractions

2.2.1 Tissue preparation

Approximate 5 mm^3 sections of tissue were used for DNA and protein extractions, while 2.5 mm^3 sections were used for RNA extractions. Frozen tissue aliquots were placed in a mortar and pestle pre-cooled with liquid nitrogen and ground in liquid nitrogen to a fine powder. Ground tissues were transferred to a 50 ml sterile plastic tube and either processed immediately or stored as is at -80°C until required for extraction.

2.2.2 Nucleic acid extraction

DNA was extracted using standard phenol-chloroform protocol as described in Sambrook and Russell (2001).

Total RNA was extracted using TRIzol Reagent (Invitrogen). Briefly, ground tissue was resuspended in 1 ml of TRIzol per 50-100 mg tissue. Samples were vortexed and DNA was sheared by passing through a 21 gauge needle a minimum of 10 times. Samples were incubated in TRIzol for 10 min at RT followed by incubation with 0.2 ml chloroform:isoamyl alcohol (24:1) per ml of TRIzol. Samples were vigorously shaken for 20s, incubated at RT for 3 min and centrifuged at 5000 rpm for 30 min at 4°C in a Sorvall centrifuge. The aqueous layer was removed from each sample and transferred to a new 50 ml tube. Five hundred µl of ice-cold isopropanol per ml of TRIzol was added to each sample followed by incubation at RT for 10 min. Samples were centrifuged at 5000 rpm for 20 min at 4°C, supernatant decanted and pellets were washed in 15 ml ice-cold 70% EtOH followed by centrifugation at 5000 rpm for 10 min. The supernatant was again decanted and RNA pellets were air dried for 10-15 min. Pellets were resuspended in 100-500 µl nanopure ddH_20 and incubated at 60°C for 5 min. Total RNA was stored at -80°C.

2.2.3 Whole cell lysate extraction

Ground tissues were resuspended in 1-2 vol of protein lysis buffer (50 mM Tris-HCl; pH 8.0, 1% SDS) of tissue. Lysates were passed through a 21 gauge needle a minimum of 10 times, transferred to a 1.5 ml tube and stored at -80°C.

2.2.4 Quantitation of nucleic acids and protein

Nucleic acids were quantitated by spectrophotometric analysis. For DNA, the concentration was calculated by multiplying the OD_{260} value by 50 μg/ml and the dilution factor. RNA concentration was determined by multiplying the OD_{260} value by 40 μg/ml and the dilution factor.

Protein concentration was determined by the colorimetric Bradford Assay (BioRad) according to manufacturer's protocol. Briefly, 200 μl of Bradford Reagent (BioRad) and 800 μl dH_20 was added to 10 μl of whole cell lysate and protein sample concentration was measured at 595 nm.

2.3 Southern and Northern Blot Hybridization

2.3.1 Southern blot analysis

Five μg of genomic tumor and corresponding normal DNA (isolated from peripheral blood leukocytes or normal kidney) were individually digested with ***Taq1*** and ***Pst1*** restriction enzymes according to standard protocols described in Sambrook and Russell (2001). Briefly, fragments were electrophoretically separated on a 1% agarose gel, stained with EtBr and photographed on an Ultralum Dual Light Transilluminator. DNA was depurinated by soaking gel in

0.25 N HCl for 20 min followed by neutralization in 0.4 N NaOH/0.6 M NaCl. The DNA was then transferred O/N in 0.4 N NaOH/0.6 M NaCl onto Hybond N+ nylon membrane (Amersham Biosciences) using standard capillary transfer as described in Sambrook and Russell (2001). Membranes were washed in 2X SSC (0.3 M NaCl, 0.03 M sodium citrate, pH 7.0); 0.1% SDS three times for 5 min each each prior to hybridization and then placed in a hybridization bottle with 20-30 ml of hybridization solution [7% PEG, 10% SDS, 1.5% 20X SSPE (3.6 M NaCl, 0.2 M sodium phosphate, 0.02 M EDTA), 0.1 mg/ml freshly denatured herring sperm DNA]. Membranes were pre-hybridized for a minimum of 4 h to O/N at 65°C in a hybridization oven (Robbins Scientific). After pre-hybridization, 10 ml of pre-warmed hybridization buffer containing the radiolabelled probe was added to the hybridization bottle, and mixed with the existing hybridization solution and hybridization was carried out O/N at 65°C. Membranes were then washed twice for 5 min with 2X SSC, 0.1% SDS at RT and twice for 1 h with 0.1X SSC, 0.1% SDS at 65°C. Membranes were sealed in a clear plastic bag and placed in an X-ray cassette with intensifying screens and exposed to X-ray film (KODAK X-OMAT) from O/N to 1 week at -80°C. Film was developed using a KODAK X-OMAT 2000A processor.

2.3.2 Northern blot analysis

Prior to electrophoresis, all gel trays, combs and glassware were washed with RNAzap (Ambion) to remove RNases. Ten to twenty μg of total RNA or 1-2 μg polyA+ RNA was added to 3.5 μl of RNA sample buffer (5.3 M formaldehyde, 43% formamide, 7% bromophenol blue, 0.5X MOPS, 1 mM EDTA) and samples were heated to 70°C for 10 min and quick chilled on ice. RNA was electrophoresed on a 1% agarose-formaldehyde gel (2.2 M formaldehyde, 1X MOPS) in 1X MOPS running buffer (0.02 M MOPs, 1 mM EDTA, 5 mM NaOAc; pH 7.0) at 100 V for 4 h. The RNA was transferred in 20X SSC O/N onto Hybond C+ nitrocellulose membrane (Amersham Biosciences) using standard capillary transfer (Sambrook and Russell, 2001). Following transfer, the membrane was baked at 80°C in a vacuum oven for 2 h and subsequently washed in 0.1X SSC, 0.1% SDS three times for 5 min each to remove excess salts. Membranes were placed in hybridization bottles with 20-30 ml hybridization solution [50% formamide, 5.5X SSPE (1M NaCl, 55 mM NaH_2P0_4, 5.5 mM EDTA; pH 7.4), 5X Denhardts, 0.1% SDS, 1% dextran sulfate and 0.5 mg/ml freshly denatured herring sperm DNA (Roche Biochemicals)] and pre-hybridized at 42°C for 4 h to O/N in a hybridization oven. Ten ml of pre-warmed hybridization solution containing the radiolabelled probe was added to the hybridization tube, mixed with the existing hybridization solution, and hybridized at 42°C O/N. Membranes were washed twice for 5 min with 2X SSC, 0.1% SDS at RT followed by twice for 1 h with 0.1X SSC, 0.1% SDS at 65°C. Membranes were sealed in a clear plastic bag and placed in an X-ray cassette with an intensifying screen and exposed to X-ray film (KODAK X-OMAT) from O/N to 1 week at -80°C and developed on a KODAK X-OMAT 2000A processor. Northern blots were stripped by incubating blots twice for 1.5 h at 65°C in 0.1X Thomas Buffer (5 mM Tris-HCl;

pH 8, 0.2 mM EDTA, 0.05% sodium pyrophosphate, 0.002% BSA, 0.002% Ficoll, 0.002% PVP).

2.3.3 Preparation of probes

GPC3 cDNA probes were kindly donated by Dr. Rhiannon Hughes, University of Calgary. The 3 *GPC3* probes represent the full length *GPC3* cDNA and consist of overlapping cDNA fragments representing exons 1-3, exons 3-5 and exons 5-8. Plasmid DNA containing the *GPC3* cDNA was isolated using a cesium chloride gradient according to a standard protocol (Sambrook and Russell, 2001): Plasmid DNA was digested with the restriction enzyme *EcoRI* and DNA was electrophoresed on a 1% low melt agarose (Invitrogen) gel and the insert excised. Excised bands were weighed, diluted with water (1ml dH_20/mg gel) and heated to 65°C for 15 min to allow the gel slice to melt into solution. Probes were sequenced using the ABI Prism 310 Genetic Analyser, as described below, to confirm they corresponded to the correct gene sequence.

2.3.4 Random primed synthesis of probes

Approximately 100 ng of cDNA probe was labelled by random primed synthesis. The excised gel fragment/dH_20 mixture was boiled for 10 min and then placed at 37°C for 10 min. Twelve μl of OLB mix (Appendix 1), 4 μl BSA, 10 U Klenow Fragment (Amersham Biosciences) and 10 μl of α-dCTP ^{32}P (3000 Ci/mmol) (Amersham Biosciences) were added and the mixture subsequently incubated for 1-2 h at 37°C. Unincorporated α-dCTP ^{32}P was removed by passing the radiolabelled probe through a Bio-Gel A 1.5 mm gel (BioRad) column (Sambrook and Russell, 2001). The radiolabelled probe was collected while the unincorporated radionucleotides remained in the column. The specific activity of the radiolabelled probes was determined and only those probes with a specific activity of >1 x 10^9 cpm/ug were used for hybridization. Radiolabelled probes were boiled for 10 min, placed on ice and the entire volume of the probe was added to 10 ml of pre-warmed hybridization solution. The probe/hybridization mixture was added directly to the hybridization tube and hybridization was carried out overnight as described previously.

2.4 Western Blot Analysis

2.4.1 SDS-polyacrylamide gel electrophoresis

A 12% separating SDS-PAGE gel [12% bis-acrylamide (2.8:30), 0.375 M Tris-HCl; pH 8.8, 0.1% SDS, 0.1% APS, 4 µl TEMED] was prepared, poured, overlaid with dH_20 and allowed to polymerize for 1 h. Once the separating gel had polymerized, the dH_20 was removed and the stacking gel (30% bis-Acrylamide (2.8:30), 0.125 M Tris-Cl; pH 6.8, 0.1% SDS, 0.1% APS, 4 µl TEMED) was prepared and layered over the separating gel. A comb was inserted and the gel was allowed to polymerize for 45 min.

2.4.2 Preparation of protein samples

Two volumes of 5X Laemmli buffer (0.35 M Tris-Cl; pH 6.8, 10% SDS, 36% glycerol, 0.6 M β-ME, 0.12% bromophenol blue) was added to each sample.

Samples were boiled for 5 min and loaded onto the SDS-PAGE gel with either the BenchMark™ Pre-stained Protein Ladder (Invitrogen) or the Prestained Protein Ladder, 10-180 kDa (Fermentas). Protein samples were electrophoresed in 1X running buffer (25 mM Tris, 192 mM glycine, 0.1% SDS) at 150 V for 2 h.

2.4.3 Western blot transfer

Hybond C+ nitrocellulose membrane (Amersham Biosciences), 3MM Whatmann filter paper and fiber pads were pre-soaked in chilled 1X transfer buffer (10 mM $NaHCO_3$, 3 mM $NaCO_3$, 20% MeOH) for a minimum of 15 min. The gel/membrane sandwich was prepared as described in Sambrook and Russell (2001) and proteins were transferred in 1X pre-chilled transfer buffer at 150 mA for 2 h at 4°C. Once proteins were transferred, the membrane was stained with 0.005% 2,4,6-Trimethylpyridinium p-toluenesulfonate (CTPS) in 12 N HCl for 5 min, placed between plastic and photocopied for documentation. The CTPS stain was removed by washing the membrane three times for 5 min each in 1X TBS on a shaking platform.

2.4.4 Western blotting

Mouse anti-Ksp cadherin monoclonal antibody directed to the C-terminus of the human *Ksp-cadherin* gene (Zymed Laboratories Inc.) was used at a concentration of 2 μg/ml. The antibody was diluted in 5% BSA, stored at 4°C and re-used for several times.

Membranes were blocked in 1X TBS + 5% skim milk powder for 4 h to O/N. Membranes were washed five times for 5 min each in 1X TBS on a shaking platform. Membranes were then incubated with the primary antibody diluted in 5% BSA as described above, O/N at 4°C. The following day, membranes were washed three times for 5 min each in 1X T-TBS (0.1% Tween 20, 1X TBS). The secondary antibody, 1:10 000 rabbit-α-mouse HRP conjugate (Jackson Laboratories) + 1% skim milk was added and membranes were incubated for a minimum of 2 hours to O/N. Membranes were washed six times for 5 minutes in T-TBS followed by two times for 5 minutes in 1X TBS.

2.4.5 Protein Detection

Proteins were detected by chemiluminesence using the Supersignal® West Pico Chemiluminescent Substrate (PIERCE). Two and a half ml each of Supersignal® West Pico Luminol/Enhancer solution and Supersignal® West Pico Stable Peroxide Solution were added to each membrane and incubated for 2 min at RT on a shaking platform. Membranes were placed on glass plates, covered with saran wrap and exposed to X-ray film (KODAX X-OMAT) from 30s to 5 min and developed using a KODAX X-OMAT 2000A processor.

2.5 Reverse Transcription

Total or polyA+ RNA was reverse transcribed for subsequent use in expression analysis and probe preparation. Samples were set up in duplicate and one tube served as a negative control to which no reverse transcriptase enzyme was added. One µl of 10 mM dNTPs and 1 µl of oligo $(dT)_{12-18}$ (Invitrogen) was added to 5 µg of total RNA or 10 ng of polyA+ RNA. Samples were heated to 65°C for 10 min and chilled on ice for 5 min. Seven µl of reverse transcription master mix [2.5X First Strand Buffer (125 mM Tric-Cl; pH 8.3, 187.5 mM Kcl, 7.5 mM $MgCl_2$) (Invitrogen), 25 mM DTT, 20 U RNAguard Ribonuclease Inhibitor (Amersham Biosciences)] was added to each RNA sample and heated to 42°C for 2 min. To one of the duplicate RNA tubes only, 200 U Superscript I (Invitrogen) was added and incubation continued at 42°C for 1 h. The reverse transcription reaction was terminated by heating to 70°C for 15 min followed by storage at -20°C.

2.6 Polymerase Chain Reaction (PCR)

The following conditions were used for all PCR amplifications unless otherwise specified. One hundred ng of DNA or 1 µl of cDNA were amplified in 1X PCR buffer (10 mM Tris-HCl; pH 9, 1.5 mM $MgCl_2$, 50 M KCl) (Amersham Biosciences), 200 µM dNTPs, 0.8 pmol of each forward and reverse primer and 1 U *Taq* polymerase (Amersham Biosciences). The following PCR parameters were used: 94°C for 5 min, followed by 30-40 cycles of 94°C for 50s, 51-58°C for 50s and 72°C for 50s with a final extension at 72°C for 7 min. All PCRs were performed in the 2400, 9600 or 9700 Gene Amp PCR Systems (Perkin Elmer). PCR products were electrophoresed on a 1% agarose gel and visualized with EtBr on the Ultralum Dual Light Transilluminator. PCR products to be sequenced were purified with the Qiaquick PCR purification kit following the manufacturer's instructions (Qiagen).

2.6.1 PCR Primers

PCR primer sequences, expected PCR product size, cycle number and annealing temperatures organized by gene name are found in Tables 2.1 – 2.5. Table 2.5 lists the primer sequences for β-actin and *GAPDH* used as controls for RNA expression, and the sequences for the M13 and the Universal primers used for plasmid sequencing.

2.7 Heteroduplex Analysis

Both normal and Wilms tumor DNA was PCR amplified for all 8 exons of the *GPC3* gene using the conditions described above and the primers listed in Table 2.1. An equal concentration of the exon-specific PCR product from the normal sample was mixed with the same exon-specific PCR product from the Wilms tumor sample to be evaluated. The normal:test mixtures were heated and denatured at 95°C for 5 minutes followed by subsequent cooling at 1°C intervals to 25°C over a 45 min duration. Sequence changes will result in the formation of heteroduplexes, following denaturation, while complementary sequences will form homoduplexes. Briefly, the hetero- and homo-duplexes are separated according to the melting temperatures, listed in Table 2.1, by denaturing HPLC using the WAVE™ DNA Fragment Analysis System (Transgenomics). This system takes advantage of the fact that the different melting temperatures and subsequent mobility of the variant duplexes result in distinct peaks (WAVES) on the chromatogram. A subset of the normal WAVES and all abnormal WAVES were sequenced to determine the precise sequence change.

2.8 Automated DNA Sequencing

PCR products from the *GPC3* study, MSP samples from the Ksp-cadherin methylation study, cDNA probes and cloned candidate fragments from the DD-PCR study were sequenced using the same general protocol on either the ABI Prism 310 Genetic Analyzer (Applied Biosystems) or the CEQ8000 Genetic Analysis System (Beckman-Coulter).

2.8.1 ABI Prism 310 Genetic Analyzer sequencing preparation

For sequencing of PCR samples, 50-100 ng purified PCR product, 4 μl Big Dye Terminator mix (Applied Biosystems), 0.16-0.32 pmol of forward or reverse PCR primer and dH_20 to 10 μl were mixed together. For MSP sequencing, 0.64-1.28 pmol of forward or reverse PCR primer was used. For sequencing of plasmid DNA, 100-200 ng of plasmid DNA, 4 μl Big Dye Terminator mix (Applied Biosciences), 4 pmol of M13 or Universal primer and dH_20 to 10 μl were mixed together.

The following cycle sequence conditions were performed in either the 2400, 9600 or 9700 Gene Amp Thermocycler (Perkin Elmer) for all PCR and plasmid DNA ABI Prism sequencing reactions: 96°C for 30s, 50°C for 5s, 60°C for 4 min for 25 cycles.

After samples had undergone cycle sequencing, DNA was EtOH precipitated. Forty microliters of 60% EtOH was added to each sample and mixed well. Samples were incubated at RT for 15 min and centrifuged at 14 000 rpm for 20 min. Supernatant was aspirated and pellets were washed twice with 125 µl 70% EtOH. Pellets were dried by heating to 95°C for 1 min and resuspended in 12.5 µl of Template Suppression Reagent (TSR) (Applied Biosystems). Samples were heated to 95°C for 5-10 min followed by a 10 min incubation on ice. Samples were transferred to septa tubes and loaded onto the 310 ABI Prism Genetic Analyzer for analysis.

2.8.2 CEQ8000 Genetic Analysis System sequencing preparation

Twenty-five to fifty ng of purified PCR product was used in each sequencing reaction together with 4 µl of DTCS Quick Start Master Mix (Beckman Coulter), 0.16-0.32 pmol of forward or reverse PCR primer and dH_20 to a final volume of 10 µl. For plasmid DNA, 100-200 ng of plasmid DNA was added to the final volume of dH_20 needed to make up a 10 µl reaction. The DNA and dH_20 only were pre-heated to 96°C for 1 minute. After pre-heating, 4 pmol of M13 or Universal sequencing primer and 4 µl of DTCS Quick Start Master Mix (Beckman Coulter) were added to each sample and mixed thoroughly.

The following cycle sequence program was used for all PCR and/or plasmid DNA sequencing reactions: 96°C for 20 s, 50°C for 20 s and 60°C for 4 min for 30 cycles in a 2400, 9600, 9700 Gene Amp Thermocycler (Perkin Elmer).

Fresh stop solution (1.2 M NaOAc; pH 5.2, 40 mM EDTA; pH 8.0, 4 mg/ml glycogen) was made prior to precipitation. Five µl of stop solution was added to a 1.5 ml tube and sequencing reactions were transferred to these tubes and samples were mixed well. Sixty µl of ice-cold 95% EtOH was added to each tube, vortexed and immediately centrifuged at 14 000 rpm for 15 minutes at 4°C. Supernatant was removed with a micropipette, and pellets were washed twice with 200 µl ice-cold 70% EtOH and centrifuged at 14 000 rpm for 5 min at 4°C. Pellets were air dried for 10-15 min, resuspended in 30 µl Sample Loading Solution (SLS) (Beckman Coulter) and incubated at RT for 10 min. Samples were then transferred to a 96-well CEQ sample plate (Beckman Coulter) and each sample was overlaid with light mineral oil (Beckman Coulter). The CEQ sample plate was loaded onto the machine for analysis.

2.9 Differential Display PCR

2.9.1 Wilms tumor samples

Six Wilms tumors were used for the initial DD-PCR study. Three tumors that have lost heterozygosity of 16q (16q-) yet retained heterozygosity on chromosomes 1p and 11p, and 3 tumors that have retained heterozygosity of chromosome 16q (16+) in addition to chromosomes 1p and 11p were evaluated.

2.9.2 Differential Display Reverse Transcription

PolyA+ RNA was extracted from tumor tissue according to standard methods as described in Sambrook and Russell (2001). Table 2.3 lists the primer sequences used for reverse transcription and PCR in the differential display analysis. To 100 ng of polyA+ RNA, 0.017 μM of external primer [T_{11}MA, T_{11}MC or T_{11}MG)] and 7 μl of dH_2O was added and samples were heat-shocked for 2 min at 65°C and then quick-chilled on ice. Twenty μl of reverse transcription master mix [1X First Strand Buffer (Invitrogen), 0.05 mM dNTPs, 10 U RNAguard Ribonuclease Inhibitor (Amersham Biosciences), 10 mM DTT, 0.5 mM spermidine, 100 U Superscript II (Invitrogen)] was added to each sample. Samples were incubated at 42°C for 1 h and then heat inactivated by heating at 95°C for 5 min, quick-chilled on ice and stored at -20°C.

2.9.3 Differential Display Polymerase Chain Reaction

Eighteen μl of PCR master mix [1X PCR buffer (Amersham Biosciences), 2 μM dNTPs, 2.5 μM external primer [T_{11}M(A,C,G)], 0.5 μM internal OPG primer (random 10-mers; Operon Technologies, Inc.), 0.5 U Taq DNA polymerase (Amersham Biosciences) and 1 μl α-dATP-^{35}S (1200 Ci/mmol) (Amersham Biosciences)] was added to 2 μl cDNA. DNA was PCR amplified using the following cycling conditions: 95°C for 5 min followed by 30 cycles of 95°C for 30s, 41°C for 90s and 72°C for 30s with a final extension at 72°C for 5 min.

2.9.4 Denaturing polyacrylamide gel electrophoresis

A 6% denaturing polyacrylamide gel (42% urea, 38% acrylamide:bis (38:2), 1X TBE, 0.1% APS, 0.001% TEMED) of standard sequencing size was used for gel electrophoresis of amplified DD-PCR products. To each RT-PCR sample, 7.3 µl of sequencing loading dye (95% formamide, 10 mM EDTA, 0.5% (w/v) xylene cyanol, 0.5% (w/v) bromophenol blue) was added and heated to 90°C for 5 minutes. Three µl of each sample was loaded onto a pre-runned, warmed sequencing gel and samples were electrophoresed for 4-6 h at 70 watts. Gels were then transferred to 3MM Whatmann filter paper, covered with saran wrap and dried using a Drygel Sr. slab gel dryer (Hoefer Scientific Instruments). Several light-sensitive markers were taped near the corners of the gel to aid with alignment. Dried gels were placed into an X-ray cassette and exposed to X-ray film (KODAK X-OMAT) for O/N-3 days and developed on a KODAK X-OMAT 2000A film processor.

2.9.5 Excision of cDNA fragments

Autoradiograms were visually screened for the presence of differentially expressed cDNAs between the two tumor groups (16q- vs. 16q+). A cDNA was deemed to be differentially expressed and considered for further evaluation if it was expressed in at least two samples of one group and not expressed in at least two samples of the other group. Highest priority was given to those cDNAs that were exclusively expressed in one group but not in the other group.

Differentially expressed cDNAs, termed candidate cDNA fragments, were identified and the autoradiogram was aligned with the light sensitive markers on the gel. With a sterile needle, holes were poked though the autoradiogram and gel at the four corners of the candidate cDNA fragment (which was represented by the presence of a band on the gel). Marked candidate transcripts were removed with a sterile scalpel and transferred to a 1.5 ml tube with 100 μl of dH_20. Samples were incubated at RT for 15 min and then boiled for 15 min. The aqueous layer was then transferred to a fresh 1.5 ml tube and 2.5 μl 20 mg/ml glycogen (Bohringer Manniheim), 1/10 vol. 3M NaOAc (pH 7) and 2 vol. 95% EtOH was added and DNA was precipitated using standard conditions (Sambrook and Russell, 2001). DNA pellets were resuspended in 10 μl dH_20 and stored at 4°C.

2.9.6 Reamplification of cDNA fragments

Four μl of candidate fragment DNA was amplified with 1X PCR buffer (Amersham Biosciences), 20 μM dNTPs, 2.5 μM external primer, 0.5 μM internal OPG primer and 0.5 U Taq DNA polymerase (Amersham Biosciences) using the DD-PCR cycle conditions as described previously. Thirty μl of PCR product were electrophoresed on a 5% PAGE gel (5% acylamide:bis (29:1), 1X TBE, 0.1% APS, 0.001% TEMED) at 180 V for 2-3 h. Gels were stained with EtBr, photographed and amplified cDNAs were excised and placed in a 1.5 ml tube with 100 μl elution buffer (0.5 M NH_4OAc, 1 mM EDTA), covered with aluminum foil and incubated at 37°C O/N. DNA was precipitated with 2 vol. 95% EtOH, resuspended in 100 μl TE and reprecipitated with the addition of 1/10 vol. 3 M NaOAc and 2 vol. 95% EtOH. DNA pellet was resuspended in 10 μl dH_20 and stored at -20°C.

2.9.7 Cloning of cDNA fragments

Reamplified and purified candidate cDNA fragments were cloned using the Original TA cloning kit (Invitrogen). One to three microlitres of DNA was ligated to 25 ng pCR®2.1 vector using 1X Ligation Buffer (Invitrogen), and 0.4 U T4 DNA Ligase (Invitrogen) in a final volume of 10 µl. Samples were incubated at 14°C O/N. The following day, transformation of the ligated DNA into bacterial cells was performed. Two µl of ligated DNA was added to a vial of TOP10F'competent cells (Invitrogen) and mixed gently. The mixture was incubated on ice for 30 min, heat shocked for 30s at 42°C and placed on ice for 2 min. Two hundred and fifty µl of SOC medium was added to each tube and samples were shaken horizontally at 37°C for 1 h. While cells were shaking, 40 µl of 40 mg/ml X-Gal and 40 µl 100 mM IPTG were spread onto LB + 50 µg/ml ampicillin agar plates to allow for blue/white colony screening. For each transformation reaction, 50 µl and 200 µl of competent cell mixture was spread onto 2 agar plates which were incubated at 37°C O/N. The next day, agar plates were removed and placed at 4°C to enhance color selection. Six to twelve white colonies per transformation were picked and inoculated into 5 ml of LB broth with 50 µg/ml ampicillin and grown O/N in a 37°C shaking incubator.

2.9.8 Plasmid isolation and restriction digest

Plasmids were isolated using a standard lysozyme/boiling lysis treatment (Sambrook and Russell, 2001) or a purchased kit [Qiagen mini-prep kit (Qiagen) or GenElute Plasmid Miniprep Kit (Sigma)].

Plasmid DNA was digested with *EcoR1*, electrophoresed on a 1% agarose gel and the DNA visualized by UV light following EtBr staining. Those plasmids in which inserts were present were further characterized by sequencing with M13 and Universal sequencing primers as described previously.

2.9.9 Characterization of sequenced cDNAs

Nucleotide-nucleotide BLAST (blastn) searches (http://www.ncbi.nlm.nih.gov/BLAST/) of the isolated differentially expressed transcripts were performed. The candidate transcripts were then separated into various categories based on the results of the sequencing. These categories were: known genes, EST/hypothetical proteins, genomic DNA, repetitive elements and no known homology. Those sequences that matched known genes or EST/hypothetical proteins were further characterized by semi-quantitative RT-PCR as described below.

2.9.10 Semi-quantitative RT-PCR

One hundred ng of polyA+ RNA were reverse transcribed with the oligo $(dT)_{12-18}$ primer as described previously. Serial dilutions from 2^{-2} to 2^{-12} for each cDNA sample were made and each diluted sample was amplified by PCR. Table

2.4 denotes primer sequence, size and annealing temperature for each gene analysed. Amplified products were electrophoresed on a 1% agarose gel and visualized by EtBr staining. The relative intensity of the bands were quantitated by calculating pixel volume obtained by scanning on the Typhoon 9400 Variable Mode Imager (Molecular Dynamics) imaging system and using the ImageQuant software program. The pixel volume can then be used to calculate relative expression of the gene of interest for each sample. Included on every gel, for normalization, was a cDNA sample amplified using *GAPDH* primers to saturation (when the PCR amplification is no longer in the linear range). The pixel volume, which corresponds to relative DNA band intensity, was plotted against the cDNA dilution factor and the resulting log-phase line can be interpolated to cross the X-axis. This value represents the dilution factor at which the cDNA representing the gene of interest has been diluted out, and the PCR amplification is in its linear range. This X-intercept value can then be used, when compared to a control, to determine the relative RNA expression for a particular sample. Using this methodology, the expression level of any given gene of interest can be compared between tumor samples.

2.10 DNA methylation analysis

2.10.1 Sodium bisulfite modification

For sodium bisulfite modification, 1.5 μl freshly prepared 10 N NaOH was added to 2 μg genomic DNA and samples were incubated at 37°C for 15 min. During incubation, 3.6 M sodium bisulfite; pH 5.5 and 10 mM hydroquinone was prepared. Five hundred and twenty µl of sodium bisulfite and 30 µl hydroquinone was added to the DNA/NaOH mixture and samples were overlaid with mineral oil and incubated at 55°C O/N. The following day, the entire modified DNA was removed from the mineral oil and transferred to a new tube and DNA was purified using the Wizard® DNA Clean-up System (Promega) according to manufacturer's instructions. To purified DNA, 1.5 µl 10 N NaOH was added and samples were incubated at RT for 15 minutes. DNA was EtOH precipitated by adding 1/10 vol. 7.5 M NH_4OAc and 2 vol. 95% EtOH. The DNA pellet was resuspended in 30 µl dH_20 and stored at -20°C.

2.10.2 Bisulfite-specific and Methylation-specific PCR

Methylation status of modified DNA was analysed by bisulfite-specific PCR (BSP) and methylation-specific PCR (MSP) followed by direct sequencing. Primers homologous to the modified DNA sequence were designed to 4 different regions within the 5' end of the *Ksp-cadherin* gene and putative promoter region between –17 to +4944 with respect to transcription start site. Two primer sets (MSP01-1M and MSP01-2M) were designed using the MethPrimer Program (http://www.ucsf.edu/urogene/methprimer/index1.html) and included a CG pair in the primer sequence, while the remaining two primer sets were designed manually and did not contain a CG pair in the primer sequence. Table 2.5 denotes primer sequence, product size and annealing temperature of the methylation specific primers. One µl of modified DNA was PCR amplified under the following conditions: 1X bisulfite buffer (16.6 mM $(NH_4)_2{\cdot}SO_4$, 67 mM Tris-Cl;

pH 8.8, 6.7 mM $MgCl_2$, 10 mM β-ME), 1.25 mM dNTPs (Amersham Biosciences), 0.8 pmol forward and reverse primers and 1.25 U platinum Taq polymerase (Invitrogen). DNA was PCR amplified with the following cycling conditions: 95°C for 5 min followed 38 cycles of 95°C for 30s, 51-58°C for 30s, and 70°C for 30s, with a final extension at 70°C for 7 min. Amplified PCR product was purified using Qiaquick PCR purification kit (Qiagen) and purified product was electrophoresed on a 1% agarose gel and visualized by EtBr. PCR products were then sequenced as described previously using the original PCR primers for sequencing.

Table 2.1: *GPC3* PCR primer sequences, PCR product sizes and PCR and WAVE annealing temperatures.

Primer Name	Primer Sequence	PCR product size (bp)	PCR anneal Tm	WAVE Tm
GPC3 Ex1AB	5' AGGTAGCTGCGAGGAAAC 3' TAGGCACGCTCAAGGGAC	349	55°C	66/67°C
GPC3 Ex2AB	5' GTTTGCCCTGTTTGCCATG 3' CAAATAATGATGCCACTAAGC	329	55°C	60/61°C
GPC3 Ex3AB	5' GGATTTTCATGCTTTAATTTG 3' AGGTCACGTCTTGCTCCTC	336	51°C	58/59°C
GPC3 Ex3CD	5' CCTGCCTGATTCAGCCTTGGAC 3' GTTGAAAAGAGACCAAGC	420	55°C	60/61°C
GPC3 Ex3EF	5' GAGAGAATACATTCTGTCC 3' CCTCTGACAACTGTAGAC	173	55°C	58/59°C
GPC3 Ex4AB	5' GAAATTGAAGTGCCTTTCAG 3' CCTTAAAATACAATTGTTAATTG	273	51°C	56/57°C
GPC3 Ex5AB	5' GCCTCTTATGCACAGATG 3' CTGGTGCAATTAATGGAG	262	55°C	58/59°C
GPC3 Ex6AB	5'GATGCCAAATACAGTCAG 3' CTCTCTCTCGGTTATTTC	252	51°C	56/57°C
GPC3 Ex7AB	5' GAAGAGCTGATGCATTCC 3' GAGCTGTATAGTCTTTCC	340	51°C	60/61°C
GPC3 Ex8AD	5' GTGTTATACTGAGGCTATG 3' AAGAGAGAACGATAGAAAGG	674	55°C	60/61°C
GPC3 Ex8EF	5' GTTTGGCTGCTAGAACATGG 3' GAGGTGGGTTTCAAGGAAC	238	55°C	57/58°C
DXS1254	5' GATCTTCTGTTCTTATTTTTAAAT 3' CCGAGAGGACTGTTAAGAG	105	55°C	N/A
DXS106	5'CCTGTACTCCTAGGTATTTGT 3'AGAGAGCCAAATCAAGAATGC	87	55°C	N/A
DXS207	5' ACAACAGCCACAGAAGAGAT 3' AGCTCATTTATTCATCACTGCC	247	55°C	N/A

Table 2.2: Primer sequences for the anchored and internal primers used in the differential display analysis.

Primer name	Primer Type	Primer Sequence
T_{11}MG	Anchored	3' TTTTTTTTTTT(M)G
T_{11}MC	Anchored	3' TTTTTTTTTTT(M)C
T_{11}MA	Anchored	3' TTTTTTTTTTT(M)A
T_{11}MT	Anchored	3' TTTTTTTTTTT(M)T
OPG-1	Internal	5' CTACGGAGGA
OPG-2	Internal	5' GGCACTGAGG
OPG-3	Internal	5' GAGCCCTCCA
OPG-4	Internal	5' AGCGTGTCTG
OPG-5	Internal	5' CTGAGACGGA
OPG-6	Internal	5' GTGCCTAACC
OPG-7	Internal	5' GAACCTGCGG
OPG-8	Internal	5' TCACGTCCAC
OPG-9	Internal	5' CTGACGTCAC
OPG-10	Internal	5' AGGGCCGTCT
OPG-11	Internal	5' TGCCCGTCGT
OPG-12	Internal	5' CAGCTCACGA
OPG-13	Internal	5' CTCTCCGCCA
OPG-14	Internal	5' GGATGAGACC
OPG-15	Internal	5' ACTGGGACTC
OPG-16	Internal	5' AGCGTCCTCC
OPG-17	Internal	5' ACGACCGACA
OPG-18	Internal	5' GGCTCATGTG
OPG-19	Internal	5' GTCAGGGCAA
OPG-20	Internal	5' TCTCCCTCAG

Table 2.3: Primer sequences, PCR product sizes and annealing temperatures of candidate genes analysed by semi-quantitative RT-PCR.

Primer Name	Primer Sequence	PCR product size (bp)	PCR Anneal Tm
MLLT10	5' CTAGTACTCCTGTCTCCAGC 3' TGCTGGCTGCTACTGGAGGC	386	51°C
PLEKHA1	5' GATAACCTAAGTCGCCATGG 3'TGTCGCTTTGCTTACATTCC	375	51°C
VPS45A	5' CAGAGGTTGAGCAAGAACTG 3' AGGTCTGTCTCTGAGTGTGC	445	51°C
POLD3	5' GTCCGCATATGGCACAGGAA 3'TATCAGCAGCACGGCAGCTC	436	51°C
OGFRL1	5' ATCTGAATGAGTCCCAGCAC 3' CTGTCTCTTCCACAGGCTCT	449	51°C
EIF4B	5' ATCAGTGCAGTGCGTTTACC 3' GAGTTTCTTCACTTCGCCAG	875	51°C
ANAPC1	5' CAGCACATCTCAGAAGCCTC 3' CATTGTGTTGGACATCGTCAG	670	51°C
COP9	5' GTGTATGGTCAGCTTCTAGC 3' TACTGACAGGCTCCATCCAG	768	51°C
SYTL2	5' GGATGAGCTTCCACAGAGTC 3' CTGCCACTCACCTCATCTTG	736	55°C
RB1CC1	5' GATGAAGCTATTCAGACTGC 3' GCAATGTTCGTTCTAACAGC	665	51°C
TAF1	5' GAACACAAGGATGGACATGG 3'TAGGCTGGAGAACAGGGAAG	365	51°C
IbtK	5' CTCTGAAGGAAGCTATGCAG 3' CCTCAATCTGAATCAGAGCC	850	58°C

Table 2.4: Ksp-cadherin gene and promoter primer sequences PCR product sizes and annealing temperatures. Primers Ksp-cad AB and Ksp-cad GH were used for RT-PCR while the remaining primers were used in the DNA methylation study.

Primer	Primer Sequence	PCR product size	Anneal Tm
Ksp-cad AB	5' CTGTCTGTGGAAGTTCCAGA 3' GCTCTCCAGGTGATAGTGCA	750	51°C
Ksp-cad GH	5' TCCAGACTCTCAATGGTTCC 3' TGACATTTGGAGCACTCCCA	550	51°C
MSP03-1M	5' TTTGTTAGAGGATGGTAGAGTAGGC 3'CATAAATAATACAACCAAACCCGA	175 bp	58°C
MSP03-1U	5' TTTGTTAGAGGATGGTAGAGTAGGTG 3' CATAAATAATACAACCAAACCCAAA	175 bp	58°C
MSP03-1 +	5' GGTAGTAAGAGATGGTAGTTG 3' ATCCCTAAAACCTATCCACC	365 bp	51°C
MSP03-2M	5' GTTTGGTTAATAAGGCGAAATTTC 3' TATCACCCAAATTAAAATAAAACGC	186 bp	58°C
MSP03-2U	5' TTTGGTTAATAAGGTGAAATTTTGT 3' ATCACCCAAATTAAAATAAAACACA	186 bp	58°C
MSP03-2 +	5' GGATGGGTTAGGTGTAGTGG 3'CAAAACAACCATTTCTATCCC	330 bp	51°C
MSP1n	5' GGTTAGGTATAAAGGGAAAT 3' ATTCAAACCTTACCTACAAC	855 bp	51°C
MSP2n	5' GAGGATTTGATTATAGGAGG 3'ACCCAATAACCTTTTCCACT	449 bp	51°C

Table 2.5: Primer sequences, PCR product sizes and annealing temperatures for β-actin and *GAPDH* as well as M13 and Universal sequencing primers.

Primer Name	**Primer Sequence**	**PCR product size (bp)**	**PCR Anneal Tm**
β-actin	5' CCTCGCCTTTGCCGATCC 3' GGATCTTCATGAGGTAGTCAGTC	626	55°C
GAPDH	5' AGCCACATCGCTCAGAACAC 3' GAGGCATTGCTGATGATCTTG	473	51°C
M13 Forward	CAGGAAACAGCTATGAC	NA	NA
Universal Reverse	GTAAACGACGGCCAG	NA	NA

CHAPTER 3

Analysis of the Simpson-Golabi-Behmel Syndrome (SGBS) gene locus, *GPC3* in sporadic Wilms tumors.

A version of this chapter has been published in:

Gillan TL, Hughes R, Godbout R, Grundy PE. (2003). The Simpson-Golabi-Behmel gene, *GPC3*, is not involved in sporadic Wilms tumorigenesis. Am J Med Genet 122A:30-36.

The Simpson-Golabi-Behmel syndrome is an overgrowth syndrome that shares considerable phenotype overlap with the Beckwith-Wiedemann syndrome making accurate clinical diagnosis between the two difficult. Individuals with either syndrome are predisposed to developing embryonal and childhood cancers, particularly Wilms tumors (Verloes et al., 1995). Most cases of SGBS arise due to a defect in the gene *Glypican 3* (*GPC3*), a proteoglycan of the GRIPs (glypican related integral membrane protein) family. *GPC3* is located on chromosome Xq26 and is the only glypican family member that has been implicated in the etiology of a disease. Expression of *GPC3* is predominantly found in fetal mesodermal-derived tissues of the kidney, liver and lung. Minimal levels of expression have been found in adult tissues including mesothelium, breast and ovary (Pilia et al., 1996). The exact function of GPC3 is not known, however it is thought to be similar to that of the other glypican family members, which are involved in cell growth and differentiation during mammalian development.

Constitutional inactivation of *WT1* and the putative *WT2* gene give rise to syndrome (WAGR, DDS, BWS) associated Wilms tumors, while somatic alterations lead to tumor formation in otherwise normal children. Since individuals with SGBS are predisposed to developing Wilms tumor, *GPC3* is expressed in fetal mesodermal tissues including kidney and *GPC3* is believed to play a role in development, we hypothesized that some sporadic Wilms tumors may also harbor somatic mutations in the SGBS gene, *GPC3*. Involvement of the X-linked *GPC3* gene could also provide a possible explanation for the observation that males are diagnosed on average six months earlier than females, as hemizygous males would be more prone to loss of gene function.

3.1 Wilms tumor sample population

Sixty-four Wilms tumors were selected for the *GPC3* study. Of the 64, 48 were from male patients, 14 from female patients and in 2 the sex was unrecorded. Due to the fact that *GPC3* is an X-linked gene, and the hemizygous state would facilitate the identification of mutations, a disproportionately high number of males were selected. Fifty-one of the Wilms tumors were sporadic cases while 12 were from individuals diagnosed with BWS and/or hemi-hypertrophy and one Wilms tumor was from an individual with SGBS and was included as a positive control. An extensive DNA analysis of the SGBS gene, *GPC3,* was performed on 64 Wilms tumors by Southern blot analysis, heteroduplex analysis via denaturing HPLC, sequencing and Northern blot analysis.

3.2 Identification of *GPC3* mutations by southern blot analysis

The search for large chromosomal deletions and/or insertions in 64 Wilms tumors and corresponding constitutional or normal kidney DNA samples was performed using Southern blot analysis. Tumor and corresponding normal kidney or constitutional DNA were digested with *Taq1* and *Pst1* restriction enzymes. Southern blots were hybridized with the full length *GPC3* cDNA probe.

A tumor-specific deletion of the entire *GPC3* gene was identified in both the *Taq1* and *Pst1* digests in one Wilms tumor (WT-42T), from a male patient (Figure 3.1). In the corresponding normal kidney, *GPC3* was present. Since the entire *GPC3* gene was deleted in this tumor, it is possible that a large portion of the X chromosome or the entire chromosome was also deleted. In order to determine whether this deletion was specific to the *GPC3* gene or if it encompassed a large part, or all of the X chromosome, microsatellite analysis was performed on DNA from this Wilms tumor, the adjacent normal kidney and a normal control. Three microsatellite markers, 2 of which flanked the *GPC3* gene and spanned a 64 Mb region and 1 marker, on the p arm of the X chromosome, were used for analysis (Figure 3.2). DNA was successfully amplified in all 3 DNA samples for all 3 microsatellite markers (Figure 3.3). These results indicate that the X chromosome is intact and the deletion is confined to the *GPC3* gene itself or a smaller chromosomal region flanking the gene within the 64 Mb region that is deleted; however, the extent of the deletion was not further defined.

Further analysis of the *Taq1* digests hybridized with *GPC3* revealed a loss of the second (8.2 kb) *Taq1* fragment in 3 Wilms tumors (WT-43, WT-44 and WT-45) and their corresponding normal kidney DNA (Figure 3.4). Samples WT-44 and WT-45 were from males while WT-43 was from a female individual. Upon initial hybridization with the full length *GPC3* cDNA, it was thought that the absence of the 8.2 kb represented a constitutional deletion. However, further evaluation of these tumors revealed that the loss of the second *Taq1* fragment represented a polymorphism. Hybridization with a probe comprised of only the

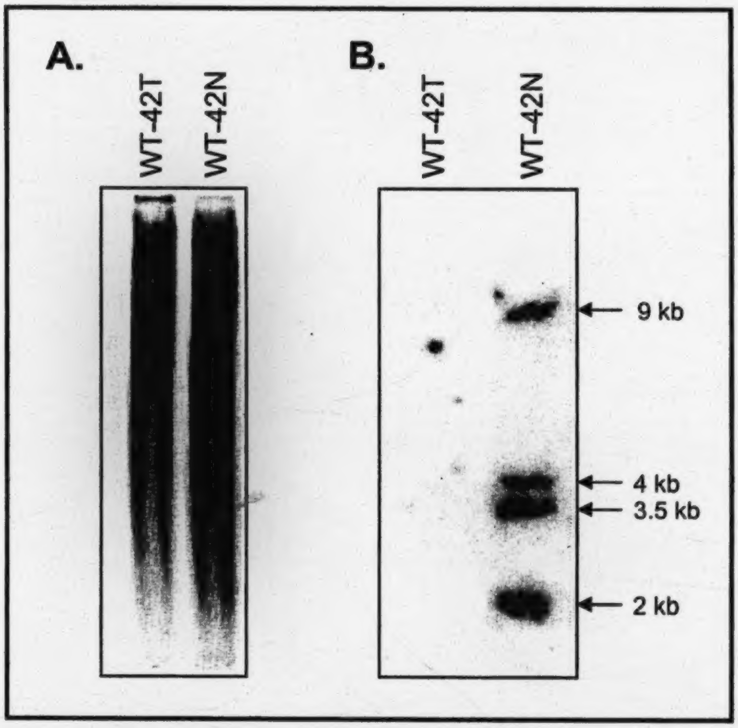

Figure 3.1: Southern blot of Wilms tumor WT-42T hybridize with GPC3. A. Ethidium bromide stained agarose gel of *Taq1* digested DNA from Wilms tumor WT-42T and its corresponding normal kidney DNA, WT-42N, demonstrating equal amounts of DNA in each lane. **B.** Autoradiogram of WT-42T and WT-42N hybridized with the full length *GPC3* cDNA probe. In Wilms tumor WT-42T the entire *GPC3* gene is absent.

Figure 3.2: Ideogram of the X chromosome. Location of the microsatellite markers, used in the microsatellite analysis, relative to the *GPC3* gene. Ideogram taken from the NCBI Mapviewer website (http://www.ncbi.nlm.nih.gov/mapview/maps.cgi?taxid=9606&chr=X).

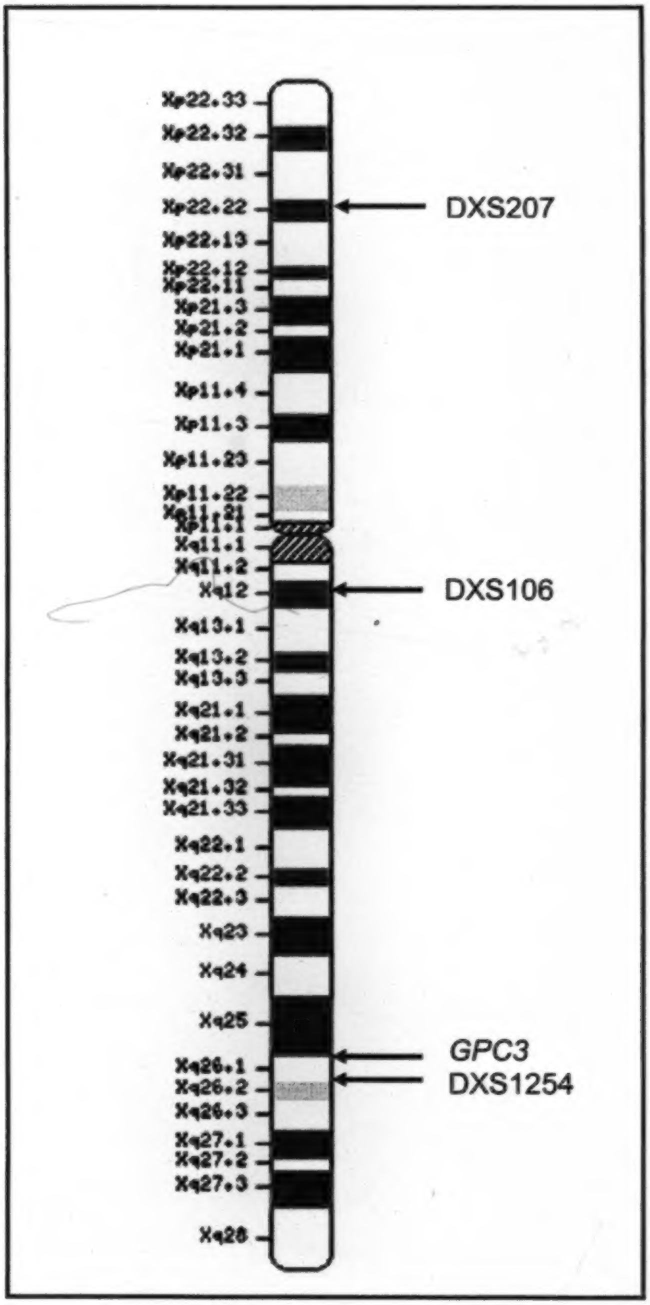
Xp22.33
Xp22.32
Xp22.31
Xp22.22
Xp22.13
Xp22.12
Xp22.11
Xp21.3
Xp21.2
Xp21.1
Xp11.4
Xp11.3
Xp11.23
Xp11.22
Xp11.21
Xp11.1
Xq11.1
Xq11.2
Xq12
Xq13.1
Xq13.2
Xq13.3
Xq21.1
Xq21.2
Xq21.31
Xq21.32
Xq21.33
Xq22.1
Xq22.2
Xq22.3
Xq23
Xq24
Xq25
Xq26.1
Xq26.2
Xq26.3
Xq27.1
Xq27.2
Xq27.3
Xq28
DXS207
DXS106
GPC3
DXS1254

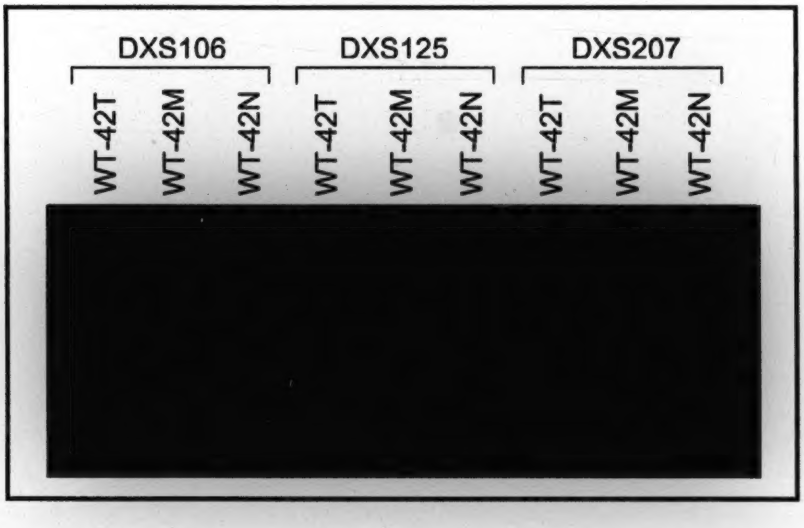
DXS106
DXS125
DXS207
WT-42T
WT-42M
WT-42N
WT-42T
WT-42M
WT-42N
WT-42T
WT-42M
WT-42N

Figure 3.3: X chromosome microsatellite analysis of sample WT-42

Microsatellite analysis was performed with 3 markers that span the X chromosome to determine if the entire chromosome or only a portion of it was deleted. WT-42T (tumor), WT-42M (maternal) and WT-42N (constitutional) DNA were analysed. The DNA was successfully amplified in all 3 samples for all 3 primer sets and the appropriate PCR product sizes for the 3 microsatellite markers [DXS106 → 87-103 bp; DXS1254 → 99-113 bp; DXS201 → 174-194 bp) were seen. These results indicate that the entire chromosome is not deleted but rather the deletion is confined between the 2 *GPC3* flanking microsatellite markers DXS106 and DXS1254.

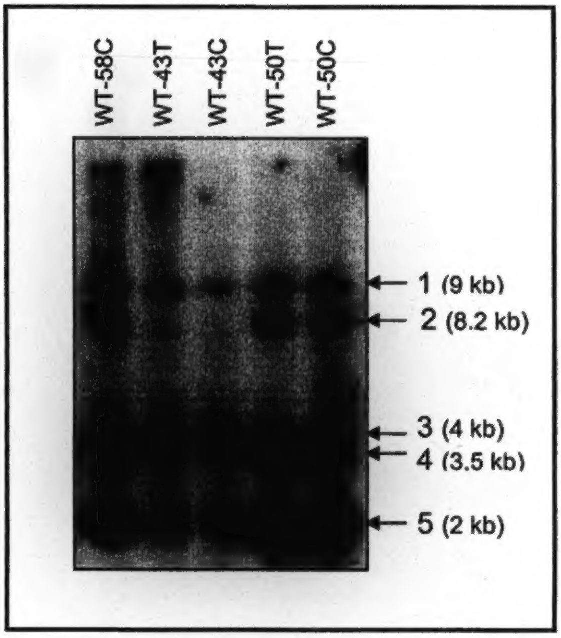
WT-58C
WT-43T
WT-43C
WT-50T
WT-50C
1 (9 kb)
2 (8.2 kb)
3 (4 kb)
4 (3.5 kb)
5 (2 kb)

Figure 3.4: Southern blot analysis of *Taq 1* digested Wilms tumor and corresponding constitutional DNA hybridized with *GPC3*. *Taq 1* digested DNA is hybridized to full length *GPC3* cDNA. Hybridization with the full length *GPC3* reveals the presence of five *Taq 1* fragments (numbered 1 – 5 on the autoradiogram). The second *Taq 1* fragment, which represents the 8.2 kb band, is deleted in samples WT-43C and WT-43T. C – constitutional DNA; T – tumor DNA.

last 3 exons of the *GPC3* gene revealed the presence of a 4 kb band in all samples missing the 8.2 kb band. This band was not present in the samples that retained the 8.2 kb band. Analysis of WT-43 maternal DNA also revealed the presence of this 4 kb band but not the 8.2 kb band, confirming that this alteration is a polymorphism rather than a deletion (Fig 3.5). Interestingly these three cases were all from patients of African American descent. Chi-square analysis was performed to test whether there is an association between these polymorphisms and African American descent. Of the 64 Wilms tumors, 12/64 (19%) were African American and of these, 3/12 (25%) were found to have the *Taq1* polymorphism versus 0/52 non-African American samples ($p < 0.001$). This indicates there is a statistically significant increase in the incidence of the *Taq1* polymorphism in the African American population. No other band shifts, deletions or insertions were found in the remaining Wilms tumor samples with either the *Taq1* or *Pst 1* digests suggesting that large deletions/insertion within the *GPC3* gene are not common in Wilms tumors.

3.3 Identification of small *GPC3* mutations by heteroduplex analysis

In order to detect small deletions, insertions and/or point mutations, heteroduplex analysis, via denaturing HPLC, using the WAVE™ DNA Fragment Analysis System, was performed for each of the 8 *GPC3* exons in all 64 Wilms tumors. Heteroduplex analysis identifies sequence changes, based on the different duplexes that form depending on whether the test and control templates are identical and, therefore form homoduplexes, or whether a sequence change

Figure 3.5: Southern blot analysis of *Taq1* digested DNA with segments of the *GPC3* gene.

A. Hybridization with *GPC3* exons 1-3 hybridizes to *Taq1* fragments 1, 3 and 4. **B.** Hybridization with *GPC3* exons 3-5 hybridizes to *Taq1* fragments 3, 4 and 5. **C.** Hybridization with *GPC3* exons 5-8 hybridizes to *Taq1* fragments 1 (which appears to be a similar size as a fragment identified with the *GPC3* exons 1-3 cDNA probe) and 2. The second *Taq1* fragment is not present in samples WT-43C, WT-43T and WT-44T as seen with hybridizations with the full length cDNA probe. In addition to deletion of the second *Taq1* fragment, hybridization with the last 3 *GPC3* exons reveals the presence of another *Taq1* fragment (3*) not present in the Wilms tumors without the deletion of fragment 2. This 3* fragment was not seen with hybridization with the full length or 5' *GPC3* probes as it is the same size as the third *Taq1* fragment and was therefore masked. The presence of this 3* fragment was also seen in samples WT-44C/T and WT-45C/T when probed with the 3' end of the gene. **D.** Hybridization of WT-43 maternal DNA with the last 3 exons of *GPC3* revealed the presence of both the second *Taq1* fragment and the 3* *Taq1* fragment confirming that this alteration is a polymorphism rather than a deletion.

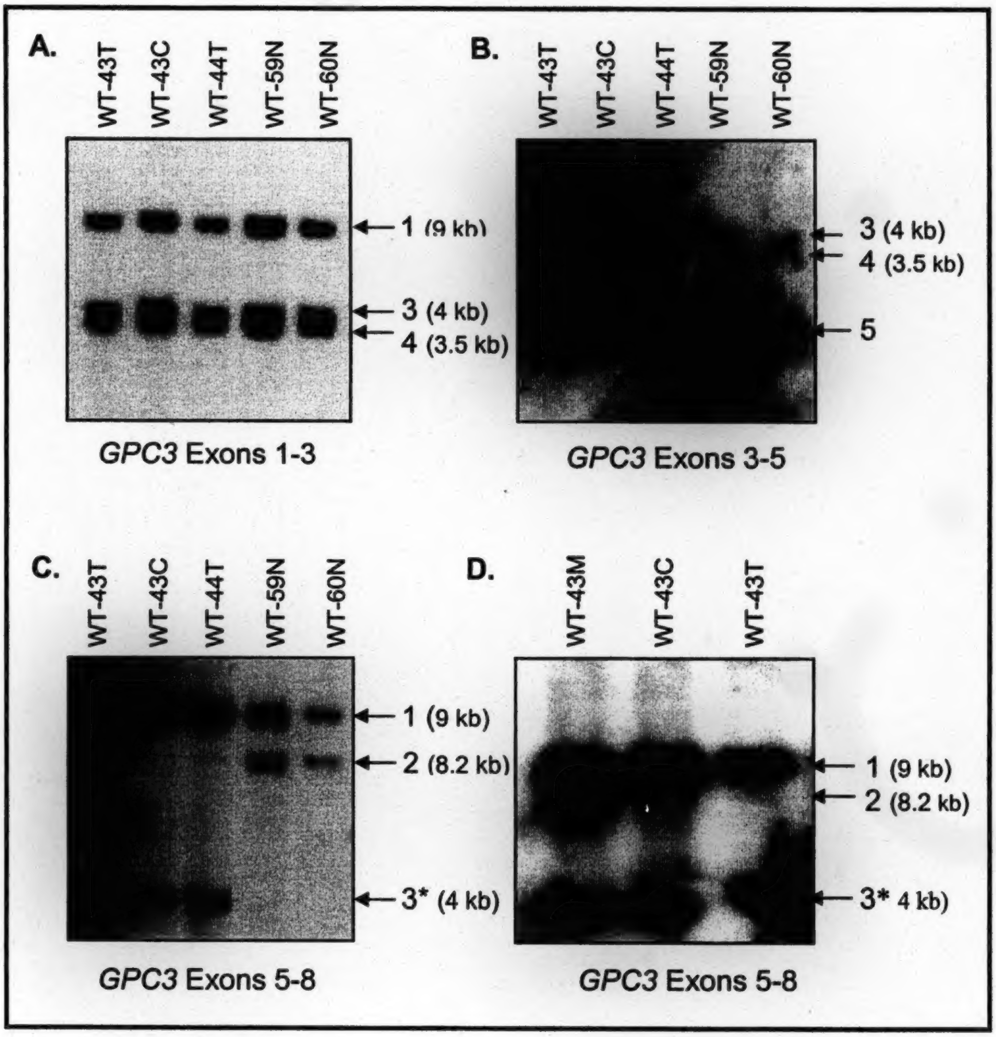
A.
WT-43T
WT-43C
WT-44T
WT-59N
WT-60N
1 (9 kb)
3 (4 kb)
4 (3.5 kb)
B.
WT-43T
WT-43C
WT-44T
WT-59N
WT-60N
3 (4 kb)
4 (3.5 kb)
5
C.
WT-43T
WT-43C
WT-44T
WT-59N
WT-60N
1 (9 kb)
2 (8.2 kb)
3* (4 kb)
D.
WT-43M
WT-43C
WT-43T
1 (9 kb)
2 (8.2 kb)
3* 4 kb)

GPC3 Exons 1-3

GPC3 Exons 3-5

GPC3 Exons 5-8

GPC3 Exons 5-8

is present creating the formation of heteroduplexes. Due to the different melting temperatures of the hetero- and homoduplexes, they elute at different times from the HPLC column and can be distinguished from one another based on the peaks or WAVEs that this creates when graphed. Heteroduplexes produce WAVEs distinctly different from the WAVEs created by the normal control homoduplex and are therefore termed abnormal WAVEs. Eleven abnormal WAVEs in nine tumors were identified and included three in exon 2, four in exon 7 and four in exon 8. Tumors that displayed abnormal WAVEs were further characterized by sequencing.

One of the tumors with an abnormal WAVE in exon 2, sample WT-46, was from a male child with SGBS who was included to serve as a positive control for mutation detection. Sequencing of this tumor revealed a 13 bp deletion at nucleotide 384 (Genbank accession number XM 029475) (Fig 3.6) resulting in the production of a premature stop codon. This deletion was also present in the corresponding constitutional DNA suggesting that this exon 2 *GPC3* deletion is the underlying defect resulting in SGBS in this child. This deletion is in concordance with that described previously by Xuan et al. (1999).

Sequencing of sample WT-47, from a male child with BWS, revealed a C_{446} → T exon 2 transition mutation resulting in a premature stop codon (CGA → UGA) (Figure 3.7) in both the tumor and corresponding constitutional DNA. The identification of the *GPC3* nonsense mutation suggests that this particular individual has SGBS and not BWS as originally diagnosed. In the third sample with an abnormal WAVE in exon 2, WT-48 (from a female child), no sequence

Figure 3.6: ***GPC3*** **exon 2 WAVE and sequencing results for sample WT-46.** Abnormal WAVEs, distinct from the normal control DNA (pink), were seen in samples WT-46T (black) and WT-46C (blue). Sequencing of both tumor and constitutional DNA revealed a 13 bp deletion as seen in the sequencing electropherogram. C = constitutional; T = tumor

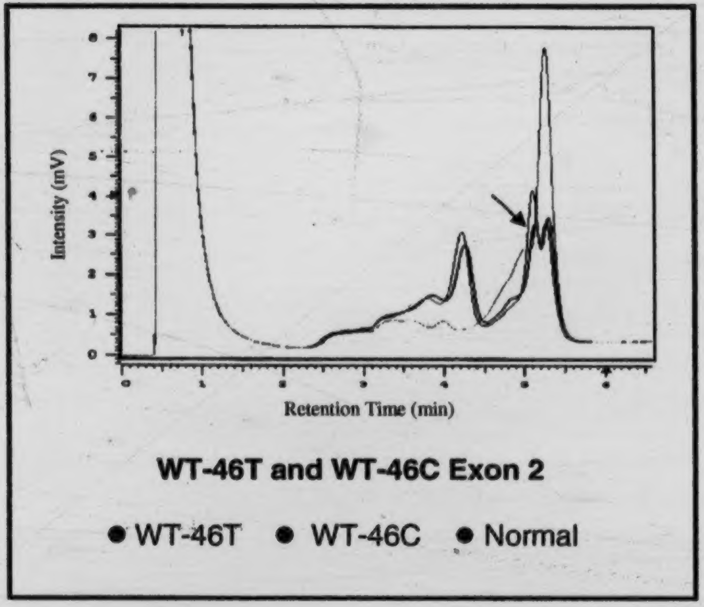

WT-46T and WT-46C Exon 2

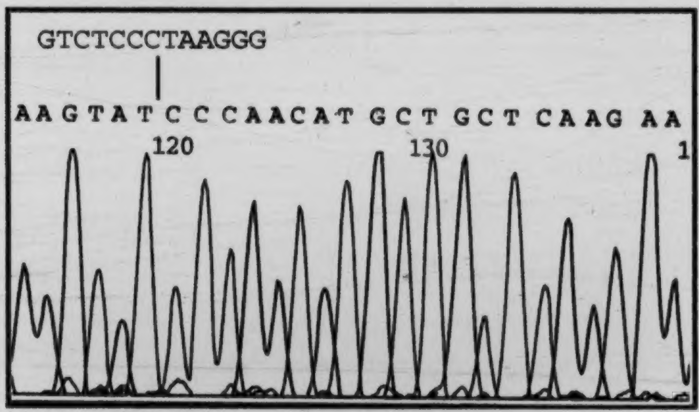

Exon 2 – WT-46T 13 bp deletion

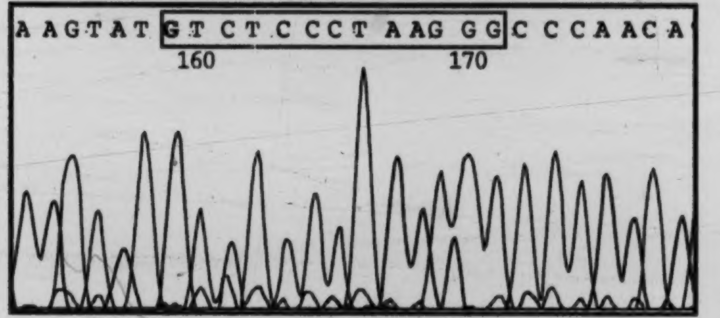

Exon 2 wild type sequence

Figure 3.7: ***GPC3*** **exon 2 WAVE and sequencing results for sample WT-47T.** An abnormal WAVE (pink) in exon 2, distinct from the WAVEs of the other tumors and normal control DNA, was seen for sample WT-47T. Sequencing of this sample revealed a C → T transition mutation that resulted in the formation of a premature stop codon as seen in the sequencing electropherogram. The same abnormal WAVE and sequence change was also found in WT-47 corresponding constitutional DNA.

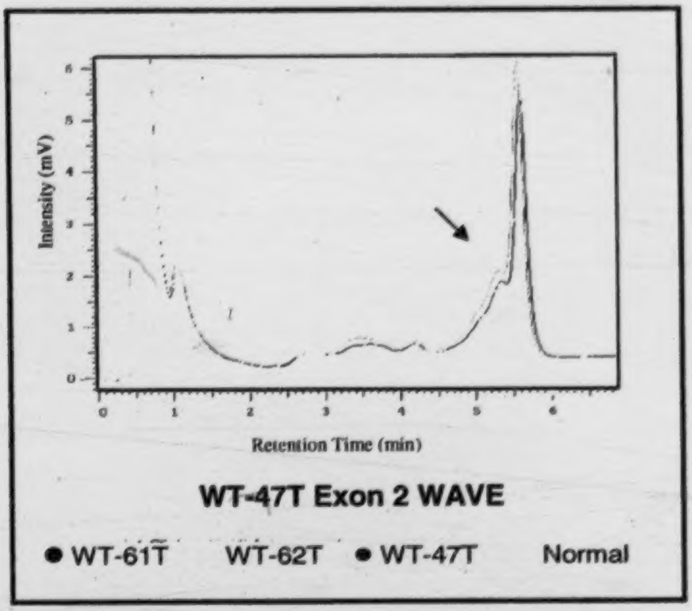

WT-47T Exon 2 WAVE

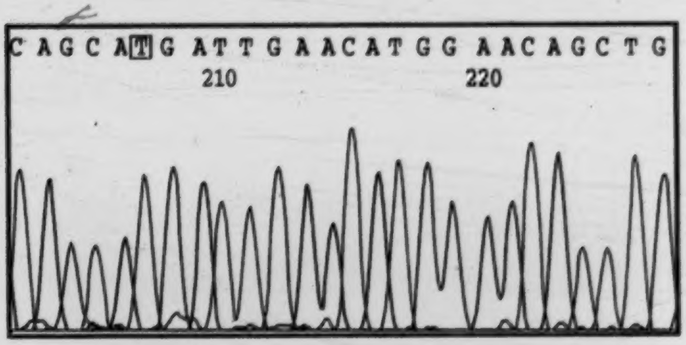

Exon 2 – WT-47T; C → T premature stop

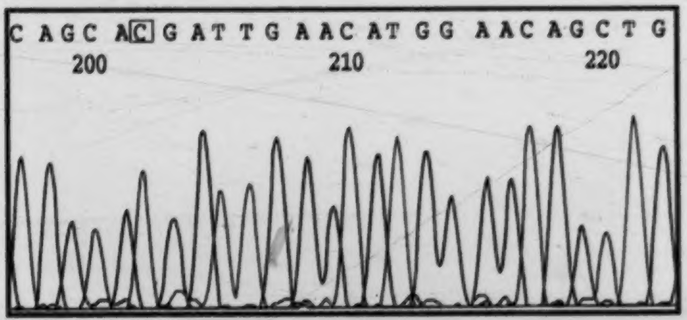

Exon 2 wild type sequence

change was found within the exon suggesting that the sequence change may reside in one of the flanking introns. Review of the sequence showed that splice sites were not affected and evaluation of this tumor by Northern analysis did not reveal any changes in transcript size.

DNA sequencing of the four tumors with abnormal WAVEs in exon 7 revealed that 3 of the 4 tumors (WT-43, WT-44 and WT-45) contained a $T_{690} \rightarrow C$, silent, single base pair change that was previously reported in ovarian cancer cell lines (Figure 3.8) (Lin et al., 1999). The corresponding constitutional DNA for these 3 tumors also had the $T_{690} \rightarrow C$ silent mutation. It is believed that this sequence change represents a polymorphism as it does not cause an amino acid change and the transition mutation is present in both the constitutional and tumor DNA. Interestingly, these 3 cases were the same cases found to have the *Taq1* polymorphism identified by Southern blot analysis. However, it is not thought that this sequence change causes the *Taq1* polymorphism as the $T_{690} \rightarrow C$ sequence change does not disrupt a *Taq1* restriction site. Since these were the identical tumor samples that contained the *Taq1* polymorphism that is associated with the African American population, this exon 7 polymorphism should also demonstrate a statistically significant association with the African American population. Chi-square analysis supports this association ($p < 0.001$).

Sequencing of exon 7 from the male patient, WT-49, revealed a C → T single base pair change within the intron between exons 7 and 8 (Figure 3.9). Examination of sequence showed no disruption of splice sites nor any changes in

Figure 3.8: *GPC3* exon 7 WAVE and sequencing results for sample WT-44. An abnormal WAVE (pink) in exon 7, distinct from the other tumors and normal control DNA, was seen for sample WT-44T. Sequencing identified a silent transition T → C mutation in tumor WT-44T as seen in the sequencing electropherogram. Abnormal WAVEs and the identical sequence change was seen in the corresponding constitutional DNA as well as in the constitutional-tumor pairs WT-45C/T and WT-43C/T. C = constitutional; T = tumor.

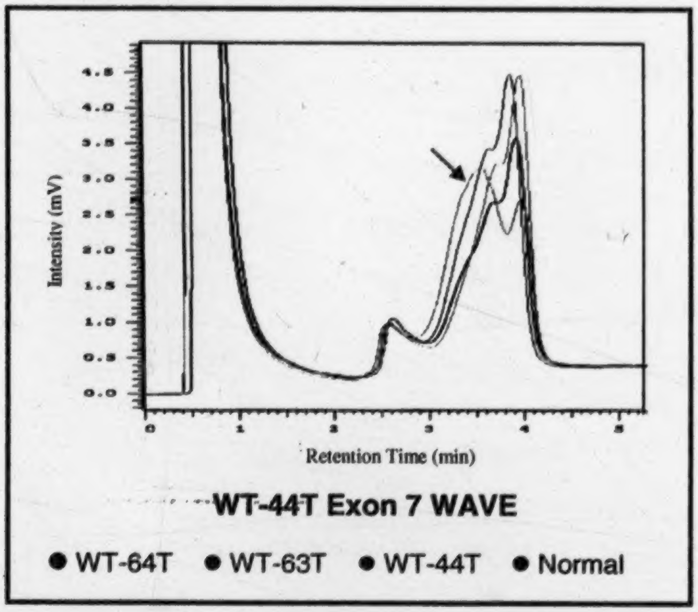

WT-44T Exon 7 WAVE

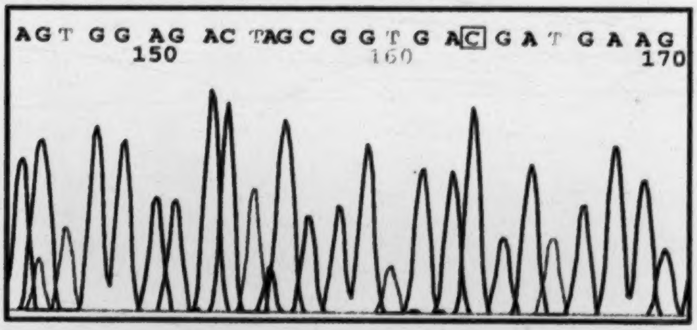

WT-44T Exon 7 T → C silent mutation

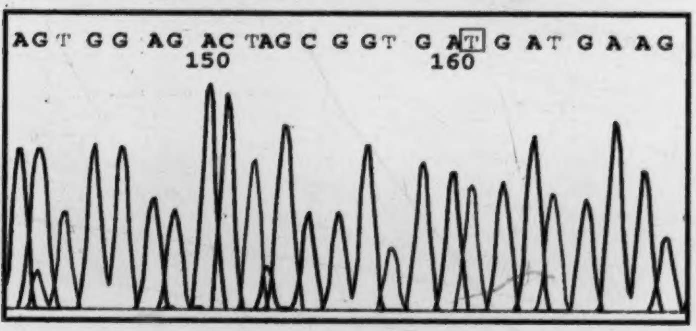

Exon 7 wild type sequence

Figure 3.9: ***GPC3*** **exon 7 WAVE and sequencing results for sample WT-49T.** An abnormal WAVE (black), as compared to the other tumors and normal control, was seen for sample WT-49T in exon 7. Sequencing identified a C → T transition mutation within the intron between exons 7 and 8 as seen in the sequencing electropherogram. Constitutional DNA was not analysed.

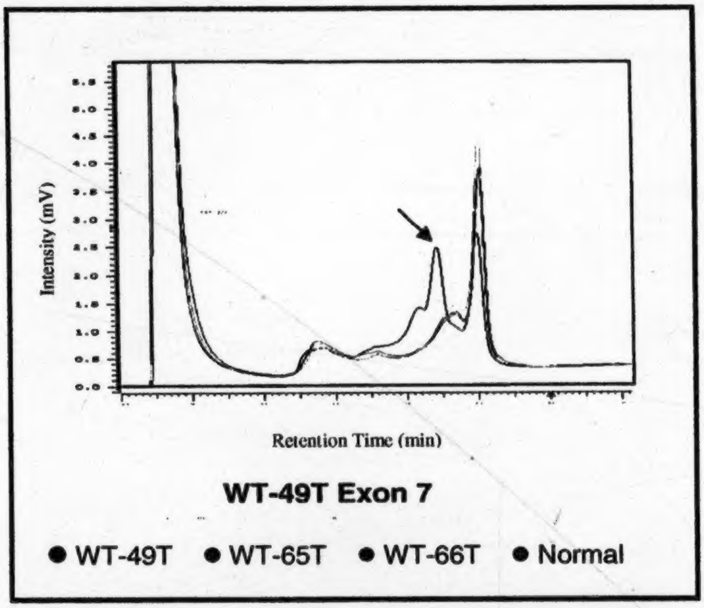

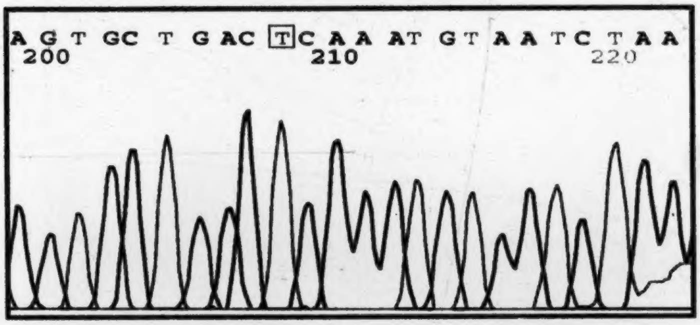

Exon 7 – WT-49T; intronic C → T transition mutation

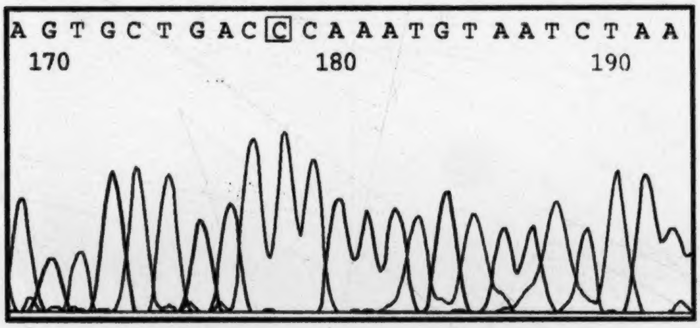

Exon 7 wild type sequence

transcript size by Northern blot analysis suggesting this sequence change also represents a polymorphism.

Two distinct sequence changes in exon 8 were found in 4 Wilms tumors. In three cases, WT-48T, WT-45T and WT-51T, a female and two males respectively, a silent single base pair polymorphism $A_{1816} \rightarrow G$ was detected. This transition mutation was also present in their corresponding constitutional DNA and was previously reported in ovarian cancer cell lines (Lin et al., 1999b) (Figure 3.10). In addition to the $A_{1816} \rightarrow G$ polymorphism, a second sequence change was detected in samples WT-48T and WT-45T, as well as in sample WT-50T, from a female patient. This 4 bp (GAAA) deletion at nucleotide 2155 (Genbank accession number XM 029475) is located in the 3' UTR (Figure 3.11). Sequencing of constitutional DNA corresponding to each tumor and parental DNA (where available) revealed the identical 4 bp deletion. Interestingly, these 3 tumors were from patients of African American descent but only one (WT-45) also contained the *Taq1* and exon 7 polymorphisms. Northern blot analysis of tumors WT-48T and WT-50T, for which RNA was available, did not reveal any differences in transcript size suggesting this deletion represents a polymorphism.

To test the possibility that this 4 bp deletion is a polymorphism rather than a deletion involved in Wilms tumorigenesis, heteroduplex and sequencing analysis (where applicable) of exon 8 in 89 samples from a non-Wilms tumor population were examined. Included in the 89 samples were 13 samples from individuals of African American descent. The 4 bp 3' UTR deletion was found in 3 of the non-Wilms tumor samples. Interestingly, all 3 were of African American

Figure 3.10: ***GPC3*** **exon 8 WAVE and sequencing results for sample WT-51T.** An abnormal WAVE (blue), as compared to the other tumors and normal control, was seen in exon 8 for sample WT-51T. Sequencing revealed a G → A silent, transition mutation as seen in the sequencing electropherogram. Abnormal WAVEs and the same sequence change was found in the constitutional DNA and in the constitution-tumor DNA pairs WT-45C/T and WT-48C/T. C = constitutional; T = tumor.

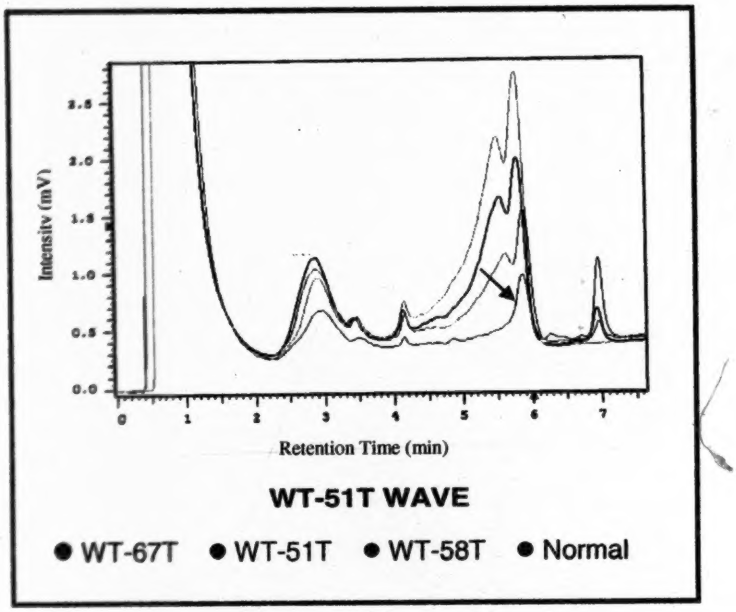

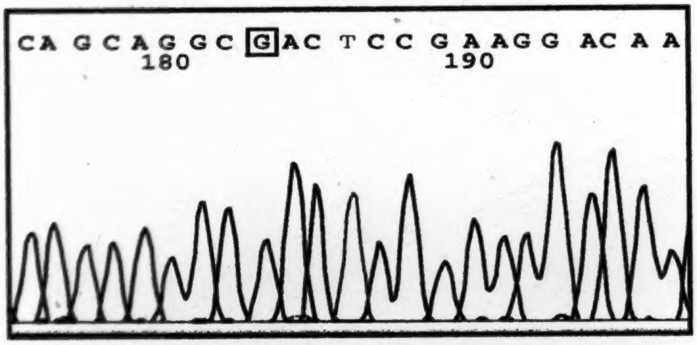

Exon 8 – WT-51T; G → A silent mutation

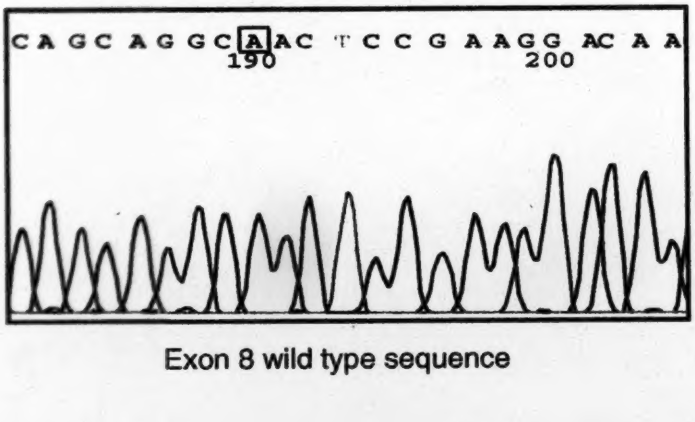

Exon 8 wild type sequence

Figure 3.11: *GPC3* exon 8 WAVE and sequencing results for sample WT-48T. An abnormal WAVE (black) in exon 8, as compared to the other tumors and normal control, was seen in sample WT-48T. Sequencing identified a 4 bp deletion in the 3' UTR. Abnormal WAVEs and the same 4 bp deletion was seen in the corresponding constitutional DNA and in the constitutional-tumor pairs WT-50C/T and WT-45C/T.

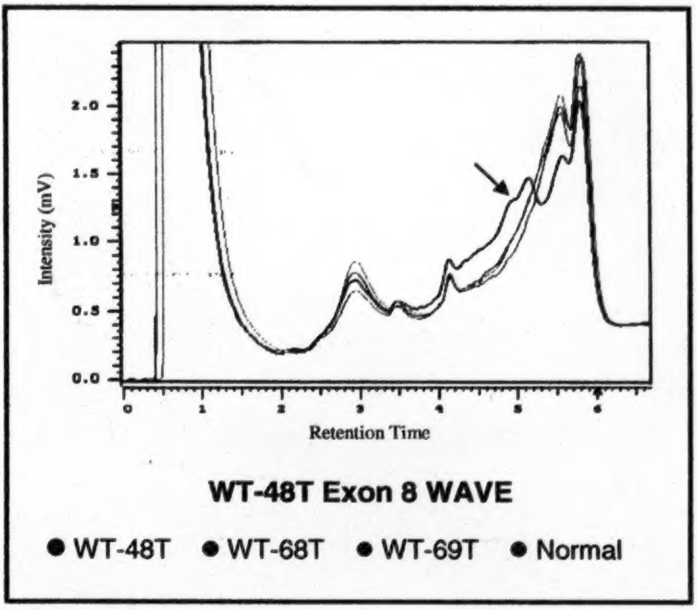

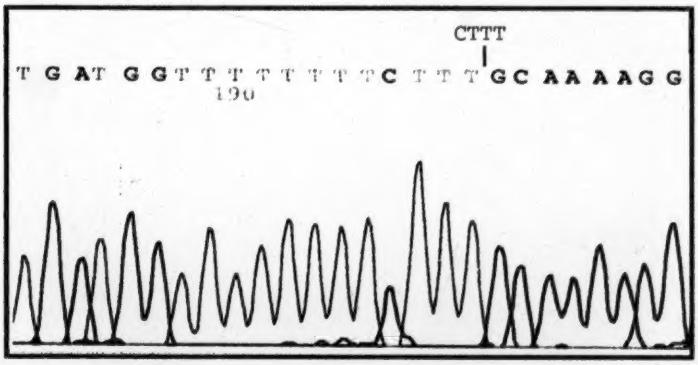

Exon 8 – WT-48T; 4 bp deletion (CTTT)

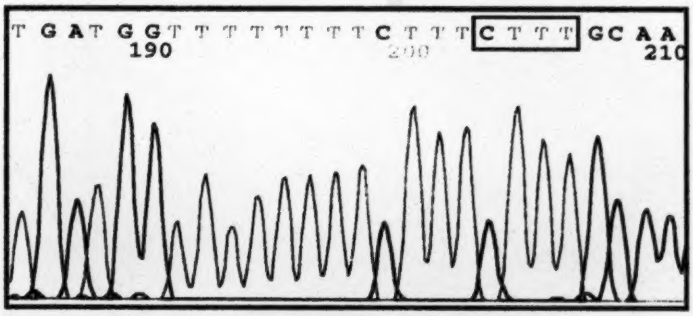

Exon 8 wild type sequence

descent. Chi-square analysis was performed to see if the exon 8 3' UTR deletion, like the *Taq1* and exon 7 polymorphisms, had statistically significant association with the African American population. Of the 153 samples evaluated by exon 8 WAVE analysis, 64/153 (42%) were Wilms tumors and 89/153 (58%) were non-Wilms tumor samples. Of the 42% of Wilms tumor, 15% were of African American descent and 25% of this population had the deletion versus 0% of the non-African American Wilms tumors. Furthermore, in the non-Wilms tumor population, 13/89 (15%) were African American and of these 13, 3/13 (13%) had the exon 8 deletion versus 0% in the non-African American population. Chi-square analysis found the association of the exon 4 bp deletion with the African American population to be statistically significant ($p<0.0001$). This supports the hypothesis that the deletion is a polymorphism exclusive to the African American population. To further confirm that this polymorphism is associated with the African American population and not with Wilms tumors, additional Chi-square analysis was performed. Three of the sixty-four (4.7%) Wilms tumor contained the 3' UTR deletion compared to 3/89 (3.4%) of the non-Wilms tumor population. Chi-square analysis determined that this association was not statistically significant ($p \leq 1$) and therefore no association exists between the 3' UTR deletion and Wilms tumors. Identification of the 3' UTR deletion in several non-Wilms tumor samples together with the Chi square results provide strong evidence that the 3' UTR deletion is a polymorphism unique to the African American population rather than a deletion involved in Wilms tumorigenesis.

3.4 RNA expression analysis of *GPC3*

Tissue for 36 Wilms tumors and 6 normal mature kidney samples was available for RNA extraction and subsequent expression analysis. Expression of *GPC3* RNA was evaluated by Northern blot analysis followed by densitometric analysis. No altered size transcripts were seen in any of the Wilms tumors or normal kidney samples ruling out splice site mutations and/or the presence of alternatively spliced transcripts. Of the 6 normal kidney tissues, *GPC3* RNA was abundantly expressed in 1/6 kidneys and either absent or significantly reduced in the remaining 5 samples. Comparable (±3 fold variation) *GPC3*:β-actin ratios, as determined by densitometric analysis, were found in 29/36 Wilms tumors including WT-51T, WT-52T, WT-53T and WT-54T. However, for the remaining 7 tumors, *GPC3* RNA expression was either significantly increased or reduced as compared to the β-actin control as seen in Figure 3.12. For the SGBS case WT-46T, which contained the premature stop codon in exon 2, *GPC3* RNA was not expressed. Other Wilms tumors, notably WT-49T and WT-55T also had significantly reduced *GPC3* RNA expression as compared to their β-actin controls. Conversely, *GPC3* RNA expression for Wilms tumors WT-56T and WT-57T was substantially increased as compared to their β-actin controls. Wilms tumors identified with *GPC3* polymorphisms, for which RNA was available for analysis, all expressed abundant levels of *GPC3* RNA. Table 3.1 provides a summary of the *GPC3* DNA and RNA results for which putative mutations/polymorphisms were identified.

Figure 3.12: RNA expression of *GPC3* in Wilms tumor and normal kidney. Representative Northern blot analysis of GPC3 expression in 11 Wilms tumors and 3 normal kidney samples. *GPC3* expression could not be evaluated in case WT-42T (which was missing the entire gene/chromosomal region) due to insufficient β-actin RNA levels. *GPC3* was abundantly expressed in most Wilms tumors and one normal sample, WT-65N. *GPC3* expression was reduced or absent in two of the normal kidney samples, WT-56N and WT-55N and in 3 Wilms tumors WT-49T, WT-55T and WT-53T.

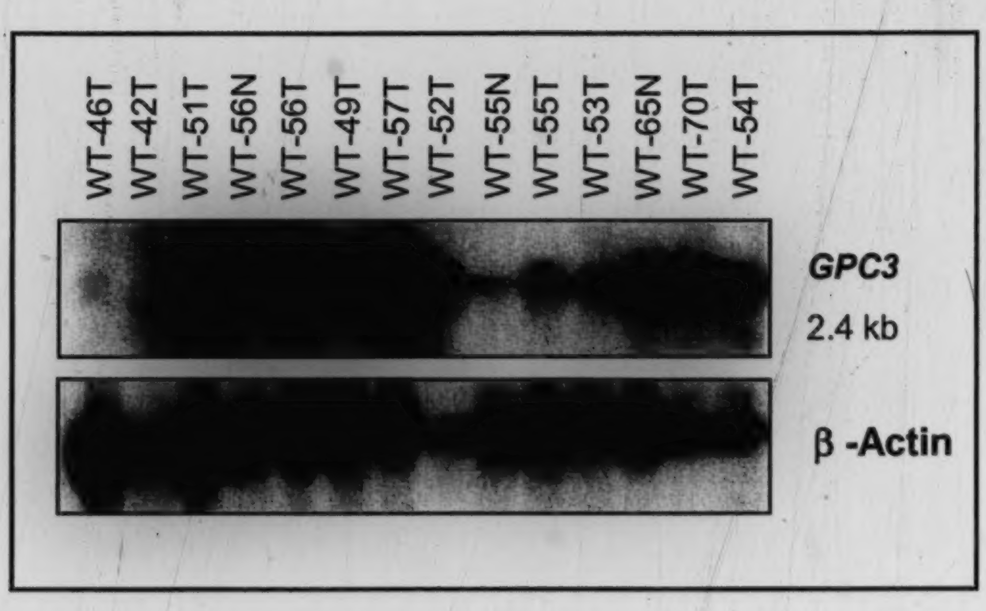
WT-46T
WT-42T
WT-51T
WT-56N
WT-56T
WT-49T
WT-57T
WT-52T
WT-55N
WT-55T
WT-53T
WT-65N
WT-70T
WT-54T
GPC3
2.4 kb
β -Actin

Table 3.1: Summary of Wilms tumor cases with *GPC3* polymorphisms/mutations.

CASE #	Anomalies	Race	Southern Blot	RNA Expression	Heteroduplex Analysis	Tumor Sequence	Constitutional Sequence
WT-42		Caucasian	Absent	NA	ND	ND	ND
WT-46	SGBS	Caucasian	Normal	Absent	Abnormal wave	Ex 2 13bp del premature stop	Same as tumor
WT-47	WBS or SGBS	Caucasian	Normal	NA	Abnormal wave	Ex 2 C → T premature stop	Same as tumor
WT-48		African American	Normal	Expressed	Abnormal waves	Ex 2 N/C in coding region; Ex 8 A → G silent; Ex 8 4bp del 3' UTR	Same as tumor
WT-49		Native American	Normal	Expressed	Abnormal wave	Ex 7 intronic C → T	ND
WT-43		African American	Taq 1 polymorphism	Expressed	Abnormal wave	Ex 7 T → C silent	ND
WT-44		African American	Taq 1 polymorphism	Expressed	Abnormal wave	Ex 7 T → C silent	Same as tumor
WT-45		African American	Taq 1 polymorphism	NA	Abnormal waves	Ex 7 T → C silent; Ex 8 A → G silent; Ex 8 4bp del 3' UTR	Same as tumor
WT-50	Hemi-hypertrophy	African American	Normal	Expressed	Abnormal wave	Ex 8 4bp del. 3' UTR	Same as tumor
WT-51		Caucasian	Normal	NA	Abnormal wave	Ex 8 A → G silent	ND

NOTE. - ND = not done, NA = RNA not available or degraded, N/C = no change, del = deletion.

3.5 Discussion

We hypothesized that non-SGBS Wilms tumors would harbor somatic alterations of *GPC3* and provide evidence of an additional pathway of Wilms tumorigenesis. Other than the tumor-specific deletion of the entire *GPC3* gene/chromosome region identified in one sporadic Wilms tumor from a male patient, no evidence of any *GPC3* functional mutations were found; however, several *GPC3* polymorphisms were identified. Variable *GPC3* expression was seen as 7/36 Wilms tumors had reduced or absent *GPC3* expression, while the remaining 29 tumors displayed moderate to high *GPC3* expression levels. This variation could be attributed to the fact that Wilms tumors are embryonal tumors made up of stromal, blastemal and epithelial cells in varying stages of differentiation and development and likely express *GPC3* at varying levels. Although the role of *GPC3* in sporadic Wilms tumor is limited, *GPC3* has been shown to have tumor suppressing abilities in other cancers. Studies in malignant mesothelioma, ovarian and breast cancer cell lines, the normal counterparts of which express *GPC3*, revealed that *GPC3* was silenced via aberrant promoter methylation (Lin et al., 1999; Xiang et al., 2001; Murthy et al., 2000). Furthermore, mutation analysis of malignant mesothelioma and breast cancer cell lines failed to reveal *GPC3* mutations, supporting aberrant *GPC3* promoter hypermethylation as the predominant mechanism of *GPC3* gene inactivation. Treatment of the cell lines with the demethylating agent, 5-aza-deoxycytidine, restored *GPC3* expression and suppressed tumor growth supporting the hypothesis that *GPC3* may function as a tumor suppressor gene in some adult cancers. Methylation analysis of the *GPC3* promoter was also evaluated in Wilms tumors and neuroblastomas and the authors found no correlation between promoter methylation in these tumors and *GPC3* expression. This suggests that promoter methylation is likely not a predominant mechanism used for regulating *GPC3* gene expression in embryonal cancers (Saikali and Sinnet, 2004).

Involvement of *GPC3* in hepatocellular carcinoma (HCC) and colorectal cancer has also been observed (Hsu et al., 1997; Filmus, 2001). Expression analyses of *GPC3* have shown that it is normally expressed in the fetal but not in the mature liver or intestine; however, it is expressed in normal malignant counterparts of these tissues (HCC and colorectal cancer). The authors propose that in these instances, *GPC3* may be acting as an oncofetal protein. Although oncofetal proteins do not have a direct role in tumorigenesis, they have been successfully used as tumor markers and targets of immunotherapy as exemplified by α-fetoprotein, carcinoembryonic antigen and prostate specific antigen. The expression pattern of *GPC3* in HCC and colorectal tumors is similar to what others and we have observed in Wilms tumor as *GPC3* is normally expressed in fetal kidney but not adult kidney. We found reduced or absent expression in 5/6 normal kidney samples and abundant expression of *GPC3* in most of the Wilms tumors with adequate RNA for evaluation. Similarly, Saikali and Sinnett (2000) and Toretsky et al. (2001) found *GPC3* to be highly expressed in Wilms tumors and absent or reduced in their normal kidney counterparts. However, the expression of *GPC3* seen in Wilms tumor is most likely to be a reflection of the stage of differentiation of this embryonal tissue rather than as a prognostic tumor marker, which appears to be the case for HCC. It is still unclear as to whether the upregulation of *GPC3* in hepatocellular and colorectal tumors is involved in tumor progression; however, *GPC3* upregulation in Wilms tumor is unlikely to be involved Wilms tumorigenesis.

Within the context that constitutional inactivation of *GPC3* predisposes to tumorigenesis, it was surprising to find a lack of evidence of *GPC3* involvement in sporadic Wilms tumors. Interestingly, a recent paper published by White et al. (2002) did provide evidence of somatic *GPC3* mutations in Wilms tumor. Two non-conservative single base pair changes were identified in their screening of 41 Wilms tumors. They suggest that GPC3 may play a role in Wilms tumor development. Our analysis of 64 Wilms tumors identified only one putative tumor specific deletion of the *GPC3* gene and/or chromosomal region. These studies taken together suggest that dysfunction of *GPC3* in Wilms tumor must only contribute to the development of a very small proportion of sporadic Wilms tumors. We therefore conclude that dysfunction *of GPC3* is not a frequent event in Wilms tumorigenesis.

CHAPTER 4

Identification of Wilms tumor genes by DD-PCR and database searching.

4.1 Loss of heterozygosity of chromosome 16q in Wilms tumors

Loss of heterozygosity of chromosome 16q is found in approximately 20% of Wilms tumors and is associated with a statistically significantly adverse outcome suggesting that the putative gene residing in this region is involved in tumor progression rather than initiation (Grundy et al., 1994). We therefore hypothesize that a putative Wilms tumor gene is located on chromosome 16q and propose to identify the gene(s) on chromosome 16q involved in Wilms tumorigenesis and/or its downstream targets.

4.2 Techniques used to identify candidate genes

The identification of candidate genes is an important step in furthering our understanding of human disease and cancer. Identification of clinically relevant genes will aid in the development of more sensitive diagnostic tools, the creation of prognostic indicators and refinement of therapies. One approach is to study differential gene expression between subsets of Wilms tumors – those that retain chromosome 16q heterozygosity versus those that exhibit 16q LOH. A variety of methods have been introduced to study differential gene expression. A common technique is differential display PCR (DD-PCR) that has successfully identified differentially expressed genes involved in hematopoeisis (Bond et al., 1998), drug resistance (Bertram et al., 1998) and various cancers including lung cancer (Manda et al., 1999), head and neck squamous cell carcinoma (Gonzalez et al., 2003). DD-PCR is a cost- and time-effective, sensitive alternative to subtraction hybridization. DD-PCR can simultaneously identify up- and down-regulated, known and unknown genes, based on the comparison of gene expression profiles of two different populations (e.g.: tumor vs. normal). The major disadvantage of DD-PCR is that it is prone to generating false positives. The sequencing of the human genome has enhanced the development of microarrays and protein arrays, which have resulted in a resurgence in the search for differentially expressed candidate genes. All of these techniques have been used with varying success in identifying differentially expressed genes.

With the advances in the Human Genome Sequencing Project, many genes and ESTs have been identified and localized to specific chromosomal regions. Databases have been created that compile lists of known genes (Ex.:NCBI's OMIM genemap database), together with their chromosomal location and gene expression and protein function information, if known. These databases are constantly being revised and updated as new genes are identified and chromosomal locations refined. We can take advantage of these powerful databases to use an *in silico* approach to identify candidate genes. With this approach, if a critical gene region has been identified via LOH, genetic linkage, translocation, etc., a thorough search of the gene information compiled and review of the literature enables one to determine if any of the genes represent good candidates. This approach, although limited to known genes, and based solely on the function and expression profiles assigned to them, is both time- and cost-effective. The identification of chromosome 16q candidate Wilms tumor genes was performed using both DD-PCR and an *in silico* approach of database searching. A portion of the DD-PCR experiments, including parts of the cloning, sequencing and RT-PCR analysis was performed by Holly Mewhort (summer student working under my direction).

4.3 Differential Display PCR

4.3.1 Tumor selection for DD-PCR

The success of DD-PCR relies, in part, on the populations selected for analysis. Often tumor vs. normal, induced vs. non-induced, different developmental stages etc. are chosen for comparison. In most of the DD-PCR experiments used to identify differentially expressed transcripts in cancer, normal tissue/cells are screened against tumor tissue/cells. In this instance transcripts are sought that are either up- or down- regulated in the tumor but not in the normal tissue. However, in an effort to specifically target genes on chromosome 16q, we chose to compare tumors that have retained chromosome 16q heterozygosity against tumors that have lost 16q heterozygosity. Furthermore, in an attempt to focus on 16q and not on Wilms tumor genes present on other chromosomes, all of the tumors selected retained heterozygosity on chromosomes 11p and 1p. We therefore compared 3 tumors that have retained chromosome 16q, 11p and 1p heterozygosity (16q+, 11p+, 1p+) against tumors that have lost 16q heterozygosity, but have retained 11p and 1p heterozygosity (16q-, 11p+, 1p+).

4.3.2 Identification of differentially expressed cDNAs

RT-PCR analysis was carried out with three of the 3' anchored primers (T_{11}MG, T_{11}MC and T_{11}MA) together with 20 of the 5' arbitrary (OPG) primers. A total of 62 differentially expressed cDNAs were identified from these 60 PCR amplifications. Of those, 25 were obtained with the T_{11}MG anchored primer, 18 with the T_{11}MC anchored primer and 19 with the T_{11}MA anchored primers. The cDNA candidate fragments were isolated, reamplified, cloned and sequenced. The results of the sequencing enabled the placement of the cDNA fragments into the following categories: (1) known genes; (2) EST/hypothetical proteins; (3) genomic DNA; (4) Alu/repetitive elements; (5) unknown sequences (6) mitochondrial DNA sequences and (7) clones with no insert. Table 4.1 provides a summary of the sequencing results of the 62 cDNA fragments identified with each anchored primer and their respective category placement. In some instances, cDNA fragments isolated by DD-PCR were found to represent the same gene. This was the case for *POLD3* and *COP9,* which were isolated twice and *GABA-1*, which was isolated three times.

cDNAs that were differentially expressed between the 2 tumor groups were identified and isolated as described previously. Only those cDNAs that were aberrantly expressed in at least 2 or more tumors of one category as compared to the second category were considered for further characterization. Examples of differentially expressed cDNAs, represented as bands on a gel are shown in the two representative DD-PCR autoradiograms in Figures 4.1 and 4.2. In Figure 4.1, band 1 is expressed only in the tumors that have retained

Table 4.1: Categorization of the sequenced candidate transcripts according to anchored primer utilized and sequencing results.

Sequence Results	**T_{11}MA**	**T_{11}MC**	**T_{11}MG**	**Total**
Known Genes	9	6	3	18
ESTs/Hypothetical proteins	2	2	5	9
Alu/repetitive elements	3	2	7	12
Genomic DNA	4	7	8	19
Unknown	0	0	1	1
Mitochondrial DNA	0	0	1	1
No insert	1	1	0	2
Total	19	18	25	62

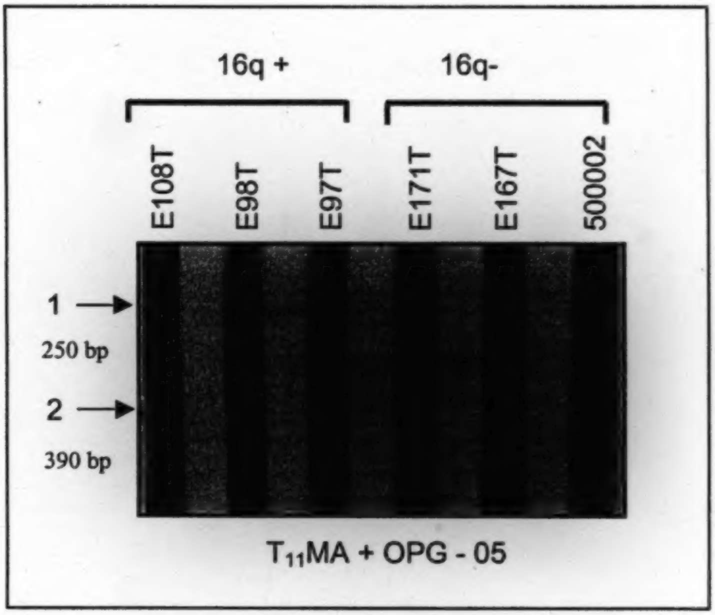
16q +
16q-
E108T
E98T
E97T
E171T
E167T
500002
1
250 bp
2
390 bp
T_{11}MA + OPG - 05

Figure 4.1: Differential display PCR autoradiogram (1). Two representative differentially expressed transcripts identified by DD-PCR using the T_{11}MA anchored primer and the OPG-05 random primer. Band 1 was considered a high priority candidate as it was expressed in the 16q+ tumor group only; however, sequencing identified it as genomic DNA. Band 2 was expressed in 2/3 16q+ tumors and 1/3 16q- tumors and was identified by sequencing as the *POLD3* gene.

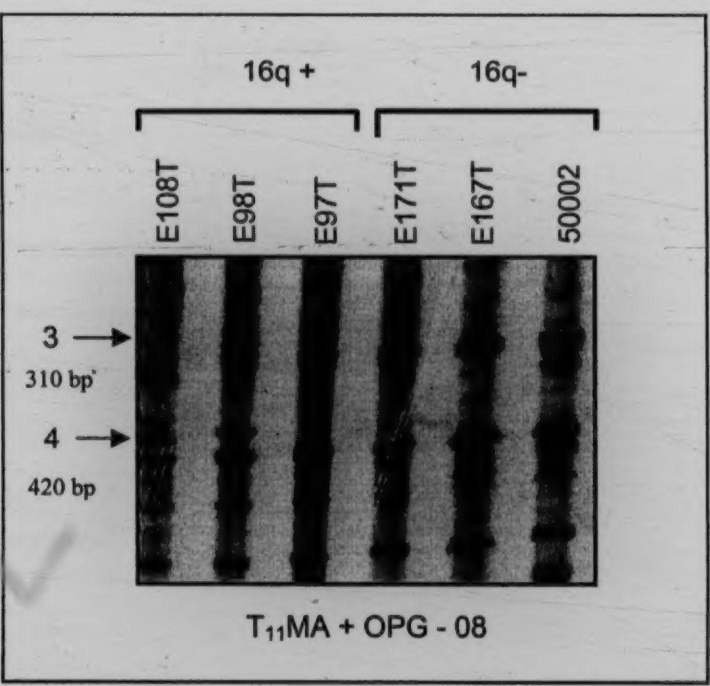
16q +
16q-
E108T
E98T
E97T
E171T
E167T
50002
3
310 bp
4
420 bp
T_{11}MA + OPG - 08

Figure 4.2: Differential display PCR autoradiogram (2). Autoradiogram showing two more representative differentially expressed cDNAs that were identified with the anchored primer T_{11}MA and random primer OPG-08. Band 3 was present in all 3 of the 16q+ tumors and in 1/3 16q- tumors. Sequencing identified the transcript as the *APC1* gene. Band 4 was present in 2/3 of the 16q+ tumors and in none of the 16q- tumors and was identified as genomic DNA by sequencing.

chromosome 16q heterozygosity but not in the tumors that have lost chromosome 16q heterozygosity. Sequencing of this cDNA identified it as genomic DNA. Band 2, however, was expressed in 2/3 tumors that have retained chromosome 16q heterozygosity and 1/3 tumors that have lost chromosome 16q heterozygosity and was identified by sequencing as the *POLD3* gene. In Figure 4.2, band 3 was expressed in all 3 tumors that have retained chromosome 16q heterozygosity and only in 1/3 tumors that have lost chromosome16q heterozygosity. Sequencing determined that this cDNA represented the *APC1* gene. Finally, band 4 was expressed in 2/3 of the tumors that retain chromosome 16q heterozygosity and not in any of the tumors that lose chromosome 16q heterozygosity. Sequencing this cDNA identified it as genomic DNA. The majority of the differentially expressed cDNAs isolated were not exclusively expressed in all three of the tumors of one group and none of the tumors in the second group as was the case for band 1, but rather displayed variable expression in the two tumor groups similar as observed for bands 2, 3 and 4.

4.3.3 Review of the differentially expressed cDNAs

Sequencing of the 62 candidate cDNA fragments identified 18 that represented known genes. Included in these are three genes (*COP9*, *POLD3* and *GABA-1*) that were isolated more than once. Therefore, in actuality, only 14 different known genes were isolated. Table 4.2 provides a list of the 14 known genes identified by DD-PCR together with their gene symbols, chromosomal

Table 4.2: List of known genes identified by DD-PCR, their chromosomal location, number of times isolated and whether they were analysed by RT-PCR.

Anchored Primer	Gene Identified	Gene Symbol	Chromosome location	Number of times isolated	Analysed by RT-PCR
T_{11}MA	COP9; subunit 8	COP9	2q37.3	2	Yes
	Vacuolar protein sorting isoform 45	VPS45A	1q21-q22	1	Yes
	DNA delta polymerase; subunit 3	POLD3	11q13.4	2	Yes
	Anaphase promoting complex; subunit 1	ANAPC1	2q12.1	1	Yes
	Gamma-aminobutyric acid receptor alpha-1	GABRA-1	5q34-q35	3	No
T_{11}MC	Eukaryotic translation initiation factor 4B	EIF4B	12q13.13	1	Yes
	RB1-inducible coiled-coil 1	RB1CC1	8q11.23	1	Yes
	Synaptotagmin-like 2, transcript variant A	SYTL2	11q14.1	1	Yes
	Pleckstrin homology domain containing family (phosphoinositide binding specific) member 1	PLEKHA1	10q26.13	1	Yes
	Coagulation factor XIII, subunit A	F13A1	6p25-p24	1	No
	ABC transporter			1	No
T_{11}MG	Myeloid/lymphoid or mixed lineage leukemia, translocated to 10	MLLT10	10p12.31	1	Yes
	Opioid growth factor receptor-like	OGFRL1	6q13	1	Yes
	TAF1 RNA polymerase II	TAF1	Xq13.1	1	Yes

location, number of times isolated and whether they were further characterized by RT-PCR. None of the 14 genes localized to chromosome 16q. However, two of the genes, *SYTL2* and *POLD3,* localized to chromosome 11q, a region which contains LOH in a subset of Wilms tumors. *SYTL2* localizes to chromosome 11q14 and has been implicated in vesicular trafficking while *POLD3* localizes to chromosome 11q13 and is involved in DNA replication and DNA mismatch repair (Fukuda et al., 2001; Hughes et al., 1999; Longley et al., 1997). The region of LOH identified in Wilms tumor is located at the distal end of chromosome 11 near 11q23-qter (Radice et al., 1995; Klamt et al., 1998; Nakadate et al., 2001). However, since *SYTL2* and *POLD3* map to 11q14 and 11q13, respectively, it is unlikely that they represent the Wilms tumor gene associated with 11q23-qter LOH.

Although the design of the DD-PCR experiment was to specifically target genes located on chromosome 16q, no genes on this chromosome were isolated. However, it is possible that some of the genes identified, although not on chromosome 16, may represent up- or downstream targets of the 16q gene and be involved in Wilms tumorigenesis. Therefore, further examination of some of the genes isolated by DD-PCR was warranted. Of the 16 known genes isolated by DD-PCR, 11 genes and 1 EST were chosen for further evaluation by semi-quantitative RT-PCR. These are listed in Table 4.3 together with their known or predicted protein function and tissue expression. The 11 genes, for which RNA expression data were available, were all expressed in the kidney; however, they were also expressed in many other tissues as well. The EST,

Table 4.3: Tissue expression pattern of the DD-PCR candidate genes. The tissue expression data was obtained from the GeneCards™ database (http://bioinfo.weizmann.ac.il/cards/index.html) (Rebhan et al., 1997).

GENE	Function	BMR	SPL	TMS	BRN	SPC	HRT	MSL	LVR	PNC	PST	KDN	LNG
VPS45	Involved in vesicle-mediated protein trafficking				+	+	+	+	+		+	+	+
POLD3	Involved in DNA binding, replication and repair	+			+				+		+	+	+
ANAPC1	Controls progression from mitosis and G1 phase of cell cycle	+	+	+	+			+	+	+	+	+	+
EIF4B	Regulator of translation initiation	+	+	+	+	+	+	+	+	+	+	+	+
RB1CC1	Proposed TF and regulator of the *RB1* gene				+	+	+	+	+	+	+	+	+
SYTL2					+	+	+	+	+		+	+	+
PLEKHA1			+		+	+	+	+	+	+	+	+	+
MLLT10	Gene fusion protein, novel TF	+			+			+	+	+	+	+	+
TAF1	Transcriptional regulator	+		+	+			+		+	+	+	+
IBtK	Tyrosine kinase required for B-cell development			+	+		+	+	+	+	+		+
COP9S8		NA	NA	NA	NA	NA	NA	NA	NA	NA	NA	NA	NA
OGFRL1		NA	NA	NA	NA	NA	NA	NA	NA	NA	NA	NA	NA

BMR – bone marrow; SPL – spleen; TMS – thymus; SPC – spinal cord; HRT – heart; MSL – muscle; LVR – liver; PNC – pancreas; PST – prostate; KDN – kidney; LNG – lung; NA – not available.

KIAA1417 [which was recently identified, after the RT-PCR analysis had been completed, as Inhibitor of Bruton agammaglobulinemia tyrosine kinase (*IBtk*)] has not been reported to be expressed in the kidney.

Two of the known genes, *GABRA-1* and *F13A1* were not considered for further evaluation, as review of their protein function did not support their having a role in Wilms tumorigenesis. *GABRA*-1 is exclusively expressed in the brain and represents a receptor for the major inhibitory neurotransmitter in vertebrate brain and mutations within the gene have been associated with juvenile myoclonic dystrophy (Cossette et al., 2002). *F13A1* is a coagulation factor important in stabilizing blood clots and is expressed in a wide variety of tissues (Takahashi et al., 1986). A third cDNA, when analysed with NCBI's blastn translation search tool, was found to encode a putative bacterial ATP-binding cassette (ABC) transporter. Although human ABC transporters have been identified and found to be important in multidrug resistance and delivery of chemotherapeutic drugs, the sequence identified by DD-PCR only showed homology to the bacterial, but not human, ABC transporters and therefore, was not considered for further evaluation.

4.3.4 Analysis of candidate Wilms tumor genes by semi-quantitative RT-PCR

Further analysis of 11 of the known genes, including *MLLT10, EIF4b, VPS45, POLD3, ANAPC1, RB1CC1, SYTL2, PLEKHA1, OGFRL1, TAF1, COP9* and 1 EST, KIAA1417 (*IBtk*), was carried out by semi-quantitative RT-PCR. This technique was employed to confirm the differential expression seen between the

2 categories of tumors in the original DD-PCR analysis. If the RT-PCR results confirmed the DD-PCR results and therefore confirmed differential expression, the gene would be considered for further evaluation. If the RT-PCR results did not confirm the original DD-PCR analysis it was considered a false positive and as such, no further evaluation was done. The RT-PCR primers for the 12 genes to be further evaluated, targeted the middle of the gene and were designed so that introns were spanned to ensure no contaminating DNA would be amplified. Typically, each set of primers amplified a 500-700 bp region. Primer sequences were also checked to ensure that they did not co-amplify psudogenes. It should be noted that although a total of 6 tumors were analysed in the DD-PCR assay, only 5 were used in the RT-PCR assay due to the fact that the RNA for one of the tumors that lost 16q LOH had become degraded and no additional RNA was available for analysis.

4.3.5 Results of semi-quantitative RT-PCR

In order to control for amount of RNA in each reverse transcription reaction, as well as RNA and/or cDNA integrity, a *GAPDH* control PCR amplification was performed at the beginning of each week or every time new cDNA serial dilutions were made, whether it was from newly transcribed RNA or stock cDNA. To determine the relative *GAPDH* expression in each of the 5 tumor samples used in the RT-PCR analysis, the relative band intensity averages (determined by calculating the pixel volume for each band) for each tumor cDNA serial dilution amplified with *GAPDH,* were calculated and plotted against one another (Figure 4.3). Comparison of the *GAPDH* relative DNA band intensity averages shows differential expression between the tumors that have lost chromosome 16q heterozygosity versus the tumors have retained chromosome 16q heterozygosity. However, the tumors within each group (16q+ vs. 16q-) exhibit similar levels of expression with respect to one another. Calculation of the X-intercept of the line representing average *GAPDH* product for each tumor group, shows that the tumors that have lost chromosome 16q heterozygosity express *GAPDH* at 18X lower levels than the tumors that retain chromosome 16q heterozygosity. These results suggest that either the RNA samples for the tumors that have lost chromosome 16q heterozygosity are less concentrated or more degraded than the tumors that have retained chromosome 16q heterozygosity, or that the difference in expression between the tumor groups represents true differential expression of *GAPDH* between these two groups of tumors. Northern blot analysis of samples E108T and E98T, which retained chromosome 16q heterozygosity and samples E171T and E167T, which lost chromosome 16q heterozygosity, with *β-actin* also revealed that the RNA from the two samples that retained 16q heterozygosity were expressed at increased levels as compared to RNA from the two samples that lost 16q heterozygosity (Figure 4.4). This suggests that the either the concentration of RNA in the 16q LOH samples is lower than the 16q+ tumors or that the RNA is slightly degraded. The differential *GAPDH* expression seen between Wilms tumors is further discussed later in the chapter.

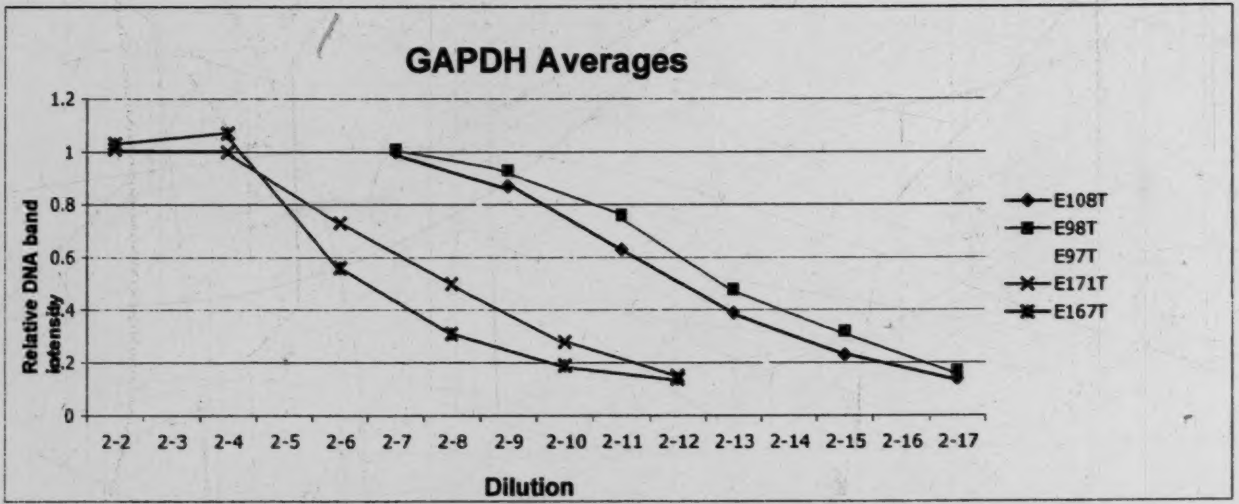

Figure 4.3: Average *GAPDH* RNA expression for each tumor sample evaluated. GAPDH RNA expression for each tumor sample was evaluated every week or every time new cDNA dilutions were made. The average relative DNA band intensity of the PCR product for each cDNA serial dilution was calculated and graphed. Samples E108T, E98T and E97T represent tumors that have retained 16q heterozygosity, while samples E171T and E167T represent tumors that have lost 16q heterozygosity.

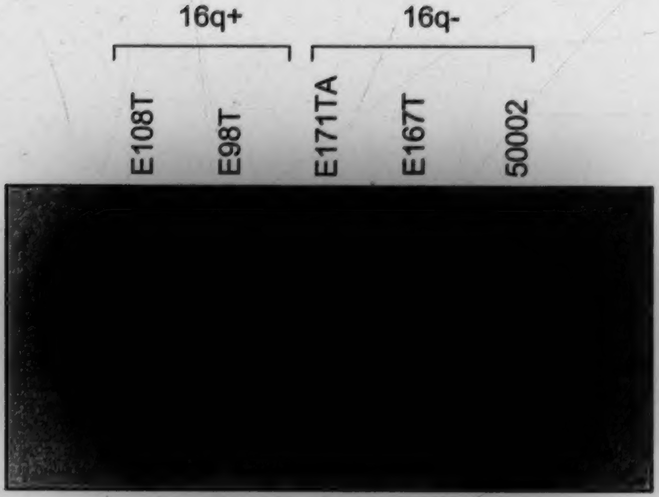

Figure 4.4: Northern blot of tumors used if the DD-PCR analysis hybridized with β-actin. It can be seen that the two tumors that retain 16q heterozygosity express β-actin at higher levels than the tumors that have lost 16q heterozygosity. It should be noted that sample E97T (16q+) is not present on the blot, while sample 50002 (16q-) is present but was not used in the semi-quantitative RT-PCR analysis due to the fact that it became degraded.

Results obtained from the semi-quantitative RT-PCR were analysed two ways. First, all samples for the gene of interest were compared against the corresponding *GAPDH* control such that expression for that particular tumor sample and gene of interest could be determined relative to corresponding *GAPDH* RNA expression. A value representing the fold-increase or decrease relative to *GAPDH* was generated for each gene of interest (Table 4.4). We were unable to confirm the DD-PCR pattern of expression for any of the 12 genes analysed, suggesting that the genes identified by DD-PCR represent false positives or that use of the *GAPDH* control may have been inappropriate for our analysis.

The second method of analysis compares the five tumor samples for a particular gene of interest against one another, independent of *GAPDH*. Expression levels from all of the tumor samples analysed for a particular gene were graphed together. Comparison of gene expression between the tumors that have retained 16q heterozygosity versus tumors that have lost 16q heterozygosity for all 12 genes of interest also did not confirm the patterns of differential expression seen in the original DD-PCR analysis (Figures 4.5 and 4.6). Interestingly, when analyzing the data independent of *GAPDH* results, most of the tumor samples showed similar expression for each gene of interest. However, *COP9*, *ANAPC1*, *TAF1* did show moderate differential expression [4-fold (*APC*, *TAF1*) to 20-fold (*COP9*)] between the 2 tumor groups but this differential expression was not seen in the original DD-PCR assay.

Table 4.4: Summary of DD-PCR and semiquantitative RT-PCR results normalized to *GAPDH*. These results were obtained by calculating RNA levels for each gene of interest relative to *GAPDH* RNA levels. This normalization was done for every sample for all 12 of the genes analysed. Tumors E108T, E98T and E97T retain 16q heterozygosity while tumors E171T, E167T and 50002 lose I6q heterozygosity. Ft. Band = faint band; NA = RNA not available.

Gene	**Expression Analysis**	**E108T**	**E98T**	**E97T**	**E171T**	**E167T**	**50002**
COP9	DD-PCR	No Data	Band	Band	No Band	No Band	
	RT-PCR + GAPDH	↓ 8X	↓ 223X	↓ 3X	↑ 4X	↓ 8X	NA
VPS45	DD-PCR	No Band	No Band	Band	Band	Band	
	RT-PCR + GAPDH	↓ 2X	↓ 4X	↓ 5X	↓ 3X	↓ 6X	NA
POLD3	DD-PCR	Band	Band	No Band	Band	Ft. Band	
	RT-PCR + GAPDH	↓ 5X	↓ 9X	↓ 1X	↓ 2X	↑ 4X	NA
ANAPC1	DD-PCR	Band	Band	Band	Band	No Band	
	RT-PCR + GAPDH	↓ 56X	↓ 39X	↓ 52X	↓ 12X	0	NA
EIF4b	DD-PCR	Ft. Band	No Band	No Band	Band	Band	
	RT-PCR + GAPDH	↑ 3X	↑ 2X	↓ 26X	↑ 5X	↑ 26X	NA
RB1CC1	DD-PCR	Band	Band	Ft. Band	Band	No Band	
	RT-PCR + GAPDH	↓ 7X	↓ 13X	↓ 2X	↑ 22X	↓ 7X	NA
SYTL2	DD-PCR	Band	No Data	Band	Ft. Band	Ft. Band	
	RT-PCR + GAPDH	↓ 256X	↓ 362X	↓ 30X	↓ 84X	↓ 3X	NA
PLEKHA1	DD-PCR	Band	Band	Band	Band	No Band	
	RT-PCR + GAPDH	↓ 3X	↓ 42X	↓ 9X	↓ 3X	↓ 1X	NA
IbtK	DD-PCR	Band	Band	Band	Ft. Band	Ft. Band	
	RT-PCR + GAPDH	↓ 4X	↓ 2X	↓ 5X	↑ 7X	↑ 6X	NA
MMLT10	DD-PCR	No Band	No Band	Band	Band	Band	
	RT-PCR + GAPDH	↓ 2X	↓ 4X	↓ 5X	↓ 3X	↓ 6X	NA
OGFRL1	DD-PCR	Band	Band	Band	Band	Band	
	RT-PCR + GAPDH	↓ 13X	↓ 13X	↓ 1259X	↓ 6X	↓ 4X	NA
TAF1	DD-PCR	Ft. Band	Ft. Band	No Band	Ft. Band	Band	
	RT-PCR + GAPDH	↓ 9X	↑ 8X	↓ 5X	↑ 2X	↑ 10X	NA

Figure 4.5: RT-PCR results, uncorrected for *GAPDH*, for 5 of the tumor samples and 6 of the genes evaluated (1). The relative DNA band intensity (pixel volume) generated by each PCR product was graphed against the cDNA serial dilution for each tumor sample. The green lines represent tumors that have retained 16q heterozygosity while the pink lines represent tumors that have lost 16q heterozygosity.

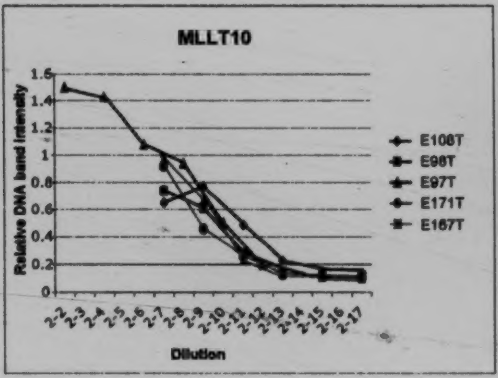
MLLT10
Relative DNA band intensity
1.6
1.4
1.2
1
0.8
0.6
0.4
0.2
0
2-2 2-3 2-4 2-5 2-6 2-7 2-8 2-9 2-10 2-11 2-12 2-13 2-14 2-15 2-16 2-17
Dilution
E108T
E98T
E97T
E171T
E167T

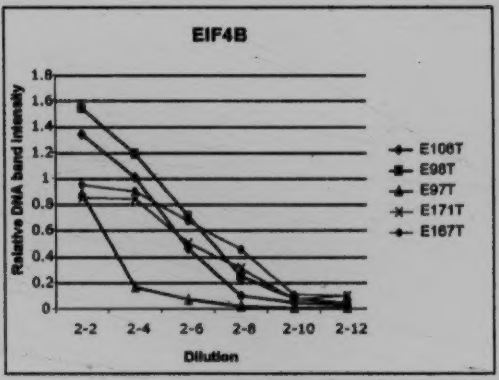
EIF4B
Relative DNA band intensity
1.8
1.6
1.4
1.2
1
0.8
0.6
0.4
0.2
0
2-2 2-4 2-6 2-8 2-10 2-12
Dilution
E108T
E98T
E97T
E171T
E167T

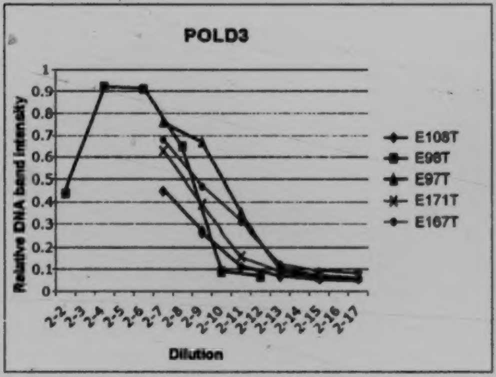
POLD3
Relative DNA band intensity
1
0.9
0.8
0.7
0.6
0.5
0.4
0.3
0.2
0.1
0
2-2 2-3 2-4 2-5 2-6 2-7 2-8 2-9 2-10 2-11 2-12 2-13 2-14 2-15 2-16 2-17
Dilution
E108T
E98T
E97T
E171T
E167T

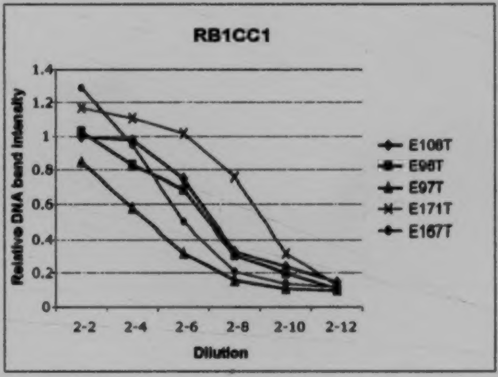
RB1CC1
Relative DNA band intensity
1.4
1.2
1
0.8
0.6
0.4
0.2
0
2-2 2-4 2-6 2-8 2-10 2-12
Dilution
E108T
E98T
E97T
E171T
E167T

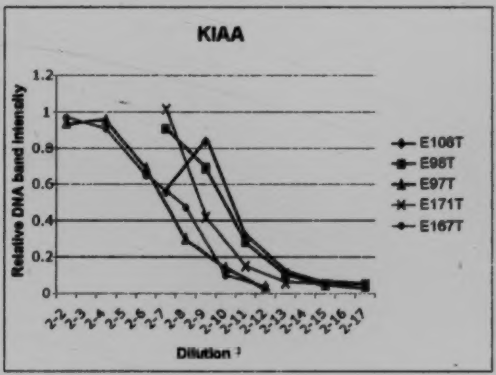
KIAA
Relative DNA band intensity
1.2
1
0.8
0.6
0.4
0.2
0
2-2 2-3 2-4 2-5 2-6 2-7 2-8 2-9 2-10 2-11 2-12 2-13 2-14 2-15 2-16 2-17
Dilution
E108T
E98T
E97T
E171T
E167T

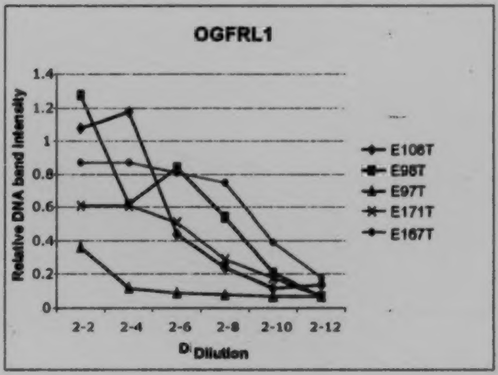
OGFRL1
Relative DNA band intensity
1.4
1.2
1
0.8
0.6
0.4
0.2
0
2-2 2-4 2-6 2-8 2-10 2-12
Dilution
E108T
E98T
E97T
E171T
E167T

Figure 4.6: RT-PCR results, uncorrected for *GAPDH,* for 5 of the tumor samples for 6 of the genes evaluated (2). The relative DNA band intensity (pixel volume) generated by each PCR product was graphed against the cDNA serial dilution for each tumor sample. The green lines represent tumors that have retained 16q heterozygosity while the pink lines represent tumors that have lost 16q heterozygosity.

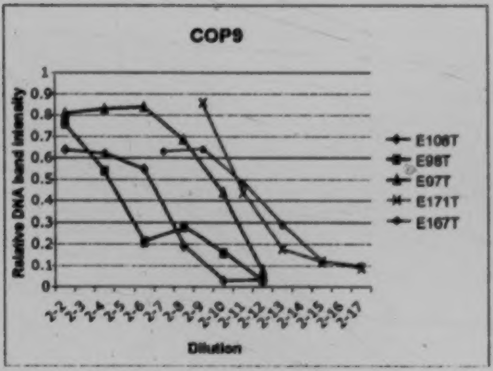
COP9
Relative DNA band intensity
1
0.9
0.8
0.7
0.6
0.5
0.4
0.3
0.2
0.1
0
2-2
2-3
2-4
2-5
2-6
2-7
2-8
2-9
2-10
2-11
2-12
2-13
2-14
2-15
2-16
2-17
Dilution
E106T
E96T
E97T
E171T
E167T

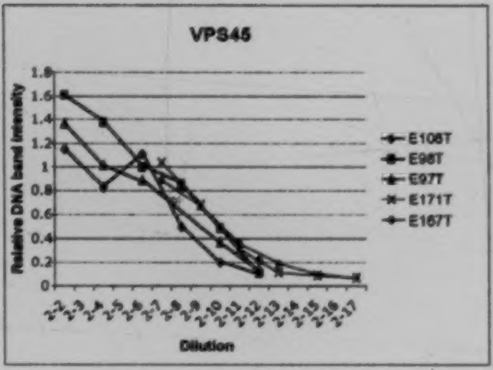
VPS45
Relative DNA band intensity
1.8
1.6
1.4
1.2
1
0.8
0.6
0.4
0.2
0
2-2
2-3
2-4
2-5
2-6
2-7
2-8
2-9
2-10
2-11
2-12
2-13
2-14
2-15
2-16
2-17
Dilution
E106T
E96T
E97T
E171T
E167T

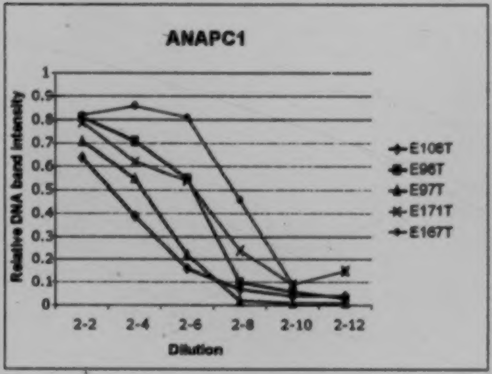
ANAPC1
Relative DNA band intensity
1
0.9
0.8
0.7
0.6
0.5
0.4
0.3
0.2
0.1
0
2-2
2-4
2-6
2-8
2-10
2-12
Dilution
E106T
E96T
E97T
E171T
E167T

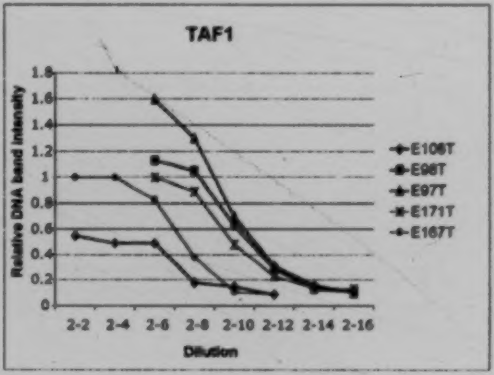
TAF1
Relative DNA band intensity
1.8
1.6
1.4
1.2
1
0.8
0.6
0.4
0.2
0
2-2
2-4
2-6
2-8
2-10
2-12
2-14
2-16
Dilution
E106T
E96T
E97T
E171T
E167T

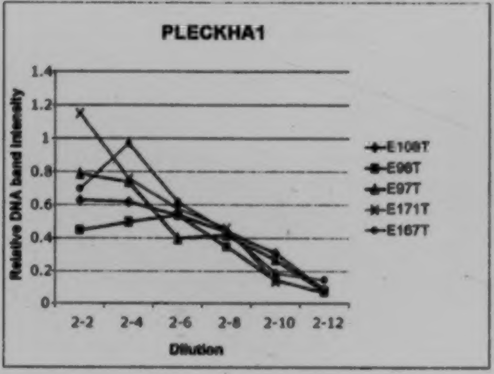
PLECKHA1
Relative DNA band intensity
1.4
1.2
1
0.8
0.6
0.4
0.2
0
2-2
2-4
2-6
2-8
2-10
2-12
Dilution
E106T
E96T
E97T
E171T
E167T

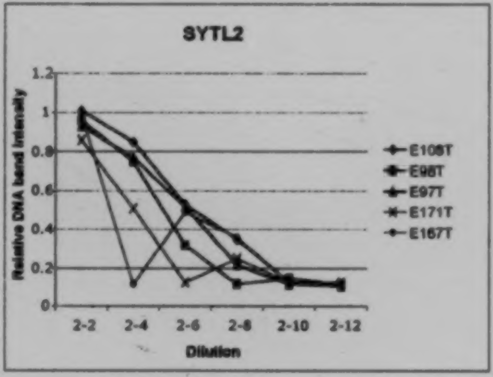
SYTL2
Relative DNA band intensity
1.2
1
0.8
0.6
0.4
0.2
0
2-2
2-4
2-6
2-8
2-10
2-12
Dilution
E106T
E96T
E97T
E171T
E167T

7

4.3.6 Analysis of MLLT10 RNA in additional Wilms tumors

Despite the fact that the expression pattern of the genes did not match the original DD-PCR results, 2 genes, *MLLT10* and *EIF4b*, were chosen for further evaluation in additional Wilms tumors by semi-quantitative RT-PCR based on the RT-PCR results as well as published information.

MLLT10 is located on chromosome 10p12 and is one of 17 known gene partners of the Myeloid/lymphoid mixed lineage leukemia (*MLL*) gene and results in the creation of a fusion gene due to a t(10;11)(p12q23) translocation (Chaplin et al., 1995). This fusion gene represents a zinc finger/leucine zipper gene that is thought to represent a novel class of transcription factors. *MLLT10* has been implicated in acute myeloid/lymphoid or mixed lineage childhood leukemias and was chosen for this reason.

MLLT10 was analysed in 13 additional Wilms tumors, 7 of which retained chromosome 16q heterozygosity and 6 of which lost chromosome 16q heterozygosity. Table 4.5 shows the *MMLT10* RT-PCR results generated for each tumor relative to its *GAPDH* control. As seen in the initial RT-PCR analysis of 5 tumors, there does not appear to be any differential expression between the 2 tumor categories. The majority of the tumors, regardless of which category they fall into, show decreased expression (between 4-fold to 32-fold) relative to *GAPDH*. A few tumors show significantly reduced *MLLT10* expression (145-fold and 424-fold) as compared to *GAPDH.*

The *MLLT10* semi-quantitative RT-PCR results obtained for each tumor, uncorrected for *GAPDH*, are shown in Figure 4.7. Interestingly, the majority of

Table 4.5: Semi-quantitative RT-PCR results for *MLLT10* RNA expression normalized to *GAPDH* RNA expression.

Sample	16q+/-	MLL	DD-PCR
E108T	+	1.4X↓	BAND
E98T	+	3.5X↓	BAND
E97T	+	3X↑	BAND
WT-33	+	15X↓	
WT-13	+	13X↓	
WT-8	+	32X↓	
WT-3	+	30X↓	
WT-19	+	424X↓	
WT-20	+	4X↓	
WT-5	+	14X↓	
E171T	-	8X↑	NO BAND
E167T	-	30X↑	BAND
WT-34	-	12X↓	
WT-29	-	145X↓	
WT-28	-	66X↓	
WT-32	-	16X↓	
WT-15	-	10X↑	
WT-1	-	10X↓	

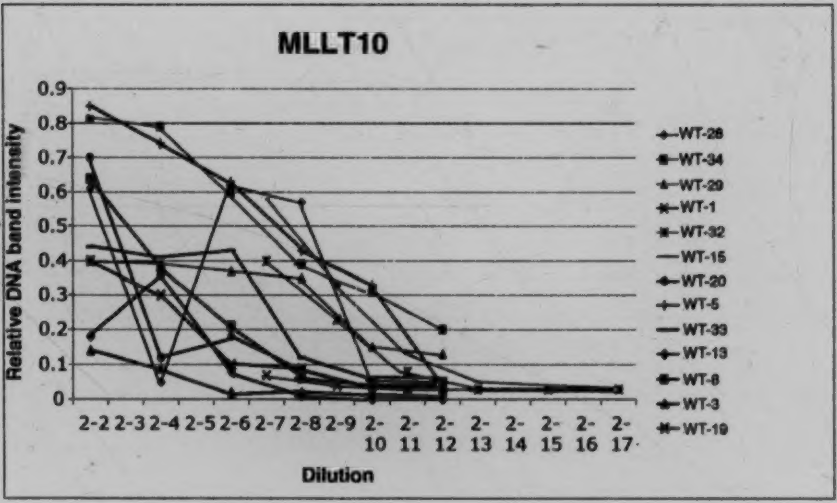

Figure 4.7: RT-PCR analysis of *MLLT10* in additional Wilms tumors uncorrected for *GAPDH*. *MLLT10* was evaluated in 13 additional Wilms tumors by semi-quantitative RT-PCR and graphed together to identify possible differential expression between the two tumor groups. Green represents tumors that retained 16q heterozygosity while pink represents tumors that have lost 16q heterozygosity.

tumors that have lost chromosome 16q LOH express *MLLT10* at a lower level than the tumors that have retained chromosome 16q heterozygosity. An average 23-fold difference is observed between the tumors that lost 16q heterozygosity versus the tumors that retained 16q heterozygosity when the average X-intercept is calculated for each tumor group. It is surprising that the RT-PCR results differ depending on whether or not RNA levels are measured relative to *GAPDH.* In the absence of normalization, the results suggest a correlation between reduced *MLLT10* expression and chromosome 16q LOH in Wilms tumors. Further study of *MLLT10* expression in Wilms tumor using another quantitative RNA expression study is warranted.

4.3.7 Analysis of EIF4b RNA in additional Wilms tumors

EIF4b (Eukaryotic Initiation Factor 4b) has been localized to chromosome 12q13.13 and is involved in the binding of mRNA to the 43S pre-initiation complex (Methot et al., 1994). Table 4.6 illustrates the semi-quantitative RT-PCR results obtained for *EIF4b* relative to *GAPDH*. No differential expression was seen between the 2 tumor groups. Most of the tumors showed either 5-fold up-regulation or down-regulation as compared to their *GAPDH* controls. Three normal kidney samples were included in this analysis, 2 from mature kidney and one from fetal kidney. Interestingly, it was found that *EIF4b* expression in all three of the normal kidney samples was significantly down-regulated (17-fold to 79-fold) relative to *GAPDH*, with the fetal kidney showing the lowest level of expression (Table 4.6).

Table 4.6: Semi-quantitative RT-PCR results for *EIF4b* RNA expression normalized to *GAPDH* RNA expression.

Sample	16q+/-	EIF4b	DD-PCR
E108T	+	3X↑	FAINT BAND
E98T	+	2X↑	NO BAND
E97T	+	26X↓	NO BAND
WT-33	+	20X↑	
WT-14	+	1.4X↓	
WT-8	+	3X↓	
WT-2	+	5X↑	
WT-4	+	2X↑	
WT-5	+	2X↑	
E171T	-	5X↑	BAND
E167T	-	26X↑	BAND
WT-31	-	2X↑	
WT-29	-	2X↓	
WT-30	-	2X↓	
WT-28	-	4X↑	
N		20X↓	
N		17X↓	
135d		79X↓	

The *EIF4b* expression results for the tumor and normal kidney samples, uncorrected for *GAPDH*, are summarized in Figure 4.8. Although this analysis does not provide evidence for differential expression between the 2 tumor groups, differential expression is seen between the normal kidney samples and the tumors. This confirms the RT-PCR results generated by comparison of tumor gene expression relative to *GAPDH* expression. Since expression of *EIF4b* did not correlate with chromosome 16q LOH, this suggests that *EIF4b* is likely not involved in the chromosome 16q Wilms tumor gene pathway. Up-regulation of *EIF4b* when compared to normal fetal and mature kidney suggests that it may have a role in Wilms tumorigenesis; however, further evaluation of *EIF4b* in Wilms tumors and normal kidney is needed to explore this possibility.

4.4 Database Searching

4.4.1 Genes localized within the minimal region of 16q LOH

A list of all the known genes residing between chromosome 16q21-q24.1 was obtained from NCBI's Online Mendelian Inheritance in Man (OMIM) (http://www.ncbi.nlm.nih.gov:80/entrez/Omim/getmap.cgi) genemap database. At the time of screening, Winter 2001, there were 102 known genes located within this region. Tissue expression, function and other details of each gene was obtained by reviewing the OMIM database (http://www.ncbi.nlm.nih.gov/entrez/query.fcgi?db=OMIM), the GeneCards™ website (http://bioinfo.weizmann.ac.il/cards/index.html) (Rebhan et al., 1997) which provides details of RNA expression studies and NCBI's PubMed gene

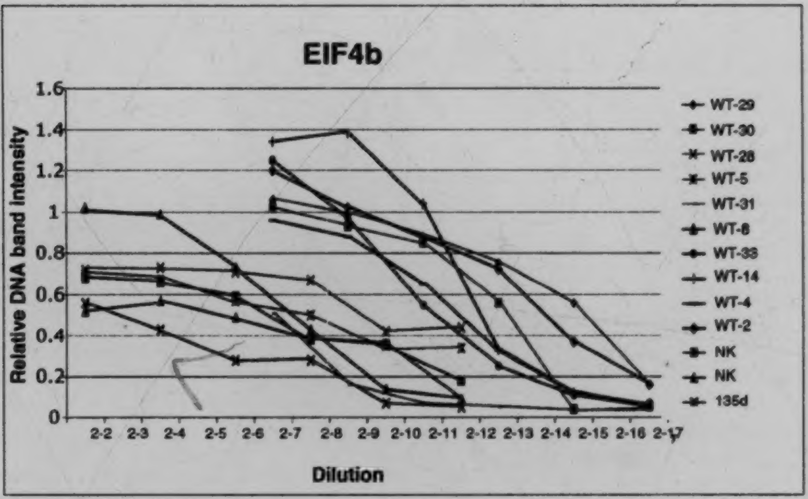

Figure 4.8: RT-PCR analysis of *E1F4b* in additional Wilms tumors and normal kidney uncorrected for *GAPDH*. *EIF4b* was evaluated in 10 additional Wilms tumors and 3 normal kidney samples by semi-quantitative RT-PCR and graphed together to identify possible differential expression between the two tumor groups. Green represents tumors that retained 16q heterozygosity, pink represents tumors that have lost 16q heterozygosity and blue represents normal kidney. T = tumor; N = normal mature kidney; d = normal embryonic kidney.

literature reviews (http://www.ncbi.nlm.nih.gov/entrez/query.fcgi?db=PubMed). Based on the information obtained from these sources, the genes could be categorized into groups according to their known or predicted protein functions including: (1) DNA synthesis and repair; (2) cell cycle; (3) RNA metabolism; (4) transcriptional regulation; (5) cell signaling; (6) protein metabolism; (7) ECM and adhesion; (8) intracellular trafficking; (9) energy metabolism; (10) cytoskeleton; (11) serum proteins; (12) unknown. These results are displayed in graphical form in Figure 4.9. A list of the gene names, gene symbols, chromosome 16 location, associated disorders and RNA tissue expression is presented in Table 4.7. Based on the information acquired for each gene, the genes could be further categorized into the following groups: (1) highly probable Wilms tumor candidate genes; (2) probable Wilms tumor candidate genes and (3) unlikely Wilms tumor candidate genes. The criteria used to categorize genes into their respective groups were: (1) involvement in other cancers particularly childhood or renal cancers; (2) RNA tissue expression limited to the kidney or the kidney plus one or two more tissues; (3) gene function or predicted protein function (if known); (4) involvement in kidney development and (5) association with a specific disease or disorder related to kidney development/cancer.

4.4.2 Exclusion of candidate Wilms tumor genes

Using these selection criteria, many of the genes could be excluded and placed in the unlikely Wilms tumor candidate gene category. The genes in this category usually displayed ubiquitous expression as seen for the gene, *ALDOA*

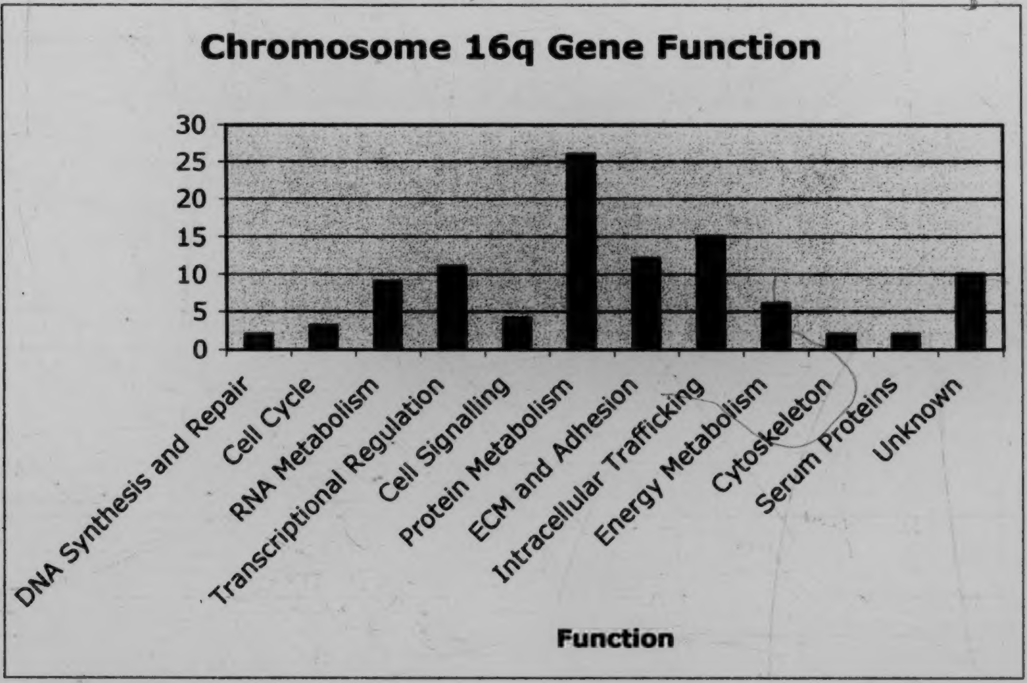

Figure 4.9: Categorization of the genes localized to the minimal region of LOH on chromosome 16q. One hundred and two genes are located in the 6.7 Mb region on chromosome 16q. These genes are classified according to their known or predicted protein function.

Table 4.7: List of known genes within the minimal region of LOH according to 16q location.
The table includes information on related disorders and tissue expression.

16q location	Gene	Symbol	Disorder	BMR	SPL	TMS	BRN	SPC	HRT	MSL	LVR	PNC	PST	KDN	LNG
16q13-q21	Anisomastia	ANMA	Anisomastia												
16q13-q21	Kinesin family member C3	KIFC3		+		+	+			+	+	+		+	+
16q13-q21	Matrix metalloproteinase 15	MMP15					+		+	+	+		+	+	
16q13-q21	RNA polymerase II, polypeptide C	POLR2C					+			+	+	+		+	+
16q13-q22	Carboxylesterase 1	CES1	Monocyte carboxylesterase deficiency							+	+	+	+	+	+
16q21	Autocrine motility factor receptor	AMFR	Metastatic tumors?	+			+		+	+	+	+	+	+	+
16q21	Bardet-Biedl syndrome	BBS2	Bardet-Biedl syndrome 2	+			+			+	+	+	+	+	+
16q21	Cholesteryl ester transfer protein	CEPT			+		+				+			+	
16q21	Glutamic-oxaloacetic transaminase-2 mitochondrial	GOT2		+			+		+	+	+	+	+	+	+
16q21	Heat-shock transcription factor 4	HSF4					+		+	+		+	+	+	
16q21	WW domain-containing	WWP2		+	+	+	+			+	+	+	+	+	+
16q21-q22	Cadherin-16	CDH16												+	
16q21-q22.1	Cadherin-8	CDH8					+			+					
16q21-q22.1	Cadherin-11	CDH11			+		+			+			+	+	+
16q21-q23	Carbonic anhydrase VII	CA7					+								
16q21-q23	Nucleolar protein 3	NOL3					+		+	+	+	+	+		+
16q21-q22.3	DEAD/H box 38	DDX38		+	+		+		+	+	+	+	+		+
16q22	Cystathionase	CTH	Cystathioninuria												
16q22	Alanyl-tRNA synthetase	AARS		+	+		+		+	+	+	+	+	+	+
16q22	Agouti-related transcript, mouse, homologue of	AGRP												+	+
16q22	Acute myeloid leukemia chromosome region 2	AMLCR2	Acute myelogenous leukemia												
16q22	Aneurysmal bone cyss	ANBC	Aneurysmal bone cysts												
16q22	Amyloid beta precursor protein-binding protein-1	APPBP1		+		+	+				+	+		+	+
16q22	Core-binding factor, beta subunit	CBFB	Myeloid leukemia, acute M4Eo subtype	+		+	+			+	+	+	+	+	+
16q22	Carbohydrate sulfotransferase-5	CHST5													
16q22	Carbohydrate sulfotransferase-6	CHST6	Macular corneal dystrophy							+	+				
16q22	North American Indian childhood cirrhosis	CIRH1A	North American Indian childhood cirrhosis	+		+	+			+	+		+	+	+
16q22	Hydroxysteroid dehydrogenase 2	HSD11B2	Hypertension, mineralocorticoid excess		+		+			+	+		+	+	+

Table 4.7: Continuation of the list of known genes within the minimal region of LOH according to 16q location. The table includes information on related disorders and tissue expression.

16q location	Gene	Symbol	Disorder	BMR	SPL	TMS	BRN	SPC	HRT	MSL	LVR	PNC	PST	KDN	LNG
16q22	Ras-related associated with diabetes	RRAD								+		+	+	+	+
16q22	Thymidine kinase, mitochondrial	TK2					+			+				+	
16q22	TNRF1-associated death domain protein	TRADD		+			+	+		+		+	+	+	+
16q22	Zinc finger protein-19	ZNF19													
16q22	Zinc finger protein-32	ZNF23					+			+	+	+	+	+	
16q22-q23	Golgi apparatus protein 1	GLG1		+	+	+	+		+	+	+	+	+	+	+
16q22-q23	Avian musculoaponeurotic fibrosarcoma protooncogene	MAF		+			+				+	+	+	+	+
16q22-q23	Syntrophin, beta-2	SNRB2					+			+	+		+	+	+
16q22-q23	Aldolase A, fructose-biphosphatase	ALDOA	Aldolase A deficiency	+	+	+	+	+	+	+	+	+	+	+	+
16q22-qter	Cytochrome c oxidase subunit IV, isoform 1	COX4I1		+	+	+	+		+	+	+	+	+	+	+
16q22-qter	Neighbor of Cox4	COX4I1					+		+	+	+	+		+	+
16q22-qter	Calbindin 2	CALB2					+								
16q22.1	E-cadherin	CDH1	Various cancers				+			+	+	+	+	+	+
16q22.1	Cadherin-3 (Placental-cadherin)	CDH3	Congenital hypotrichosis with juvenile macular dystrophy							+	+	+	+		+
16q22.1	Cadherin-5	CDH5		+			+	+	+	+	+		+		+
16q22.1	Cataract, Marner type	CTM													
16q22.1	Chymotrypsin-like protease	CTRL										+	+	+	+
16q22.1	E2F transcription factor 4	E2F4		+			+	+	+	+	+	+	+	+	+
16q22.1	Hyaluronan synthase 3	HAS3		+									+	+	+
16q22.1	Haptoglobin	HP	Hypohaptoglobinemia	+			+			+	+				+
16q22.1	Haptoglobin-related locus	HPR													
16q22.1	Lecithin-cholesterol acyltransferase	LCAT	Norun and Fish-eye diseases		+		+				+		+		+
16q22.1	Proteosome subunit MECL1	MECL1		+	+		+			+	+		+	+	+
16q22.1	NAD(P)H dehydrogenase quinone 1	NQO1	Polymorphisms linked to cancer susceptibility				+	+	+	+	+	+	+	+	+
16q22.1	Putative serine kinase H1	PSKH1			+						+	+	+	+	
16q22.1	Spinocerebellar ataxia 4	SCA4	Spinocerebellar ataxia												
16q22.1	Solute carrier family 9, isoform 5	SLC9A5			+		+				+	+			+

Table 4.7: Continuation of the list of known genes within the minimal region of LOH according to 16q location. The table includes information on related disorders and tissue expression.

16q location	Gene	Symbol	Disorder	BMR	SPL	TMS	BRN	SPC	HRT	MSL	LVR	PNC	PST	KDN	LNG
16q22.1	Solute carrier family 12, member 4	SLC12A4		+	+	+	+			+	+		+		+
16q22.1	Telomeric repeat-binding factor-2	TERF2					+		+		+			+	+
16q22.1	DEAD/H box 19	DDX19		+			+			+	+	+	+	+	+
16q22.1	Splicing factor 3B, subunit 3	MF3B3		+	+		+			+	+	+	+	+	+
16q22.1	Solute carrier family 7, member 6	SLC7A6		+	+					+	+		+		+
16q22.1-q22.3	Tyrosine aminotransferase	TAT	Tyrosinemia, type II												
16q22.2-q22.3	Adenosine deaminase tRNA-specific 1	ADAT1					+			+	+				+
16q22.2-q22.3	Lysyl-tRNA synthetase	KARS				+	+		+	+	+	+	+	+	+
16q22.3-q23.1	AT motif-binding factor 1	ATBF1		+			+		+	+	+		+	+	
16q23	Adaptor-related protein complex 1, gamma 1	AP1G1		+		+	+		+	+	+	+	+	+	+
16q23-q24	Dehydrated hereditary stomatocytosis	DHS	Dehydrated hereditary stomatocytosis												
16q23-q24	Proteasome 25S subunit, non-ATPase, 7	PSMD7					+			+	+		+	+	+
16q23.1	Breast cancer antiestrogen resistance 1	BCAR1					+					+	+		+
16q23.2-q23.3	Chemotrypsinogen B1	CTRB1										+			
16q23.3	M-phase phosphoprotein 6	MPP					+				+	+	+	+	+
16q23.3-q24.1	WW domain-containing oxidoreductase	WWOX					+			+		+	+	+	
16q24	ATPase family gne 3	AFG3L1		+			+			+	+	+	+	+	+
16q24	Core-binding factor, alpha subunit 2, translocated to 3	CBFA2T3		+	+		+	+			+		+		+
16q24	Cyclin-dependant kinase 10	CDK10					+			+	+	+	+	+	+
16q24	Cytochrome b-245, alpha polypeptide	CYBA	Chronic granulomatous disease	+			+	+	+	+		+		+	+
16q24	Forkhead box F1	FOXF1											+	+	+
16q24	Glycine cleavage system H protein	GCSH	Glycine encephalopathy				+			+	+	+		+	+
16q24	Interleukin 17C	IL17C											+		
16q24	Membrane-bound trancription factor protease, site 1	MBTPS1		+	+	+	+			+	+	+	+	+	+

Table 4.7: Continuation of the list of known genes within the minimal region of LOH according to 16q location. The table includes information on related disorders and tissue expression.

16q location	Gene	Symbol	Disorder	BMR	SPL	TMS	BRN	SPC	HRT	MSL	LVR	PNC	PST	KDN	LNG
16q24	Malonyl-CoA decarboxylae	MLYCD		+						+	+	+	+	+	+
16q24	TATA box-binding protein associated factor 1C	TAF1C					+	+			+		+	+	+
16q24.1	Gigaxonin	GAN	Giant axonal neuropathy-1												
16q24.1	Phospholipase C, gamma 2	PLCG2		+	+		+			+	+			+	
16q24.1-q24.2	Hydroxysteroid (17-beta) dehydrogenase 2	HSD17B2									+				
16q24.2-q24.3	Cadherin-13	CDH13					+		+	+	+		+	+	+
16q24.2-q24.3	Fibrosis of extracellular muscles congenital, 3	FEOM3	Fibrosis of extracellular muscles, congenital												
16q24.3	Adenine phosphoribosyltransferase	APRT	Urolithiasis				+			+		+	+	+	+
16q24.3	E1A-like inhibitor of differentiation 1	EID1					+							+	+
16q24.3	Carbonic anhydrase V	CA5									+				
16q24.3	Cadherin-15	CDH15		+			+		+	+				+	
16q24.3	Cell matrix adhesion regulator	CMAR		+	+	+	+		+	+	+	+	+	+	+
16q24.3	Copine VII	CPNE7					+								
16q24.3	Dipeptidase-1, renal	DPEP1					+					+		+	
16q24.3	Fanconi anemia complementation group A	FANCA	Fanconi anemia	+	+		+			+	+				+
16q24.3	Forkhead box C2	FOXC2	Lymphedema-distichiasis syndrome											+	+
16q24.3	Galactosamine (N-acetyl)-6-sulfate sulfatase	GALNS	Mucopolysaccharidosis IVA	+			+							+	+
16q24.3	Growth arrest-specific 11	GAS11		+			+		+		+	+		+	+
16q24.3	Junctophilin 3	JPH3	Huntington disease-like 2				+				+				
16q24.3	Melanocortin-1 receptor	MC1R	Vulnerability to UV-induced skin damage				+	+		+	+		+	+	
16q24.3	Procollagen, type III, N-endopeptidase	PCOLN3	Cancer metastasis	+	+	+	+	+		+	+	+	+	+	+
16q24.3	Paraplegin	PGN	Spastic paraplegia-7	+	+		+			+	+		+	+	+
16q24.3	Solute carrier family 7, member 5	SLC7A5		+	+		+					+	+		+

BMR = bone marrow; SPL = spleen; TMS = thymus; BRN = brain; SPC = spinal cord; HRT = heart; MSL = muscle; LVR = liver; PNC = pancreas; PST = prostate; KDN = kidney; LNG = lung.

(Adolase A, fructose-biphosphatase) (Rebhan et al., 1997; http://bioinfo.weizmann.ac.il/cards-bin/carddisp?ALDOA) or conversely, exhibited very limited tissue expression not including the kidney as is the case for Chemotrysinogen B1 (*CTRB1*) which is exclusively expressed in the pancreas (Rebhan et al., 1997; http://bioinfo.weizmann.ac.il/cards-bin/carddisp?CTRB1). Other genes could be excluded based on their known or predicted protein function, which was unlikely contribute to renal development. This is seen for Interleukin 17C (*IL17C*), a cytokine involved in the induction the T helper 1 (Th1) response (Hurst et al., 2002). Other genes were excluded on the basis that the disorder they are involved in shows no association or potential association with renal carcinogenesis, as seen for the gene Gigaxonin (*GAN*). Defects in the *GAN* gene cause Giant Axonal Neuropathy leading to segmental distention of the neurons (Bomont et al., 2000). The majority of genes located on chromosome 16q were excluded as candidate Wilms tumor genes and are listed in Table 4.8.

4.4.3 Candidate Wilms tumor genes

Of the 102 genes, 30 were placed in either the highly probably candidate gene category or the probable candidate gene category. These genes were chosen as candidates as they fell under one or more of the selection criteria categories described previously. Of the 30 putative candidate genes, 15 were identified as being implicated in a wide variety of cancers or involved in cancer pathways as shown in Table 4.9. Eight were chosen based on their known or predicted function and interestingly, all 8 belonged to the cadherin family of

Table 4.8: List of known genes on chromosome 16q excluded as Wilms tumor candidates

16q location	Gene	16q location	Gene
16q13-q21	Anisomastia	16q22.3-q23.1	AT motif-binding factor 1
16q13-q21	Kinesin family member C3	16q23	Adaptor-related protein complex 1, gamma 1
16q13-q21	RNA polymerase II, polypeptide C	16q23-q24	Dehydrated hereditary stomatocytosis
16q13-q22	Carboxylesterase 1	16q23-q24	Proteasome 25S subunit, non-ATPase, 7
16q21	Cholesteryl ester transfer protein	16q23.1	Breast cancer antiestrogen resistance 1
16q21	Glutamic-oxaloacetic transaminase-2 mitochondrial	16q23.2-q23.3	Chemotrypsinogen B1
16q21	Heat-shock transcription factor 4	16q23.3	M-phase phosphoprotein 6
16q21	WW domain-containing	16q23.3-q24.1	WW domain-containing oxidoreductase
16q21-q23	Carbonic anhydrase VII	16q24	ATPase family gne 3
16q21-q22.3	DEAD/H box 38	16q24	Cyclin-dependant kinase 10
16q22	Cystathionase	16q24	Cytochrome b-245, alpha polypeptide
16q22	Alanyl-tRNA synthetase	16q24	Glycine cleavage system H protein
16q22	Aneurysmal bone cyss	16q24	Interleukin 17C
16q22	Amyloid beta precursor protein-binding protein-1	16q24	Membrane-bound trancription factor protease, site 1
16q22	Carbohydrate sulfotransferase-5	16q24	Malonyl-CoA decarboxylae
16q22	Carbohydrate sulfotransferase-6	16q24	TATA box-binding protein associated factor 1C
16q22	North American Indian childhood cirrhosis	16q24.1	Gigaxonin
16q22	Hydroxysteroid dehydrogenase 2	16q24.1	Phospholipase C, gamma 2
16q22	Ras-related associated with diabetes	16q24.1-q24.2	Hydroxysteroid (17-beta) dehydrogenase 2
16q22	Zinc finger protein-19	16q24.2-q24.3	Fibrosis of extracellular muscles congenital, 3
16q22-q23	Golgi apparatus protein 1	16q24.3	Adenine phosphoribosyltransferase
16q22-q23	Syntrophin, beta-2	16q24.3	Carbonic anhydrase V
16q22-q23	Aldolase A, fructose-biphosphatase	16q24.3	Copine VII
16q22-qter	Cytochrome c oxidase subunit IV, isoform 1	16q24.3	Fanconi anemia complementation group A
16q22-qter	Neighbor of Cox4	16q24.3	Galactosamine (N-acetyl)-6-sulfate sulfatase
16q22-qter	Calbindin 2	16q24.3	Growth arrest-specific 11
16q22.1	Cataract, Marner type	16q24.3	Junctophilin 3
16q22.1	Chymotrypsin-like protease	16q24.3	Paraplegin
16q22.1	Haptoglobin	16q24.3	Solute carrier family 7, member 5
16q22.1	Haptoglobin-related locus		
16q22.1	Lecithin-cholesterol acyltransferase		
16q22.1	Proteosome subunit MECL1		
16q22.1	Putative serine kinase H1		
16q22.1	Spinocerebellar ataxia 4		
16q22.1	Solute carrier family 9, isoform 5		
16q22.1	Solute carrier family 12, member 4		
16q22.1	Telomeric repeat-binding factor-2		
16q22.1	DEAD/H box 19		
16q22.1	Splicing factor 3B, subunit 3		
16q22.1	Solute carrier family 7, member 6		
16q22.1-q22.3	Tyrosine aminotransferase		
16q22.2-q22.3	Adenosine deaminase tRNA-specific 1		
16q22.2-q22.3	Lysyl-tRNA synthetase		

Table 4.9: List of genes from chromosome 16q that are known or believed to be implicated in tumorigenesis.

Gene	Expression	Function	Cancer
MMP15	BRN, HRT, MSL, LVR, PST, KDN	Zn^{2+} binding enzyme that degrades ECM	Implicated in angiogenesis and tumor invasion
AMFR	BMR, BRN, HRT, MSL, LVR, PNC, PST, KDN, LNG	Secreted by tumor cells and aids tumor motility	Implicated in poor prognosis gastric cancer
NOL3	BRN, HRT, MSL, LVR, PNC, PST, LNG	Cytoplasmic isoform my inhibit apoptosis	
AMLCR2	N/A	NA	Linked to familial myelogenous leukemia
CBFB	BMR, THM, BRN, MSL, LVR, PNC, PST, KDN, LNG	Transcription factor regulating AML1	Implicated in leukemia
TRADD	BMR, BRN, SPC, MSL, PNC, PST, KDN, LNG	Signalling	Involved in apoptosis signaling pathway
ZNF23	BRN, MSL, LVR, PNC, PST, KDN	May be involved in transcriptional regulation	Possible involvement in acute myloid leukemia???
MAF	BMR, BRN, LVR, PNC, PST, KDN, LNG	Leucine zipper transcription factor	Part of a translocation with IgH in some multiple myeloma cells
E2F4	PNC, PST, KDN, LNG, BMR, BRN, SPC, HRT, MSL, LVR	Transcription factor	Part of Rb signaling pathway
HAS3	BMR, PST, KDN, LNG	Part of ECM, role in development	Implicated in tumorigenesis
NQO1	BRN, SPC, HRT, MSL, LVR, PNC, PST, KDN, LNG	N/A	Polymorphism may increase susceptibility to certain cancers
CBFA2T3	BMR, SL, BRN, SPC, LVR, PST, LNG		Part of transloction common in acute myeloid leukemia
CMAR	BMR, SPL, TMS, BRN, HRT, MSL, LVR, PNC PST, KDN, LNG	Mitochondrial metalloprotease	May be a suppressor of tumor invasion
MCIR	BRN, SPC, MSL, LVR, PST, KDN	Involved in skin pigmentation	Defects associated with increase in skin cancer
PCOLN3	BMR, SPL, TMS, BRN, SPC, MSL, LVR, PNC, PST, KDN, LNG	Synthesis of ECM	May be involved in cancer metastasis

genes (Table 4.10). Six were chosen based on limited kidney expression (Table 4.11) and one gene was chosen based on its related disorder (Table 4.12). There is some overlap between the categories as many of the genes can be placed in more than one category; however, for simplicity, an attempt was made to place them in their best fit category. From the genes and information obtained from the database search, 10 highly probable candidate genes could be identified and these include: *BBS2*, *DPEP1* and all 8 of the cadherin genes.

4.4.4 Highest priority Wilms tumor candidate genes

Defects in the *BBS2* gene are responsible for Bardet-Beidl syndrome, a multigenic, autosomal recessive disorder characterized by obesity, pigmented retinopathy, polydactyly, hypogenitalism, mental retardation and renal anomalies (Beales et al., 1997). To date, there are 6 *BBS* genes identified, with *BBS2* being the only one localized to chromosome 16q. *BBS2* is expressed in a wide variety of tissues including the kidney. Beales et al. (2000) proposed that the *BBS* genes, including *BBS2* might be implicated in renal tumors and malformation. Since defects in *WT1* and the putative *WT2* loci not only give rise to Wilms tumors but also syndromes such as DDS, BWS and WAGR syndrome, which are often accompanied by renal malformations, defects of *BBS2* may also predispose to the development of Wilms tumor. Although there is no evidence to date that individuals with BBS are predisposed to developing Wilms tumor, it is possible that defects in the *BBS2* gene may contribute to

Table 4.10: List of cadherin genes located within the minimal region of LOH on chromosome 16q.

Gene	Expression	Function	Cancer/diseases
Ksp-cad	KDN	Cell adhesion	?
CDH8	BRN, MSL	Synaptic cell adhesion	?
CDH11	SPL, BRN, MSL, PST, KDN, LNG	Cell adhesion	Involved in ABC translocation; putative oncongenic marker
CDH1	BRN, MSL, LVR, PNC, PST, KDN, LNG	Cell adhesion	Putative tumor suppressor in many cancers
CDH3	MSL, LVR, PNC, PST, LNG	Cell adhesion	Defects in CDH3 cause HJMD
CDH5	BMR, BRN, SPC, HRT, MSL, LVR, PST, LNG	Cell adhesion	?
CDH13	BRN, HRT, MSL, LVR, PST, KDN, LNG	Cell adhesion; regulator of neural cell growth	Putative tumor suppressor in many cancers
CDH15	BMR, BRN, HRT, MSL, KDN	Cell adhesion	Deleted in breast cancer

Table 4.11: List of genes located on chromosome 16q with limited tissue expression including the kidney.

Gene	Expression	Function	Cancer/diseases
DPEP1	BRN, PNC, KDN	Renal metabolism	
AGRP	BRN, KDN, LNG	Weight homeostasis	
TK2	BRN, MSL, KDN	Mitochondrial deoxyribonucleoside kinase	Activation of chemotherapeutic drugs
FOXF1	HRT, PST, KDN, LNG	Putative TF for lung related gene	
FOXC2	KDN, LNG	Formatioin of special mesenchymal tissues	Defects in FOXC2 cause lymphedema-distichiasis syndrome
EIDI	BRN, KDN, LNG	Unknown	

Table 4.12: List of genes on chromosome 16q implicated in a potential Wilms tumor associated syndrome.

Gene	Expression	Function	Cancer/diseases
BBS2	BMR, BRN, SPC, HRT, MSL, LVR, PNC, PST, KDN, LNG	Renal development?	Defects in BBS2 cause Bardet-Beidl syndrome Type II

Wilms tumorigenesis and therefore, evaluation of *BBS2* in Wilms tumors may be warranted.

DPEP1 is a kidney membrane enzyme that hydrolyses dipeptides and is responsible for renal metabolism of glutathione and its conjugates. *DPEP1* has a fairly limited tissue expression restricted to brain, pancreas, lungs and kidney, specifically the brush borders of the kidney (Kosak and Tate, 1982). Interestingly, a subtractive hybridization experiment designed to identify differentially expressed genes between Wilms tumors and normal kidney identified the *DPEP1* gene (Austruy et al., 1993). Further characterization of this gene in Wilms tumors by Northern blot analysis revealed that RNA expression was significantly reduced or lost in the majority of Wilms tumors (Austruy et al., 1993). However, the absence of *DPEP1* in Wilms tumors could be a reflection of the fact that the cell types that express *DPEP1* may not be present in Wilms tumors. Interestingly, no further work has been published on this gene with respect to Wilms tumorigenesis; however, preliminary results support further evaluation of *DPEP1* in fetal kidney and Wilms tumor.

Eight cadherin genes, including Ksp-cadherin, E-cadherin, *CDH8*, *CDH11*, *CDH5*, *CDH3*, *CDH13* and *CDH15*, localize to the minimal region of chromosome 16q LOH. Cadherins are cell adhesion molecules that aid in the establishment and maintenance of cell-cell contacts (Takeichi, 1988; Takeichi et al., 1988). The best characterized cadherin family member *is E-cadherin* and loss of E-cadherin expression is thought to contribute to the behavior of numerous carcinomas including breast, gastric and lung cancers (reviewed in

Hirohasi, 1998). In addition to E-cadherin, other cadherin genes have also been implicated in carcinogenesis. *CDH13* has been found to be silenced in lung (Sato et al., 1998) and breast cancers (Lee, 1996 and Toyooka et al., 2001). Based on the initial candidate gene selection criteria: protein function, kidney expression, renal development and carcinogenic implication, one cadherin gene, Ksp (kidney-specific)-cadherin fulfilled all of the requirements of a candidate Wilms tumor gene. Ksp-cadherin was found to be an attractive Wilms tumor candidate gene and therefore was given highest priority for evaluation in Wilms tumors as discussed in Chapter 5.

4.5 Discussion

DD-PCR and *in silico* database searching was employed to identify candidate Wilms tumor genes located on chromosome 16q. However, each approach comes with its own advantages and disadvantages directly impacting its ability to specifically target Wilms tumor genes as discussed below.

DD-PCR is a technique that has been successfully used to identify differentially expressed transcripts/genes in cancer, development, infection, hematopoiesis and others (Liang and Pardee, 1992). It was chosen for our study to identify putative candidate Wilms tumor genes, as at the time of the proposal, it was the preferred method of gene profiling as microarrays were just being introduced and the human genome had not yet been sequenced. Other reasons for selecting DD-PCR include: (1) not as labour intensive as compared to some of the other differential gene profiling methods; (2) ability to simultaneously identify known and unknown genes; (3) ability to identify genes that are both up- and down-regulated; and (4) requirement for small amounts of RNA.

For the DD-PCR assay, we used a combination of 3 anchored primers (T_{11}MG, T_{11}MC, T_{11}MA) together with 20 arbitrary primers for a total of 60 PCR reactions. The fourth anchored primer (T_{11}MT) was not used as it has been shown that it amplifies the least number of cDNAs and yields the least number of true differentially expressed fragments (Mou et al., 1994; Malhotra et al., 1998). It has been estimated that there are 30 000 – 35 000 genes in the human genome, and each cell type expresses only 10-15% of the genes. Therefore, any cell should theoretically express 3 000 – 5 000 genes (The Genome International Sequencing Consortium, 2001). The three anchored primer sets were found to have similar efficiencies, as all three generated approximately the same number of cDNAs. It was found that each DD-PCR reaction typically produced about 100 cDNA fragments that could be resolved by gel electrophoresis. This may actually represent more than 100 cDNAs due to the fact that several cDNAs can co-migrate producing the illusion of only one band. Therefore, 100 cDNAs multiplied by 60 PCR amplifications equals 6000 cDNAs indicating that the DD-PCR assay should have provided an accurate representation of the majority of expressed transcripts in Wilms tumor cells. These findings are in accordance with those of Liang and Pardee (1992) who found that 60-100 bands per lane were optimally resolved by electrophoresis.

Since we were comparing 3 tumors that had retained 16q heterozygosity against 3 tumors that had lost 16q heterozygosity, it was proposed that only fragments that were up- or down-regulated in all 3 tumors of one group compared to the second group would be isolated. However, this was rarely observed and more often than not, variations between the 3 tumors of one group occurred, making the isolation of differentially expressed transcripts exclusively expressed in one tumor group but not the other difficult. Due to the lack of transcripts expressed exclusively in one tumor group, candidate transcripts were selected if they were expressed in at least 2/3 of one tumor group and not expressed in at least 2/3 of the other group. The differential expression often seen between each of the tumor samples within the same group (16q+ or 16q-) is most likely due to the fact that Wilms tumors are genetically heterogeneous, and even though we tried to control for genetic variation introduced by genes on chromosomes 11p and 1p, tumor heterogeneity was still evident. Many of the successful DD-PCR experiments have been carried out with cell lines, which often are not as heterogeneous as primary tumor tissue; however, as a truly representational Wilms tumor cell line is not available this was not an option for us (Gardner-Thorpe et al., 2002). Other successful DD-PCR experiments used a single cell line treated with a specific agent (drug, radiation, etc.) and isolated genes that are up- or down-regulated as a response to the induction (Kaneko et al., 2002). This minimizes variation/heterogeneity and increases the likelihood of identifying gene(s) specifically targeted by the inducing agent.

Sixty-two differentially expressed fragments were isolated, reamplified, cloned and sequenced. Of these 62, only 18 represented known genes and/or ESTs, while the remainder were found to be genomic DNA, repetitive elements, mitochondrial DNA or unknown genes. The DD-PCR assay was designed to target genes on chromosome 16q by comparing tumors that have lost chromosome 16q heterozygosity against tumors that have retained chromosome 16q heterozygosity. Surprisingly, none of the identified genes localized to chromosome 16. Based on these results, one might conclude that the DD-PCR assay was not successful in identifying genes specific to chromosome 16q. However, it is still possible that the genes identified are indirectly involved in pathways related to chromosome 16q. Furthermore, we have not ruled out the possibility that one of our unknown genes may in fact localize to chromosome 16q and be the 16q Wilms tumor gene.

It is possible that inactivation of the putative Wilms tumor gene on chromosome 16q may occur as a result of inactivation of another Wilms tumor gene. For example, it is possible that inactivation of Wilms tumor genes located on chromosomes 11p and/or 1p may lead to inactivation of the gene on 16q or vice versa. Since we selected tumors that not only had lost or retained 16q heterozygosity, but had also retained 11p and 1p heterozygosity (which suggests that the putative genes in these regions are intact), this may have interfered with the DD-PCR results. It is therefore possible that instead of specifically targeting Wilms tumor genes on chromosome 16q, we may in fact have been selectively omitting genes on chromosome 16q as it was presumed that the putative Wilms tumor genes on chromosomes 11p and 1p were functional in the tumors chosen for our study.

As no chromosome 16q genes were identified, and it is possible that some of the isolated genes may be indirectly involved in the chromosome 16q Wilms tumor-related pathway, 12 genes were further characterized by semi-quantitative RT-PCR to confirm the differential expression seen in the DD-PCR assay. The semi-quantitative RT-PCR approach was used over Northern blot analysis because: (1) only a limited amount of mRNA was available for each of the tumors; (2) RT-PCR has increased sensitivity and can detect lower levels of expression; and (3) some of the mRNA was of poorer quality and could not easily be visualized by northern blotting. However, there are limitations with the RT-PCR assay. The sensitivity of RT-PCR can complicate expression analyses as amplification of contaminating material as well as variation in PCR amplification efficiencies can result in over- or under-estimation of gene expression. Furthermore, many of the genes used as controls (*GAPDH*, *β-actin*, *28S rRNA*) have been reported to be differentially expressed between different tissues samples, tumors and tissues from different developmental stages (Thellin et al., 1999). In fact, it is possible that *GAPDH* is differentially expressed in Wilms tumors as seen by the results of our RT-PCR analysis. Interestingly, a study of telomerase RNA expression in Wilms tumors that used *GAPDH* as an expression control also revealed differential *GAPDH* expression in tumors and normal kidney. Therefore *GAPDH* RNA levels were not incorporated into final calculations of telomerase expression, but rather levels of telomerase expression were compared across tumors. (Jeffrey Dome, St. Jude's Children's Research

Hospital, personal communication). Therefore, we evaluated gene expression between tumors with and without normalizing for *GAPDH*.

We carried out semi-quantitative RT-PCR based on cycle number and cDNA dilutions rather than real time RT-PCR due to the high cost associated with generating the many gene-specific primers needed for the real time assay. A complimentary method (such as Northern blotting) to evaluate RNA levels in our tumor samples would be needed to validate our semi-quantitative RT-PCR data. Future experiments should be carried with tumors for which adequate, high quality RNA or tissue is available.

Two methods of analyzing the data generated from the RT-PCR analysis were used to allow for a more accurate and reliable measurement of gene expression levels. Neither method confirmed the original DD-PCR expression data for any of the 12 genes evaluated. This suggests that most, if not all, of the genes isolated are artifacts generated by the DD-PCR assay and represent false positives. Furthermore, all of the genes analysed by semi-quantitative RT-PCR, showed significant levels of RNA, indicating that none of the genes were completely silenced or inactivated in the Wilms tumors analysed. This provides further evidence that the isolated cDNAs may represent artifacts, as it is generally believed that LOH of chromosome 16q would result in the loss of a tumor suppressor gene. However, if one of the genes identified by DD-PCR represented a downstream target of Wilms tumorigenesis, rather than a Wilms tumor gene, complete loss or reduction of RNA would not necessarily occur.

The high number of false positives seen in our study is in accordance with studies published in the literature. In fact, Sompayrac et al. (1995) have reported that up to 90% of the cDNAs isolated by DD-PCR are in fact false positives and Kociok et al. (1998) found that approximately 40% of the cDNAs are not reproducible. The false positives generated in our DD-PCR analysis may be attributed to the presence of more than one cDNA per band in some cases. Therefore, isolation and re-amplification of the cDNA fragments may have resulted in the wrong cDNA being isolated. Furthermore, the cloning of PCR products consisting of more than one cDNA would lead to the production of clones containing different cDNAs, some of which would contain differentially expressed cDNAs, while others would not. Therefore, depending on which clone is picked and sequenced, there is a chance that the clone containing the differentially expressed cDNA could be overlooked. It would be beneficial to sequence several clones to ensure that the differentially expressed cDNA is not missed and to get a true representation of the cDNA isolated; however, this would add considerable time and cost to the analysis. Furthermore, because of co-migration, cDNAs that are truly differentially expressed may be overlooked. This is due to the fact that another cDNA, that is not differentially expressed, can migrate to the same position as a cDNA that is differentially expressed, resulting in a non-differential, uniform band in all samples.

The DD-PCR analysis was successful in amplifying a high percentage of the transcripts expressed by Wilms tumors. However, none of the genes isolated, based on their putative function, gene location and/or RT-PCR results, are likely to be the chromosome 16q Wilms tumor gene with the possible exception of *MLLT10.* Attempts to specifically target genes on chromosome 16q were unsuccessful as no chromosome 16q genes were isolated. Furthermore, none of the genes isolated mapped to any of the putative Wilms tumor loci suggesting that this method of gene profiling may not have been the best technique for identifying Wilms tumor genes. Due to time constraints, evaluation of the majority of ESTs and unknown genes was not performed. However, it is possible that some of the uncharacterized ESTs and sequences representing unknown genes isolated by the DD-PCR assay may be the chromosome 16q Wilms tumor gene and may be involved Wilms tumorigenesis. Therefore, further evaluation of these transcripts by semi-quantitative RT-PCR should be performed. Despite the fact that many of the genes isolated by DD-PCR may represent false positives, two genes were selected for further analysis in an expanded series of Wilms tumors. *MLLT10* was selected based on the fact that it is involved in childhood leukemias while *EIF4b* was selected as initial RT-PCR results were thought to confirm the differential expression seen in the original DD-PCR assay.

MLLT10 is one of the *MLL* partner genes involved in t(10;11)(p12;q23) translocations. *MLLT10* is expressed in many tissues but is predominantly found in the testis and encodes a N-terminal zinc finger and a C-terminal leucine zipper. The *MLLT10 – MLL* translocation creates a fusion protein in which the *MLL* zinc fingers are replaced with the *MLLT10* leucine zipper which is thought to produce a novel class of transcription factor (Chaplin et al., 1995). Comparison of *MLLT10* expression levels, independent of *GAPDH*, revealed that the tumors that had lost 16q heterozygosity expressed slightly lower levels of *MLLT10* than tumors that had retained 16q heterozygosity. Initial studies in mice found that *MLLT10* may function as a regulator of cellular proliferation and therefore inactivation of *MLLT10* could result in cell growth; however, no further studies in mice or humans to confirm this have been conducted (Linder et al., 1998). Confirmation of the semi-quantitative RT-PCR results by either Northern blot analysis or real time RT-PCR would be beneficial to confirm that *MLLT10* is in fact differentially expressed in Wilms tumors. If this were the case, further evaluation of *MLLT10* in an expanded study of more Wilms tumors and normal mature and fetal kidney would be warranted. If *MLLT10* is in fact a regulator of cellular proliferation and it is found to be down-regulated in Wilms tumors that have lost chromosome 16q, *MLLT10* would then likely have to be regulated by the putative Wilms tumor gene on chromosome 16q. Further evaluation of *MLLT10* would be interesting to determine if it represents one of the up- or downstream targets of the chromosome 16q gene believed to be involved in the progression of a subset of Wilms tumors.

Further analysis of *EIF4b* in Wilms tumors and normal kidney was also performed. *EIF4b* aids in the binding of mRNA to the ribosome by unwinding the secondary structure in the 5' untranslated region (Methot et al., 1994). No mutations or dysregulation of *EIF4b* in disease or cancer have been reported in the literature. The RT-PCR analysis did not show any evidence of differential expression; however, interestingly, *EIF4b* was up-regulated in the majority of

Wilms tumors as compared to normal mature and fetal kidney. A recent report studying *Drosophila EIF4b (dEIF4b)* has demonstrated that overexpression of *dEIF4b* increased cell proliferation in differentiated imaginal discs (Hernandez et al., 2004). This is the first report providing evidence that *EIF4b* may function as a regulator of cell growth and proliferation in addition to translation initiation. If EIF4b can in fact regulate cell proliferation, its up-regulation in Wilms tumors may contribute to tumorigenesis, acting as an oncogene rather than the expected tumor suppressor gene. However, the increase in *EIF4b* expression in Wilms tumors could be attributed to the increase in cellular proliferation associated with tumorigenesis. Both the *EIF4b* functional data and our RT-PCR results are preliminary. Additional information of the role of *EIF4b* as a putative regulator of cell proliferation in humans and confirmation of the RT-PCR results by Northern blot analysis or real time PCR would be beneficial prior to initiating further studies.

Numerous gene profiling techniques have been developed to identify differentially expressed genes. Subtractive hybridization was one of the first techniques that was successful in identifying up-regulated genes between two different populations. The advantage of subtractive hybridization is that it is not prone to generating false positives; however, it is unable to detect low abundance transcripts. Furthermore, subtractive hybridization is labour intensive due to the fact that several rounds of subtraction (hybridization) are needed and the subtraction process has to be performed in the reverse direction in order to ensure both up and down-regulated genes are identified (reviewed in Byers et al., 2000).

In recent years, microarray analysis has become the method of choice for studying differential gene expression and has identified differentially expressed genes in cancer, human disease and drug discovery (DeRisi et al., 1996; Mirnics et al., 2001; Braxton and Bedilion, 2001). Microarrays are comprised of a solid support system onto which DNA from up to 20 000 transcripts have been spotted. RNA from the cell/tissue population of interest is labeled and hybridized to the array, binding only to complementary sequences (Watson et al., 1998). The patterns obtained from the 2 populations of interest are compared and differentially expressed genes can be identified. Microarray analysis is advantageous as it allows the simultaneous quantitative evaluation of 10 000-20 000 genes/ESTs between several different populations. However, its high throughput nature is also one of its biggest disadvantages as it is prone to generating large volumes of data that need to be evaluated. Additional disadvantages of microarray analysis is that it is costly, only known genes can be evaluated, it can generate false positives and it lacks reproducibility, a common problem among many of the gene expression techniques (reviewed in Bustin and Dorudi, 2002).

The most recent technique developed for identifying candidate genes is the use of proteomics and the protein chip arrays. They are similar in design as microarrays; however, instead of comparing expression of genes or transcripts between cell populations, they allow comparison of protein levels in different populations. Similar to microarrays, proteins in their native conformation are immobilized on a chip and then protein lysates from the cells/tissue of interest are bound. Protein chips are useful for identifying prognostic and diagnostic tumor markers, altered proteins that cause disease and evaluation of post-translation modifications, options that are not available with RNA expression methodologies (reviewed in Fung et al., 2001). However, cost, data management and reproducibility are variables that can complicate the analyses.

The *in silico* approach of database searching proved to be a successful method of identifying candidate Wilms tumor genes. This method, which has become more widely used since the sequencing of the human genome, is both a cost- and time-effective approach for identifying candidate genes. Although this method is only useful in situations where a gene region has been identified for the disease or cancer of interest, if this information is known, it can be successful at identifying relevant disease-causing genes. The critical Wilms tumor gene region on chromosome 16q was narrowed down to a 6.7 Mb region between 21-q24 and 102 genes have been localized to this region. Review of the literature of these genes enabled their placement into one of three categories: (1) high-priority Wilms tumor candidate genes; (2) low-priority Wilms tumor candidate genes and (3) unlikely Wilms tumor candidate genes. Thirty genes were placed in the high priority category, and of these 10 were believed to represent the highest priority candidates. The gene, *Ksp-cadherin*, was chosen as the top candidate based on its expression profile and putative function and was evaluated in a series of Wilms tumors as discussed in Chapter 5. It would be of interest to perform RT-PCR and/or Northern blot analysis on the remaining high priority candidates (*BBS2*, *DPEP1* and the 7 other cadherin genes) as one or more of them may have a role in Wilms tumorigenesis.

It is apparent that the *in silico* approach to identifying candidate Wilms tumor genes was successful and has significant advantages over some of the more traditional approaches. The major limitations of this method is that a defined candidate region has to be known, and only known genes can be evaluated. Although, it is probable that numerous genes will reside in the critical gene region, simple literature searches aided by the OMIM genemap database can eliminate the majority of candidates based on their expression and function. The ease of designing and obtaining primers for RT-PCR or Northern analysis, allows one to screen through numerous genes quickly.

The ultimate goal of both of these approaches was not only to identify Wilms tumor genes, but those that are specifically located on chromosome 16q. DD-PCR analysis did not identify any genes located on chromosome 16q, although the genes identified may represent upstream or downstream targets of the chromosome 16q Wilms tumor gene. However, the *in silico* approach exclusively examined genes located on chromosome 16q. Although the *in silico* approach initially does not reveal any information on gene expression as is the case for DD-PCR, it does minimize the number of candidates to evaluate as only genes that, by function and expression link them to the cancer or disease of interest, are selected. Thus, screening databases for candidate genes in the minimal region of LOH of Wilms tumor loci may represent the most effective approach. If no high priority candidates are identified, then another approach like microarray analysis could be initiated.

In summary, DD-PCR does not appear to be the best method for identifying candidate Wilms tumor genes, as a large number of false positives and irrelevant candidates were isolated. If a Wilms tumor gene profiling assay were to be proposed for present day, some of the more recently developed technologies such as microarrays or protein arrays would likely be better approaches.

Chapter 5

Evaluation of Ksp-cadherin in Wilms tumor

A portion of this chapter has been submitted for publication: Gillan TL, Dietrich K, Perlman EJ, Godbout R, Grundy PE. Ksp-cadherin represents a new candidate Wilms tumor gene. (Submitted to Cancer Research).

5.1 Ksp-cadherin

Kidney-specific cadherin (Ksp-cadherin) was identified as a potential Wilms tumor gene, via *in silico* database searching and fulfills many of the requirements of a chromosome 16q Wilms tumor candidate gene. It localizes to the minimal region of chromosome 16q LOH in Wilms tumors, is exclusively expressed in the epithelial tubular cells of the developing and adult kidney (Thomson et al., 1998; Thompson and Aronson, 1999) and is believed to regulate cell adhesion and proliferation.

Cadherins are a superfamily of calcium-dependent cell adhesion molecules important in the establishment and maintenance of cell-cell contacts and have also been implicated in development and cell polarity (Takeichi et al., 1988; Takeichi et al., 1991). Several of the cadherins mediate homophilic cell-cell adhesion via interaction with the actin cytoskeleton within adherens junctions in normal epithelium (Ozawa et al., 1989). Many of the cadherin genes localize to one of three chromosomal regions: 5p, 16q and 18q (Kremmidiotis et al., 1998). Interestingly, these 3 chromosomal regions have been shown to undergo LOH in many cancers. Chromosome 16q LOH has been documented in Wilms tumors (Maw et al., 1992), breast cancer (Doggett et al., 1995), hepatocellular carcinoma (Nishida et al., 1992) and prostate cancer (Cher et al., 1995); chromosome 18q LOH is seen in gastric cancer, colorectal cancer and head and neck squamous cell carcinoma (Jones et al., 1997); while some sporadic colorectal cancers exhibit chromosome 5p LOH (Xu et al., 2003).

The proposed functions of cadherins make them prime candidates for tumor suppressor genes. Loss of cadherin function leads to loss of cell-cell adhesion, which may then result in tumor growth, proliferation and metastasis (Hirohashi, 1998). The best characterized cadherin gene is the classical cadherin, E-cadherin. Inactivation of E-cadherin by both somatic and germline mutations, as well as epigenetic events such as hypermethylation, have been reported in lobular breast cancer (Berx et al., 1996; Graff et al., 1995), gastric cancer (Hirohashi et al., 1998) and prostate cancer (Umbas et al., 1994). Additional cadherin genes such as N-cadherin and P-cadherin have been shown to be silenced in prostate cancer (Arenas et al., 2000). Interestingly, up-regulation of LI-cadherin is seen in hepatocellular carcinoma, gastric intestinal metaplasia and pancreatic duct adenocarcinoma in contrast to the down-regulation seen with several of the cadherin genes in cancer (Wong et al., 2003).

Several cadherin genes have been evaluated in Wilms tumors including E-cadherin, cadherin-11 and P-cadherin, all of which localize to chromosome 16q22-q24. Neither significant reduction of RNA expression nor altered size transcripts of cadherin-11 and P-cadherin were detected; however, E-cadherin expression was reduced in some of the poorly differentiated Wilms tumors (Alami et al., 2003; Schulz et al., 2000; Safford et al., 2003).

The Ksp-cadherin gene is comprised of 18 exons, which is transcribed into a 2.2 Kb mRNA, producing a 130 kDa protein. Alternative splicing has also been demonstrated. Ksp-cadherin belongs to the 7D-cadherin subfamily that also includes LI-cadherin. The 7D-cadherins differ from the prototypic classical cadherins, such as E-cadherin in that they: (1) contain 2 additional cadherin binding domains; (2) lack the HAV prosequence and (3) have a truncated cytoplasmic tail (Thomson, 1995; Wendeler et al., 2004). Although the exact function of Ksp-cadherin is not known, it is thought to be similar to other cadherins and play a role in cell polarity, development and the establishment and maintenance of cell-cell contacts. Studies have shown that Ksp-cadherin can mediate homophilic, calcium-dependent cell-cell adhesion, however, unlike the classical cadherins, the 7D-cadherins do not associate with members of the Armadillo family of proteins (catenins) and the actin cytoskeleton (Wendeler et al., 2004). The exact manner of how the 7D-cadherins modulate calcium-dependant cell adhesion independent of catenin binding remains unanswered. It has also recently been demonstrated that Ksp-cadherin is regulated by Hepatocyte nuclear factor-1β (*HNF-1β*) and mutations within the *HNF-1β* binding site or the two associated GC boxes located within the Ksp-cadherin promoter, can abolish Ksp-cadherin expression (Bai et al., 2002).

We hypothesized that Ksp-cadherin could be the chromosome 16q Wilms tumor gene associated with poor prognosis, and inactivation of Ksp-cadherin would be seen in these tumors. We therefore proposed to evaluate RNA and protein expression of Ksp-cadherin in Wilms tumors and if evidence of gene silencing was found, attempt to identify the mechanism of gene inactivation by performing gene and promoter mutation analyses and promoter methylation analysis would be initiated.

5.2 Tumor sample population

Ksp-cadherin was evaluated in 34 Wilms tumors previously analysed in our laboratory for chromosome 16q LOH status. Of the 34 Wilms tumors evaluated, 12 tumors lost heterozygosity of 16q and 20 retained heterozygosity of 16q. LOH status could not be determined in two cases because normal DNA was not available. Ksp-cadherin is exclusively expressed in renal epithelial cells. Therefore, a higher proportion of epithelial predominant Wilms tumors, comprised of a minimum of 60% epithelial cells, were specifically selected for the study. Of the 34 tumors, 18 were epithelial-predominant while the remaining 16 tumors consisted of varying proportions (0-60%) of epithelial, stromal and/or blastemal cells. Of the 12 tumors with chromosome 16q LOH, 5 were epithelial predominant. Of the 20 tumors that retained chromosome 16q heterozygosity, 11 were epithelial predominant. Both tumors with unknown LOH status were predominantly epithelial. Included in the immunohistochemical analysis were 6 additional Wilms tumors selected for their association with nephrogenic rests, which are thought to represent Wilms tumor precursor lesions. Mature kidney tissue obtained from the normal kidney of Wilms tumor patients and fetal kidney tissues were also included in the study.

5.3 RNA analysis of Ksp-cadherin

Ksp-cadherin RNA levels in 34 Wilms tumors, 5 normal mature kidney and 5 normal fetal kidney samples were examined by RT-PCR. The 5' and 3' ends of Ksp-cadherin were evaluated separately. Of the 34 tumors, 14 (41%) contained both the 5' and 3' ends of the Ksp-cadherin transcript, while 11 (32%) expressed the 3' end only. The remaining 9 tumors (27%) did not express Ksp-cadherin RNA. Representative results are shown in Figure 5.1. Both the 5' and 3' ends of the Ksp-cadherin transcript were expressed in all of the mature and fetal kidney samples. *GAPDH* was expressed in all 34 Wilms tumors confirming that adequate intact RNA was present. Northern blot analysis was carried out using nine representative Wilms tumor samples (Fig. 5.2). Only one of the tumors, WT-2, expressed significant levels of Ksp-cadherin RNA. A low level of Ksp-cadherin was also observed in WT-14, while no transcripts, full length or truncated, were detected in the remaining tumors. β-actin was expressed at similar levels between tumors confirming the presence of intact RNA in all but one tumor, WT-33. The comparison of RNA expression by Northern blot analysis versus RT-PCR for the 8 tumors with intact RNA is shown in Table 5.1. The two tumors that expressed Ksp-cadherin by Northern blot analysis also expressed the 5' and 3' ends of the transcript by RT-PCR analysis. Of the six tumors that did not express RNA by Northern analysis, by RT-PCR analysis, two of the tumors expressed both the 5' and 3' ends of the transcripts, two expressed the 3' end only and two generated no products.

To determine whether there was a correlation between loss of Ksp-cadherin expression and chromosome 16q LOH, we examined our RT-PCR results based on chromosome 16q LOH status. Of the 34 Wilms tumors, 20 (59%) retained chromosome 16q and of these, 8 (40%) expressed both the 5' and 3' ends of the Ksp-cadherin transcript, 6 (30%) expressed 3' Ksp-cadherin

Figure 5.1: RT-PCR analysis of Ksp-cadherin in Wilms tumor. Representative RT-PCR gel showing the presence or absence of Ksp-cadherin mRNA in Wilms tumors and a normal mature kidney sample. In tumors WT-1 and WT-4, Ksp-cadherin is not expressed, tumor WT-3 expresses the 3' end of the gene only and tumor WT-2 and normal kidney (N) express both the 5' and 3' ends of the transcript. The -RT lanes represent the control samples to which no reverse transcriptase enzyme was added. Included in the bottom panel are the 16q LOH and epithelial status.

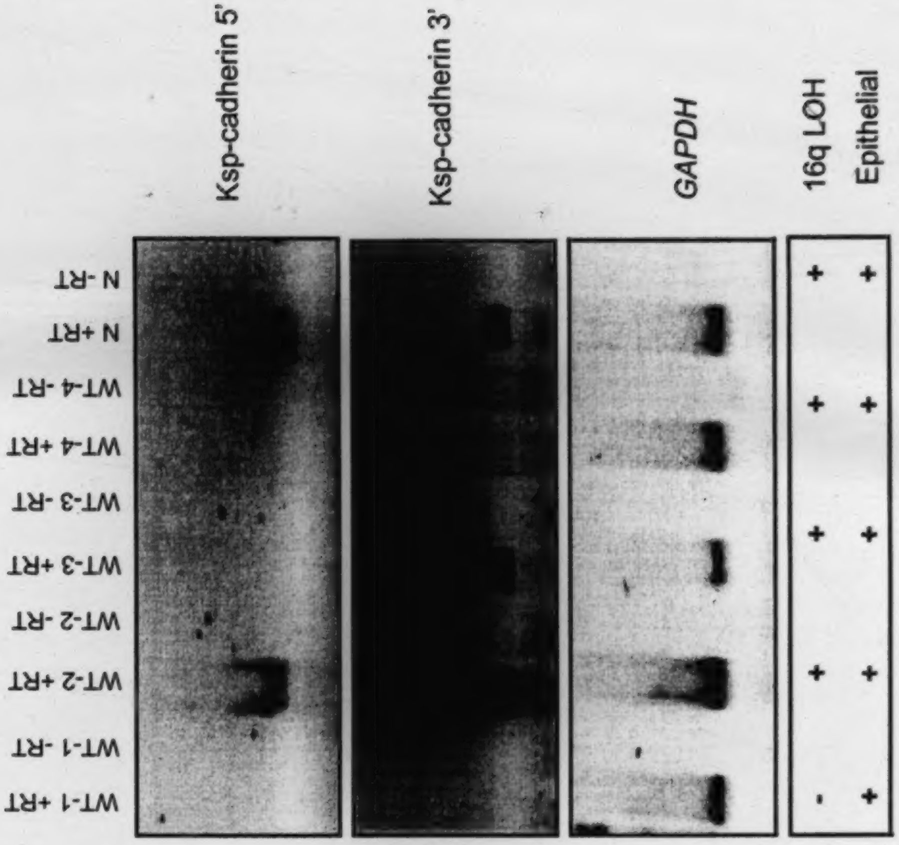
Ksp-cadherin 5'
Ksp-cadherin 3'
GAPDH
16q LOH
Epithelial
N -RT
N +RT
WT-4 -RT
WT-4 +RT
WT-3 -RT
WT-3 +RT
WT-2 -RT
WT-2 +RT
WT-1 -RT
WT-1 +RT
+
+
+
+
+
+
+
+
-
+

Figure 5.2: Northern blot analysis of Ksp-cadherin in Wilms tumor. Analysis of 9 Wilms tumors by Northern blot analysis with hybridization to a full length Ksp-cadherin cDNA probe. Only 2 tumors express Ksp-cadherin mRNA. Tumor WT-2 expresses high levels of Ksp-cadherin RNA while WT-14 expresses low levels of this transcript. The RNA from tumor WT-33 is degraded and therefore was excluded from this analysis.

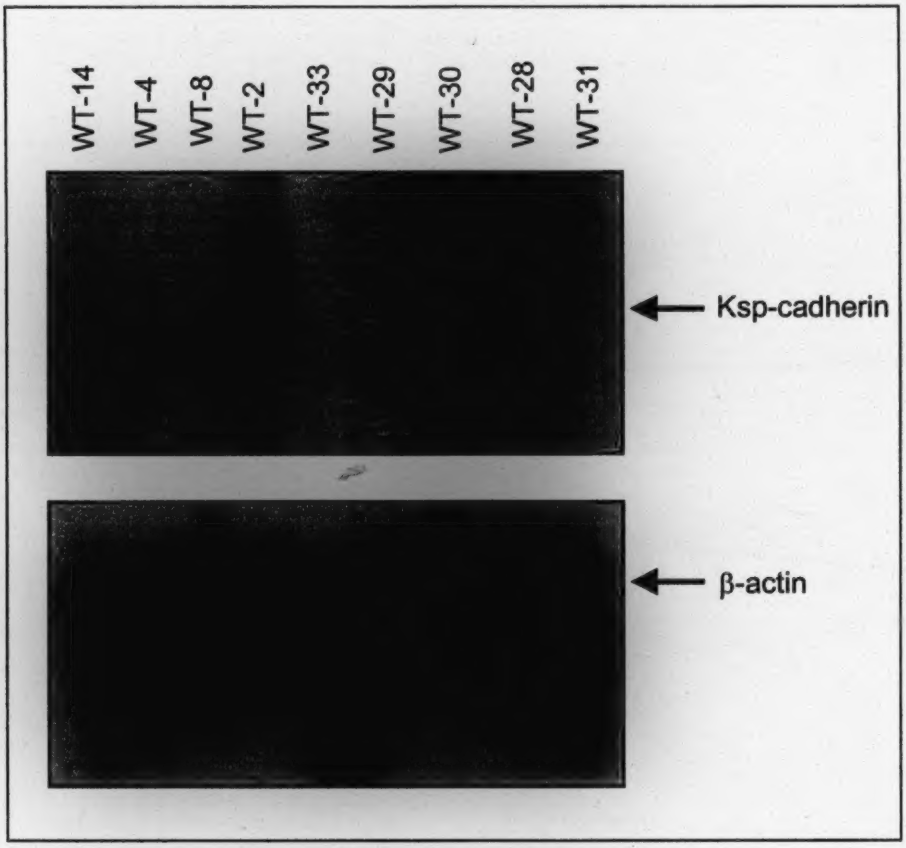
WT-14
WT-4
WT-8
WT-2
WT-33
WT-29
WT-30
WT-28
WT-31
Ksp-cadherin
β-actin

Table 5.1: Comparison of Northern blot and RT-PCR results, chromosome 16q LOH status and histology in 8 representative Wilms tumors.

Wilms tumor	Northern	RT-PCR 5'	RT-PCR 3'	16q LOH	Epithelial
WT-14	+	+	+	+	+
WT-4	-	-	-	+	+
WT-8	-	-	+	+	+
WT-2	++	+	+	+	+
WT-29	-	-	+	-	-
WT-30	-	+	+	-	-
WT-28	-	-	-	-	-
WT-31	-	+	+	-	+

Note: + indicates positive Ksp-cadherin expression; ++ very strong Ksp-cadherin expression; - no Ksp-cadherin expression.

only, and 6 (30%) did not express Ksp-cadherin. Of the 12 Wilms tumors that lost heterozygosity of chromosome 16q, 5 (42%) expressed both the 5' and 3' Ksp-cadherin transcripts, 5 (42%) expressed the 3' end only, and 2 (16%) did not express Ksp-cadherin. Of the two tumors for which no LOH data was available, 1 expressed both the 5' and 3' ends while the other did not express Ksp-cadherin. Loss of Ksp-cadherin RNA expression is slightly higher in the tumors that retain chromosome 16q LOH; however, based on Chi square analysis, this association is not statistically significant ($X^2 = 0.835$; $p \leq 1$).

Next, we analysed our RT-PCR results based on epithelial cell status. Of the 34 Wilms tumors, 18 (53%) were comprised of a minimum of 60% epithelial cells based on histology results at the time of collection and are thus classified as epithelial predominant. The remaining 16 (47%) had less than 60% epithelial cells, if any. Of the 18 epithelial predominant Wilms tumors, 10 (55%) expressed both the 5' and 3' ends of the Ksp-cadherin transcript, 5 (28%) expressed the 3' end only and 3 (17%) did not express Ksp-cadherin RNA. Figure 5.3 provides a summary of the Ksp-cadherin RT-PCR results for the tumors that lost and retained chromosome 16q heterozygosity and the epithelial predominant tumors. Results of the RNA studies indicate that a large percentage of Wilms tumors evaluated have either absent or defective Ksp-cadherin RNA expression.

5.4 Western blot analysis of Ksp-cadherin in Wilms tumor

Ksp-cadherin protein expression levels were determined by Western blot analysis using a monoclonal Ksp-cadherin antibody targeted to the C-terminus.

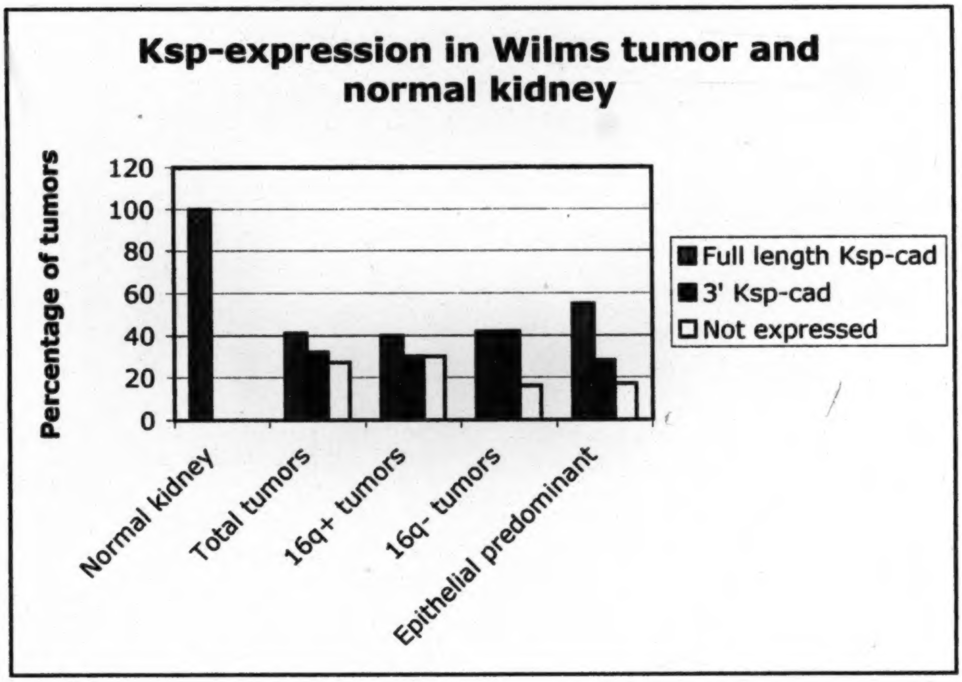

Figure 5.3: Summary of Ksp-cadherin RNA expression in Wilms tumors. Breakdown of the Ksp-cadherin RT-PCR results in Wilms tumors and normal kidney. The figure shows the total number of Wilms tumors that display full length Ksp-cadherin, the 3' end only and those that do not express Ksp-cadherin. The distribution of Ksp-cadherin expression is also shown by chromosome 16q LOH status as well as for epithelial predominant tumors.

Thirty-four Wilms tumors, 13 normal mature kidney and 2 normal fetal kidney samples were evaluated. Of the 34 Wilms tumors, only 1, WT-7 expressed the Ksp-cadherin protein while 13/13 mature and 2/2 fetal kidney samples abundantly expressed the Ksp-cadherin protein (Fig. 5.4). The one Wilms tumor that expressed Ksp-cadherin protein also expressed the full length *Ksp-cadherin* cDNA, did not lose 16q heterozygosity and was epithelial predominant.

5.5 Ksp-cadherin immunohistochemistry *(done by Chiler Hassan, Dr. Perlman's Laboratory, University of Northwestern).*

Paraffin embedded blocks were available for 15 of the 34 Wilms tumors. Nine of these tumors were comprised of ≥60% epithelial cells while the remaining 6 were composed of mixed cell types some of which included epithelial cells. In addition to these 15 Wilms tumors, slides from 6 additional tumors were selected for the presence of intralobar or perilobar nephrogenic rests. All were also evaluated by immunohistochemistry. Ten mature and 4 fetal kidney samples at 12, 18, 25, and 36 weeks gestation were included as normal controls. Eleven of fifteen Wilms tumors were completely negative for Ksp-cadherin protein expression while the remaining four tumors had areas of positive staining in rare microscopic foci comprised of epithelial tubular cells (Fig. 5.5). Although these foci were positive for Ksp-cadherin, the vast majority of epithelial tubular structures in these 4 tumors were negative for this protein. All of the mature and fetal kidney samples showed a positive Ksp-cadherin signal which increased with gestational age and was confined to the distal tubules and collecting ducts (Fig.

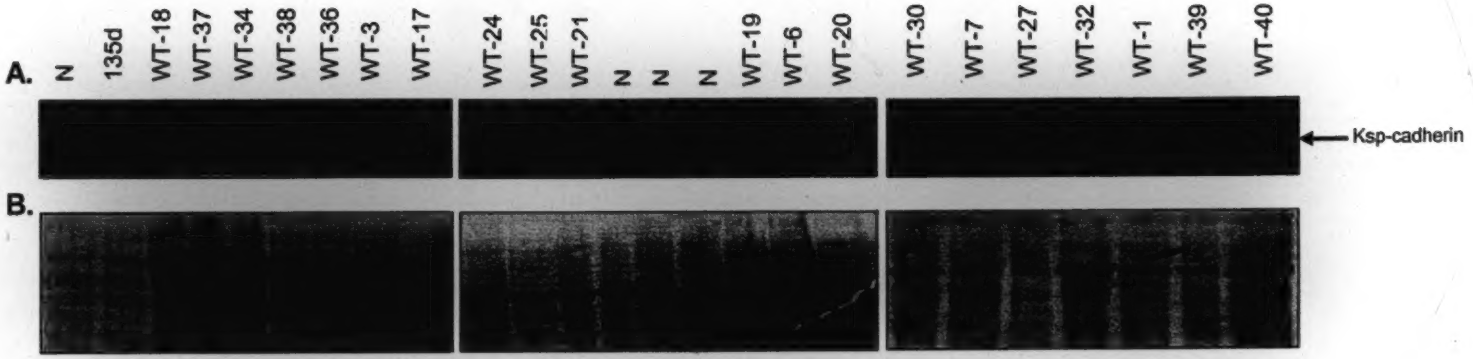
A.
N
135d
WT-18
WT-37
WT-34
WT-38
WT-36
WT-3
WT-17
WT-24
WT-25
WT-21
N
N
N
WT-19
WT-6
WT-20
WT-30
WT-7
WT-27
WT-32
WT-1
WT-39
WT-40
Ksp-cadherin
B.

Figure 5.4: Western Blot Analysis of Ksp-cadherin. A. Wilms tumors as well as fetal (d) and normal mature kidney (N) were evaluated for Ksp-cadherin protein expression by Western Blot analysis. These figures are a representation of the results seen in each tissue type. All fetal and mature kidneys were positive for Ksp-cadherin protein as seen in panels A and B, while all tumors were negative for Ksp-cadherin protein with the exception of Wilms tumor WT-7. **B.** Membranes were stained with CPTS to illustrate amount of protein loaded.

36 week fetal kidney Wilms tumor Nephrogenic rest

Figure 5.5: Representative immunohistochemistry results. Panel A shows Ksp-cadherin staining in the fetal kidney (as designated by arrows); Panel B shows Ksp-cadherin staining of a microscopic foci comprised of epithelial tubular cells in a Wilms tumor (black arrow). Multiple additional epithelial tubular structures are also present that are negative for Ksp-cadherin staining (blue arrow); Panel C shows the absence of staining in a large hyperplastic perilobar nephrogenic rest (left) and strong positivity in the distal tubules of the adjacent normal kidney (right).

5.5). Surprisingly, the Wilms tumor that was positive for Ksp-cadherin expression by RT-PCR and Western blot analysis was negative for Ksp-cadherin in the immunohistochemistry study. Furthermore, the four tumors with positive staining for rare epithelial tubules were negative by Western blot analysis. Evaluation of both the intralobar and perilobar nephrogenic rests associated with 6 of the Wilms tumors were also negative for Ksp-cadherin protein expression.

5.6 Methylation analysis of the *Ksp-cadherin* promoter region

5.6.1 Review of the methylation detection techniques used

Inactivation of tumor suppressor genes can occur via germline and somatic mutations, gross chromosomal aberrations and epigenetic events such as hypermethylation. Methylation of CpG dinucleotides, usually present in CpG islands, is one mechanism of inactivation of tumor suppressor genes. In this type of methylation, only the cytosines located 5' to guanines (CpG) are subject to methylation (Bird, 1986). Determining methylation patterns associated with CpG islands and CG-rich regions has become an increasingly common method of evaluating and understanding gene regulation and expression. The criteria needed for a region to be considered a CpG island are: (1) the DNA region must be at least 200 bp; (2) the G + C content must be ≥50% and (3) the observed/expected ratio of CpG must be ≥0.6 (Gardiner-Garden and Frommer, 1987). CpG islands are associated with gene promoters and are usually hypomethylated (Larsen et al., 1992). However, increasingly, many of the CpG islands associated with cancer-related genes are found to be hypermethylated resulting in gene inactivation. A variety of techniques have been developed to analyse the methylation patterns in these regions. Many of the techniques are based on sodium bisulfite modification of DNA. This method takes advantage of the fact that in DNA chemically treated with sodium bisulfite, all unmethylated cytosines are converted to uracil, while methylated cytosines are resistant to this modification and remain as cytosines (Frommer et al., 1992). Therefore, sequencing of the modified DNA allows the discrimination between methylated cytosines and unmethylated cytosines (which have become modified to uracils which are subsequently converted to thymines upon PCR amplification). The two approaches used to analyse the methylation status of the Ksp-cadherin promoter were: (1) bisulfite sequencing PCR (BSP) and (2) methylation-specific PCR (MSP) (Figure 5.6). BSP amplifies sodium bisulfite modified DNA using PCR primers that do not contain any CpG dinucleotides. The amplified region is then either cloned and sequenced or directly sequenced. The methylation status of each of the CpG dinucleotides present in the amplified region can then be determined (Frommer et al., 1992). MSP also amplifies sodium bisulfite modified DNA. However, the primers used in this assay contain at least one CpG pair and thus discriminate between methylated and unmethylated DNA. For this assay two different sets of primers are generated, one set which contains at least one CpG dinucleotide and assume methylated DNA (in which the cytosines remains as cytosines), and a second pair encompassing the same region but that assume unmethylated DNA (the cytosine has been changed to uracil) (Figure 5.7). With these two primer pairs, one can theoretically distinguish between regions

Figure 5.6: Sodium bisulfite modification and BSP and MSP analysis. For sodium bisulfite modification, DNA is denatured and treated with sodium bisulfite. This causes a chemical modification that converts all unmethylated cytosines to uracils (which subsequently become modified to thymines upon PCR amplification). Methylated cytosines are resistant to modification and remain as cyotosines. The modified DNA is then PCR amplified with either BSP or MSP primers designed against the modified DNA. BSP products are sequenced and the methylation status of each CpG site within the amplified region is determined. The methylation status of DNA amplified by MSP can be determined by gel electrophoresis of PCR products, due to primer specificity for either methylated or unmethylated DNA. Sequencing of the PCR products can then be performed to determine the methylation status of each individual CpG dinucleotide within the amplified region.

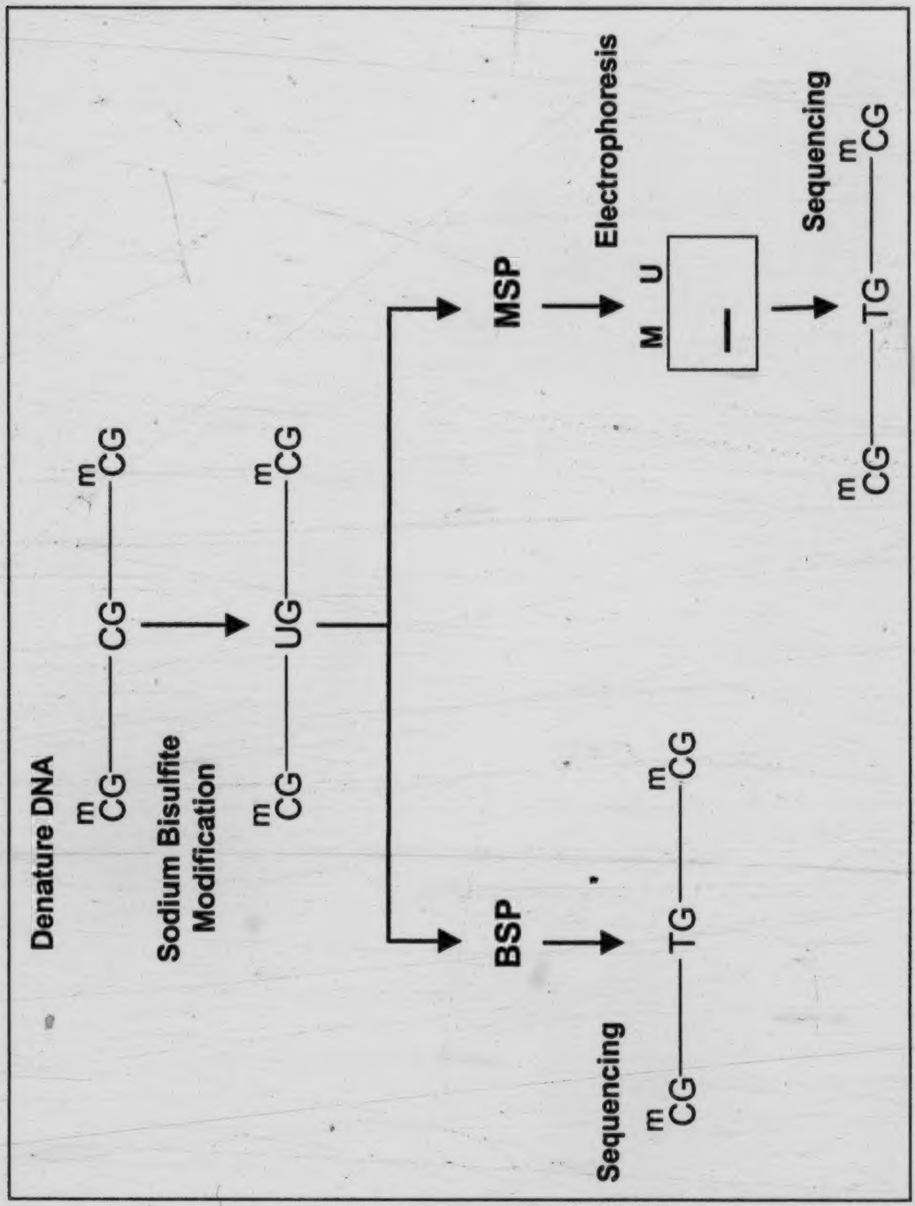
Denature DNA
mCG——CG——mCG
Sodium Bisulfite Modification
mCG——UG——mCG
BSP
Sequencing
mCG——TG——mCG
MSP
Electrophoresis
M
U
Sequencing
mCG——TG——mCG

MSP03-1 Forward (5') primer:

5' WT - CCT GCT AGA GGA TGG CAG AGC AGG CG 3'
5' M - TTT GTT AGA GGA TGG TAG AGT AGG CG 3'
5' U - TTT GTT AGA GGA TGG TAG AGT AGG TG 3'

MSP03-1 Reverse (3') primer:

3' WT - CAT GGA TGG TGC AGC CAG GCC CGT 5'
3' M - CAT AAA TAA TAC AAC CAA ACC CGA 5'
3' U - CAT AAA TAA TAC AAC CAA ACC CAA 5'

Figure 5.7: Design of MSP primers. This figure illustrates the wild type, methylated and unmethylated primer sequence for the MSP primer MSP03-1. The red nucleotides represent unmethylated cytosines that have been modified to thymines, while the blue nucleotides represent methylated cytosines resistant to bisulfite modification. It is the presence or absence of a CpG dinucleotide in the primer sequence that allows the primer to preferentially amplify methylated or unmethylated sequences respectively. WT = wild type; M = methylated; U = unmethylated.

that are methylated versus regions that are unmethylated by each primer pair's ability to amplify the region. If the region is methylated, then only primers with a methylated CpG pair should amplify this region. Conversely, if the region is unmethylated, then only primers that have been designed to reflect the modification of cytosine to thymine (CpG to TpG) should amplify the region. Subsequent electrophoresis of PCR products should result in the presence of a band with the methylated primers if the region was methylated and absence of a band with the unmethylated primers and vice versa (Herman et al., 1996). MSP provides a relatively simple and efficient way to screen regions for the presence or absence of methylation and further detailed analysis of the CpG dinucleotides amplified by the MSP primers can be done by sequencing of PCR products.

5.6.2 Methylation Primers

Two sets of MSP primers, MSP03-1 and MSP03-2, were designed using the MethPrimer program (http://www.ucsf.edu/urogene/methprimer/index1.html). Two additional primer sets were designed manually for BSP analysis. All of the amplified regions were sequenced for individual CpG analysis. Figure 5.8 shows the relative positions of the amplified region with respect to the transcription and translational start sites and the first 5 exons of the Ksp-cadherin gene. The primer set MSP03-1 spanned a 175 bp intronic region between exons 4 and 5 of the Ksp-cadherin gene and contained 4 CpG sites. MSP03-2 primers spanned 186 bp of the intronic region between exons 3 and 4 of Ksp-cadherin and

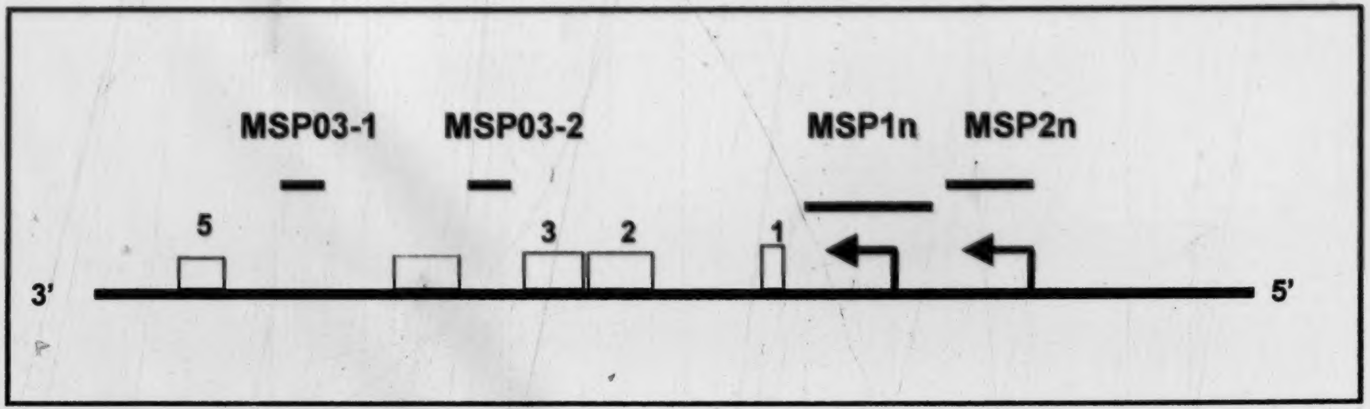

Figure 5.8: Regions of the Ksp-cadherin gene and promoter analysed for methylation. Red bars correspond to the regions analysed by either MSP or BSP analysis. The boxes represent Ksp-cadherin exons 1-5; black arrow represents the translational start site; pink arrow represents the transcriptional start site. MSP03-1 and MSP03-2 are MSP primers while MSP1n and MSP2n are BSP primers.

contained 4 CpG sites. Primers MSP1n and MSP2n were designed for BSP analysis and do not discriminate between methylated and unmethylated sequences. Primer MSP1n spanned an 855 bp region, which included the translational start site between +1205 to +463 with respect to the transcription start site and contained 12 CpG sites. The final region was evaluated with the MSP2n primer set, which amplified a 449 bp region, included the transcriptional start site and contained 7 CpG sites.

5.6.3 Ksp-cadherin promoter methylation is not found in Wilms tumors

Several Wilms tumors, mature kidney and fetal kidney samples were analysed for the presence or absence of methylated cytosines by MSP and BSP analysis. In the four regions evaluated, no evidence of aberrant promoter methylation was seen. Tables 5.2 – 5.5 provides a summary of the CpG dinucleotide methylation status obtained for each sample analysed and corresponding primer set. In all regions evaluated, the fetal kidney DNA was either completely methylated or partially methylated for almost every CpG site analysed. Similar results were seen with the tumor samples and normal mature kidney samples. In some cases, occasional CpG sites were unmethylated; however, in these instances the majority of the CpG sites analysed in that particular region were completely or partially methylated. Figure 5.9 shows a representative sequencing result illustrating the presence of methylated and partially methylated cytosines identified in the normal kidney and Wilms tumor samples.

Table 5.2: Methylation sequencing results from the MSP primer set MSP03-1. The region of DNA amplified is located +4944 to +4771 with respect to the transcription start site. ● = methylated; ⊙ = partially methylated; CG - C_pG site; T = tumor; N = normal mature kidney; d = embryonic day (fetal kidney).

Sample	**CG-1**	**CG-2**
98d	●	●
112d	⊙	⊙
135d	⊙	⊙
WT-13 N	●	●
WT-23 T	●	●
WT-24 N	●	●
WT-8 T	⊙	⊙
WT-30 T	⊙	⊙
WT-27 T	●	●
WT-17 T	●	●
WT-5 T	⊙	⊙
WT-19 T	●	●
WT-8 T	●	●
WT-21 T	⊙	⊙

Table 5.3: Methylation sequencing results from the MSP primer set MSP03-2. The region of DNA amplified is located at +3252 to +3068 with respect to the transcription start site. ● = methylated; ⊙ = partially methylated; ND = not done; CG - C_pG site; T = tumor; N = normal mature kidney; d = embryonic day (fetal kidney).

Sample	CG-1	CG-2	CG-3	CG-4
98d	●	●	●	●
112d	●	●	●	●
WT-13 N	●	●	●	●
WT-13 T	●	●	●	●
WT-23 N	●	●	●	●
WT-23 T	●	●	●	●
WT-24 N	⊙	⊙	⊙	⊙
WT-24 T	●	●	●	●
WT-11 T	●	●	ND	ND
WT-7 T	●	●	ND	ND
WT-8 T	⊙	●	⊙	⊙
WT-14 T	⊙	⊙	⊙	⊙
WT-18 N	●	●	●	●
WT-18 T	●	●	●	●
WT-34 T	●	●	⊙	⊙
WT-30 T	●	●	●	●
WT-27 T	●	●	●	●
WT-17 T	●	●	●	●
WT-5 T	⊙	⊙	⊙	⊙
WT-19 T	⊙	●	⊙	⊙
WT-8 T	●	●	●	●
WT-21 T	●	●	●	●

Table 5.4: Methylation sequencing results from the BSP primer set MSP1n. The DNA amplified is located +1205 to +463 with respect to the translation start site. ● = methylated; ⊙ = partially methylated; ○ = unmethylated; ND = not done; CG - C_pG site; T = tumor; N = normal mature kidney; d = embryonic day (fetal kidney).

Sample	CG-1	CG-2	CG-3	CG-4	CG-5	CG-6	CG-7	CG-8	CG-9	CG-10	CG-11	CG-12
98d	ND	●	●	●	●	⊙	⊙	⊙	⊙	ND	●	●
112d	○	⊙	⊙	⊙	⊙	⊙	⊙	⊙	⊙	⊙	⊙	⊙
135d	○	⊙	⊙	⊙	⊙	⊙	⊙	⊙	⊙	⊙	⊙	⊙
WT-13N	ND	⊙	●	●	●	⊙	⊙	⊙	ND	ND	⊙	⊙
WT-13T	ND	●	●	●	●	●	●	⊙	⊙	ND	●	●
WT-23N	ND	●	●	●	●	●	⊙	●	●	ND	●	●
WT-23T	○	⊙	ND	⊙	●	⊙	⊙	ND	⊙	⊙	⊙	●

Table 5.5: Methylation sequencing results from the BSP primer set MSP2n. The region of DNA amplified is located +485 to-17 with respect to the translation start site. ● = methylated; ⊙ = partially methylated; ○ = unmethylated; ND = not done; CG - C_pG site; T = tumor; N = normal mature kidney; d = embryonic day (fetal kidney).

Sample	CG-1	CG-2	CG-3	CG-4	CG-5	CG-6	CG-7
98d	⊙	⊙	⊙	⊙	⊙	⊙	⊙
112d	⊙	⊙	⊙	⊙	⊙	⊙	⊙
135d	⊙	⊙	⊙	⊙	⊙	ND	ND
WT-13 N	ND	ND	ND	ND	ND	○	○
WT-13 T	ND	⊙	●	●	●	○	○
WT-23 N	⊙	●	●	●	⊙	ND	ND
WT-23 T	●	●	●	⊙	●	ND	ND

Figure 5.9: Representative BSP methylation sequencing results. BSP methylation sequencing results from fetal kidney, mature kidney and a Wilms tumor. Pink boxes highlight the unmodified cytosines present in the CpG dinucleotide which represent methylated cytosines. Black underlines represent unmethylated cytosines that have been successfully converted to thymines due to sodium bisulfite modification and represent an internal positive control for bisulfite converstion.

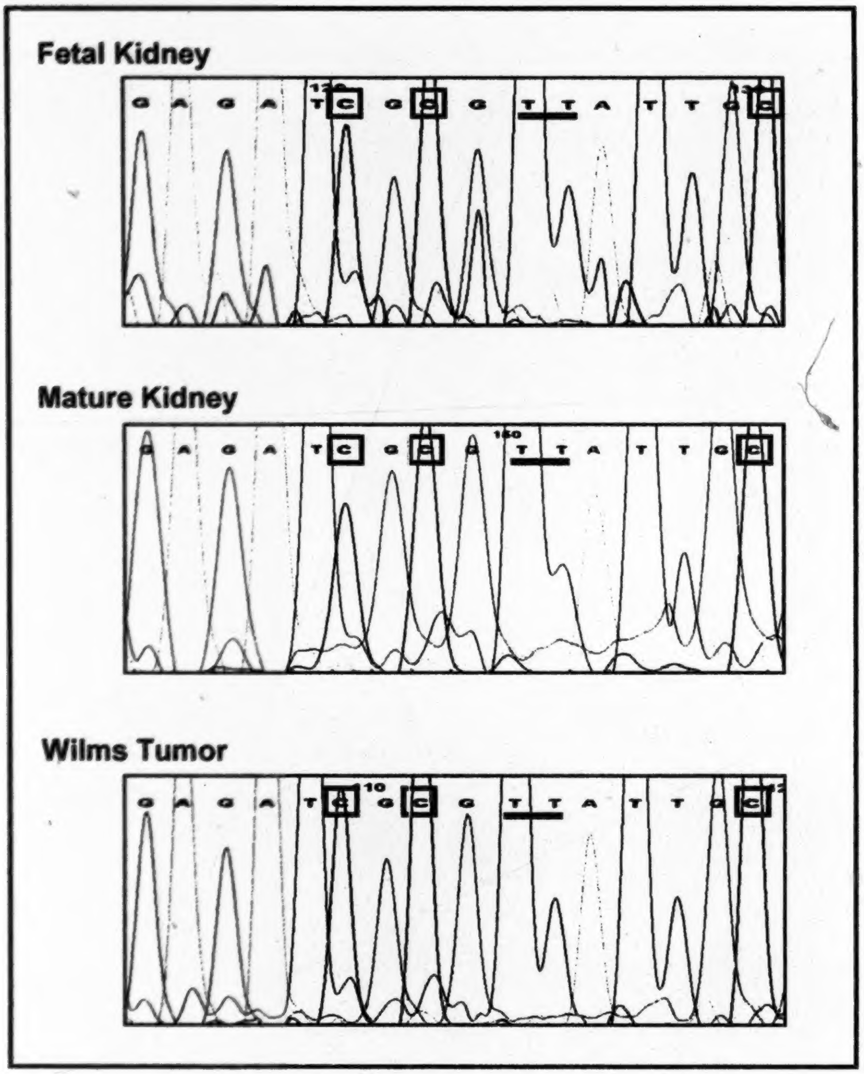
Fetal Kidney
G A G A T C G C G T T A T T G C
Mature Kidney
G A G A T C G C G T T A T T G C
Wilms Tumor
G A G A T C G C G T T A T T G C

For the MSP analysis, all of the normal fetal kidney, mature kidney and Wilms tumor DNA were successfully amplified with the MSP primers designed to amplify methylated sequences. Amplification of the same samples with methylated and unmethylated primers resulted in the presence of a band from both primer sets upon subsequent gel electrophoresis. This suggests that in these samples, both methylated and unmethylated sequences are present. However, sequencing of both methylated and unmethylated PCR products revealed that all CpG sites within the region amplified were methylated regardless of whether the methylated or unmethylated primer was used in the PCR amplification. This suggests that the PCR conditions that were used for amplification were not stringent enough to allow primers to specifically bind to either the methylated or unmethylated sequences.

The results obtained from the methylation study suggest that the regions of the Ksp-cadherin gene and promoter region evaluated are not affected by aberrant methylation. Virtually all of the CpG dinucleotides analysed in the fetal kidney, mature kidney and Wilms tumors were methylated. This would indicate that either aberrant methylation of the Ksp-cadherin promoter region is not a mechanism of inactivation or that the gene and promoter regions evaluated are outside the relevant region of gene silencing by hypermethylation.

5.7 Mutation analysis of the *Ksp-cadherin* gene *(Done by Kevin Dietrich and Kay Ziebart, Dr. Grundy's Laboratory, University of Alberta).*

The 34 Wilms tumors were evaluated for the presence of large DNA alterations (deletions/insertions) within the Ksp-cadherin gene by Southern blot analysis. The full length Ksp-cadherin cDNA was used as the hybridization probe. No deletions or insertions of fragments were visible in the 34 Wilms tumors and corresponding constitutional and/or normal kidney DNA double digested with *Taq 1* and *Pst 1* enzymes. Furthermore, no shifts in band sizes or alterations in band intensities were seen in any of the samples. A representative Southern blot of *Taq 1* plus *Pst 1* digested tumor and corresponding normal DNA hybridized with the full length Ksp-cadherin cDNA probe is seen in Figure 5.10. These results indicate that gross DNA alterations of the Ksp-cadherin gene are not common in Wilms tumors and are therefore not the primary mechanism of gene inactivation in these tumors.

5.8 Sequencing of the *HNF-1* binding region *(Done by Kevin Dietrich, Dr. Grundy's Laboratory, University of Alberta).*

Three hundred and twenty base pairs of the Ksp-cadherin promoter, between –178 to +144 bp relative to the transcription start site, were sequenced in all 34 Wilms tumors. The sequenced region included the 2 GC boxes and the *HNF-1β* DNA binding site as defined by Bai et al. (2002). No sequence changes were identified in any of the tumors sequenced and all tumors and normal kidney samples were identical to the Ksp-cadherin promoter wild-type sequence (Fig. 5.11). These results indicate that mutations within the *HNF-1β* DNA binding region, which could prevent *HNF-1β* binding and Ksp-cadherin promoter

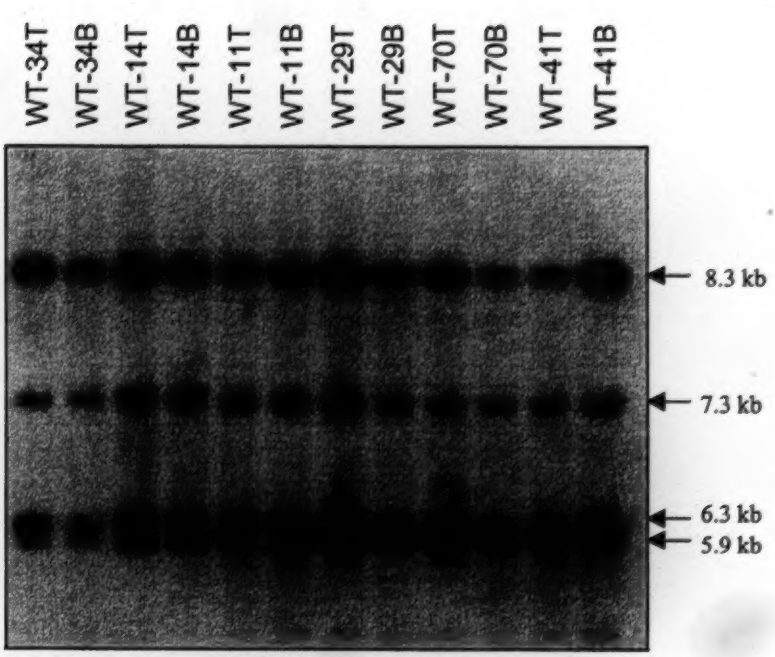
WT-34T
WT-34B
WT-14T
WT-14B
WT-11T
WT-11B
WT-29T
WT-29B
WT-70T
WT-70B
WT-41T
WT-41B
8.3 kb
7.3 kb
6.3 kb
5.9 kb

Figure 5.10: Southern blot analysis of digested Wilms tumor DNA hybridized with Ksp-cadherin cDNA. Representational Southern blot of constitutional (B) and Wilms tumor (T) DNA pairs digested with *Taq1* and *Pst1* and hybridized with the full length Ksp-cadherin cDNA. The double digest creates 4 distinct fragments as seen on the autoradiogram. Neither altered size fragments nor deletions or insertions of fragments were seen in any of the Wilms tumors versus their normal constitutional DNA counterpart.

Figure 5.11: Sequencing results of *HNF-1ß* binding region. The two GC boxes are underline in pink while the *HNF-1ß* site is underlined in black. No sequences changes were found between the Wilms tumors and wild-type sequence.

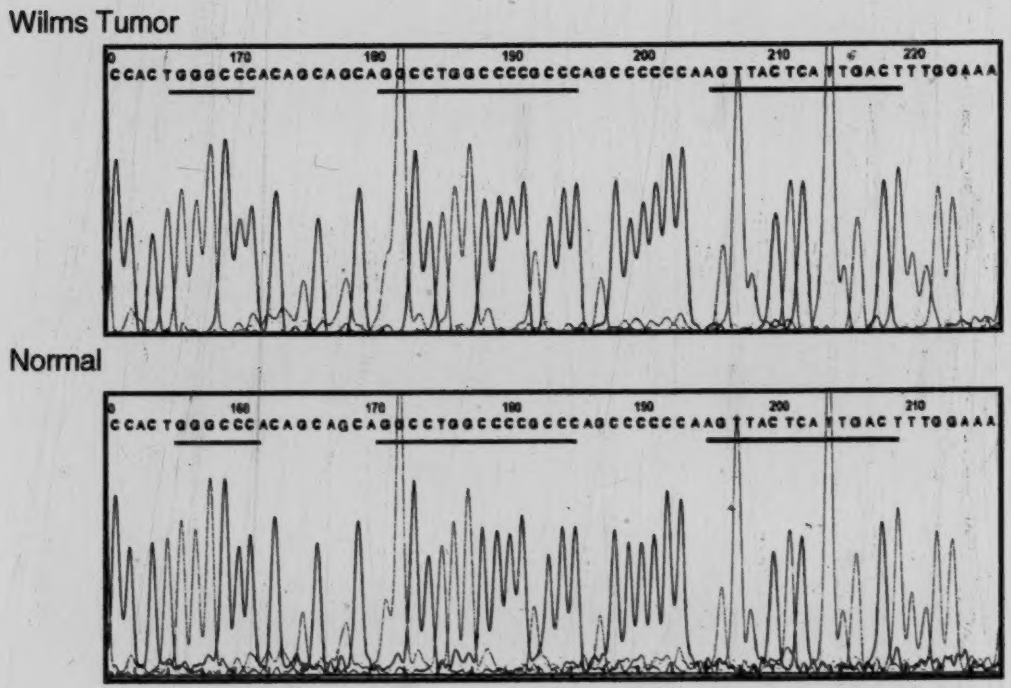
Wilms Tumor
0
170
180
190
200
210
220
CCACTGGGCCCACAGCAGCAGGCCTGGCCCCGCCCAGCCCCCCAAGTTACTCATTGACTTTGGAAA
Normal
0
160
170
180
190
200
210
CCACTGGGCCCACAGCAGCAGGCCTGGCCCCGCCCAGCCCCCCAAGTTACTCATTGACTTTGGAAA

activation, are not present in any of the Wilms tumors examined and therefore are not likely to represent a mechanism of Ksp-cadherin inactivation.

5.9 Discussion

Evaluation of Ksp-cadherin in Wilms tumors revealed that it is not expressed in the majority of Wilms tumors analysed. An independent study was published by Baudry et al. (2003) that evaluated RNA expression of 38 Wilms tumors by real time RT-PCR. In their study, they also found that Ksp-cadherin RNA was not expressed in the majority of Wilms tumors. Our study is the first to address Ksp-cadherin protein expression in Wilms tumors. Our results indicate that while Ksp-cadherin protein is abundant in normal fetal and mature kidney epithelial cells, neither epithelial-predominant nor mixed-cell Wilms tumors express Ksp-cadherin with the exception of a very minor population of epithelial tubular cells found in only a subset of tumors. Included in the immunohistochemical analysis were 6 Wilms tumors positive for either perilobar (PLNR) and intralobar (ILNR) nephrogenic rests. Nephrogenic rests are commonly associated with Wilms tumors and are believed to represent Wilms tumor precursor lesions. PLNRs are confined to the periphery of the renal lobe and are composed mainly of blastemal and epithelial cell types while ILNRs can occur anywhere in the renal lobe, are comprised of multiple cell types and are thought to arise early in development (Beckwith et al., 1990). Neither PLNRs nor ILNRs expressed Ksp-cadherin, suggesting that this gene may be silenced early in Wilms tumor development. In agreement with this hypothesis, Charles et al.

(1998) examined *WT1* status in nephrogenic rests associated with Wilms tumors and found that loss of *WT1* expression was found in the tumors as well as both types of nephrogenic rests. Based on these results, the investigators proposed that *WT1* is inactivated early in Wilms tumorigenesis.

In all assays, Ksp-cadherin was abundantly expressed in the epithelial cells of fetal and mature normal kidneys indicating that it should be expressed in the epithelial cells of Wilms tumors. However, in combination, and with particular emphasis on the immunohistochemical analysis, which provides the most detailed and accurate analysis of Ksp-cadherin expression in Wilms tumor cells, our results clearly demonstrate that Ksp-cadherin is absent in most, if not all, Wilms tumor cells with the exception of rare epithelial tubular cells. It does however remain possible that Ksp-cadherin is expressed in a portion of the renal collecting system that simply isn't involved in Wilms tumors. The discrepancy between the Western blot and immunohistochemical results of tumor WT-7, can be explained by the fact that different tumor sections or parts of the tumor were used for the different analyses.

The study by Baudry et al. (2003) evaluated RNA expression of the 3' region of the Ksp-cadherin transcript in 38 Wilms tumors by real-time RT-PCR analysis. Of note, 90 nucleotides of the region that they analysed overlapped with the 3' region that we evaluated. The majority of the Wilms tumors included in their analysis were either triphasic or blastemal- or stromal-predominant rather than epithelial-predominant. They compared levels of Ksp-cadherin RNA in Wilms tumors and normal kidney and used a variation of greater than 2 standard deviations from that found in normal kidney as their criteria for a significant change in expression. Of the 38 tumors analysed, 14/38 (37%) expressed Ksp-cadherin RNA to varying levels while 24/38 (63%) tumors did not express Ksp-cadherin RNA. The preponderance of non-epithelial Wilms tumors in their study may have resulted in the lower frequency of Ksp-cadherin positive tumors as compared to our study as Ksp-cadherin is primarily expressed in epithelial tubular cells. In our study, we specifically selected 18 Wilms tumors that were comprised predominantly of epithelial cells to ensure that lack of expression was not due to the lack of epithelial cells. RT-PCR analysis of the 18 epithelial predominant Wilms tumors revealed that 56% expressed both the 5' and 3' ends of the transcript, 27% expressed the 3' end only and 17% did not express Ksp-cadherin. Surprisingly, of these 18 Wilms tumors, only one expressed the Ksp-cadherin protein by Western blot analysis but protein was not detected in the immunohistochemical analysis. The remaining 16 tumors with mixed stromal, blastemal and epithelial cell populations, expressed both ends of the Ksp-cadherin transcript less frequently and had a higher frequency of complete lack of RNA expression than the epithelial dominant tumors. The relative abundance of Ksp-cadherin positive Wilms tumors (14/34) detected by RT-PCR, a highly sensitive detection method, in our study as compared to Baudry et al. (2003), may be a reflection of the presence of rare contaminating normal kidney cells and/or tumor heterogeneity which would also explain the discrepancy between RT-PCR and Northern blot results. The discrepancy could also be due to a very low copy number of transcripts in some tumors and the different RT-PCR assays used.

Our RT-PCR analysis revealed a significant number of Wilms tumors that expressed only the 3' end of the Ksp-cadherin transcript. The presence of these truncated transcripts may be indicative of the method by which Ksp-cadherin expression is lost in Wilms tumors. One possibility is that the Ksp-cadherin transcript is actively degraded in these tumor cells, with the 3' end being degraded at a slower rate than the 5' end, as a 5' → 3' degradation pathway has recently been described in mammalian cells (van Hoof and Parker, 2002). A related possibility is that the Ksp-cadherin transcript is inherently unstable in Wilms tumor cells, due to loss or gain of factors involved in RNA stability. Alternatively, expression of the 3' end of the Ksp-cadherin transcript may be due to alternative splicing, gene mutation or another start site if the 5' promoter is silenced. Further analysis will be required to resolve the mechanism underlying loss of Ksp-cadherin RNA expression in Wilms tumor.

Since both our results and those of Baudry et al. (2003) indicate that Ksp-cadherin is not expressed in the majority of Wilms tumors, we attempted to identify a mechanism of gene inactivation. However, evaluation of the 34 Wilms tumors for large mutations by Southern blot analysis indicate that gross chromosomal alterations of the Ksp-cadherin gene are not a common occurrence in Wilms tumors. This suggests that mutations, undetectable by Southern blot analysis or other epigenetic events, may be responsible for loss of Ksp-cadherin in Wilms tumor. A more extensive mutation analysis using denaturing HPLC and

WAVE™ analysis for each of the Ksp-cadherin exons would be of interest to determine whether or not small mutations (deletions/insertions, point mutations, etc) are present and cause inactivation of the Ksp-cadherin gene.

A region of the Ksp-cadherin promoter has been identified as a DNA binding domain for *HNF-1α* and *HNF-1β.* Overexpression and deletion studies have revealed that *HNF-1β,* but not *HNF-1α,* acts as a regulator of Ksp-cadherin (Bai et al., 2002). Deletion studies by Whyte et al. (1999) have shown that the Ksp-cadherin promoter region from –113 to –31, which contains the *HNF-1* DNA binding site, is crucial for normal promoter regulation. Furthermore mutations in the *HNF-1* consensus recognition site or the 2 GC boxes have been shown to significantly impair promoter activity subsequently reducing or abolishing Ksp-cadherin expression (Bai et al., 2002). We postulated that inactivation of Ksp-cadherin may occur via mutations in this region which would prevent *HNF-1* binding and disrupt promoter activity. However, sequencing of 320 bp of the Ksp-cadherin promoter located –178 bp to +144 bp relative to the transcription start site, which included the *HNF-1* binding site and the two GC boxes, did not identify sequence changes in any of the 34 Wilms tumors suggesting that this is also not a common mechanism of Ksp-cadherin inactivation in Wilms tumor. Since binding of *HNF-1β* to its binding site within the Ksp-cadherin promoter regulates Ksp-cadherin gene activity, it is possible that dysregulation of *HNF-1β,* which could interfere with it binding to its binding site, may also lead to the down-regulation of Ksp-cadherin in Wilms tumors. It would therefore be of interest to evaluate *HNF-1β* RNA expression in Wilms tumors. If loss of *HNF-1β* is seen, this may explain why Ksp-cadherin RNA and protein is also lost in the majority of Wilms tumors. In fact, loss of E-cadherin expression has been correlated with an increase in the transcriptional repressor *SNAIL*, which has been proposed to regulate E-cadherin, in numerous primary tumors and cancer cell lines (Batlle et al., 2000; Yokoyama et al., 2001; Poser et al., 2001).

Mutations of *HNF-1β* give rise to maturity-onset diabetes of the young, type V as well as progressive diabetic nephropathy, non-diabetic renal disease, and familial hypoplastic glomerulocystic kidney disease. This suggests that HNF-1β is likely involved in kidney development and/or regulation and its alteration may contribute to Wilms tumorigenesis. Interestingly, *HNF-1β* is located on chromosome 17cen-q21.3, which is in the same region as the familial Wilms tumor gene (*FWT1*), raising the possibility that *HNF-1β* may be the *FWT1* gene. If *HNF-1β* is the familial Wilms tumor gene you may expect some of the renal abnormalities listed above to be present in the Wilms tumor families. However, there is no evidence of such abnormalities in these families suggesting that *HNF-1β* is not the familial Wilms tumor gene. However, it is possible for a situation similar to that described for DDS and Wilms tumor to arise. It is therefore possible that different types of mutations (inactivating tumor suppressing mutation, dominant negative mutations, etc.) give rise to different or more severe phenotypes. This further supports the evaluation of *HNF-1β* expression in both sporadic and familial Wilms tumors as well as normal fetal and mature kidney to see if its expression is altered in Wilms tumors.

A third possible mechanism of Ksp-cadherin inactivation that was studied evaluates the promoter region for evidence of hypermethylation. Studies have found that hypermethylation of genes and their promoters, including many of the cadherin genes, contributes to tumorigenesis and can be another mechanism of gene inactivation. Evidence that hypermethylation of cadherins can lead to gene silencing and tumorigenesis has been demonstrated in studies with mice. Nam et al. (2004) injected SCID mice with cancer cells in which E-cadherin was silenced via hypermethylation. Treatment of the mice with the demethylating agent 5-aza-2'-deoxycytidine restored E-cadherin expression and suppressed tumor growth and metastasis in the mice as compared to the untreated controls (Nam et al., 2004). Hypermethylation of E-cadherin has been found in breast and prostate cancers (Graff et al., 1995), pancreatic cancer (Seidel et al., 2004), hepatocellular carcinoma (Kanai et al., 1997) and gastric cancer (Tamura et al., 2000), while hypermethylation of N-cadherin in pancreatic and prostate cancers (Arenas et al., 2000; Seidel et al., 2004) and H-cadherin in colorectal, breast, prostate and lung cancers (Hibi et al., 2004; Toyooka et al., 2001; Arenas et al., 2000) has also been demonstrated. We therefore examined the promoter region of Ksp-cadherin for evidence of hypermethylation. However, no evidence of hypermethylation was found in any of the four regions evaluated as all of the fetal kidney and mature kidney DNA displayed the same degree of methylation as did the Wilms tumors. Regions of partial methylation and localized CpG sites that were unmethylated were found, but overall, the majority of CpG dinucleotides in all three sample types (fetal kidney, mature kidney, tumors) were methylated.

These results indicate several possibilities: (1) the bisulfite modification was incomplete and therefore some of the cytosines that should have been modified to uracils were not, hence, leading to an inaccurate over-representation of methylated cytosines; (2) the MSP assay was not sensitive enough to distinguish between methylated and unmethylated sequences; (3) methylation may be involved in gene inactivation; however, the incorrect regions were analysed; (4) methylation is not a mode of gene inactivation for Ksp-cadherin. It is unlikely that the bisulfite conversion was incomplete as review of the sequencing results show that the majority (90%) of the cytosines not part of a CG dinucleotide were modified to uracils and subsequently converted to thymines upon PCR amplification. These cytosines act as a positive control for bisulfite modification. Furthermore, the primers are designed so that they contain several thymine residues which correspond to modified cytosines and therefore, they should only bind to DNA that has been modified. However, incomplete sodium bisulfite conversion resulting in the co-amplification of methylated and unmodified or partly modified DNA by MSP primers has been reported (Sasaki et al., 2003; Warnecke et al., 2002). Furthermore, our MSP analysis was not sufficiently sensitive to distinguish between methylated and unmethylated sequences. Review of the promoter region immediately upstream of the Ksp-cadherin transcription start site using the CpG island prediction program, CpG Island Searcher (http://www.uscnorris.com/cpgislands/cpg.cgi), did not show any evidence of a CpG island in this region. Furthermore, review of the 4 regions analysed by either BSP or MSP, revealed that they did not meet all 3 of the requirements for a CpG island. However, analysis of the region 3000 bp and beyond, upstream of the transcription start site did reveal the presence of several CpG islands. Although it is possible that the wrong region of the Ksp-cadherin promoter was analysed, a review of genes inactivated by hypermethylation including E-cadherin (Nojima et al., 2001; Nakayama et al., 2001), H-cadherin (Toyooka et al., 2001), *SLIT-2* (Dallol et al., 2003), *DLC-1* (Yuan et al., 2003), *TFPI-2* (Konduri et al., 2003) and *hMLH1* (Strazzullo et al., 2003), exhibit hypermethylation of CpG islands that are near and often include the transcriptional start site. The lack of CpG islands near the transcriptional start site of the Ksp-cadherin gene and the normal methylation pattern seen in both normal kidney and Wilms tumor DNA suggests that hypermethylation is not a mechanism of Ksp-cadherin gene inactivation. However, analysis of the CpG islands located upstream of the Ksp-cadherin gene would be interesting to confirm or exclude this possibility as hypermethylation of the CpG islands upstream of the Ksp-cadherin promoter may be involved in regulating its expression.

Given the fact that Ksp-cadherin protein is lost or absent in almost all Wilms tumors, it is surprising that we have not uncovered a mechanism of Ksp-cadherin gene inactivation. A more extensive mutational analysis of the Ksp-cadherin exons, methylation analysis of the CpG island located upstream of the Ksp-cadherin gene, and further evaluation of the *HNF-1β* gene and binding region is warranted. The generation of Ksp-cadherin knock-out mice and/or the use of antisense/siRNA technologies to inactivate Ksp-cadherin in normal embryonic kidney cells would provide functional support for Ksp-cadherin involvement in Wilms tumor. If a tumor-like phenotype results from these studies, then this would provide further evidence supporting the fact that loss of Ksp-cadherin is involved in Wilms tumorigenesis.

Although this study was designed to identify chromosome 16q candidate genes for Wilms tumors with adverse outcome, our results suggest that Ksp-cadherin is likely not the gene specifically involved in this subset of tumors. Analysis of both RNA and protein indicate that Ksp-cadherin is absent in the majority of Wilms tumors evaluated and we found no correlation between chromosome 16q LOH and loss of Ksp-cadherin expression. Our data together with that of Baudry et al. (2003) indicate the Ksp-cadherin gene is inactivated in the majority of Wilms tumors, however, attempts to identify a mechanism of gene inactivation have been unsuccessful. Furthermore, the lack of Ksp-cadherin protein in both PLNRs and ILNRs supports the possibility that inactivation of Ksp-cadherin may be a requirement for the development of Wilms tumor. Future studies should shed light on the role of Ksp-cadherin in the etiology of Wilms tumor.

In summary, this study provides compelling evidence that inactivation of Ksp-cadherin may be a requirement for Wilms tumorigenesis. Although more work needs to be done to elucidate the role of Ksp-cadherin we propose that Ksp-cadherin may represent a third Wilms tumor gene in addition to *WT1* and *WT2*. Further analysis of Ksp-cadherin will lead to a better understanding of the genetics and biochemistry of Wilms tumorigenesis.

Chapter 6

6.1 Final Discussion

The goal of this study was to identify and characterize genes involved in the initiation and/or progression of Wilms tumor. Although greater than 85% of Wilms tumors are treated successfully with current therapies, little is known about the genetics of this childhood cancer. *WT1* is the only gene proven to be involved in Wilms tumor but accounts for only 10-15% of Wilms tumors. Identification of the genes implicated in Wilms tumorigenesis will not only provide insight into the genetic basis of this cancer but may also aid in the development of diagnostic and/or prognostic markers which could ultimately lead to refinement of current therapies and minimization of late side effects. In order to identify candidate Wilms tumor genes, three different approaches were used: (1) evaluation of the gene, *GPC3*, which is responsible for the Wilms tumor-predisposing syndrome SGBS; (2) identification of candidate genes using DD-PCR and (3) identification of candidate genes via *in silico* database searching of known genes located within a candidate gene region.

Based on these three approaches, it was thought that the first approach would be the most successful in identifying a new gene implicated in Wilms tumorigenesis. Since it is known that defects in the *GPC3* gene give rise to SGBS and predispose these individuals to developing Wilms tumor, we hypothesized that defects in the *GCP3* gene may also contribute to the development of non-syndrome associated Wilms tumors. It was therefore surprising, that after an extensive mutation analysis of *GPC3* in sporadic Wilms tumors we did not find convincing evidence of its involvement. There was one individual identified with a tumor-specific deletion encompassing a portion of the X chromosome; however, it is not known if this deletion is confined to the *GPC3* gene or if is spans a portion of the X chromosome. Therefore, the presence of this deletion does not conclusively implicate *GPC3* in the genesis of this Wilms tumor since it is possible that the chromosomal region deleted could represent a random event or include loss of another gene on the X-chromosome that contributes to Wilms tumorigenesis. The lack of involvement of *GPC3* in the development of Wilms tumor is surprising as constitutional and somatic defects of *WT1* give rise to both DDS and WAGR associated Wilms tumor and sporadic Wilms tumor respectively. Similarly, it has also been suggested that alteration of the same gene that results in the Wilms tumor predisposing syndrome, BWS also contributes to sporadic Wilms tumorigenesis. The lack of *GPC3* mutations in non-syndrome associate Wilms tumors could be due to the fact that *GPC3* may need to be inactivated at a very early stage in kidney development in order to promote tumorigenesis. Alternatively, inactivation of *GPC3* may be a rare event in Wilms tumorigenesis, and our study, due to its small sample size, may have been unable to detect *GPC3* mutations. However, we can not exclude the possibility that the loss of *GPC3* resulting from the tumor-specific deletion seen in case WT-42 contributes to Wilms tumorigenesis and thus represents a somatic *GPC3* alteration in Wilms tumor. Interestingly, White et al. (2002) did find evidence of somatic tumor-specific *GPC3* alterations in 2/41 Wilms tumors.

Nonetheless, the results of their study and ours suggest that dysfunction of *GPC3* is not a frequent event in Wilms tumorigenesis.

The second method used to identify candidate Wilms tumor genes was DD-PCR. Although this method has been used successfully in other labs for the identification of genes involved in development, cancer, hematopoeisis and other processes, in our hands it was not successful in identifying novel Wilms tumor genes. Approximately half of the cDNAs identified were found to represent genomic DNA, mitochondrial DNA or repetitive elements. The remaining sequences were identified either as known genes or cDNAs that did not share homology with any of the known genes in the NCBI database. Further evaluation of the known genes by RT-PCR, however, failed to confirm the differential expression profile seen in the original DD-PCR assay.

The factors contributing to the unsuccessful results of the DD-PCR assay include: (1) the genetic heterogeneity of Wilms tumors; (2) the use of tumor tissue instead of cell lines (3) the fact that tumors were screened against tumors instead of against normal tissue and (4) DD-PCR is prone to generating false positives. If appropriate Wilms tumor cell lines were available, the technique may have been more successful as this would have limited some of the genetic heterogeneity associated with using tumor tissue. Furthermore, comparison of Wilms tumors against normal kidney, rather than other tumors could also reduce the amount of variation in differential expression seen, as the normal kidney samples should be considerably less heterogeneous. However, comparison to normal tissue would still not eliminate heterogeneity present among the tumors and would not specifically target genes on chromosome 16q.

Given that the DD-PCR method was unsuccessful, if a study for Wilms tumor gene identification was to be undertaken again, one of the newer gene profiling technologies such as microarrays or protein arrays may be a better choice. Although the starting cost of these methodologies can be expensive, the time it takes to actually perform the analysis and generate data on differentially expressed genes is substantially less. Genes can be screened within weeks of performing the array analysis as compared to months with DD-PCR. Also, there is less chance with the array technologies for the introduction of contamination and production of artifacts as the many stages of manipulation (excision, re-amplification, cloning) needed to purify and identify the differentially expressed cDNA fragments are not required. However, there are still limitations with the microarray analysis including sample quality, generation of false positives and reproducibility, all of which need to be taken into account and can obscure the results of the study. Furthermore, since the arrays also rely on detecting differential expression of RNA and/or protein between samples, the fact that Wilms tumors are genetically heterogeneous will still complicate the assay.

There have been several reports of microarray analysis performed on Wilms tumors. One study compared FH non-relapsed tumors against FH tumors that had relapsed in an attempt to identify genes that represent predictors of outcome. One hundred and thirty-seven differentially expressed genes were identified which were further narrowed down to a small subset that may represent useful markers for predicting outcome (Williams et al., 2004). Interestingly, this study identified genes that have been previously implicated in Wilms tumor including *WT1* and *GPC3*. Another study by Li et al. (2002) compared Wilms tumors to normal fetal kidney and identified 357 differentially expressed genes that they were able to narrow down to 29 high priority candidate genes. Northern blot analysis with cDNA probes that represented six of these genes confirmed the differential expression seen on the microarray. Many of these genes were transcription factors, some of which are known to be involved in kidney development, while some of the other identified genes may represent members of the Wnt signaling pathway. The results of these microarray analyses indicate that this may be a good methodology for identifying candidate Wilms tumor genes.

Although the final method of candidate gene identification, the approach of searching *in silico*, is a relatively new and simple procedure, we found it to be the most successful at identifying chromosome 16q Wilms tumor candidate genes. This approach, as mentioned previously, is the most time- and cost-effective of all of the candidate gene identification methods. Its usefulness relies on whether or not the critical gene region for the disease being studied has been defined together with the information published including expression and predicted or known protein function. This approach eliminates much of the cost and labor involved in the expression profiling techniques and identified several high priority Wilms tumor candidate genes, including several from the cadherin gene family. The strongest Wilms tumor candidate gene identified was Ksp-cadherin.

Ksp-cadherin is a cell adhesion molecule thought to be involved in the establishment and maintenance of cell-cell contacts (Thomson et al., 1998). It is localized to chromosome 16q21-q22.1 and is flanked by cadherin-8 and cadherin-11, all of which are in the minimal region of 16q LOH identified in Wilms tumors. Furthermore, it is expressed in both fetal and mature renal epithelial cells and is postulated to play a role in kidney morphogenesis. Based on the pattern of expression of Ksp-cadherin in normal kidneys, Ksp-cadherin should be expressed in at least a subset of the Wilms tumors. Indeed, we found that Ksp-cadherin was expressed in all of the fetal and mature kidney samples evaluated; however, its RNA expression was reduced or absent in many of the Wilms tumors, even those that were comprised predominantly of epithelial cells. Furthermore, Ksp-cadherin protein expression was absent in almost all of the Wilms tumors analysed. Given the expectation that Ksp-cadherin should be expressed in Wilms tumors, these findings suggest that Ksp-cadherin inactivation may be involved in the development of Wilms tumor. However, the exact role and extent of involvement of Ksp-cadherin in Wilms tumorigenesis is not known.

Ksp-cadherin has several characteristics which are consistent with a role as a tumor progression or invasion gene including: (1) it is a cell adhesion molecule in which loss of function leads to loss of cell-cell contacts which could lead to tumor cell motility and invasiveness and (2) other cadherin genes including E-cadherin and N-cadherin, have been associated with tumor invasiveness and metastasis. Therefore in our analysis of Ksp-cadherin, we evaluated both tumors that had lost chromosome 16q heterozygosity and tumors that had retained 16q heterozygosity. The presence of chromosome 16q LOH implies the location of a tumor suppressor gene at least in this subset of tumors. Thus, it would be expected that the gene on chromosome 16q would be down-regulated or absent in the tumors that have lost 16q heterozygosity but be expressed in the tumors that have retained 16q heterozygosity. Therefore, it was surprising to find that Ksp-cadherin was not expressed in both Wilms tumors that lost or retained 16q heterozygosity. These results indicate that Ksp-cadherin is likely not the chromosome 16q gene specifically implicated in Wilms tumorigenesis by LOH. Rather than being associated with an adverse prognosis, Ksp-cadherin may have a developmentally earlier and more widespread role in Wilms tumorigenesis.

Certainly the immunohistochemical analysis of the nephrogenic rests revealed that Ksp-cadherin was not expressed in either the perilobar or intralobar nephrogenic rests suggesting that loss of Ksp-cadherin may be an early event in Wilms tumorigenesis. Studies of *WT1* and other putative Wilms tumor loci in nephrogenic rests have provided insight into the genes that are relevant early in Wilms tumorigenesis versus those that are implicated later in development. Mutations of *WT1* have been found in both types of nephrogenic rests associated with Wilms tumors that also contain somatic defects of *WT1* and it has therefore been proposed that dysregulation of *WT1* occurs early in Wilms tumorigenesis (Park et al., 1993). In contrast, similar studies have been performed in nephrogenic rests associated with Wilms tumors that lose chromosome 16q heterozygosity. It has been found that these nephrogenic rests retain chromosome 16q heterozygosity (Charles et al., 1998). This provides evidence that loss of 16q heterozygosity is associated with the later stages of development or progression of Wilms tumors, in accordance with the previous association with adverse outcome (Grundy, unpublished results). However, the absence of Ksp-cadherin in the nephrogenic rests could also be due to the fact that the specific cell types that express Ksp-cadherin may not be present in the rests.

Due to the fact that Ksp-cadherin is only expressed in a subset of renal epithelial cells, which some Wilms tumors do not contain, Ksp-cadherin expression would not be expected in these tumors. Lack of Ksp-cadherin in these tumors does not therefore provide evidence for a role in their tumorigenesis. The evidence for expression in all of the fetal kidney samples however, does suggest that Ksp-cadherin should be expressed in at least some Wilms tumors.

Since it is believed that Ksp-cadherin has a role in normal kidney development, its loss could prevent normal differentiation, contribute to the malignant phenotype and result in a tumor that does not contain Ksp-cadherin-expressing renal collecting duct cells. Therefore, loss of Ksp-cadherin may disrupt or prevent the development of a subset of epithelial cells from the differentiating mesenchyme, thus predisposing to tumor formation. However, no evidence for pathologic inactivation of the Ksp-cadherin gene has been identified and until such evidence is found, loss of Ksp-cadherin cannot be directly linked to the etiology of Wilms tumor. Further study into the relationship of Ksp-cadherin in Wilms tumor is warranted.

The other Wilms tumor loci including *WT1*, WT2, and putative loci on chromosomes 16q, 1p, 7p, and the *FWT1* and *FWT2* loci are each implicated, to varying degrees, in the development of subsets of Wilms tumors. It is therefore surprising that almost all Wilms tumors lose Ksp-cadherin expression, as the apparent genetic heterogeneity of Wilms tumor does not support the theory of a single gene contributing to tumorigenesis. It is also therefore possible that loss of Ksp-cadherin occurs because of Wilms tumorigenesis. Inactivation of *WT1*, *WT2* or another Wilms tumor gene (putative *WT3*) may lead to the loss of Ksp-cadherin. Therefore, Ksp-cadherin may be physiologically a part of Wilms tumorigenesis but not the cause. If this is the case, Ksp-cadherin could prove to be a valuable therapeutic target, since it appears to be involved in the majority of Wilms tumors. Therefore, gene therapies specifically targeting Ksp-cadherin could represent a new form of treatment, which may prove beneficial to the Wilms tumors that do not respond to any of the current therapies.

Although the exact relationship between Ksp-cadherin and Wilms tumor is not known, results from our study clearly suggest its involvement. Further studies need to be performed to elucidate the role of Ksp-cadherin in Wilms tumorigenesis. Identification of the mechanism of Ksp-cadherin inactivation would add evidence to support its involvement in Wilms tumorigenesis.

6.1.1 Ksp-cadherin and Wilms tumor: Models for tumorigenesis

If loss of *Ksp-cadherin* leads to the development of Wilms tumor, one can speculate a pathogenic model. Expression of Ksp-cadherin occurs very early in kidney development, specifically at E10.5 in the ureteric bud (Thomson and Aronson, 1999). In normal kidney development, the ureteric bud moves into the metanephric mesencyme which signals the ureteric bud to begin to branch. The branching of the ureteric bud in turn provides a signal to induce the metanephric blastema to begin differentiating into epithelial and stromal cells (reviewed in Davies, 1993). This is a repetitive process that leads to undifferentiated, partly differentiated and differentiated cells being present at the same time. One could speculate that inactivation of Ksp-cadherin very early in kidney development could interfere with the development of the ureteric bud. If the ureteric bud is not properly formed, it may be unable to grow into the metanephic mesenchyme and the reciprocal induction, which leads to differentiation of the metanephric mesenchyme, may not occur. Conversely, lack of Ksp-cadherin may not disrupt formation of the ureteric bud and its extension into the metanephric mesenchyme, but rather Ksp-cadherin may be necessary to provide the signal needed to induce differentiation. Therefore, lack of Ksp-cadherin, could lead to loss of the inductive signal, subsequently resulting in failure of the metanephric mesenchyme to differentiate. Both of these scenarios, lack of Ksp-cadherin interfering with development of ureteric bud or failure to send a signal to induce differentiation, could result in the accumulation of cells in an undifferentiated state, which could predispose and ultimately give rise to a Wilms tumor. The types of mutations and whether or not they resulted in complete or partial loss of function as well as the stage of kidney development at which Ksp-cadherin became inactivated, could explain why Wilms tumors are at various stages of differentiation. In order to prove this theory, evidence that loss of Ksp-cadherin in the ureteric bud results in its inability to grow into and/or signal the metanephric blastema to differentiate, would be needed. If the entire ureteric bud were affected, one would anticipate complete failure of development of that kidney. Of course Wilms tumors occur in the setting of more or less an otherwise normal kidney so if these hypotheses were correct, inactivation of Ksp-cadherin would have to be restricted to a small area of the ureteric bud. One could propose that this area may represent a nephrogenic rest, which could ultimately give rise to a Wilms tumor.

6.2 Future Directions

Although the question of *GPC3* involvement in sporadic Wilms tumor is answered, additional work remains for the other two projects. Further characterization of the potentially differentially expressed cDNAs isolated by DD-PCR which were not homologous to known genes should be performed, as well as further characterization of some of the high priority candidates identified by the database searching approach. Furthermore, elucidating the role of Ksp-cadherin in Wilms tumors is warranted. Additional experiments will not only aid in determining if Ksp-cadherin has a causative role in this childhood kidney cancer, but may aid in a better understanding of the function of Ksp-cadherin.

6.2.1 Further evaluation of Wilms tumor candidate genes

A portion of the DD-PCR project remains incomplete as several ESTs and unknown transcripts require further analysis. Since the DD-PCR assay did not identify any genes located on chromosome 16q, it is possible that one of the uncharacterized transcripts may represent the 16q Wilms tumor gene. Re-analysis of the sequences corresponding to unknown genes with NCBI's blastn search tool should be performed again as the last blastn search was performed in Summer 2003. It is possible that some of the EST/hypothetical proteins and unknown genes may now show homology to newly identified genes whose sequence has recently been submitted to the genbank database. Even if the sequence is still unknown, primers can be designed, based on the sequence obtained from sequencing the cDNA fragment and RNA expression can be further evaluated by semi-quantitative RT-PCR or Northern blot analysis to identify candidates that are truly differentially expressed.

6.2.2 Mutation Analysis of the Ksp-cadherin gene

In an attempt to identify a mechanism of Ksp-cadherin inactivation in Wilms tumor, mutation analysis of the gene is warranted. Since the Southern blot analysis did not reveal any DNA alterations, indicating that large scale deletions/insertions of Ksp-cadherin are not common in Wilms tumor, further analysis of each exon is warranted. The Ksp-cadherin gene is a large gene comprised of 18 exons. An efficient method of detecting sequence changes in such a large gene would be to perform heteroduplex analysis using denaturing

HPLC and the WAVE™ DNA Fragment analysis system as described for the *GPC3* mutation analysis study. If an abnormal WAVE was detected in any of the Ksp-cadherin exons, these samples would then be sequenced to determine if the sequence change represented a mutation or polymorphism. If mutations are found within the Ksp-cadherin gene, this would provide evidence that inactivation of Ksp-cadherin is truly pathologic.

6.2.3 Ksp-cadherin gene knock-out studies

Convincing evidence that loss of Ksp-cadherin is pathologically involved in Wilms tumorigenesis is needed. Direct manipulation of the Ksp-cadherin gene, and assessment of the functional outcome could provide the evidence needed to confirm that loss of Ksp-cadherin leads to tumorigenesis. Ksp-cadherin gene knock-out studies in animal models and cells lines would be able to address the question, does inactivation of Ksp-cadherin produce a tumorigenic-like phenotype? Unfortunately, Wilms tumor cell line studies are difficult as there are no reliable Wilms tumor cell lines available for use in transfection studies. However, repressing Ksp-cadherin expression in a normal embryonic kidney cell line, via siRNA technology, would be able to provide information as to whether loss of this gene leads to a tumorigenic phenotype. This approach has been successfully used to repress *WT1* expression in mouse metanephric M15 cells in order to determine the effects of loss of *WT1* during different stages of kidney development (Davies et al., 2003). If the resultant cellular phenotype is tumorigenic and re-expression of Ksp-cadherin reduces or halts this process, then this would provide convincing evidence that loss of Ksp-cadherin can induce tumorigenesis. Again similar studies have been performed with the *WT1* gene in which introduction of *WT1* into a rhabdoid tumor of the kidney-derived cell line that lacks *WT1* expression, suppressed tumorigenicity (McMaster et al., 1995).

Mouse models of *WT1* have provided some clues to its role in renal development and Wilms tumor. In homozygous *WT1* knockout mice, renal and gonadal systems fail to develop and mice die in *utero.* If a similar phenotype were found in homozygous Ksp-cadherin deficient mice, this would provide evidence that Ksp-cadherin is important in kidney development. If the generation of Ksp-cadherin heterozygous mice developed renal abnormalities and were predisposed to the development of tumors, this would provide further evidence that loss of Ksp-cadherin contributes to the development of Wilms tumor.

6.2.4 Evaluation of epigenetic events controlling gene regulation

Many primary tumors and cancer cell lines, including breast and prostate, show loss of E-cadherin expression without evidence of mutations. In these instances, it has been proposed that epigenetic events including: (1) hypermethylation of the E-cadherin promoter; (2) alteration of the trans-acting factors regulating E-cadherin expression and (3) chromatin-mediated effects, may contribute to E-cadherin silencing (reviewed in Hajra and Fearon, 2002).

In our study, a portion of the Ksp-cadherin gene and promoter region was evaluated for aberrant methylation, but no evidence of hypermethylation was found in these regions. Further analysis of these CpG rich regions revealed that they did not meet the criteria of CpG islands. However, four putative promoter regions:(1) -2950 to -3452; (2) -5484 to -6963; (3) -14791 to -16284 and (4) -16620 to -17154, relative to the Ksp-cadherin transcriptional start site are predicted to contain CpG islands. It may be beneficial to evaluate these regions for aberrant methylation patterns. Although most, if not all, CpG islands associated with gene promoters are methylated in regions within or near the transcription start site, it is possible that one of these CpG islands located upstream in the Ksp-cadherin promoter region may be involved in regulating its expression and may reveal new information on location of CpG islands and gene regulation.

Dysregulation of transcription factors and disruption of transcription factor binding sites may also play a role in gene silencing. Deletion analysis of the E-cadherin promoter revealed that simultaneous disruption of the two E-boxes (enhancer elements important in regulating transcription) located within the promoter region, significantly reduces E-cadherin expression (Giroldi et al., 1997). Furthermore, defects in the transcription factors that bind to this region and regulate gene expression can also lead to decreased E-cadherin expression, as the defective transcription factors may no longer be able to bind to the E-box element in the promoter and induce E-cadherin transcription. One of the transcription factors found to bind to E-cadherin is *Snail*, and increased expression of *Snail* has been found to coincide with loss *of* E-cadherin expression in bladder, pancreas, colon, breast, oral squamous carcinoma and melanoma cell lines (Batlle et al., 2000; Yokoyama et al., 2001; Poser et al., 2001). Interestingly, analysis of the Ksp-cadherin promoter has revealed that the minimal region of promoter needed for gene expression includes 2 GC boxes and an *HNF-1* binding site (Bai et al., 2002). Furthermore, HNF-1β has been shown to directly regulate Ksp-cadherin expression. Sequencing of the promoter region including the *HNF-1* binding domain and GC boxes did not reveal any mutations in all 34 Wilms tumors evaluated, suggesting that the Ksp-cadherin promoter is functional in Wilms tumor. Therefore, it would be of interest to see if *HNF-1β* expression is altered in Wilms tumors as this may represent a mechanism of Ksp-cadherin gene silencing. If additional Ksp-cadherin transcriptional regulators and binding domains become identified these regions would also warrant further study.

Chromatin condensation has also been implicated in the down-regulation of E-cadherin expression in cancer. DNase 1 hypersensitivity experiments of the E-cadherin promoter revealed that the chromatin structure was loosened in cells that expressed E-cadherin, but the chromatin was condensed in cells that did not express E-cadherin (Hennig et al., 1995). This chromatin condensation also coincided with hypermethylation suggesting that these two processes work together and are dependant on one another. Since our methylation analysis did not find evidence of Ksp-cadherin promoter hypermethylation, it is unlikely that chromatin condensation would be present. However, as a complement or an alternative to further methylation studies it may be of interest to analyse the chromatin conformation of the Ksp-cadherin promoter and gene in Wilms tumors as compared to normal fetal kidney to see if it is in a condensed, non-functional state in Wilms tumors. The role of these epigenetic mechanisms (methylation, transcription factors, chromatin structure) in the development of cancer is still unclear but it is believed that these 3 events may work with one another to induce gene inactivation, rather than functioning as independent events.

6.2.5 Evaluation of additional cadherins and the role of cadherin switching in Wilms tumor

In addition to aberrant silencing of cadherins in cancer cells, sometimes up-regulation of a cadherin that is not normally expressed in the tissue of interest can occur. This process is called cadherin switching and has been identified in various cancers including breast (Hazan et al., 1997), prostate (Tomita et al., 2000) and melanoma (Sanders et al., 1999). In these instances loss of E-cadherin is associated with up-regulation of N-cadherin and is associated with a more invasive, metastatic phenotype. The mesenchymal cadherin, N-cadherin, has been found to be frequently involved in cadherin switching. It has been proposed that the down-regulation of epithelial cadherins such as E-cadherin combined with the up-regulation and inappropriate expression of the mesenchymal cadherins such as N-cadherin may result in a more invasive/aggressive phenotype. This is supported by *in vitro* studies in which forced expression of N-cadherin in breast cancer cell lines that endogenously express E-cadherin, caused the cells to become more motile and invasive upon injection into nude mice (Neiman et al., 1999; Hazan et al., 2000). Surprisingly, E-cadherin expression was unaffected in these cells. Reciprocal experiments with forced expression of E-cadherin in N-cadherin positive cells, did not reduce N-cadherin expression nor did it suppress cell motility or invasiveness suggesting that N-cadherin may be responsible for the more invasive properties of the cells. The studies also suggest that E-cadherin, and possibly other cadherins, may not be the primary or exclusive cadherin involved in tumor progression as N-cadherin can induce invasive and metastatic properties with or without expression of E-cadherin. H-cadherin has also been shown to have a role in tumorigenesis. Loss of H-cadherin was documented in the very early stages of breast carcinogenesis as well as colorectal and lung cancers (Toyooka et al., 2001; Toyooka et al., 2002). Forced expression of H-cadherin, but not E-cadherin, in highly invasive breast cancer cells that endogenously expressed N-cadherin, suppressed tumorigenecity and invasion (Lee et al., 1998). This suggests that loss of H-cadherin may be an early event in breast carcinogenesis necessary to induce other genetic events, such as up-regulation of N-cadherin, which is needed for the cancer to progress to an invasive or metastatic form. Therefore, it is possible that inactivation of Ksp-cadherin in Wilms tumors, which may occur early in Wilms tumorigenesis, may be one of the first events needed for tumor formation and dysfunction of additional cadherins are then needed in order for the tumor to become invasive.

Therefore, it would be of interest to evaluate expression of N-cadherin in Wilms tumors to see if it is aberrantly up-regulated and if so, if this up-regulation correlates with more aggressive tumors. It could be possible that since N-cadherin is a mesenchyme cadherin that its overexpression could be responsible for the development of blastemal predominant tumors unable to undergo the mesenchyme to epithelial differentiation transition. This could also provide an explanation as to why Wilms tumors predominantly comprised of blastemal cells are often more aggressive (Murphy et al., 2004). Another mesenchyme cadherin is cadherin-11, which has been evaluated in Wilms tumors by Schultz et al. (2000). They found that cadherin-11 RNA was expressed at higher levels as compared to E-cadherin in Wilms tumors. However, no mention was made of cadherin-11 expression in Wilms tumor versus normal fetal or mature kidney or clinicopathological correlations. It is possible that cadherin-11 may in fact be overexpressed in at least some Wilms tumors contributing to a more aggressive tumor. Interestingly, cadherin-11 is also located on chromosome 16q within the minimal region of 16q LOH in Wilms tumors and may represent the chromosome 16q gene. Evaluation of these mesenchyme cadherins by either RNA studies using real time RT-PCR or Northern blot analysis or protein expression via immunohistochemistry would be valuable and may provide additional clues as to the role of cadherins in Wilms tumorigenesis.

6.3 Concluding Remarks

The global objective of this dissertation was to identify a gene(s) involved in the initiation and/or progression of Wilms tumor. Identification of such genes would ultimately translate into a better understanding of Wilms tumorigenesis and lead to improved therapies and minimization of late side effects. Three very diverse approaches were used to identify novel Wilms tumor genes. From the different studies, valuable knowledge was gained, both with respect to Wilms tumorigenesis and also with respect to current methodologies. Furthermore, the importance of using a variety of different approaches for candidate gene identification was also illustrated. Surprisingly, evaluation of the SGBS gene, *GPC3*, which was hypothesized to be altered in Wilms tumor revealed no evidence for frequent involvement in sporadic Wilms tumor. The DD-PCR approach, which has been used successfully to identify differentially expressed genes in other cancers, was unsuccessful in identifying candidate Wilms tumor genes. Finally, a high priority candidate gene, Ksp-cadherin, was identified, via an *in silico* database searching method, which is not expressed in most Wilms tumors.

At this point in time it can not be determined whether loss of Ksp-cadherin is involved in the development of Wilms tumor, or rather if it is an effect of the development of Wilms tumor. If Ksp-cadherin is found to be directly linked to the initiation of Wilms tumors, this finding would have huge implications to Wilms tumor biology. Conversely, if loss Ksp-cadherin is found to occur as a result of Wilms tumor development and not a cause of it, this would still be relevant to Wilms tumor biology, possibly as a method of targeted therapy if most pathways to Wilms tumorigenesis converge on this one. This study has provided some exciting and valuable insight into additional genes and/or pathways that may be either directly or indirectly involved in Wilms tumorigenesis.

Chapter 7 - References

Alami J, Williams BR, Yeger H. (2003). Derivation and characterization of a Wilms' tumour cell line, WiT 49. Int J Cancer 107:365-74.

Angst BD, Marcozzi C, Magee AI. (2001). The cadherin superfamily: diversity in form and function. Journal of Cell Science 114:629-641.

Arenas MI, Romo E, Royuela M, Fraile B, Paniagua R. (2000). E-, N- and P-cadherin, and alpha-, beta- and gamma-catenin protein expression in normal, hyperplastic and carcinomatous human prostate. Histochem J 32:659-67.

Armstrong JF, Pritchard-Jones K, Bickmore WA, Hastie ND, Bard JBL. (1992). The expression of the Wilms tumor gene, WT1, in the developing mammalian embryo. Mech Dev 4:85-97.

Aron B. (1974). Wilms' tumor – a clinical study of eighty-one children. Cancer 33:637-646.

Austruy E, Cohen-Salmon M, Antignac C, Beroud C, Henry I, Nguyen VC, Brugieres L, Junien C, Jeanpierre C. (1993). Isolation of kidney complementary DNAs down-expressed in Wilms' tumor by a subtractive hybridization approach. Cancer Res 53:2888-94.

Baeg GH, Lin X, Khare N, Baumgartner S, Perrimon N. (2001). Heparan sulfate proteoglycans are critical for the organization of the extracellular distribution of Wingless. Development 126:87-94.

Bai Y, Pontoglio M, Hiesberger T, Sinclair AM, Igarashi P. (2002). Regulation of kidney-specific Ksp-cadherin gene promoter by hepatocyte nuclear factor-1β. Am J Physiol (Renal Physiol) 283:F839-F851.

Barbaux S, Niaudet P, Gubler MC, Grunfeld JP, Jaubert F, Kutten F, Fekete CN, Souleyreau-Therville N, Thibaud E, Fellous M, McElreavey K. (1997). Donor splice-site mutations in WT1 are responsible for Frasier syndrome. Nat Genet 17:467-470.

Bardeesy N, Beckwith JB, Pelletier J. (1995). Clonal expansion and attenuated apoptosis in Wilms' tumors are associated with p53 gene mutations. Cancer Res 55:215-9.

Bard JBL, McConnell JE, Davies JA. (1994). Towards a genetic basis for kidney development. Mechanisms of Development 48:3-11.

Bartolomei MS, Zemel S, Tilghman SM. (1991). Parental imprinting of the mouse H19 region. Nature 351:153-155.

Batlle E, Sancho E, Franci C, Dominguez D, Monfar M, Baulida J, Garcia de Hereros A. (2000). The transcription factor Snail is a repressor of E-cadherin gene expression in epithelial tumour cells. Nat Cell Biol 2:84-89.

Baudry D, Cabanis MO, Patte C, Zucker JM, Pein F, Fournet JC, Sarnacki S, Junien C, Jeanpierre C. (2003). Cadherins in Wilms' tumor: E-cadherin expression despite absence of WT1. Anticancer Res 23(1A):475-8.

Beales PL, Reid HA, Griffiths MH, Maher ER, Flinter FA, Woolf AS. (2000). Renal cancer and malformations in relatives of patients with Bardet-Biedl syndrome. Nephrol Dial Transplant 15:1977-85.

Beales PL, Warner AM, Hitman GA, Thakker R, Flinter FA. (1997). Bardet-Biedl syndrome: a molecular and phenotypic study of 18 families. J Med Genet 34:92-8.

Becker KR, Atkinson MJ, Reich U, Becker I, Nekarda H, Siewert JR, Hofler H. (1994). E-cadherin gene mutations provide clues to diffuse type gastic carcinomas. Cancer Research 54:3845-3852.

Beckwith JB. (1969). Macroglossia, omphalocele, adrenal cytomegaly, gigantism and hyperplastic visceromegaly. Birth Defects 5:188-1986.

Beckwith, JB. (1986). Wilms tumor and other renal tumors of childhood: An update. J Urol 136:320-324.

Beckwith JB. (1993). Precursor lesions of Wilms tumor: Clinical and biological implications. Medical and Pediatric Oncology 21:158-168.

Beckwith JB. (1998). Nephrogenic rests and the Pathogenesis of Wilms tumor: Developmental and clinical considerations. Am J Med Gen 79:268-273.

Beckwith JB, Kiviat NB, Bonadio JF. (1990). Nephrogenic rests, nephroblastomatosis and the pathogenesis of Wilms tumor. Ped Pathol 10:1-36.

Beckwith JB and Palmer NF. (1978). Histopathology and prognosis of Wilms tumor. Cancer 41:1937-1948.

Behrens J, von Kries JP, Kuhl M, Bruhn L, Wedlich D, Grosschedl R, Birchmeier W. (1996). Functional interaction of beta-catenin with the transcription factor LEF-1. Nature 382:638-42.

Bello MJ, Vaquero J, de Campos JM, Kusak ME, Sarasa JL, Saez-Castresana J, Pestana A, Rey JA. (1994). Molecular analysis of chromosome 1 abnormalities in human gliomas reveals frequent loss of 1p in oligodendroglial tumors. Int J Cancer 15:172-5.

Berfield M, Götte M, Park PW, Reizes O, Fitzgerald ML, Lincecum J, Zako M. (1999). Functions of cell surface heparan sulfate proteoglycans. Annu Rev Biochem 68:729-777.

Bertioli DJ, Schlichter UHA, Adams MJ, Burrows PR, Steinbiss HH, Antoniw JF. (1995). An analysis of differential display shows a strong bias towards high copy number mRNAs. Nucleic Acids Res 23:4520-4523.

Bertram J, Palfner K, Hiddemann W, Kneba. (1998). Elevated expression of S100P, CAP and MAGE 3 in doxorubicin-resistant cel lines: comparison of mRNA differential display reverse transcription-polymerase chain reaction and subtractive suppressive hybridization for the analysis of differential gene expression. Anti-Cancer Drugs 9:311-317.

Berx G, Becker KF, Hofler H, van Roy F. (1998). Mutations of the human E-cadherin (CDH1) gene. Hum Mutat 12:226-37.

Berx G, Cleton-Jansen AM, Strumane K, deLeeuw WJ, Nollet F, van Roy F, Cornelisse C. (1996). E-cadherin is inactivated in a majority of invasive human lobular breast cancer by truncation mutations throughout its extracellular domain. Oncogene 13:1919-1925.

Bird AP. (1986). CpG-rich islands and the function of DNA methylation. Nature 321:209-213.

Bond HM, Bonelli P, Mesuraca M, Agosti V, Cuomo C, Nistico A, Tassone P, Tuccillo F, Iacopino CI, Barbieri V, Cerra M, Costanzo FS, Morrone G, Venuta S. (1998). Identification by differential display of transcripts regulated during hemtopoietic differentiation. Stem Cells 16:136-143.

Bonneh-Barkay D, Shlissel M, Berman B, Shaoul E, Admon A, Vlodavsky I, Carey DJ, Asundi VK, Reich-Slotky R, Ron D. (1997). Identification of glypican as a dual modulator of the biological activity of fibroblast growth factors. J Biol Chem 272:12415-12421.

Bomont P, Cavalier L, Blondeau F, Ben Hamida C, Belal S, Tazir M, Demir E, Topaloglu H, Korinthenberg R, Tuysuz B, Landrieu P, Hentati F, Koenig M. (2000). The gene encoding gigaxonin, a new member of the cytoskeletal BTB/kelch repeat family, is mutated in giant axonal neuropathy. Nat Genet 26:370-4.

Braxton S, Bedilion T. (1998). The integration of microarray information in the drug development process. Curr Opin Biotechnol 9:643-9.

Breen E, Clarke A, Steele GJ, Mercurio AM. (1993). Poorly differentiated colon carcinoma cell lines deficient in α-catenin expression express high levels of surface E-cadherin but lack Ca^{2+}-dependent cell-cell adhesion. Cell Adhes Commun 1:239-250.

Breslow N, Beckwith JB, Ciol M, Sharples K. (1988). Age distribution of Wilms' tumor: report from the National Wilms' tumor study. Cancer Research 48:1653-1657.

Breslow NE, Chruchill G, Nesmith B, Thomas PR, Beckwith JB, Othersen HB, D'Angio GJ. (1986). Clinicopathologic features and prognosis for Wilms' tumor patients with metastases at diagnosis. Cancer 58:2501-2511.

Breslow N, Olshan A, Beckwith JB, Green DM. (1993). Epidemiology of Wilms tumor. Med Pediatr Oncol 3:321-6.

Breslow NE, Takashima JR, Ritchey ML, Strong LC, Green DM. (2000). Renal failure in the Denys-Drash and Wilms' tumor-aniridia syndromes. Cancer Res 60:4030-4032.

Brown KW, Malik, KTA. (2001) The molecular biology of Wilms' tumour. Exp. Rev. Mol. Med. 14 May, http://www.expertreviews.org/01003027h.htm.

Bruening W, Winnett E, Pelletier J. (1995). Wilms' tumor: a paradigm for insights into development and cancer. Cancer Invest 13:431-43.

Brzustowicz LM, Farrell S, Khan MB, Weksberg R. (1999). Mapping of a new SGBS locus to chromosome Xp22 in a family with a severe form of Simpson-Golabi-Behmel syndrome. Am J Hum Genet 65:779-783.

Bullions LC, Notterman DA, Chung LS, Levine Aj. (1997). Expression of wild-type α-catenin protein in cells with a mutant α-catenin gene restores both growth regulation and tumor suppressor activities. Mol Cell Biol 17:4501-4508.

Bustin SA and Dorudi S. (2002). The value of microarray techniques for quantitative gene profiling in molecular diagnostics. TRENDS in Molecular Medicine 8:269-272.

Byers RJ, Hoyland JA, Dixon J, Freemont AJ. (2000). Subtractive hybridization – genetic takeaways and the search for meaning. International Journal of Experimental Pathology. 81:391-404.

Call KM, Glaser T, Ito CY, Buckler AJ, Pelletier J, Haber DA, Rose EA, Kral A, Yeger H, Lewis WH, Jones C, Housman DE. (1990). Isolation and characterization of a zinc finger polypeptide gene at the human chromosome 11 Wilms tumor locus. Cell 60:509-520.

Cano-Gauci DF, Song JJ, Yang J, McKerlie C, Choo B, Shi W, Pullano R, Piscione TD, Grisaru S, Soon S, Sedlackova L, Tanswell AK, Mak TW, Yeger H, Lockwood GA, Rosenblum ND, Filmus J. (1999). Glypican-3 – deficient mice exhibit developmental overgrowth and some of the abnormalities typical of Simpson-Golabi-Behmel syndrome. J Cell Bio 146:255-264.

Caricasole A, DuarteA, Larsson S, Hastie ND, Little M, Holmes G, Todorov I, Ward A. (1996). RNA binding by the Wilms' tumor suppressor (WT1) zinc finger proteins. Proc Natl Acad Sci USA 93:7562-7566.

Chaplin T, Ayton P, Bernard OA, Saha V, Della Valle V, Hillion J, Gregorini A, Lillington D, Berger R, Young BD. (1995). A novel class of zinc finger/leucine zipper genes identified from the molecular cloning of the t(10;11) translocation in acute leukemia. Blood 85:1435-41.

Cher ML, Ito T, Weidner N, Carroll PR, Jensen RH. (1995). Mapping of regions of physical deletion on chromosome 16q in prostate cancer cells by fluorescence in situ hybridization (FISH). J Urol 153:249-54.

Chernos JE, Fowlow SB, Cox DM. (1990). A case of Perlman syndrome associated with a cytogenetic abnormality of chromosome 11. Am J Hum Genet 47(suppl):A28.

Coppes MJ, Haber DA, Grundy PE. (1994). Genetic events in the development of Wilms' tumor. N Engl J Med 331:586-90.

Coppes MJ, Huff V, Pelletier J. (1993). Denys-Drash syndrome: relating a clinical disorder to genetic alterations in the tumor suppressor gene WT1. J Pediatr 123:673-8.

Cossette P, Lie L, Brisebois K, Dong H, Lortie A, Vanasse M, Saint-Hilaire J-M, Carmant L, Verner A, Lu W-Y, Wang YT, Rouleau GA. (2002). Mutation of GABRA1 in an autosomal dominant form of juvenile myoclonic epilepsy. Nature Genet 31:184-189.

Dallol A, Krex D, Hesson L, Eng C, Maher ER, Latif F. (2003). Frequent epigenetic inactivation of the SLIT2 gene in gliomas. Oncogene 22:4611-6.

D'Angio GJ, Evans AE, Breslow N, Beckwith B, Bishop H , Farewell V, Goodwin W, Leape L, Palmer N, Sinks L, Sutow W, Tefft M, Wolff J. (1988). The treatment of Wilms tumor. Results of the second National Wilms tumor study (NWTS). Cancer 47:2302-2311.

Davies J. (1993). How to build a kidney. Seminars in Cell Biology 4:213-219.

DeBaun MR, Ess J, Saunders S. (2001). Simpson Golabi Behmel Syndrome: Progress toward understanding the molecular basis for overgrowth, malformation, and cancer predisposition. Molecular Genetics and Metabolism 72:279-286.

DeRisi J, Penland L, Brown PO, Bittner ML, Meltzer PS, Ray M, Chen Y, Su YA, Trent JM. (1996). Use of a cDNA microarray to analyse gene expression patterns in human cancer. Nat Genet 14:457-60.

Diatchenko L, Lau YFC, Campbell AP, Chenchik A, Moqadam F, Huang B, Lukyanov S, Lukyanov K, Gurskaya N, Sverdlow ED, Siebert PD. (1996). Suppression subtractive hybridization: a method for generating differentially regulated or tissue-specific cDNA probes and libraries. Proc Natl Acad Sci USA 93:6025-6030.

Domachowske JB, Bonville CA, Mortelliti AJ, Colella CB, Kim U, Rosenberg HF. (2000). Respiratory syncytial virus infection induces expression of the anti-apoptosis gene IEX-1L in human respiratory epithelial cells. J Infect Dis 191:824-830.

Dome JS and Coppes MJ. (2002). Recent advances in Wilms tumor genetics. Current Opinion in Pediatrics 14:5-11.

Donohue PJ, Alberts GF, Guo Y, Winkles JA. (1995). Identification by targeted differential display of an immediate early gene encoding a putative serin/threonine kinase. J Biol Chem 270:10351-10357.

Ebert CJ. (1872). Myoma sarconatodes renum. Vichous Arch Pathol Anat Physiol 55:518-520.

Eggenschwiler J, Ludwig T, Fisher P, Leighton PA, Tilghman SM, Efstratiadis A. (1997). Mouse mutant embryos overexpressing IGF-II exhibt phenotypic features of the Beckwith-Weidemann ad Simpson-Golabi-Behmel syndromes. Genes and Develop 11:3128-3142.

Farber S. (1966). Chemotherapy in the treatment of leukemia and Wilms tumor. JAMA 198:826-836.

Farber S, Toch R, Sears EM, Pinkel D. (1956). Advances in chemotherapy of cancer in man. Advances in Cancer Research 4:1-71.

Filmus J, Shi W, Wong ZM, Wong MJ. (1995). Identification of a new membrane-bound heparan sulphate proteoglycan. Biochem J 311:561-5.

Fong C-T, White PS, Peterson K, Sapienza C, Cavenee Wk, Kern Se, Vogelstein B, Cantor AB, Look AT, Brodeur GM. (1992). Loss of heterozygosity for chromosomes 1 or 14 defines subsets of advanced neuroblastomas. Cancer Research 52:1780-1785.

Frommer M, McDonald LE, Millar DS, Collis CM, Watt F, Grigs GW, Molloy PL, Paul CL. (1992). A genomic sequencing protocol that yields a positive display of 5' methylcytosine residues in individual DNA strands. PNAS USA 89:1827-1831.

Fukuda M, Mikoshiba K. (2001). Synaptotagmin-like protein 1-3: a novel family of C-terminal-type tandem C2 proteins. Biochem Biophys Res Commun 281:1226-33.

Fukata M, Kuronda S, Nakagawa M, Kawajiri A, Itoh N, Shoji I, Matsuura Y, Yonehara S, Fujisawa H, Kikuchi A, Kaibuchi K. (1999). Cdc42 and Rac1 regulate the interaction of IQGAP1 with β-catenin. J Biol Chem 274:26044-26050.

Fukuzawa R, Breslow NE, Morison IM, Dwyer P, Kusafuka T, Kobayashi Y, Becroft DM, Beckwith JB, Perlman EJ, Reeve AE. (2004). Epigenetic differences between Wilms tumor in white and east-Asian children. Lancet 363:446-451.

Fung ET, Thulasiraman V, Weinberger SR, Dalmasso EA. (2001). Protein biochips for differential profiling. Current Opinion in Biotechnology 12:65-69.

Gardiner-Garden M, Frommer M. (1994). Transcripts and CpG islands associated with the pro-opiomelanocortin gene and other neurally expressed genes. J Mol Endocrinol 12:365-82.

Gardner-Thorpe J, Ito H, Ashley SW, Whang EE. (2002). Differential display of expressed genes in pancreatic cancer cells. Biochem Biophys Res Commun 293(1):391-5.

Gayther SA, Gorringe LK, Ramus SJ, Huntsman D, Roviello F, Grehan N, Machado JC, Pinto E, Seruca R, Halling K, MacLeod P, Powell SM, Jackson CE, Ponder BAJ, Caldas C. (1998). Identification of germline E-cadherin mutations in gastric cancer families of European origin. Cancer Research 58:4086-4089.

Gessler M, Proustka A, Cavenee W, Neve RL, Orkin SH, Bruns GAP. (1990). Homozygous deletion in Wilms tumours of a zinc-finger gene identified by chromosome jumping. Nature 343:774-778.

Gillan TL, Dietrich K, Perlman EJ, Godbout R, Grundy PE. Ksp-cadherin represents a new candidate Wilms tumor gene. (In prep).

Gillan TL, Hughes R, Godbout R, Grundy PE. (2003). The Simpson-Golabi-Behmel gene, GPC3, is not involved in sporadic Wilms tumorigenesis. Am J Med Genet 122A:30-36.

Giroldi LA, Bringuier P-P, de Weijert M, Jansen C, van Bokhoven A, Schalken JA. (1997). Role of E boxes in the repression of E-cadherin expression. Biochemical and Biophysical Research communications 241:453-458.

Gonzalez, AD, Kaya M, Shi W, Song H, Testa JR, Penn LZ, Filmus J. (1998). OCI-5/GPC3, a glypican encoded by a gene that is mutated in the Simpson-Golabi-Behmel overgrowth syndrome, induces apoptosis in a cell line-specific manner. J Cell Bio 141:1407-1414.

Gonzalez HE, Gujrati M, Frederick M, Henderson Y, Arumugam J, Spring PW, Mitsudo K, Kim HW, Clayman GL. (2003). Identification of 9 genes differentially expressed in head and neck squamous cell carcinoma. Arch Otolaryngol Head Neck Surg 129:754-9.

Graff JR, Herman JG, Lapidus RG, Chopra H, Xu R, Jarrad DF, Isaacs WB, Pitha PM, Davidson NE, Baylin SB. (1995). E-cadherin expression is silenced by DNA hypermethylation in human breast and prostate carcinoma. Cancer Research 55:5195-5199.

Green DM, Donckerwolcke R, Evans AE, D'Angio GJ. (1995). Late effects of treatment for Wilms tumor. Hematology/Oncology Clinics of North America 9:1317-1327.

Greenwood MF, Holland P. (1984). Clinical and biochemical manifestations of Wilms tumor. In: Wilms' tumor. Pochedly C and Baum ED (eds) Elsvier, NY p9-30.

Grisaru S, Rosenblum ND. (2001). Glypicans and the biology of renal malformations. Pediatr Nephrol 16:302-6

Grundy PE, Breslow NE, Green DM, Sharples K, Evans A, D'Angio GJ. (1989). Prognostic factors of children with recurrent Wilms tumor: Results from the second and third National Wilms Tumor Study. J Clin Oncol &:638-647.

Grundy PE, Telzerow PE, Breslow N, Moksness J, Huff V, Paterson MC. (1994). Loss of heterozygosity for chromosomes 16q and 1p in Wilms' tumors predicts an adverse outcome. Cancer Research 54:2331-2333.

Grundy P, Telzerow P, Haber D, Berman B, Li F, Paterson MC, Garber J. (1991). Chromosome 11 uniparental isodisomy predisposing to embryonal neoplasms. Lancet 338:1079-1080.

Guilford P, Hopkins J, Harraway J, McLeod M, McLeod N, Harawira P, Taite H, Scoular R, Miller A, Reeve AE. (1998). E-cadherin germline mutations in familial gastric cancer. Nature 392:402-405.

Häcker U, Lin X, Perrimon N. (1997). The Drosophila sugarless gene modulates wingless signaling and encodes an enzyme involved in polysaccharide biosynthesis. Development 124:3565-3573.

Haber DA, Sohn RL, Buckler AJ, Pelletier J, Call KM, Housman DE. (1991). Alternative splicing and genomic structure of the Wilms' tumor gene WT1. Proc Natl Acad Sci USA 88:9618-9622.

Haber DA, Timmers HT, Pelletier J, Sharp PA, Housman DE. (1992). A dominant mutation in the Wilms tumor gene WT1 cooperates with the viral oncogene E1A in transformation of primary kidney cells. PNAS USA 89:6010-4.

Hajra KM and Fearon ER. (2002). Cadherin and catenin alterations in human cancer. Genes, Chromosomes and Cancer 34:255-268.

Hao Y, Crenshaw T, Moulton T, Newcomb E, Tycko B. (1993). Tumor-suppressor activity of H19 RNA. Nature 365:764-767.

Hastie ND. (1994). The genetics of Wilms' tumor--a case of disrupted development. Annu Rev Genet 28:523-58.

Hatada I, Inazawa J, Abe T, Nakayama M, Kaneko Y, Jinno Y, Niikawa N, Ohashi H, Fukushima Y, Lida K, Yutani C, Takahashi S, Chiba Y, Ohishi S, Mukai T. (1996). Genomic Imprinting of human $p57^{KIP2}$ and its reduced expression in Wilms tumor. Hum Mol Genet 5:783-788.

Hatta K, Takagi S, Fujisawa H, Takeichi M. (1987). Spatial and temporal expression pattern of N-cadherin cell adhesion molecules correlated with morphogenetic processes of chicken embryos. Dev Biol 120:215-27.

Hazan RB, Qiao R, Keren R, Badano I, Suyama K. (2004). Cadherin switch in tumor progression. Ann N.Y. Acad Sci 1014:155-163.

Hazan RB, Phillips GR, Qiao RF, Norton L, Aaronson SA. (2000). Exogenous expression of N-cadherin in breast cancer cells induces cell migration, invasion, and metastasis. JBC 148:779-790.

Hazan RB, Kang L, Whooly BP, Borgen PI. (1997). N-cadherin promotes adhesion between invasive breast cancer cells and the stroma. Cell Adhes Commun 4:399-411.

Hennig G, Behrens J, Truss M, Frisch S, Reichmann E, Birchmeier W. (1995).

Progression of carcinoma cells is associated with alterations in chromatin structure and factor binding at the E-cadherin promoter in vivo. Oncogene 11:475-84.

Henneveld HT, van Lingen RA, Hamel BCJ, Stolte-Dijkstra I, van Essen AJ. (1999). Perlman Syndrome: Four additional cases and review. Am J Med Genet 86:439-446.

Henry I, Bonaiti-Pellie C, Chehensse V, Beldjord C, Schwartz C, Utermann G, Junien C. (1991). Uniparental paternal disomy in a genetic cancer-predisposing syndrome. Nature 351:665-667.

Hernandez G, Vazquez-Pianzola P, Zurbriggen A, Altmann M, Sierra JM, Rivera-Pomar R. (2004). Two functionally redundant isoforms of Drosophila melanogaster eukaryotic initiation factor 4B are involved in cap-dependent translation, cell survival, and proliferation. Eur J Biochem 271:2923-36.

Hippo Y, Watanabe K, Watanabe A, Midorikawa Y, Yamamoto S, Ihara S, Tokita S, Iwanari H, Ito Y, Nakano K, Nezu J, Tsunoda H, Yoshino T, Ohizumi I, Tsuchiya M, OhnishiS, Makuuchi M, Hamakubo T, Kodama T, Aburatani H. (2004). Identification of Soluble NH_2-terminal fragment of Glypican-3 as a serological marker for early stage Hepatocellular carcinoma. Cancer Research 64:2418-2423.

Hirohashi S. (1998). Inactivation of the E-cadherin-mediated cell adhesion system in human cancers. Am J Pathol 153:333-339.

Hollstein M, Sidransky D, Vogelstein B. (1991). p53 mutations in human cancers. Science 253:49-53.

Hsu, H-C, Chen W, Lai P-L. (1997). Cloning and expression of a developmentally regulated transcript MXR7 in Hepatocellular carcinoma: Biological significance and temporal-spatial distribution. Cancer Research 57:5179-5184.

Hubank M and Schatz DG. (1994). Identifying differences in mRNA expression by representational difference analysis of cDNA. Nucleic Acids Research 22:5640-5648.

Huber R, Crisponi L Mazzarell R, Chen CN, Su Y, Shizuya H, Chen EY, Cao A, Pilia G. (1997). Analysis of exon/intron structure and 400 kb of genomic sequence surrounding the 5'-promoter and 3'-terminal ends of the human Glypican 3 (GPC3) gene. Genomics 45:48-58.

Huber R, Mazzarella R, Chen CN, Chen E, Ireland M, Lindsay S, Pilia G, Crisponi L. (1998). Glypican 3 and glypican 4 are juxtaposed in Xq26.1. Gene 225:9-16.

Huff V. (1998). Genotype/phenotype correlations in Wilms tumor. Medical and Pediatric Oncology 27:408-414.
Hughes P, Tratner I, Ducoux M, Piard K, Baldacci G. (1999). Isolation and identification of the third subunit of mammalian DNA polymerase delta by PCNA-affinity chromatography of mouse FM3A cell extracts. Nucleic Acids Res 27:2108-14.

Hughes-Benzie RM, Hunter AGW, Allanson JE, MacKenzie AE. (1992). Simpson-Golabi-Behmel syndrome associated with renal dysplasia and emybryonal tumor: localization of the gene to Xqcen-q21. Am J Med Genet 43:428-435.

Herman JG, Graff JR, Myohanen S, Nelkin BD, Baylin SB. (1996). Methylation-specific-PCR: a novel PCR assay for methylation status of CpG islands. PNAS USA 93:9821-9826.

Hurst SD, Muchamuel T, Gorman D M, Gilbert J M, Clifford T, Kwan S, Menon S, Seymour B, Jackson C, Kung TT, Brieland JK, Zurawski SM, Chapman RW, Zurawski G, Coffman RL. (2002). New IL-17 family members promote Th1 or Th2 responses in the lung: in vivo function of the novel cytokine IL-25. J. Immun 169:443-453

Huser J, Grignon DJ, Ro JY, Ayala AG, Shannon RL, Papadopoulous NJ. (1990). Adult Wilms tumor: A clinicopathologic study of 11 cases. Mol Pathol 3:321-326.

Igarashi P. (2003). Following the expression of a kidney-specific gene from early development to adulthood. Exp Nephrology 94:e1-e6.

Igarashi J, Nimura Y, Fujimori M, Mihara M, Adachi W, Kageyama H, Nakagawara A. (2000). Allelic loss of the region of chromosome 1p35-pter is associated with progression of human gastric carcinoma. Jpn J Cancer Res 91:797-801.

Igarashi P, Shashikant CS, Thomson RB, Whyite DA, Liu-Chen S, Ruddle FH, Aronson PS. (1999). Ksp-cadherin gene promoter. II. Kidney-specific activity in transgenic mice. Am J Physiol (Renal Physiol) 277:F599-F610.

Jackson SM, Nakato H, Sugiura M, Jannuzi A, Oakes R, Kaluza V, Golden C, Selleck SB. (1997). Dally, a Drosophila glypican, controls cellular responses to the TGF-β-related morphogen, Dpp. Development 124:4113-4120.

Jadresic L, Leake J, Gordon I, Dillon MJ, Grant DB, Pritchard J, Risdon RA, Barratt TM. (1990). Clinicopathologic review of twelve children with nephropathy, Wilms tumor and genital abnormalities (Drash syndrome). J Pediatrics 117:717-25.

Jo H, Zhang H, Zhang R, Liang. (1998). Cloning oncogenic Ras-regulated genes by differential display. Methods: A comparison to methods in enzymology 16:365-372.

Jones JW, Raval JR, Beals TF, Worsham MJ, Van Dyke DL, Esclamado RM, Wolf GT, Bradford CR, Miller T, Carey TE. (1997). Frequent loss of heterozygosity on chromosome arm 18q in squamous cell carcinomas. Identification of 2 regions of loss--18q11.1-q12.3 and 18q21.1-q23. Arch Otolaryngol Head Neck Surg 123:610-4

Joshi CP and Nguyen HT. (1996). Differential display-mediated rapid identification of different members of a multigene family HSP 16.9 in wheat. Plant Mol Biol 31:1125-1131.

Kanai Y, Ushijima S, Hui AM, Ochiai A, Tsuda H, Sakamoto M, Hirohashi S. (1997). The E-cadherin gene is silenced by CpG methylation in human hepatocellular carcinomas. Int J Cancer 71:355-9.

Kaneko H, Inoue R, Teramoto T, Morimoto W, Isogai K, Kasahara K, Kondo N. Detection of the genes induced in activated lymphocytes by modified differential display. (2002). J Investig Allergol Clin Immunol 12:86-90

Keller G, Vogelsany H, Becker I, Hutter J, Ott K, Candidus S, Grundei T, Becker K-F, Mueller J, Siewart JR, Hofler H. (1999). Diffuse type gastric and lobular breast carcinoma in a familial gastric patient with an E-cadherin germline mutation. Am J Pathol 155:337-342.

Klamt B, Schulze M, Thate C, Mares J, Goetz P, Kodet R, Scheurlen W, Weirich A, Graf N, Gessler M. (1998). Allele loss in Wilms tumors of chromosome arms 11q, 16q, and 22q correlates with clinicopathological parameters. Genes, Chromosomes and Cancer 22:287-294.

Knudson AG Jr, Hetcote HW, Brown BW. (1975). Mutation and childhood cancer: A probalistic model for the incidence of Retinoblastoma. PNAS USA 72:5116-20.

Kociok N, Unfried K, Esser P, Krott R, Schraermeyer U, Heimann K. (1998). The nonradioisotopic representation of differentially expressed mRNA by a combination of RNA fingerprinting and differential display. Mol Biotechnol 9:25-33.

Koesters R, Ridder R, Kopp-Schneider A, Betts D, Adams V, Niggli F, Briner J, von Knebel Doeberitz M. (1999). Mutational activation of the *β-catenin* proto-oncogene is a common event in the development of Wilms tumors. Cancer Research 59:3880-3882.

Koi M, Johnson LA, Kalikin LM, Little PFR, Nakamura Y, Feinberg AP. (1993). Tumor cell growth arrest caused by subchromosomal transferable DNA fragments from chromosome 11. Science 260:361-364.

Konduri SD, Srivenugopal KS, Yanamandra N, Dinh DH, Olivero WC, Gujrati M, Foster DC, Kisiel W, Ali-Osman F, Kondraganti S, Lakka SS, Rao JS. (2003). Promoter methylation and silencing of the tissue factor pathway inhibitor-2 (TFPI-2), a gene encoding an inhibitor of matrix metalloproteinases in human glioma cells. Oncogene 22:4509-16.

Koufos A, Grundy P, Morgan K, Aleck KA, Hadro T, Lampkin BC, Kalbakji A, Cavenee WK. (1989). Familial Wiedemann-Beckwith syndrome and a second Wilms tumor locus both maps to 11p15.5. Am J Hum Genet 44:711-719.

Koufos Y, Hansen MF, Lampkin BC, Workman ML, Copeland NG, Jenkins NA, Cavenee WK. (1984). Loss of alleles at loci on human chromosome 11 during genesis of Wilms' tumour. Nature 309:170-172.

Kramers S, Meadows AT, Jarrett P. (1984). Racial variation in incidence of Wilms tumor: relationship to congential anomalies. Med Pediatr Oncol 12:410-405.

Kremmidiotis G, Baker E, Crawford J, Eyre HJ, Nahmias J, Callen DF. (1998). Localization of human cadherin genes to chromosome regions exhibiting cancer-related loss of heterozygosity. Genomics 49:467-71.

Kreidberg JA, Sarida H, Loring JM, Maeda M, Pelletier J, Housman D, Jaenisch R. 1993. WT-1 is required for early kidney development. Cell 74:679-691.

Kuroda S, Fukata M, Nakagawa M, Fujii K, Nakamura T, Ookubo T, Izawa I, Nagase T, Nomura N, Tani H, Shoji I, Matsuura Y, onehara S, Kaibuchi K. (1998). Role of IQGAP1, a target of the small GTPases Cdc-42 and Rac1, in regulation of E-cadherin-mediated cell-cell adhesion. Science 281:832-835.

Larson F, Gundusen G, Lopez R, Prydz H. (1992). CpG islands are gene markers in the human genome. Genomics 3:1095-1107.

Larsson SH, Charlieu J-P, Miyagawa K, Engelkamp D, Rassoulzadegan M, Ross A, Cuzin F, van Heyningen V, Hastie ND. (1995). Subnuclear localization of WT1 in splicing or transcription factor domains is regulated by alternative splicing. Cell 81:391-401.

Lee SW, Reimer CL, Campbell DB, Cheresh P, Duda RB, Kocher O. (1998). H-cadherin expression inhibits in vitro invasiveness and tumor formation in vivo. Carcinogenesis 19:1157-1159.

Li M, Shuman C, Fei YL, Cutiongco E, Bender HA, Stevens C, Wilkins-Haug L, Day-Salvatore D, Yong SL, Geraghty MT, Squire J, Weksberg R. (2001). GPC3 mutation analysis in a spectrum of patients with overgrowth expands the phenotype of Simpson-Golabi-Behmel syndrome. Am J Med Genet 102:161-168.

Liang P, Averboukh L, Pardee A. (1993). Distribution and cloning of eukaryotic mRNAs by means of differential display: refinements and optimization. Nucleic Acids Research 21:3269-3275.

Liang P, Pardee AB. (1992). Differential display of eukaryotic messenger RNA by means of the polymerase chain reaction. Science 257:967-971.

Lin E, Huber R, Schlessinger D, Morin PJ. (1999). Frequent silencing of the GPC3 gene in ovarian cancer cell lines. Cancer Research 59:807-810.

Linder B, Jones LK, Chaplin T, Mohd-Sarip A, Heinlein UA, Young BD, Saha V. (1998). Expression pattern and cellular distribution of the murine homologue of AF10. Biochim Biophys Acta 1443:285-96.

Linskens MHK, Feng J, Andrews WH, Enlow BE, Saati SM, Tonkin LA, Funk WD, Villeponteau B. (1995). Cataloging altered gene expression in young and senescent cells using enhanced differential display. Nucleic Acids Research 23:3244-3251.

Little M, Holmes G, Walsh P. 1999. WT1: what has the last decade told us? BioEssays 21:191-202.

Little MH, Williamson KA, Mannens M, Kelsey A, Gosden C, Hastie ND, van Heyningen V. (1993). Evidence that WT1 mutations in Denys-Drash syndrome patients may act in a dominant-negative fashion. Hum Mol Genet 2:259-64.

Longley MJ, Pierce AJ, Modrich P. (1997). DNA polymerase delta is required for human mismatch repair in vitro. J Biol Chem 272:10917-21.

Maeda I, Takano T, Matsuzuka F, Maruyama T, Higashiyama T, Liu G, Kuma K, Amino N. (1999). Rapid screening of specific changes in mRNA thyroid carcinomas by sequence specific-differential display: Decreased expression of acid ceramidase mRNA in malignant and benign thyroid tumors. Int J Cancer 81:700-704.

Maiti S, Alam R, Amos CI, Huff V. (2000). Frequent association of *β-catenin* and WT1 mutations in Wilms tumors. Cancer Research 60:688-6292.

Malhotra K, Foltz L, Mahoney WC, Schueler PA. (1998). Interaction and effect of annealing temperature on primers used in differential display RT-PCR. Nucleic Acids Res 26:854-6.

Malkin D, Sexsmith E, Yeger H, Williams BRG, Coppes MJ. (1994). Mutations of the p53 tumor suppressor gene occur infrequently in Wilms' tumor. Cancer Res 54:2077-2079.

Manda R, Kohno T, Matsuno Y, Takenoshita S, Kuwano H, Yokota J. (1999). Identification of genes (SPON2 and C20orf2) differentially expressed between cancerous and noncancerous lung cells by mRNA differential display. Genomics 61:5-14.

Matsuoka E. (1981). Genetics of Wilms tumor. Hum Genet 57:231-246.

Matsuoka S, Thompson JS, Edwards MC, Barletta JM, Grundy P, Kalikin LM, Harper JW, Elledge SJ, Feinberg AP. (1996). Imprinting of the gene encoding a human cyclin-dependent kinase inhibitor, p57(KIP2), on chromosome 11p15. PNAS 93:3026-3030.

Matz M, Usman N, Shagin D, Bogdanova E, Lukyanov S. (1997). Ordered differential display: a simple method for systematic comparison of gene expression profiles. Nucl Acid Res 25:2541-2542.

Maw MA, Grundy PE, Millow LJ, Eccles MR, Dunn RS, Smith PJ, Feinberg AP, Law DJ, Paterson MC, Telzerow PE, et al. (1992). A third Wilms' tumor locus on chromosome 16q. Cancer Res 52:3094-8.

McDonald JM, Douglass EC, Fisher R, Geiser CF, Krischer J, Strong LC, Virshup D, Huff V. (1998). Linkage of familial Wilms' tumor predisposition to chromosome 19 and a two-locus model for the etiology of familial tumors. Cancer Res 58:1387-1390.

McMaster ML, Gessler M, Stanbridge EJ, Weissman BE. (1995). WT1 expression alters tumorigenicity of the G401 kidney-derived cell line. Cell Growth Differ 6:1609-17.

Methot N, Pause A, Hershey JW, Sonenberg N. (1994). The translation initiation factor eIF-4B contains an RNA-binding region that is distinct and independent from its ribonucleoprotein consensus sequence. *Molec Cell Biol* 14:2307-2316.

Michiels EM, Oussoren E, Van Groenigen M, Pauws E, Bossuyt PM, Voute PA, Baas F. (1999). Genes differentially expressed in medulloblastoma and fetal brain. Physiol Genomics 1:83-91.

Miller FR, Barnibabas N, Liu X, Wang B, Park J. (1999). Differential display, subtractive hybridization, and application of methodology to search to point mutations to identify genetic defects responsible for progression in MCF10AT model of human breast disease. Electrophoresis 20:256-260.

Miller RW, Young JLJ, Novakovic B. (1995). Childhood cancer. Cancer 75:395-405.

Mirnics K, Middleton FA, Lewis DA, Levitt P. (2001). Analysis of complex brain disorders with gene expression microarrays: schizophrenia as a disease of the synapse. Trends Neurosci 24:479-86.

Morin FJ. (1999). β-catenin signaling and cancer. Bioessays 21:1021-1030.

Morton RA, Ewing CM, Nagafuchi A, Tsukita S, Issacs WB. (1993). Reduction of E-cadherin levels and deletion of the α-catenin gene in human prostate cancer cells. Cancer Research 53:3585-3590.

Mou L, Miller H, Li J, Wang E, Chalifour L. (1994). Improvements to the differential display method for gene analysis. Biochem Biophys Res Commun 199:564-9.

Murphy WM, Gringnon DJ, Perlman EJ. (2004). Kidney tumors in children. In: Tumors of the Kidney, Bladder, and Related Urinary Structures. American Registry of Pathology, Washington, DC:1-99.

Murthy SS, Shen T, De Rienzo A, Lee WC, Ferriola PC, Jhanwar SC, Mossman BT, Filmus J, Testa JR. (2000). Expression of GPC3, an X-linked recessive overgrowth gene, is silenced in malignant mesothelioma. Oncogene 19:410-416.

Nagar B, Overduin M, Ikura M, Rini JM. (1996). Structural basis of calcium-induced E-cadherin rigidification and dimerization. Nature 380:360-4.

Nakadate H, Yokomori K, Watanabe N, Tsuchiya T, Namiki T, Kobayshi H, Suita S, Tsunematsu Y, Horikoshi Y, Hatae Y, Endo M, Komada Y, Eguchi H, Toyoda Y, Kikuta A, Kobayashi R, Kaneko Y. (2001). Mutations/deletions of the WT1 gene, loss of heterozygosity on chromosome arms 11p and 11q, chromosome ploidy and histology in Wilms' tumors in Japan. Int J Cancer 94:396-400.

Nakato H, Futch TA, Selleck SB. (1995). The division abnormally delayed (dally) gene: a putative intergral membrane proteoglycan required for cell division patterning during postembryonic development of the nervous system in Drosophila. Development 121:3687-3702.

Nam JS, Ino Y, Kanai Y, Sakamoto M, Hirohashi S. (2004). 5-aza-2'-deoxycytidine restores the E-cadherin system in E-cadherin-silenced cancer cells and reduces cancer metastasis. Clin Exp Metastasis 21:49-56.

Neri G, Marini R, Cappa M, Borrelli P, Opitz JM. (1988). An X-linked encephalo-troho-schisis sydrome. Am J Med Genet 30:287-299.

Niemann MR, Prudoff RS, Johnson KR, Wheelock MJ. (1999). N-cadherin promotes motility in human breast cancer cells regardless of their E-cadherin expression. JCB 147:631-643.

Nishida N, Fukuda Y, Kokuryu H, Sadamoto T, Isowa G, Honda K, Yamaoka Y, Ikenaga M, Imura H, Ishizaki K. (1992). Accumulation of allelic loss on arms of chromosomes 13q, 16q and 17p in the advanced stages of human hepatocellular carcinoma. Int J Cancer 51:862-8.

Nojima D, Nakajima K, Li LC, Franks J, Ribeiro-Filho L, Ishii N, Dahiya R. (2001). CpG methylation of promoter region inactivates E-cadherin gene in renal cell carcinoma. Mol Carcinog 321:19-27.

Ogawa O, Eccles MR, Szeto J, McNoe LA, Yun K, Maw MA, Smith PJ, Reeve AE. (1993). Relaxation of insulin-like growth factor II gene imprinting implicated in Wilms tumor. Nature 362:749-751.

Orkin SH, Goldman DS, Sallan SE. (1984). Development of homozygosity of chromosome 11p markers in Wilms' tumour. Nature 362:749-741.

Ozawa M, Baribault H, Kemler R. (1989). The cytoplasmic domain of the cell adhesion molecule uvomorulin associates with three independent proteins structurally related in different species. EMBO J 8:1711-7.

Park S, Bernard A, Bove KE, Sens DA, Hazen-Martin DJ, Garvin AJ, Haber DA. (1993). Inactivation of WT1 in nephrogenic rests, genetic precursors to Wilms' tumour. Nat Genet 5:363-7.

Pardinas JR, Combates NJ, Prouty SM, Stenin KS, Parimoo S. (1998). Differential subtraction display: a unified approach for isolation of cDNAs from differentially expressed genes. Anal. Biochem 257:161-168.

Pedone PV, Tirabosco R, Cavazzana AO, Ungaro P, Basso G, Luksch R, Carli M, Bruni CB, Frunzio R, Riccio A. (1994). Mono- and bi-allelic expression of insulin-like growth factor II gene in human muscle tumors. Hum Mol Genet 3: 1117-1121.

Pellegrini M, Pilia G, Pantoano S, Lucchini F, Uda M, Fumi M, Cao A, Schlessinger D, Forabosco A. (1998). GPC3 expression correlates with the phenotype of the Simpson-Golabi-Behmel syndrome. Developmental Dynamics 213:431-439.

Pelletier J, Bruening W, Li FP, Haber DA, Glaser T, Housman DE. (1991). WT1 mutations contribute to abnormal genital system development and hereditary Wilms tumor. Nature 353:431-4.

Peyrieras N, Hyafil F, Louvard D, Ploegh HL, Jacob F. (1983). Uvomorulin: a nonintegral membrane protein of early mouse embryo. PNAS USA 80:6274-7.

Perrimon N, Bernfield M. (2000). Specificities of heparan sulphate proteoglycans in developmental processes. Nature 404:725-8.

Pilia G, Hughes-Benzie RM, MacKenzie, Baybayan P, Chen EY, Huber R, Neri G, Cao A, Forabosco A, Schlessinger D. (1996). Mutations in GPC3, a glypican gene, cause the Simpson-Golabi-Behmel overgrowth syndrome. Nature Genetics 12:241-247.

Pishvaian MJ, Feltes CM, Thompson P, Bussemakers MJ, Schalken JA, Byers SW. (1999). Cadherin-11 is expressed in invasive breast cancer cell lines. Cancer Res 59:947-52.

Polakis P. (2000). Wnt signaling and cancer. Genes Dev 5:66-71.

Polakis P. (2001). More than one way to skin a catenin. Cell 105:563-6.

Polyak K, Riggins GJ. (2001). Gene discovery using the serial analysis of gene expression technique: Implications for cancer research. J Clin Oncology 19:2948-2958.

Polyak K, Xia Y, Zweier JL, Kinzler KW, Vogelstein B. (1997). A model for p53-induced apoptosis. Nature 389:300-305.

Poser I, Dominguez D, de Herreros AG, Varnai A, Buettner R, Bosserhoff AK. (2001). Loss of E-cadherin expression in melanoma cells involves up-regulation of the transcriptional repressor Snail. J Biol Chem 276:24661-24666.

Pritchard-Jones K, Fleming S. (1991). Cell types expressing the Wilms' tumor gene (WT1) in Wilms' tumours: Implications for tumour histogenesis. Oncogene 6;2211-2220.

Pritchard-Jones K, Fleming S, Davidson D, Bickmore W, Porteus D, Gosden C, Bard J, Buckler A, Pelletier J, Housman D, van Heyningen V, Hastie N. (1990).

The candidate Wilms' tumor gene is involved in genitourinary development. Nature 346:194-197.

Radice P, Perotti D, De Benedetti V, Mondini P, Radice MT, Pilotti S, Luksch R, Fossati Bellani F, Pierotti MA. (1995). Allelotyping in Wilms tumors identifies a putative third tumor suppressor gene on chromosome 11. Genomics 27:497-501.

Rahman N, Arbour L, Tonin P, Baruchel S, Pritchard-Jones K, Narod S and Stratton MR. (1997). The familial Wilms' tumor susceptibility gene, FWT1, may not be a tumor suppressor gene. Oncogene 14:3099-3102.

Rance TF. (1814). Case of fungus Haematodes of the kidnies. Edinburgh Med Surg J 29:312-315.

Rauscher FJ III. (1993). The WT1 Wilms tumor gene product: A developmentally regulated transcription factor in the kidney that functions as a tumor suppressor. Faseb Journal 7:896-903.

Rebhan, M., Chalifa-Caspi, V., Prilusky, J., Lancet, D.: GeneCards: encyclopedia for genes, proteins and diseases. Weizmann Institute of Science, Bioinformatics Unit and Genome Center (Rehovot, Israel). (1997). GeneCard for [gene] [Last Update]. World Wide Web URL: http://bioinformatics.weizmann.ac.il/cards-bin/carddisp?

Reeve AE, Shi SA, Raizis AM, Feinberg AP. (1989). Loss of allelic heterozygosity at a second locus on chromosome 11 in sporadic Wilms' tumours. Mol Cell Biol 9:1799-1803.

Riccardi VM, Sujansky E, Smith AC, Francke U. (1978). Chromosomal imbalance in aniridia, hemihypertrophy and other congential anomalies. NEJM 270:922-927.

Richards FM, McKee SA, Rajpar MH, Cole TR, Evans DG, Jankowski JA, McKeown C, Sanders DS, Maher ER. (1999). Germline E-cadherin gene (CDH1) mutations predispose to familial gastric cancer and colorectal cancer. Hum Mol Genet 8:607-610.

Ritchey ML, Lelailis PP, Hease GM, Schochet SJ, Green DM, D'Angio G. (1993). Preoperative therapy for intracaval and atrial extension of Wilms tumor. Cancer 71:4104-4110.

Rupprecht H, Drummond I, Madden S, Rauscher F, Sukhatme V. (1994). The Wilms' tumour suppressor gene WT1 is negatively autoregulated. J Biol Chem 269:6198-6206.

Safford SD, Goyeau D, Freemerman AJ, Bentley R, Everett ML, Grundy PE, Skinner MA. (2003). Fine mapping of Wilms' tumors with 16q loss of heterozygosity localizes the putative tumor suppressor gene to a region of 6.7 megabases. Ann Surg Oncol 10:136-43.

Saikali Z and Sinnett D. (2000). Expression of Glypican-3 (GPC3) in embryonal tumors. Int J Cancer 89:418-422.

Saikali Z and SinnettD. (2004). Methylation analysis of the glypican 3 gene in embryonal tumors. Br J Cancer 90:1606-1611

Sambrook and Russell. (2001). Molecular Cloning: A Laboratory Manual. Cold Spring Harbor Laboratory Press, Cold Spring Harbor, New York.

Sanders DS, Blessing K, Hassan GA, Bruton R, Marsden JR, Jankowski J. (1999). Alterations in cadherin and catenin expression during the biological progression of melanocytic tumours. Mol Pathol 52:151-157.

Sano K, Tanihara H, Heimark RL, Obata S, Davidson M, St John T, Taketani S, Suzuki S. (1993). Protocadherins: a large family of cadherin-related molecules in central nervous system. EMBO J 12:2249-2256.

Sariola H, Sainio K. (1998). Cell lineages in the embryonic kidney: their inductive interactions and signaling molecules. Biochem Cell Biol 76:1009-1016.

Sasaki M, Anast J, Bassett W, Kawakami T, Sakuragi N, Dahiya R. (2003). Bisulfite conversion-specific and methylation-specific PCR: a sensitive technique for accurate evaluation of CpG methylation. Biochemical and Biophysical Research Communications 309:305-309.

Sato M, Mori Y, Sakurada A, Fujimura S, Horii A. (1998). The H-cadherin (CDH13) gene is inactivated in human lung cancer. Hum Genet 103:96-101.

Saunders S, Paine-Saunders S, Lander AD. (1997). Expression of the cell surface proteoglycan glypican-5 is developmentally regulated in kidney, liimib, and brain. Dev Biol 190:78-93.

Schroeder WT, Chao LY, Dao DD, Strong LC, Pathak S, Riccardi V, Lewis WH, Saunders GF. (1987). Non-random loss of maternal chromosome 11 alleles in Wilms tumors. Am J Hum Genet 4:413-420.

Schulz S, Becker KF, Braungart E, Reichmuth C, Klamt B, Becker I, Atkinson M, Gessler M, Hofler H. (2000). Molecular analysis of E-cadherin and cadherin-11 in Wilms' tumours. J Pathol 191:162-9.

Scott J, Cowell J, Robertson ME, Priestly LM, Wooley R, Hopkins B, Pritchard J, Bell GI, Rall LB, Graham CF, Knott TJ. (1985). Insulin-like growth factor II gene expression in Wilms tumor and embryonic tissues. Nature 317:260-262.

Seidel B, Braeg S, Adler G, Wedlich D, Menke A. (2004). E- and N-cadherin differ with respect to their associated p120ctn isoforms and their ability to suppress invasive growth in pancreatic cancer cells. Oncogene 23:5532-42.

Selleck SB. (1999). Overgrowth syndromes and the regulation of signaling complexes by proteoglycans. Am J Hum Gen 64:372-377.

Shapiro L, Fannon AM, Kwong PD, Thompson A, Lehmann MS, Grubel G, Legrand JF, Als-Nielsen J, Colman DR, Hendrickson WA. (1995). Structural basis of cell-cell adhesion by cadherins. Nature 374:327-37.

Shapiro L, Kwong PD, Fannon AM, Colman DR, Hendrickson WA. (1995). Considerations on the folding topology and evolutionary origin of cadherin domains. Proc Natl Acad Sci USA 92:6793-7.

Shibata T, Ochiai A, Gotoh M, Machinami R, Hirohashi S. (1996). Simultaneous expression of cadherin-11 in signet-ring cell carcinoma and stromal cells of diffuse-type gastric cancer. Cancer Lett. 99:147-53.

Simpson JL, Landey S, New M, German J. (1975). A previously unrecognized X-linked syndrome of dysmorphia. Birth Defects:OAS XI:18-24.

Sompayrac L, Jane S, Burn TC, Tenen DG, Danna KJ. (1995). Overcoming limitations of the mRNA differential display technique. Nucleic Acids Res 23:4738-9.

Song HH, Filmus J. (2002). The role of glypicans in mammalian development. BBA 1573:241-246.

Song, HH, Shi W, Filmus J. (1997). OCI-5/Rat Glypican-3 binds to fibroblast growth factor-2 but not to insulin-like growth factor-2. J Bio Chem 272:7574-7577.

Srisaru S, Rosenblum ND. (2001). Glypicans and the biology of renal malformations. Pediatr Nephrol 16:302-306.

Strazzullo M, Cossu A, Baldinu P, Colombino M, Satta MP, Tanda F, De Bonis ML, Cerase A, D'Urso M, D'Esposito M, Palmieri G. (2003). High-resolution methylation analysis of the hMLH1 promoter in sporadic endometrial and colorectal carcinomas. Cancer 98:1540-6.

Takahashi N, Takahashi Y, Putnam FW. (1986). Primary stucture of blood coagulation factor XIIIa (fibrinoligase, transglutaminase) from human placenta. Proc Nat Acad Sci 83:8019-8023.

Takeichi M. (1988). The cadherins: cell-cell adhesion molecules controlling animal morphogenesis. Development 102:639-55.

Takeichi M, Hatta K, Nose A, Nagafuchi A. (1988). Identification of a gene family of cadherin cell adhesion molecules. Cell Differ Dev 25 Suppl:91-4.

Tamura G, Yin J, Wang S, Fleisher AS, Zou T, Abraham JM, Kong D, Smolinski KN, Wilson KT, James SP, Silverberg SG, Nishizuka S, Terashima M, Motoyama T, Meltzer SJ. (2000). E-cadherin gene promoter hypermethylation in primary human gastric carcinomas. J Natl Cancer Inst 92:569-573.

Tepass U, Truon K, Godt D, Ikura M, Peifer M. (2000). Cadherins in embryonic and neural morphogenesis. Nature Reviews 1:91-100.

The Genome International Sequencing Consortium. (2001). Initial sequencing and analysis of the human genome. Nature 409:860-921.

Thellin O, Zorzi W, Lakaye B, De Borman B, Coumans B, Hennen G, Grisar T, Igout A, Heinen E. (1999). Housekeeping genes as internal standards: use and limits. J Biotechnol 75:291-5.

Thomas PRM, Tefft M, Compaan PJ, Norkool P, Breslow NE, D'Angio GJ (1991). Results of two radiotherapy randomizations in the third National Wilms Tumor Study (NWTS-3). Cancer 58:1703-1707.

Thompson JS, Reeve KJ, DeBaun MR, Perlman EJ, Feinberg AP. (1996). Reduced expression of the cyclin-dependent kinase inhibitor gene p57^{KIP2} in Wilms tumor. Cancer Research 56:5723-5727.

Thomson RB, Aronson PS. (1999). Immunolocalization of Ksp-cadherin in the adult and developing rabbit kidney. Am J Physiol 277:F146-F156.

Thomsom RB, Igarashi P, Biemesderfer D, Kim R, Abu-Alfa A, Soleimani M, Aronson PS. (1995). Isolation and cDNA cloning of Ksp-cadherin, a novel kidney-specific member of the cadherin multigene family. J Biol Chem 270:17594-17601.

Tomita K, van Bokhoven A, van Leeders GJ, Ruijter ET, Jansen CF, Bussemakers MJ, Schalken JA. (2000). Cadherin switching in human prostate cancer progression. Cancer Res 60:3650-3654.

Toretsky JA, Zitomersky NL, Eskenazi AE, Voigt RW, Strauch ED, Sun CC, Huber R, Meltzer SJ, Schlessinger D. (2001). Glypican-3 expression in Wilms tumor and Hepatoblastoma. J Ped Hematology/Oncology 23:496-499.

Toyooka KO, Toyooka S, Virmani AK, Sathyanarayana UG, Euhus DM, Gilcrease M, Minna JD, Gazdar AF. (2001). Loss of expression and aberrant methylation of the CDH13 (H-cadherin) gene in breast and lung carcinomas. Cancer Research 61:4556-4560.

Toyooka S, Toyooka KO, Harada K, Miyajima K, Makarla P, Sathyanarayana UG, Yin J, Sato F, Shivapurkar N, Meltzer SJ, Gazdar AF. (2002). Aberrant methylation of the CDH13 (h-cadherin) promoter region in colorectal cancers and adenomas. Cancer Research 62:3382-3386.

Troyanovsky SM, Troyanovsky RB, Eshkind LG, Leube RE, Franke WW. (1994). Identification of amino acid sequence motifs in desmocollin, a desmosomal glycoprotein, that are required for plakoglobin binding and plaque formation. Proc Natl Acad Sci USA 91:10790-10794.

Umbas R, Isaacs WB, Bringuier PP, Schaafsma HE, Karthaus HF, Oosterhof GO, Debruyne FM, Schalken JA. (1994) Decreased E-cadherin expression is associated with poor prognosis in patients with prostate cancer. Cancer Res 54:3929-33.

van Hoof A, Parker R. (2002). Messenger RNA degradation: Beginning at the end. Current Biology 12:R285-R287.

Verkoczy LK, Berinstein NL. (1998). Isolation of genes negatively or positively co-expressed with human recombination activating gene 1 (RAG1) by differential display PCR (DD RT-PCR). Nucleic Acids Research 26:4497-4507.

Verloes A, Massart B, DeHalleux I, Lanherndries J-P, Koulischer L. (1995). Clinical overlap of Beckwith-Wiedemann, Perlman and Simpson-Golabi-Behmel syndromes: A diagnostic pitfall. Clin Genet 47:257-262.

Vermeulen SJ, Nollet F, Teugels E, Vennekens KM, Malfait F, Philippe J, Speleman F, Bracke ME, van Roy FM, Mareel MM. (1999). The α-catenin gene (CTNNA1) acts as an invasion-suppressor gene in human colon cancer cells. Oncogene 18:905-915.

Veugelers M, De Cat B, Ceulemans H, Bruystens A-M, Coomans C, Durr J, Vermeesch J, Marynen P, David G. (1999). Glypican-6, a new member of the glypican family of cell surface heparan sulfate proteoglycans. J Biol Chem 274:26968-26977.

Veugelers M, De Cat B, Reekmans G, Delande N, Frints S, Legius E, Fryns JP, Schrander-Stumpel C, Weidle B, Magdalena N, David G. (2000). Mutational analysis of the GPC3/GPC4 glypican gene cluster on Xq26 in patients with Simpson-Golabi-Behmel syndrome: identification of loss-of-function mutations in the GPC3 gene. Human Molecular Genetics 9:1321-1328.

Veugelers M, Vermeesch J, Watanabe K, Yamaguchi Y, Marynen P, David G. (1998). GPC4, the gene for human K-glypican, flanks GPC3 on Xq26: Deletion of the GPC3-GPC4 gene cluster in one family with Simpson-Golabi-Behmel syndrome. Genomics 53:1-11.

Vujanic GM, Harms D, Sndstedt B, Weirich A, de Kraker J, Delemarre JFM. (1999). New definitions of focal and diffuse anaplasia in Wilms tumor: the international society of paediatric oncology (SIOP) experience. Medical and Pediatric Oncology 32:317-323.

Wang Z, Qui Q, Deuel T. (1993). The Wilms' tumour gene product WT1 activates or suppresses transcription through separate functional domains. J Biol Chem 268:9172-9175.

Warnecke PM, Stirzaker C, Song J, Grunau C, Melki JR, Clark SJ. (2002). Identification and resolution of artifacts in bisulfite sequencing. Methods 27:101-107.

Watanabe K, Yamada H, Yamaguchi Y. (1995). K-glypican: A novel GPI-anchored heparan sulfate proteoglycan that is highly expressed in developing brain and kidney. J Cell Biol. 130:1207-1218.

Watson A, Mazumder A, Stewart M, Balasubramanian S. (1998). Technology for microarray analysis of gene expression. Curr Opin Biotechnol 9:609-14.

Weksberg R, Squire JA, Templeton DM. (1996). Glypicans: a growing trend. Nature Genetics 12:225-227.

Wendeler MW, Praus M, Jung R, Hecking M, Metzig C, Geβner R. (2004). Ksp-cadherin is a functional cell-cell adhesion molecule related to LI-cadherin. Experimental Cell Research 294:345-355.

Wertz K, Herrmann BG. (1999). Kidney-specific cadherin (cdh16) is expressed in embryonic kidney, lung, and sex ducts. Mechanisms of Development 84:185-188.

Wheelock MJ, Johnson KR. (2003). Cadherins as modulators of cellular phenotype. Annu Rev Cell Dev Biol 19:207-235.

White GRM, Kelsey AM, Varley JM, Birch JM. (2002). Somatic glypican 3 (GPC3) mutations in Wilms' tumour. Br J Cancer 86:1920-1922.

Whyte DA, Li C, Thomson B, Nix SL, Zanjani R, Karp SL, Aronson PS, Igarashi P. (1999). Ksp-cadherin gene promoter. I. Characterization and renal epithelial cell-specific activity. Am J Physiol (Renal Physiol) 277:F587-F598.

Wilmore HP, White GFJ, Howell RT, Brown KW. (1994). Germline and somatic abnormalities of chromosome 7 in Wilms' tumor. Cancer Genetics and Cytogenetics 77:93-98.

Wilms M. 1899. Mischgeschwulste der Niere. Die Mishgeschwulste Leipzig: a Georgi:5-90.

Wong BW, Luk JM, Ng IO, Hu MY, Kiu KD, Fan ST. (2003). Identification of liver-intestine cadherin in hepatocellular carcinoma – a potential disease marker. Biochemical and Biophysical Res Comm 311:618-624.

Xiang YY, Ladeda V, Filmus J. (2001). Glypican-3 expression is silenced in human breast cancer. Oncogene 20:7408-7412.

Xu SF, Peng ZH, Li DP, Qiu GQ, Zhang F. (2003). Refinement of heterozygosity loss on chromosome 5p15 in sporadic colorectal cancer. World J Gastroenterol 9:1713-8.

Xuan JY, Besner A, Ireland M, Hughes-Benzie RM, MacKenzie AE. (1994). Mapping of Simpson-Golabi-Behmel syndrome to Xq25-q27. Human Molecular Genetics 3:133-137.

Yagi T, Takeichi M. (2000). Cadherin superfamily genes: functions, genomic organization, and neurologic diversity. Genes and Devel 14:1169-1180.

Yap AS, Brieher WM, Pruschy M, Gumbiner BM. (1997). Lateral clustering of the adhesive ectodomain: a fundamental determinant of cadherin function. Curr Biol 7:308-15.

Yokoyama K, Kamata N, Hayashi E, Hoteiya T, Ueda N, Fujimoto R, Nagayama M. (2001). Reverse correlation of E-cadherin and snail expression in oral squamous cell carcinoma cells in vitro. Oral Oncol 37:65-71.

Yoshiura K, Kanai Y, Ochiai A, Shimoyama Y, Sugimura T, Hirohashi S. (1995). Silencing of the E-cadherin invasion-suppressor gene by CpG methylation in human cancers. PNAS USA 92:7416-7419.

Yuan BZ, Durkin ME, Popescu NC. (2003). Promoter hypermethylation of DLC-1, a candidate tumor suppressor gene, in several common human cancers.

Cancer Genet Cytogenet 140:113-7.

Zhang JS, Duncan EL, Chang AC-M, Reddel RR. (1998). Differential Display of mRNA. Molecular Biotechnology 10:155-165.

Zhang Y, Shields T, Crenshaw T, Hao Y, Moulton T, Tycko B. (1993). Imprinting of human H19: allele-specific CpG mehtylation, loss of the active allele in Wilms tumor, and potential for somatic allele switching. Am J Hum Genet 53:113-124.

Zhang Y, Tycko B. (1992). Monoallelic expression of the human H19 gene. Nat Genet 1:40-4.

Appendix 1

Recipe for random priming labelling mix:

Solution 1

1.25 M Tris-Cl; H 8.0

0.25 M $MgCl_2$

Solution 2

18 µl β-mercaptoethanol

5 µl 100 mM dATP

5 µl 100 mM dGTP

5 µl 100 mM dCTP

5 µl 100 mM dTTP

715 µl Solution 1

250 µl dH_20

Solution 3

2 M Hepes; pH 6.6

Solution 4

Random hexanucleotides resuspended to 90 O.D. units per ml

To make random priming labelling mix, combine solutions 2, 3 and 4 at a ratio of 100:250:150 and freeze in aliquots at -20°C.